AD711129

FTD-HC-23-361-69

FOREIGN TECHNOLOGY DIVISION

INVESTIGATIONS OF ELASTICITY AND PLASTICITY
(Collection of Articles)

DDC

SEP 10 1970

B

Distribution of this document is
unlimited. It may be released to the
Clearinghouse, Department of Commerce,
for sale to the general public.

279

EDITED TRANSLATION

INVESTIGATIONS OF ELASTICITY AND PLASTICITY
(Collection of Articles)

English pages: 241

Source: Leningrad. Universitet. Matematiko-
Mekhanicheskiy Fakul'tet. Issledovaniya
po Uprugosti i Plastichnosti, 1965,
Nr. 4, pp. 1-64, 72-219

Translated Under: F33657-70-D-0607

PREPARED BY:

TRANSLATION DIVISION
FOREIGN TECHNOLOGY DIVISION
WP-AFB, OHIO.

Date 20 April 19 70

TABLE OF CONTENTS

Published with the approval of the
Editorial and Publishing Council of
Leningrad University

This collection consists of studies carried out in the
Division of Elasticity Theory of the Mathematics and Mechanics
Department of Leningrad University. The articles cover questions
of elasticity theory, plasticity theory, statics and dynamics of
thin shells, and experimental methods for studying stresses and
fracture conditions.

The volume is intended for scientific personnel and engineers
working in the strength field.

Editor: Professor L. M. Kachanov

EQUATIONS OF ANISOTROPIC PLATE THEORY

V. V. Ponyatovskiy

In this paper the method of [1] is used to construct a theory of anisotrop'c plates. It is assumed that the plate is elastically uniform through its thickness and has at every point a plane of elastic symmetry parallel to the median plane. As is known, in this case the problem of the stresses in the plate breaks down into two independent problems which are symmetric and antisymmetric with respect to the median plane, respectively.

The equations of the bending problem for transversely isotropic plates are examined in detail. In this case, the stress state is represented as the sum of two qualitatively different stress states: "rotational" and "potential" [2].

To solve the bending problem we use asymptotic integration of differential equations with a small parameter in the derivatives [3,4].

§ 1. Three-dimensional Problem Formulation. Basic Relations

1. We refer the plate median plane to the arbitrary curvilinear coordinates x^1, x^2 and denote by $g_{\alpha\beta}$ the metric tensor of the median plane in these coordinates. Let z be the distance of any point of

FTD-HC-23-361-69

the plate to the median plane, so that

$$-h < z < h,$$

where 2h is the plate thickness, which we will consider constant. We denote the components of the stress tensor and the deformations by $\sigma_{\alpha\beta}$, $\sigma_{\alpha z} = \sigma_\alpha^z = \sigma_\alpha$, $\sigma_{zz} = \sigma^{zz} = \sigma$ and $e_{\alpha\beta}$, $e_{\alpha z} = e_\alpha$, $e_{zz} = e$, respectively. Here and in the following the Greek indices of a tensor symbol take the values 1, 2.

We assume that the material from which the plate is made obeys the generalized Hooke's law and at every point has a plane of elastic symmetry parallel to the median plane. In this case the Hooke's law formulas are written as

$$e_{\alpha\beta} = a_{\alpha\beta\pi\rho}\sigma^{\pi\rho} + a_{\alpha\beta}\sigma,$$
$$e_\alpha = b_{\alpha\beta}\sigma^\beta, \quad e = a_{\alpha\beta}\sigma^{\alpha\beta} + a\sigma, \tag{1.1}$$

where $a_{\alpha\beta\pi\rho}$, $a_{\alpha\beta}$, a, $b_{\alpha\beta}$ are the deformation coefficients. In the plane x^1, x^2 $a_{\alpha\beta\pi\rho}$ is a tensor which is symmetric relative to both the first and last two indices and also their pairs; $a_{\alpha\beta}$ and $b_{\alpha\beta}$ are symmetric tensors and a is a scalar. In the following we assume that the deformation coefficients are independent of z.

In the absence of mass forces, the equilibrium equations have the form

$$\nabla_\beta\sigma^{\alpha\beta} + \frac{\partial\sigma^\alpha}{\partial z} = 0, \quad \nabla_\alpha\sigma^\alpha + \frac{\partial\sigma}{\partial z} = 0, \tag{1.2}$$

where ∇_α is the symbol of covariant differentiation in the metric established in the median plane. The static boundary conditions

$$\sigma_\alpha|_{z=\pm h} = 0, \quad \sigma|_{z=\pm h} = \frac{q \pm p}{2}. \tag{1.3}$$

will be given at the boundaries of the plate surfaces z = ±h, where $q = q(x^1, x^2)$ gives the load on the surfaces z = ±h, which is symmetric relative to the median plane, while $p = p(x^1, x^2)$ gives the antisymmetric load.

2. We represent the plate stresses $\sigma_{\alpha\beta}$ in the form of Legendre polynomial series in the variable $\zeta = \frac{z}{h}$, and retain in these series a finite number of terms

$$\sigma_{\alpha\beta} = \sum_{k=0}^{N} \sigma_{\alpha\beta}^{(k)} P_k(\zeta).$$

(1.4)

The expansion coefficients, which in the following we will call k-th order "moments", are unknown functions of a point of the plate median plane.

Substituting (1.4) into the equilibrium equation (1.2) and integrating the resulting equations with respect to z with account for the boundary conditions (1.3), we obtain the expressions for the remaining stresses

$$\sigma_{\alpha 3} = h \sum_{k=0}^{N+1} \left(\frac{\sigma_{\alpha}^{(k+1)}}{2k+3} - \frac{\sigma_{\alpha}^{(k-1)}}{2k-1} \right) P_k(\zeta),$$

$$\sigma_{33} = \frac{p}{2} + \frac{3p}{2}\zeta - \frac{p}{10} P_2(\zeta) + h^2 \sum_{k=0}^{N+2} \left[\frac{\sigma_{(k-2)}}{(2k-3)(2k-1)} - \frac{2\sigma_{(k)}}{(2k-1)(2k+3)} + \frac{\sigma_{(k+2)}}{(2k+3)(2k+5)} \right] P_k(\zeta)$$

(1.5)

and the equations

$$\nabla_\beta \sigma_{(0)}^{\alpha\beta} = 0, \quad \frac{2h^2}{3} \nabla_\alpha \nabla_\beta \sigma_{(1)}^{\alpha\beta} + p = 0.$$

(1.6)

In (1.5) we have used the notations

$$\sigma_{(k)}^{\alpha} = \nabla_\beta \sigma_{(k)}^{\alpha\beta}, \quad \sigma_{(0)} = 0,$$
$$\sigma_{(k)} = \nabla_\alpha \sigma_{(k)}^{\alpha} = \nabla_\alpha \nabla_\beta \sigma_{(k)}^{\alpha\beta}, \quad k = 2, 3, \ldots, N,$$
$$\sigma_{(k)} = 0, \quad k = 0, 1.$$

(1.7)

Moreover, here and below we shall consider that $\sigma_{(k)}^{\alpha\beta} \equiv 0$ for $k < 0$ and $k > N$.

3. We note that, by virtue of the orthogonality of the Legendre polynomials, the zero and first order "moments" $\sigma_{\alpha\beta}^{(0)}, \sigma_{\alpha\beta}^{(1)}$ are proportional to the conventional forces and moments $T_{\alpha\beta}$, $M_{\alpha\beta}$

$$T_{\alpha\beta} = \int_{-h}^{h} \sigma_{\alpha\beta}\,dz = 2h\,\sigma_{\alpha\beta}^{(0)}, \quad M_{\alpha\beta} = \int_{-h}^{h} z\,\sigma_{\alpha\beta}\,dz = \frac{2h^3}{3}\,\sigma_{\alpha\beta}^{(1)}. \tag{1.8}$$

However, "moments" of higher order $\sigma_{\alpha\beta}^{(k)}$ (k> 1) define stresses which are self-equilibrating through the plate thickness.

Similarly,

$$\sigma_{(1)}^{\alpha} = \nabla_{\beta}\,\sigma_{(1)}^{\alpha\beta} \tag{1.9}$$

is proportional to the shearing force N_{α}

$$N_{\alpha} = \int_{-h}^{h} \sigma_{\alpha}\,dz = \frac{2h^3}{3}\,\sigma_{\alpha}^{(1)}, \tag{1.10}$$

while $\sigma_{\alpha}^{(k)}$ (k $\neq$ 1) defines the self-equilibrating tangential stresses. We see from (1.8), 1·10) that (1·9) and (1·6) are simply the usual plate equilibrium equations in terms of forces and moments.

§ 2. Application of the Castigliano Principle
to the Derivation of Plate Theory Equations

1. We introduce the plate deformation potential energy

$$\Pi = \frac{1}{2}\iint\left\{\int_{-h}^{h}(\sigma^{\alpha\beta}e_{\alpha\beta} + 2\sigma^{\alpha}e_{\alpha} + \sigma e)\,dz\right\}\sqrt{g}\,dx^1\,dx^2, \tag{2.1}$$
$$g = g_{11}g_{22} - g_{12}^2.$$

where the double integral is taken over the entire median plane of the plate.

Substituting (1·1), (1-4), (1·5) into (2·1) and integrating with respect to z we obtain

$$\Pi = h \iint \sum_{k=-2}^{N} \left[\frac{h^4 a\, \sigma_{(k-4)}\, \sigma_{(k)}}{(2k-7)(2k-5)(2k-3)(2k-1)(2k+1)} - \right.$$

$$- \frac{4h^4 a\, \tau_{(k-2)}\sigma_{(k)}}{(2k-5)(2k-3)(2k-1)(2k+1)(2k+3)} +$$

$$+ \frac{h^2 a_{\alpha\beta}\left(\sigma_{(k-2)}\sigma_{(k)}^{\alpha\beta} + \sigma_{(k-2)}^{\alpha\beta}\sigma_{(k)}\right)}{(2k-3)(2k-1)(2k+1)} - \frac{2h^2 b_{\alpha\beta}\sigma_{(k-2)}^{\alpha\beta}\sigma_{(k)}^{\beta}}{(2k-3)(2k-1)(2k+1)} +$$

$$+ \frac{a_{\alpha\beta\gamma}\sigma_{(k)}^{\alpha\beta}\sigma_{(k)}^{\gamma}}{2k+1} + \frac{4h^2 b_{\alpha\beta}\sigma_{(k)}^{\alpha}\sigma_{(k)}^{\beta}}{(2k-1)(2k+1)(2k+3)} - \frac{2h^2 a_{\alpha\beta}\left(\sigma_{(k)}\sigma_{(k)}^{\alpha\beta} + \sigma_{(k)}^{\alpha\beta}\sigma_{(k)}\right)}{(2k-1)(2k+1)(2k+3)} +$$

$$+ \frac{6h^4 a\, \tau_{(k)}\sigma_{(k)}}{(2k-3)(2k-1)(2k+1)(2k+3)(2k+5)} - \frac{2h^2 b_{\alpha\beta}\sigma_{(k+2)}^{\alpha}\sigma_{(k)}^{\beta}}{(2k+1)(2k+3)(2k+5)} +$$

$$+ \frac{h^2 a_{\alpha\beta}\left(\sigma_{(k+2)}\sigma_{(k)}^{\alpha\beta} + \sigma_{(k+2)}^{\alpha\beta}\sigma_{(k)}\right)}{(2k+1)(2k+3)(2k+5)} -$$

$$- \frac{4h^4 a\, \tau_{(k+2)}\sigma_{(k)}}{(2k-1)(2k+1)(2k+3)(2k+5)(2k+7)} +$$

$$\left. + \frac{h^4 a\, \tau_{(k+4)}\sigma_{(k)}}{(2k+1)(2k+3)(2k+5)(2k+7)(2k+9)} \right] \sqrt{g}\, dx^1 dx^2 +$$

$$+ 2h \iint \left[\frac{q}{2} a_{\alpha\beta}\sigma_{(0)}^{\alpha\beta} + \frac{p}{5} a_{\alpha\beta}\tau_{(1)}^{\alpha\beta} - \frac{p}{70} a_{\alpha\beta}\tau_{(3)}^{\alpha\beta} + \frac{h^2 q}{30} a\, \sigma_{(2)} + \right.$$

$$\left. + \frac{10h^2 p}{1575} a\, \tau_{(3)} - \frac{h^2 p}{6930} a\, \tau_{(5)} \right] \sqrt{g}\, dx^1 dx^2 + \text{const.}$$

$$(2.2)$$

The energy expression is written so that, to obtain its variation δΠ, we must in each term of the integrands place the variation sign δ in front of the last cofactor and then double the first integral.

Let us minimize the expression for the potential energy with the aid of the equilibrium equations (1.6), which play the role of auxiliary conditions. In order to take these auxiliary conditions into account, we use the Lagrange multiplier method. We multiply (1.6) by $2hu_\alpha$ and w, respectively, and substitute the results into the integrand of (2.2). We obtain the functional

$$I = \Pi + \iint \left[2h\, u_\alpha \nabla_\beta \tau_{(0)}^{\alpha\beta} + \left(\frac{2h^2}{3} \nabla_\alpha \nabla_\beta \tau_{(1)}^{\alpha\beta} + p \right) w \right] \sqrt{g}\, dx^1 dx^2. \qquad (2.3)$$

The Lagrange multipliers u_α are the covariant components of the characteristic tangential displacement and w is the characteristic deflection [5]. In classical thin plate theory u_1, u_2, w are the components of the displacement vector of a point of the median plane.

For convenience in writing the subsequent formulas, we introduce the notations:

$$c_{ij}^{(k)} = \frac{k^2 a_{ij} c_{(k-2)}}{(2k-3)(2k-1)(2k+1)} + \frac{a_{ij} c_{(k)}^0}{2k+1} - \frac{2k^2 a_{ij} c_{(k)}}{(2k-1)(2k+1)(2k+3)} +$$
$$+ \frac{k^2 a_{ij} c_{(k+2)}}{(2k+1)(2k+3)(2k+5)} + \frac{a_{ij} P_{(k)}}{2k+1} \qquad (k=0,\,1,\,2,\,...,\,N);$$

$$P_{(0)} = \frac{2}{3};\; P_{(1)} = \frac{2}{7};\; P_{(2)} = 0;\; P_{(3)} = -\frac{p}{15};\; P_{(k)} = 0,\; k>3;$$

$$n_c^{(0)} = n_c;$$

$$n_c^{(k)} = -\frac{2k^2 b_{ij} c_{(k-2)}}{(2k-3)(2k-1)(2k+1)} + \frac{4k^2 b_{ij} c_{(k)}}{(2k-1)(2k+1)(2k+3)} -$$
$$- \frac{2k^2 b_{ij} c_{(k+2)}}{(2k+1)(2k+3)(2k+5)} \qquad (k=1,\,2,\,...,\,N);$$

$$n_{(0)} = 0,\; n_{(1)} = \frac{kn}{3};$$

$$n_{(k)} = \frac{k^2 a\, c_{(k-4)}}{(2k-7)(2k-5)(2k-3)(2k-1)(2k+1)} -$$
$$- \frac{4k^2 a\, c_{(k-2)}}{(2k-5)(2k-3)(2k-1)(2k+1)(2k+3)} + \frac{k^2 a_{ij} c_{(k-2)}^0}{(2k-3)(2k-1)(2k+1)} -$$
$$- \frac{2k^2 a_{ij} c_{(k)}^0}{(2k-1)(2k+1)(2k+3)} + \frac{6k^2 a\, c_{(k)}}{(2k-3)(2k-1)(2k+1)(2k+3)(2k+5)} +$$
$$+ \frac{k^2 a_{ij} c_{(k+2)}^0}{(2k+1)(2k+3)(2k+5)} - \frac{4k^2 a\, c_{(k+2)}}{(2k-1)(2k+1)(2k+3)(2k+5)(2k+7)} +$$
$$+ \frac{k^2 a\, c_{(k+4)}}{(2k+1)(2k+3)(2k+5)(2k+7)(2k+9)} + \frac{k^2 a\, P_{(k)}}{(2k-3)(2k-1)(2k+1)} \qquad (2.4)$$
$$(k=2,\,3,\,...,\,N);$$

$$P_{(2)} = P_{(0)};\; P_{(3)} = P_{(1)} - \frac{3}{5} P_{(3)};\; P_{(4)} = 0;\; P_{(5)} = P_{(3)};\; P_{(k)} = 0,\; k>5.$$

With the aid of these notations the variation of functional (2.3) may be written as

$$\delta I = 2k \sum_{k=0}^{N} \iint \left(c_{ij}^{(k)} \delta \sigma_{(k)}^{ij} + u_{(k)} \nabla_\alpha \nabla_\beta \delta \sigma_{(k)}^{\alpha\beta} + n_c^{(k)} \nabla_\beta \delta \sigma_{(k)}^{c\beta} \right) \sqrt{g}\, dx^1\, dx^2. \qquad (2.5)$$

Equating δI to zero, after the usual transformations we obtain the following variational equation:

$$\sum_{k=0}^{N} \iint \left[c_{ij}^{(k)} - \frac{1}{2}\left(\nabla_\beta u_c^{(k)} + \nabla_c u_\beta^{(k)} \right) + \nabla_c \nabla_\beta u_{(k)} \right] \delta \sigma_{(k)}^{c\beta} \sqrt{g}\, dx^1\, dx^2 +$$
$$+ \sum_{k=0}^{N} \int \left[\left(n_c^{(k)} n^c - \frac{\partial n_{(k)}}{\partial x^2} n^c \right) \delta \left(\sigma_{(k)}^{c\beta} n_c\, n_\beta \right) +$$
$$+ \left(n_c^{(k)} s^c - \frac{\partial n_{(k)}}{\partial x^2} s^c \right) \delta \left(\sigma_{(k)}^{c\beta} n_c\, s_\beta \right) + u_{(k)} \delta \left(\sigma_{(k)}^{c\beta} n_c \right) \right] ds = 0. \qquad (2.6)$$

7

Here n_α, n^α are the covariant and contravariant components of the vector of the unit outward normal to the contour of the region occupied by the plate median plane; s_α, s^α are the components of the unit tangential vector, whose direction coincides with the direction of integration along the region boundary; ds is the contour length element.

Variational equation (2.6) leads to the differential equations (compatability equations)

$$\sigma_\alpha^{(k)} + \frac{1}{2}(\nabla_\beta u_\alpha^{(k)} + \nabla_\alpha u_\beta^{(k)}) + \nabla_\alpha \nabla_\beta u_{(k)} = 0 \tag{2.7}$$

and the homogeneous geometric boundary conditions

$$u_\alpha^{(k)} n^\alpha - \frac{\partial u_{(k)}}{\partial s^\alpha} n^\alpha = 0, \quad u_\alpha^{(k)} s^\alpha - \frac{\partial u_{(k)}}{\partial s^\alpha} s^\alpha = 0, \quad u_{(k)} = 0. \tag{2.8}$$

The corresponding static boundary conditions are

$$\sigma_{(k)}^\alpha n_\alpha n_\beta = \sigma_{nn}^{(k)}, \quad \sigma_{(k)}^\alpha n_\alpha s_\beta = \sigma_{ns}^{(k)}, \quad \sigma_{(k)}^\alpha n_\alpha = \sigma_n^{(k)}. \tag{2.9}$$

By virtue of the assumption of elastic symmetry, the stress state of the plate may be considered as the sum of two stress states, one of which is symmetric, while the other is antisymmetric with respect to the median plane. Correspondingly, we have two independent problems: stretching and bending of the plate, for which the equations and boundary conditions are obtained from the problems presented above for even and odd k, respectively.

2. The compatibility equations (2.7) may be derived by integrating the Hooke's law equations with respect to z after first writing them in the form:

$$\frac{\partial v}{\partial z} = a_{\alpha\beta} \sigma^{\alpha\beta} + a\sigma, \quad \frac{\partial v_\alpha}{\partial z} = -\frac{\partial v}{\partial x^\alpha} + 2b_{\alpha\beta} \sigma^\beta,$$

$$a_{\alpha\beta\gamma} \sigma^{\gamma} + a_{\alpha\beta} \sigma - \frac{1}{2}(\nabla_\alpha v_\beta + \nabla_\beta v_\alpha) = 0, \tag{2.10}$$

where $(v_1 v_2, v)$ is the displacement vector of an arbitrary point of the plate.

Displacements v_α and v can be determined if we integrate the first two equations (2.10) with respect to z, after first substituting

into them the expressions (1.4) and (1.5) for the stresses. Substituting the displacements v_α thus found into the third equation and expanding the left side into a series in Legendre polynomials, we obtain equations of the form (2.7). The variational method has the advantage that it permits obtaining simultaneously the natural geometric boundary conditions.

§ 3. Bending Equations for a Homogeneous Transversely Isotropic Plate.

1. Consider a transversely isotropic homogeneous plate whose plane of isotropy coincides with the median plane. Let E be Young's modulus for the directions in the plane of isotropy; E_z is Young's modulus for the directions perpendicular to the plane of isotropy; v is Poisson's ratio, characterizing the contraction in the plane of isotropy for stretch in this same plane; v_z is Poisson's ratio characterizing the contraction in the plane of isotropy for stretch in the direction perpendicular to this plane; G is the shear modulus for planes normal to the isotropy plane.

The deformation coefficient tensor has the form
$$a_{\alpha\beta\gamma\eta} = \frac{1}{E}[(1+v)\,\varepsilon_{\alpha\gamma}\varepsilon_{\beta\eta} - v\varepsilon_{\alpha\beta}\varepsilon_{\gamma\eta}],\quad a_{\alpha\beta} = -\frac{v_z}{E_z}\,\varepsilon_{\alpha\beta},$$
$$b_{\alpha\beta} = \frac{1}{2G}\varepsilon_{\alpha\beta},\quad a = \frac{1}{E_z}. \tag{3.1}$$

We rewrite the equilibrium equations (1.6) for the case of plate bending and the compatibility equations (2.7), substituting therein the deformation coefficients from (3.1)

$$\frac{2h^3}{3}\nabla_\alpha\nabla_\beta\sigma^\alpha_{(1)} + p = 0,$$

$$\frac{(1+v)\sigma^{(1)}_{\alpha\beta} - v\varepsilon_{\alpha\beta}\sigma^\gamma_{\alpha(1)}}{3} + \frac{Eh}{3}\nabla_\alpha\nabla_\beta w - \frac{E}{G}\cdot\frac{h^2}{15}(\nabla_\alpha\sigma^{(1)}_\beta + \nabla_\beta\sigma^{(1)}_\alpha) +$$
$$+ \frac{E}{2G}\cdot\frac{h^2}{105}(\nabla_\alpha\sigma^{(3)}_\beta + \nabla_\beta\sigma^{(3)}_\alpha) - \frac{E}{E_z}\cdot\frac{h^2}{105}\varepsilon_{\alpha\beta}\sigma_{(3)} = \frac{v_z}{5}\cdot\frac{E}{E_z}\varepsilon_{\alpha\beta}p.$$

$$\frac{E}{E_z}\cdot\frac{h^2\nabla_\alpha\nabla_\beta\sigma_{(k-4)}}{(2k-7)(2k-5)(2k-3)(2k-1)(2k+1)} -$$
$$- \frac{E}{E_z}\cdot\frac{4h^2\nabla_\alpha\nabla_\beta\sigma_{(k-2)}}{(2k-5)(2k-3)(2k-1)(2k+1)(2k+3)} -$$
$$- \frac{E}{E_z}\cdot\frac{h^2v_z(\nabla_\alpha\nabla_\beta\sigma^c_{\alpha(k-2)} + \varepsilon_{\alpha\beta}\sigma_{(k-2)})}{(2k-3)(2k-1)(2k+1)} + \frac{E}{2G}\cdot\frac{h^2(\nabla_\eta\sigma^{(k-2)}_\beta + \nabla_\beta\sigma^{(k-2)}_\alpha)}{(2k-3)(2k-1)(2k+1)} +$$
$$+ \frac{(1+v)\sigma^{(2)}_{\alpha\beta} - v\varepsilon_{\alpha\beta}\sigma^\gamma_{\alpha(k)}}{2k+1} + \frac{E}{E_z}\cdot\frac{2v_z h^2(\nabla_\alpha\nabla_\beta\sigma^c_{\alpha(k)} + \varepsilon_{\alpha\beta}\sigma_{(k)})}{(2k-1)(2k+1)(2k+3)} - \tag{3.2}$$

(Continued on following page)

(Continued from preceding page)

$$-\frac{E}{G}\cdot\frac{h^6(\nabla_a\sigma_a^{(h)}+\nabla_\beta\sigma_a^{(h)})}{(2k-1)(2k+1)(2k+3)}+$$
$$+\frac{E}{E_z}\cdot\frac{6h^4\nabla_a\nabla_\beta\sigma_{(h)}}{(2k-3)(2k-1)(2k+1)(2k+3)(2k+5)}+$$
$$+\frac{E}{2G}\cdot\frac{h^2(\nabla_a\sigma_a^{(h+2)}+\nabla_\beta\sigma_a^{(h+2)})}{(2k+1)(2k+3)(2k+5)}-\frac{E}{E_z}\cdot\frac{h^6\nu_z(\nabla_a\nabla_\beta\sigma_{z(h+2)}^2+E_{a\beta}\sigma_{(h+2)})}{(2k+1)(2k+3)(2k+5)}$$
$$-\frac{E}{E_z}\cdot\frac{4h^4\nabla_a\nabla_\beta\sigma_{(h+2)}}{(2k-1)(2k+1)(2k+3)(2k+5)(2k+7)}+$$
$$+\frac{E}{E_z}\cdot\frac{h^6\nabla_a\nabla_\beta\sigma_{(h+4)}}{(2k+1)(2k+3)(2k+5)(2k+7)(2k+9)}=$$
$$=\frac{E}{E_z}\cdot\frac{\nu_z}{2k+1}\mathcal{E}_{a\beta}P_{(h)}-\frac{E}{E_z}\cdot\frac{h^6\nabla_a\nabla_\beta P_{(h)}}{(2k-3)(2k-1)(2k+1)}\quad(k=3,5,\ldots,N).$$

(3.2)

The geometric boundary conditions (2.8) for the transversely isotropic plate take the form:

$$\frac{2h^4}{15G}\sigma_a^{(1)}n^a-\frac{h^3}{105G}\sigma_a^{(3)}n^a-\frac{h}{3}\cdot\frac{\partial w}{\partial x^a}n^a=0,$$
$$\frac{2h^4}{15G}\sigma_a^{(1)}s^a-\frac{h^3}{105G}\sigma_a^{(3)}s^a-\frac{h}{3}\cdot\frac{\partial w}{\partial x^a}s^a=0,$$
$$w=0,$$

$$-\frac{h^4}{E_z(2k-7)(2k-5)(2k-3)(2k-1)(2k+1)}\cdot\frac{\partial\sigma_{(h-4)}}{\partial x^a}n^a+$$
$$+\frac{4h^4}{E_z(2k-5)(2k-3)(2k-1)(2k+1)(2k+3)}\cdot\frac{\partial\sigma_{(h-2)}}{\partial x^a}n^a+$$
$$+\frac{h^2}{(2k-3)(2k-1)(2k+1)}\left(\frac{\nu_z}{E_z}\cdot\frac{\partial\sigma_{z(h-2)}^a}{\partial x^b}n^b-\frac{1}{G}\sigma_a^{(h-2)}n^a\right)+$$
$$+\frac{2h^2}{(2k-1)(2k+1)(2k+3)}\left(\frac{1}{G}\sigma_a^{(h)}n^a-\frac{\nu_z}{E_z}\cdot\frac{\partial\sigma_{z(h)}^a}{\partial x^b}n^b\right)-$$
$$-\frac{8h^4}{E_z(2k-3)(2k-1)(2k+1)(2k+3)(2k+5)}\cdot\frac{\partial\sigma_{(h)}}{\partial x^a}n^a+$$
$$+\frac{h^2}{(2k+1)(2k+3)(2k+5)}\left(\frac{\nu_z}{E_z}\cdot\frac{\partial\sigma_{z(h+2)}^a}{\partial x^b}n^b-\frac{1}{G}\sigma_a^{(h+2)}n^a\right)+$$
$$+\frac{4h^4}{E_z(2k-1)(2k+1)(2k+3)(2k+5)(2k+7)}\cdot\frac{\partial\sigma_{(h+2)}}{\partial x^a}n^a-$$
$$-\frac{h^4}{E_z(2k+1)(2k+3)(2k+5)(2k+7)(2k+9)}\cdot\frac{\partial\sigma_{(h+4)}}{\partial x^a}n^a-$$
$$-\frac{h^2}{E_z(2k-3)(2k-1)(2k+1)}\cdot\frac{\partial P_{(h)}}{\partial x^a}n^a=0\quad(n^a\sim s^a),$$

$$(k=3,5,\ldots,N),$$

(3.2$_1$)

(Continued on following page)

(Continued from preceding page)

$$
\begin{aligned}
& \frac{N^2 c_{(k-4)}}{(2k-7)(2k-5)(2k-3)(2k-1)(2k+1)} - \\
& - \frac{4N^2 a_{(k-2)}}{(2k-5)(2k-3)(2k-1)(2k+1)(2k+3)} - \\
& - \frac{N^2 v_2 c_{0\,(k-2)}}{(2k-3)(2k-1)(2k+1)} + \frac{2N^2 v_2 c_{0\,(k)}}{(2k-1)(2k+1)(2k+3)} + \\
& + \frac{6N^2 c_{(k)}}{(2k-3)(2k-1)(2k+1)(2k+3)(2k+5)} - \frac{N^2 v_2 c_{0\,(k+2)}}{(2k+1)(2k+3)(2k+5)} - \\
& - \frac{4N^2 c_{(k+2)}}{(2k-1)(2k+1)(2k+3)(2k+5)(2k+7)} + \\
& + \frac{N^2 c_{(k+4)}}{(2k+1)(2k+3)(2k+5)(2k+7)(2k+9)} + \\
& + \frac{N^2 P_{(k)}}{(2k-3)(2k-1)(2k+1)} = 0 \quad (k=3,\,5,\,\ldots,\,N).
\end{aligned}
\tag{$3\cdot2_1$}
$$

The symbol ($n^{\alpha} \sim s^{\alpha}$) indicates that the relation obtained from the given expression by replacement of n^{α} by s^{α} holds.

2. Let us introduce the stress functions. To do this, we divide the vector $\sigma_{\alpha}^{(k)}$ into potential and rotational parts $t_{\alpha}^{(k)}$, $\tau_{\alpha}^{(k)}$ such that

$$
\sigma_{\alpha}^{(k)} = t_{\alpha}^{(k)} + \tau_{\alpha}^{(k)} \quad (k=1,\,3,\,\ldots,\,N).
\tag{3-3}
$$

The latter may be expressed in terms of the scalar functions $\Phi_{(k)}, \omega_{(k)}$ by the formulas

$$
t_{\alpha}^{(k)} = \nabla_{\alpha} \Phi_{(k)}, \quad \tau_{\alpha}^{(k)} = \varepsilon_{\cdot\alpha}^{\beta} \nabla_{\beta} \omega_{(k)} \quad (k=1,\,3,\,\ldots,\,N),
\tag{3-4}
$$

where $\varepsilon_{\cdot\alpha}^{\beta}$ is the mixed form of the discriminant tensor $\varepsilon_{\alpha\beta}$ [6]

$$
\varepsilon_{11} = \varepsilon_{22} = 0, \; \varepsilon_{12} = -\varepsilon_{21} = \sqrt{g}.
\tag{3-5}
$$

From (3.3), (3.4) we have ($\Delta = g^{\alpha\beta} \nabla_{\alpha} \nabla_{\beta}$)

$$
\begin{aligned}
& \nabla_{\alpha} \sigma_{\beta}^{(k)} + \nabla_{\beta} \sigma_{\alpha}^{(k)} = 2\nabla_{\alpha} \nabla_{\beta} \Phi_{(k)} + \nabla_{\alpha}(\varepsilon_{\cdot\beta}^{\tau} \nabla_{\tau} \omega_{(k)} + \varepsilon_{\cdot\alpha}^{\tau} \nabla_{\beta} \omega_{(k)}), \\
& \nabla_{\alpha} \sigma_{(k)}^{\alpha} = \Delta \Phi_{(k)} \quad (k=1,\,3,\,\ldots,\,N).
\end{aligned}
\tag{3-6}
$$

Substituting (3.6) into (3.2), we obtain

$$\frac{2h^2}{3}\Delta\Phi_{(1)}+p=0,$$

$$\frac{(1+\nu)\left(\sigma_\varphi^{(1)}-\sigma_\psi^{(1)}\right)-\nu\,\varepsilon_{\alpha\beta}\,\sigma_\alpha^\varepsilon{}_{(1)}}{3}+\frac{Eh}{3}\,\nabla_\alpha\nabla_\beta w-\frac{E}{G}\cdot\frac{2h^2}{15}\,\nabla_\alpha\nabla_\beta\Phi_{(1)}+$$
$$+\frac{E}{G}\cdot\frac{h^2}{105}\,\nabla_\alpha\nabla_\beta\Phi_{(3)}-\frac{E}{E_z}\cdot\frac{\nu_z h^2}{105}\,\varepsilon_{\alpha\beta}\,\Delta\Phi_{(3)}=\frac{\nu_z}{3}\cdot\frac{E}{E_z}\,\varepsilon_{\alpha\beta}\,p,$$

$$\frac{E}{E_z}\cdot\frac{h^4\,\nabla_\alpha\nabla_\beta\Delta\Phi_{(k-4)}}{(2k-7)(2k-5)(2k-3)(2k-1)(2k+1)}-$$
$$-\frac{E}{E_z}\cdot\frac{4h^4\,\nabla_\alpha\nabla_\beta\Delta\Phi_{(k-2)}}{(2k-5)(2k-3)(2k-1)(2k+1)(2k+3)}-$$
$$-\frac{E}{E_z}\cdot\frac{h^2\,\nu_z\left(\nabla_\alpha\nabla_\beta\sigma_\alpha^\varepsilon{}_{(k-2)}+\varepsilon_{\alpha\beta}\,\Delta\Phi_{(k-2)}\right)}{(2k-3)(2k-1)(2k+1)}+\frac{E}{G}\cdot\frac{h^2\,\nabla_\alpha\nabla_\beta\Phi_{(k-2)}}{(2k-3)(2k-1)(2k+1)}+$$
$$+\frac{(1+\nu)\left(\sigma_\varphi^{(k)}-\sigma_\psi^{(k)}\right)-\nu\,\varepsilon_{\alpha\beta}\,\sigma_\alpha^\varepsilon{}_{(k)}}{2k+1}+\frac{E}{E_z}\cdot\frac{2\nu_z h^2\left(\nabla_\alpha\nabla_\beta\sigma_\alpha^\varepsilon{}_{(k)}+\varepsilon_{\alpha\beta}\,\Delta\Phi_{(k)}\right)}{(2k-1)(2k+1)(2k+3)}-$$
$$-\frac{E}{G}\cdot\frac{2h^2\,\nabla_\alpha\nabla_\beta\Phi_{(k)}}{(2k-1)(2k+1)(2k+3)}+$$
$$+\frac{E}{E_z}\cdot\frac{6h^4\,\nabla_\alpha\nabla_\beta\Delta\Phi_{(k)}}{(2k-3)(2k-1)(2k+1)(2k+3)(2k+5)}+$$
$$+\frac{E}{G}\cdot\frac{h^2\,\nabla_\alpha\nabla_\beta\Phi_{(k+2)}}{(2k+1)(2k+3)(2k+5)}-\frac{E}{E_z}\cdot\frac{h^2\,\nu_z\left(\nabla_\alpha\nabla_\beta\sigma_\alpha^\varepsilon{}_{(k+2)}+\varepsilon_{\alpha\beta}\,\Delta\Phi_{(k+2)}\right)}{(2k+1)(2k+3)(2k+5)}-$$
$$-\frac{E}{E_z}\cdot\frac{4h^4\,\nabla_\alpha\nabla_\beta\Delta\Phi_{(k+2)}}{(2k-1)(2k+1)(2k+3)(2k+5)(2k+7)}+$$
$$+\frac{E}{E_z}\cdot\frac{h^4\,\nabla_\alpha\nabla_\beta\Delta\Phi_{(k+4)}}{(2k+1)(2k+3)(2k+5)(2k+7)(2k+9)}=$$
$$=-\frac{E}{E_z}\cdot\frac{p_z}{2k+1}\,\varepsilon_{\alpha\beta}\,p_{(k)}-\frac{E}{E_z}\cdot\frac{h^2\,\nabla_\alpha\nabla_\beta\,p_{(k)}}{(2k-3)(2k-1)(2k+1)}\quad(k=3,5,\ldots,N),$$

<div></div>(3.7)

where $\tau_{\alpha\beta}^{(k)}$ denotes the symmetric tensor

$$\frac{\tau_{\alpha\beta}^{(k)}}{2k+1}=-\frac{Eh^3}{2(1+\nu)G}\cdot\frac{\nabla_\alpha\left(\sigma_\beta^\varepsilon\nabla_\alpha\omega_{(k-2)}+\sigma_{\alpha}^\varepsilon\nabla_\beta\omega_{(k-2)}\right)}{(2k-3)(2k-1)(2k+1)}+$$
$$+\frac{Eh^3}{(1+\nu)G}\cdot\frac{\nabla_\alpha\left(\sigma_\beta^\varepsilon\nabla_\alpha\omega_{(k)}+\sigma_\alpha^\varepsilon\nabla_\beta\omega_{(k)}\right)}{(2k-1)(2k+1)(2k+3)}-$$
$$-\frac{Eh^3}{2(1+\nu)G}\cdot\frac{\nabla_\alpha\left(\sigma_\beta^\varepsilon\nabla_\alpha\omega_{(k+2)}+\sigma_\alpha^\varepsilon\nabla_\beta\omega_{(k+2)}\right)}{(2k+1)(2k+3)(2k+5)}\quad(k=1,3,\ldots,N).$$

<div></div>(3.8)

We require that the tensor $\tau_{\alpha\beta}^{(k)}$ satisfy the equation

$$\nabla_\beta\,\tau_{\alpha\beta}^{(k)}=\tau_\alpha^\varepsilon{}_{(k)}=s^{2k}\nabla_\beta\,\omega_{(k)}\quad(k=1,3,\ldots,N).$$

<div></div>(3.9)

Then in accordance with (3.8)

$$\frac{h^2\,E\,\sigma_{\alpha}^\beta\nabla_\beta\Delta\omega_{(k-2)}}{2(1+\nu)G(2k-3)(2k-1)(2k+1)}+\frac{\sigma_\alpha^\varepsilon\nabla_\beta\omega_{(k)}}{2k+1}-$$
$$-\frac{h^2\,E\,\sigma_{\alpha}^\beta\nabla_\beta\Delta\omega_{(k)}}{(1+\nu)G(2k-1)(2k+1)(2k+3)}+$$
$$+\frac{h^2\,E\,\sigma_{\alpha}^\beta\nabla_\beta\Delta\omega_{(k+2)}}{2(1+\nu)G(2k+1)(2k+3)(2k+5)}=0.$$

We convolve the left side of this equality with respect to α with the tensor $\varepsilon_{\pi}^{\cdot\alpha}$. Considering that

$$\varepsilon_{\alpha}^{\cdot\nu}\partial_{\nu}^{\cdot}\nabla_{\beta} = g_{\alpha}^{\beta}\nabla_{\beta} = \nabla_{\alpha}$$

we integrate the resulting equalities and drop the nonessential abritrary constant. We obtain the following equations for determining the functions $\omega_{(k)}$

$$\frac{EN^2\Delta\omega_{(k-2)}}{3(1+\nu)G(2k-3)(2k-1)(2k+1)} + \frac{\omega_{(k)}}{2k+1} -$$
$$- \frac{EN^2\Delta\omega_{(k)}}{(1+\nu)G(2k-1)(2k+1)(2k+3)} +$$
$$+ \frac{EN^2\Delta\omega_{(k+2)}}{2(1+\nu)G(2k+1)(2k+3)(2k+5)} = 0 \quad (k = 1, 3, ..., N). \qquad (3\cdot10)$$

We further take

$$\sigma_{\alpha\beta}^{(k)} - \tau_{\alpha\beta}^{(k)} = t_{\alpha\beta}^{(k)} \quad (k = 1, 3, ..., N). \qquad (3.11)$$

Thus, from (3.3), (3.4) we have

$$\nabla_{\beta} t_{(k)}^{\alpha\beta} = \sigma_{(k)}^{\alpha} - \tau_{(k)}^{\alpha} = f_{(k)}^{\alpha}, \quad f_{\alpha}^{(k)} = \nabla_{\alpha}\Phi_{(k)}. \qquad (3.12)$$

Moreover, by virtue of (3.8)

$$t_{(k)}^{\alpha} = f_{(k)}^{\alpha}. \qquad (3\cdot13)$$

It follows from (3.11) and (3.13) that (3.7) may be considered as the equations which determine the tensors $t_{\alpha\beta}^{(k)}$.

Thus we have a representation of the tensor $\sigma_{\alpha\beta}^{(k)}$ as the sum of two independent tensors $\tau_{\alpha\beta}^{(k)}$ and $t_{\alpha\beta}^{(k)}$. The former is defined by (3.8), in which the scalar functions $\omega_{(k)}$ must satisfy (3.10), and is characterized by the fact that $\tau_{\alpha(k)}^{\alpha} = 0$ and the vector $\nabla_{\beta}\tau_{(k)}^{\alpha\beta}$ are solenoidal. The second tensor $t_{\alpha\beta}^{(k)}$ is characterized only by the property that its divergence $\nabla_{\beta}t_{(k)}^{\alpha\beta}$ is a potential vector.

We shall designate the stress states corresponding to the tensors $\tau_{\alpha\beta}^{(k)}$ and $t_{\alpha\beta}^{(k)}$ as "rotational" and "potential" [2].

We express the "moments" $t_{\alpha\beta}^{(k)}$ of the "potential" stress state in terms of the stress functions $\Phi_{(k)}$ and the deflection function w, and we derive the differential equations for determining these functions. For simplicity, we set $p = 0$ and denote (3·7) briefly as

$$\Delta\Phi_{(1)}=0, \quad L_{\alpha\beta}^{(k)}=0 \quad (k=1, 3, \ldots, N) \tag{3.14}$$

($L_{\alpha\beta}^{(k)}$ is a symmetric tensor).

We form the equalities $\nabla_\beta L_{\alpha(k)}^{\beta} = 0$ and integrate them, discarding the nonessential arbitrary constant. We obtain the equations

$$
\frac{1+v}{3}\Phi_{(1)} - \frac{v}{3}\sigma_{a(1)}^{c} + \frac{Eh}{3}\Delta w + \frac{h^2 E}{105}\left(\frac{1}{G} - \frac{v_z}{E_z}\right)\Delta\Phi_{(3)} = 0,
$$

$$
\frac{E}{E_z} \cdot \frac{h^4\Delta\Delta\Phi_{(k-4)}}{(2k-7)(2k-5)(2k-3)(2k-1)(2k+1)} -
$$
$$
-\frac{E}{E_z} \cdot \frac{4h^4\Delta\Delta\Phi_{(k-2)}}{(2k-5)(2k-3)(2k-1)(2k+1)(2k+3)} -
$$
$$
-\frac{E}{E_z} \cdot \frac{h^2 v_z(\Delta\sigma_{a(k-2)}^{c}+\Delta\Phi_{(k-2)})}{(2k-3)(2k-1)(2k+1)} + \frac{E}{G} \cdot \frac{h^2\Delta\Phi_{(k-2)}}{(2k-3)(2k-1)(2k+1)} +
$$
$$
+ \frac{1+v}{2k+1}\Phi_{(k)} - \frac{v}{2k+1}\sigma_{a(k)}^{c} +
$$
$$
+ \frac{E}{E_z} \cdot \frac{2v_z h^2(\Delta\sigma_{a(k)}^{c}+\Delta\Phi_{(k)})}{(2k-1)(2k+1)(2k+3)} - \frac{E}{G} \cdot \frac{2h^2\Delta\Phi_{(k)}}{(2k-1)(2k+1)(2k+3)} +
$$
$$
+ \frac{E}{E_z} \cdot \frac{6h^4\Delta\Delta\Phi_{(k)}}{(2k-3)(2k-1)(2k+1)(2k+3)(2k+5)} +
$$
$$
+ \frac{E}{G} \cdot \frac{h^2\Delta\Phi_{(k+2)}}{(2k+1)(2k+3)(2k+5)} - \frac{E}{E_z} \cdot \frac{h^2 v_z(\Delta\sigma_{a(k+2)}^{c}+\Delta\Phi_{(k+2)})}{(2k+1)(2k+3)(2k+5)} -
$$
$$
- \frac{E}{E_z} \cdot \frac{4h^4\Delta\Delta\Phi_{(k+2)}}{(2k-1)(2k+1)(2k+3)(2k+5)(2k+7)} +
$$
$$
+ \frac{E}{E_z} \cdot \frac{h^4\Delta\Delta\Phi_{(k+4)}}{(2k+1)(2k+3)(2k+5)(2k+7)(2k+9)} = 0 \tag{3.15}
$$
$$
(k=3, 5, \ldots, N).
$$

Subtracting from these equations the equalities $L_{\alpha(k)}^{\alpha} = 0$ we obtain

$$
\frac{E}{E_z} \cdot \frac{v_z h^2\Delta\Phi_{(k-2)}}{(2k-3)(2k-1)(2k+1)} + \frac{1+v}{2k+1}\Phi_{(k)} - \frac{\sigma_{a(k)}^{c}}{2k+1} -
$$
$$
-\frac{E}{E_z} \cdot \frac{2v_z h^2\Delta\Phi_{(k)}}{(2k-1)(2k+1)(2k+3)} + \frac{E}{E_z} \cdot \frac{h^2 v_z\Delta\Phi_{(k+2)}}{(2k+1)(2k+3)(2k+5)} = 0
$$
$$
(k=1, 3, \ldots, N). \tag{3.16}
$$

Excluding $t_{\alpha(k)}^{\alpha} = \sigma_{\alpha(k)}^{\alpha}$ from (3.15) with the aid of these relations, we obtain the following system of equations for finding the functions w, $\Phi_{(k)}$

$$Eh\,\Delta w+(1-\nu^2)\Phi_{(1)}+\frac{h^2E}{35}\left(\frac{1}{G}-\frac{\nu_z(1+\nu)}{E_z}\right)\Delta\Phi_{(3)}=0;\qquad(3.17_1)$$

$$\frac{E}{E_z}\left(1-\frac{E}{E_z}\nu_z^2\right)\frac{h^4\,\Delta\Delta\Phi_{(k-4)}}{(2k-7)(2k-5)(2k-3)(2k-1)(2k+1)}-$$

$$-\frac{E}{E_z}\left(1-\frac{E}{E_z}\nu_z^2\right)\frac{4h^4\,\Delta\Delta\Phi_{(k-2)}}{(2k-5)(2k-3)(2k-1)(2k+1)(2k+3)}+$$

$$+\left(\frac{E}{G}-2\nu_z(1+\nu)\frac{E}{E_z}\right)\frac{h^2\,\Delta\Phi_{(k-2)}}{(2k-3)(2k-1)(2k+1)}+\frac{1-\nu^2}{2k+1}\Phi_{(k)}-$$

$$-\left(\frac{E}{G}-2\nu_z(1+\nu)\frac{E}{E_z}\right)\frac{2h^2\,\Delta\Phi_{(k)}}{(2k-1)(2k+1)(2k+3)}+$$

$$+\frac{E}{E_z}\left(1-\frac{E}{E_z}\nu_z^2\right)\frac{6h^4\,\Delta\Delta\Phi_{(k)}}{(2k-3)(2k-1)(2k+1)(2k+3)(2k+5)}+$$

$$+\left(\frac{E}{G}-2\nu_z(1+\nu)\frac{E}{E_z}\right)\frac{h^2\,\Delta\Phi_{(k+2)}}{(2k+1)(2k+3)(2k+5)}-$$

$$-\frac{E}{E_z}\left(1-\frac{E}{E_z}\nu_z^2\right)\frac{4h^4\,\Delta\Delta\Phi_{(k+2)}}{(2k-1)(2k+1)(2k+3)(2k+5)(2k+7)}+$$

$$+\frac{E}{E_z}\left(1-\frac{E}{E_z}\nu_z^2\right)\frac{h^4\,\Delta\Delta\Phi_{(k+4)}}{(2k+1)(2k+3)(2k+5)(2k+7)(2k+9)}=0$$

$$(k=3,\ 5,\ \ldots,\ N-2);\qquad(3.17_2)$$

For k = N, the following term is added to the left side of (3.17$_2$)

$$\left(\frac{E}{E_z}\nu_z\right)^2\frac{h^4\,\Delta\Delta\Phi_{(N)}}{(2N+1)^2(2N+3)^2(2N+5)}.$$

To obtain the formulas expressing the moments $t_{\alpha\beta}^{(k)}$ in terms of the scalar functions w and $\Phi_{(k)}$, we must exclude $t_{\alpha(k)}^{\alpha}$ from (3.7) with the aid of (3.16). We obtain the formulas

$$(1+\nu)t_{\alpha\beta}^{(1)}=-Eh\,\nabla_\alpha\nabla_\beta w+\nu(1+\nu)g_{\alpha\beta}\Phi_{(1)}+\frac{E}{G}\cdot\frac{2h^2}{5}\nabla_\alpha\nabla_\beta\Phi_{(1)}-$$

$$-\frac{E}{G}\cdot\frac{h^2}{35}\nabla_\alpha\nabla_\beta\Phi_{(3)}+\frac{E}{E_z}\cdot\frac{\nu_z(1+\nu)h^2}{35}g_{\alpha\beta}\Delta\Phi_{(3)},\qquad(3.18_1)$$

$$\frac{1+\nu}{2k+1}t_{\alpha\beta}^{(k)}=\frac{E}{E_z}\left(1-\frac{E}{E_z}\nu_z^2\right)\frac{h^4\,\nabla_\alpha\nabla_\beta\Delta\Phi_{(k-4)}}{(2k-7)(2k-5)(2k-3)(2k-1)(2k+1)}-$$

$$-\frac{E}{E_z}\left(1-\frac{E}{E_z}\nu_z^2\right)\frac{4h^4\,\nabla_\alpha\nabla_\beta\Delta\Phi_{(k-2)}}{(2k-5)(2k-3)(2k-1)(2k+1)(2k+3)}+$$

$$+\left(\frac{E}{G}-2\nu_z(1+\nu)\frac{E}{E_z}\right)\frac{h^2\,\nabla_\alpha\nabla_\beta\Phi_{(k-2)}}{(2k-3)(2k-1)(2k+1)}-$$

$$-\frac{E}{E_z}\nu_z(1+\nu)\frac{h^2\,g_{\alpha\beta}^{z}g_{\alpha\beta}\nabla_\alpha\nabla_\beta\Phi_{(k-2)}}{(2k-3)(2k-1)(2k+1)}-\frac{\nu(1+\nu)}{2k+1}g_{\alpha\beta}\Phi_{(k)}-$$

$$-\left(\frac{E}{G}-2\nu_z(1+\nu)\frac{E}{E_z}\right)\frac{2h^2\,\nabla_\alpha\nabla_\beta\Phi_{(k)}}{(2k-1)(2k+1)(2k+3)}+\qquad(3.18_2)$$

(Continued on following page)

15

(Continued from preceding page)

$$
\begin{aligned}
&+ \frac{E}{E_z}\nu_z(1+\nu)\frac{2h^2 c_{sa}^z c_{sa}^\prime \nabla_\alpha \nabla_\beta \Phi_{(k)}}{(2k-1)(2k+1)(2k+3)} + \\
&+ \frac{E}{E_z}\left(1-\frac{E}{E_z}\nu_z^2\right)\frac{6h^4 \nabla_\alpha \nabla_\beta \Delta\Phi_{(k)}}{(2k-3)(2k-1)(2k+1)(2k+3)(2k+5)} - \\
&+ \left(\frac{E}{G}-2\nu_z(1+\nu)\frac{E}{E_z}\right)\frac{h^2 \nabla_\alpha \nabla_\beta \Phi_{(k+2)}}{(2k+1)(2k+3)(2k+5)} - \\
&- \frac{E}{E_z}\nu_z(1+\nu)\frac{h^2 c_{sa}^z c_{sa}^\prime \nabla_\alpha \nabla_\beta \Phi_{(k+2)}}{(2k+1)(2k+3)(2k+5)} - \\
&- \frac{E}{E_z}\left(1-\frac{E}{E_z}\nu_z^2\right)\frac{4h^4 \nabla_\alpha \nabla_\beta \Delta\Phi_{(k+2)}}{(2k-1)(2k+1)(2k+3)(2k+5)(2k+7)} + \\
&+ \frac{E}{E_z}\left(1-\frac{E}{E_z}\nu_z^2\right)\frac{h^4 \nabla_\alpha \nabla_\beta \Delta\Phi_{(k+4)}}{(2k+1)(2k+3)(2k+5)(2k+7)(2k+9)} \\
&\hspace{6cm}(k=3,\ 5,\ \ldots,\ N-2);
\end{aligned}
\tag{3.18_2}
$$

For k = N, the following term is added to the left side of (3.18_2)

$$
\left(\frac{E}{E_z}\nu_z\right)^2 \frac{h^4 \nabla_\alpha \nabla_\beta \Phi_{(N)}}{(2N+1)^2(2N+3)^2(2N+5)}.
$$

Reissner's plate theory equations [7, 8] are obtained from the relations obtained in this section for N = 1. Therefore, the present theory may be considered to be a generalization of Reissner's theory.

The plate bending theory equations, which are obtained from the relations above for N = 3, include all the correction terms for classical theory which were obtained in [9, 10] and also include some others which permit the establishment of more general boundary conditions than those of [9, 10].

§ 4. Asymptotic Integration of the Bending
Equations for Transversely Isotropic
Plates

1. We can use the method of asymptotic integration of differential equations with a small parameter in the derivatives [3, 4] to solve the problem of transversely isotropic plate bending.

We take as the small parameter the plate half-thickness h, considering it a small quantity in comparison with the characteristic linear dimension a of the plate median plane.

Hereafter, it is assumed everywhere that the problem parameters and the desired solution are sufficiently smooth point functions of the plate median plane.

The integrals of (3.2) which are not rapidly varying (regular part of the asymptotic solution) are sought with the aid of the usual small parameter method. Namely, setting

$$\sigma_{\alpha\beta}^{(s)} = h^{-2}\left(\overset{(0)}{\sigma_{\alpha\beta}^{(s)}} + h\overset{(1)}{\sigma_{\alpha\beta}^{(s)}} + \ldots\right),$$
$$w = h^{-3}\left(\overset{(0)}{w} + h\overset{(1)}{w} + \ldots\right) \tag{4.1}$$

and substituting (4.1) into (3.2), we require that the coefficients of like powers of h be the same in the left and right sides. Then we obtain for determining $\overset{(s)}{\sigma_{\alpha\beta}}{(k)}$, $\overset{(s)}{w}$ a recursive sequence of sets of equations, each of which is equivalent to a single biharmonic equation for the function $\overset{(s)}{w}$.

The equations for the first three approximations follow:

$$\left. \begin{array}{l} \overset{(0)}{\sigma_{\alpha\beta}^{(k)}} = 0 \quad (k>1), \\[4pt] \nabla_\alpha \nabla_\beta \overset{(0)}{\sigma_{(1)}} + \frac{3\nu}{2} = 0, \\[4pt] (1+\nu)\overset{(0)}{\sigma_{\alpha\beta}^{(1)}} - \nu g_{\alpha\beta}\overset{(0)}{\sigma_{\varepsilon(1)}^{\varepsilon}} + E\nabla_\alpha \nabla_\beta \overset{(0)}{w} = 0; \end{array} \right\} \tag{4.2$_0$}$$

$$\left. \begin{array}{l} \overset{(1)}{\sigma_{\alpha\beta}^{(k)}} = 0 \quad (k>1), \\[4pt] \nabla_\alpha \nabla_\beta \overset{(1)}{\sigma_{(1)}} = 0, \\[4pt] (1+\nu)\overset{(1)}{\sigma_{\alpha\beta}^{(1)}} - \nu g_{\alpha\beta}\overset{(1)}{\sigma_{\varepsilon(1)}^{\varepsilon}} + E\nabla_\alpha \nabla_\beta \overset{(1)}{w} = 0; \end{array} \right\} \tag{4.2$_1$}$$

where $\qquad\qquad\qquad\qquad \overset{(s)}{\sigma_{\alpha\beta}} = \nabla_\beta \overset{(s)}{\sigma_{\alpha\beta}}.$

$$
\begin{aligned}
&\overset{(2)}{\sigma_{\alpha\beta}^{(k)}}=0 \quad (k>3), \\
&(1+\nu)\overset{(2)}{\sigma_{\alpha\beta}^{(3)}}-\nu g_{\alpha\beta}\overset{(2)}{\sigma_{\tau(3)}}=\frac{E}{E_s}\cdot\frac{\nu}{15}\nabla_\alpha\nabla_\beta\overset{(0)}{\sigma_{\tau(1)}}- \\
&\qquad -\frac{E}{G}\cdot\frac{1}{30}\left(\nabla_\alpha\overset{(0)}{\sigma_\beta^{(1)}}+\nabla_\beta\overset{(0)}{\sigma_\alpha^{(1)}}\right), \\
&\nabla_\alpha\nabla_\beta\overset{(2)}{\sigma_{(1)}}=0, \\
&(1+\nu)\overset{(2)}{\sigma_{\alpha\beta}^{(2)}}-\nu g_{\alpha\beta}\overset{(2)}{\sigma_{(1)}}+E\nabla_\alpha\nabla_\beta\overset{(2)}{w}= \\
&\qquad -\frac{E}{5G}\left(\nabla_\alpha\overset{(0)}{\sigma_\beta^{(1)}}+\nabla_\beta\overset{(0)}{\sigma_\alpha^{(1)}}\right)+\frac{3\nu_s}{5}\cdot\frac{E}{E_s}g_{\alpha\beta}P,
\end{aligned}
\qquad (4.2_2)
$$

2. The integrals (4.1), (4.2) can be subjected to only two
boundary conditions at the edge of the plate. In order to obtain a
sufficiently broad class of solutions which permit satisfying all
the boundary conditions at the plate edge, we must introduce into
consideration integrals of the homogeneous equation (3.2) of the boun-
dary layer type [3]. These integrals, differing markedly from zero
only near the boundary Γ of the plate median plane, disappear rapidly
with increasing distance from the boundary into the depth of the
region. For their construction we use a small parameter method which
is based on a different expansion of the differential operators in
powers of the small parameter h than that used in § 3; this decomposi-
tion holds only in a small vicinity of the boundary Γ [3].

In order to obtain this decomposition, we introduce in the vicinity
of the boundary Γ of the region occupied by the plate median plane, a
local orthogonal coordinate system $x^1 = r$, $x^2 = s$. Here r is the
distance measured from points of the curve Γ along the inward normal,
and s is the arc length of the contour Γ, whose direction is taken
opposite that of the unit tangent vector s_α (see (2.6), (2.8), (2.9)).

We denote by $R = R(s)$ the radius of curvature of the curve Γ
and consider it positive at points of convexity and negative at points
of concavity of the region occupied by the plate median plane.

We write out the expressions for the components of the metric and discriminant tensors and the second-order Christoffel symbols $\Gamma^{\gamma}_{\alpha\beta}$ in the local coordinate system which we have introduced

$$g_{11} = 1, \quad g_{12} = 0, \quad g_{22} = \left(1 - \frac{r}{R}\right)^2.$$

$$e_{12} = 0, \quad e_{22} = 1 - \frac{r}{R},$$

$$\Gamma^1_{22} = -\frac{r}{1 - \frac{r}{R}} \cdot \frac{d}{ds}\left(\frac{1}{R}\right), \quad \Gamma^1_{22} = \frac{1}{R}\left(1 - \frac{r}{R}\right), \qquad (4.3)$$

$$\Gamma^2_{22} = -\frac{1}{R\left(1 - \frac{r}{R}\right)}, \quad \Gamma^2_{11} = \Gamma^2_{11} = \Gamma^1_{12} = 0.$$

Using (4.3), we obtain the following expressions for the differential operations $\nabla_{\alpha}\nabla_{\beta}$

$$\nabla_1\nabla_1 = \frac{\partial^2}{\partial r^2}, \quad \nabla_1\nabla_2 = \frac{\partial^2}{\partial r \partial s} + \frac{1}{R\left(1 - \frac{r}{R}\right)} \cdot \frac{\partial}{\partial s},$$

$$\nabla_2\nabla_2 = -\frac{1}{R}\left(1 - \frac{r}{R}\right)\frac{\partial}{\partial r} + \frac{\partial^2}{\partial s^2} + \frac{r}{1 - \frac{r}{R}} \cdot \frac{d}{ds}\left(\frac{1}{R}\right)\frac{\partial}{\partial s} \qquad (4.4)$$

and the expression for the Laplace operator

$$\Delta = \frac{\partial^2}{\partial r^2} - \frac{1}{R\left(1 - \frac{r}{R}\right)}\frac{\partial}{\partial r} + \frac{1}{1 - \frac{r}{R}} \cdot \frac{\partial}{\partial s}\left(\frac{1}{1 - \frac{r}{R}} \cdot \frac{\partial}{\partial s}\right). \qquad (4.5)$$

The coefficients in (4.4), (4.5) may be expanded in the vicinity of the boundary into series in powers of r. Performing this operation and changing the independent variable r by means of the formula

$$r = ht, \qquad (4.6)$$

we obtain the following decompositions for the differential operations (4.4), (4.5) in powers of h:

$$h^2\nabla_1\nabla_1 = \frac{\partial^2}{\partial t^2}, \qquad (4.7)$$

$$h^3\nabla_1\nabla_2 = h\frac{\partial^2}{\partial t \partial s} + \frac{h^2}{R} \cdot \frac{\partial}{\partial s} + \dots,$$

$$h^2\nabla_2\nabla_2 = -\frac{h}{R} \cdot \frac{\partial}{\partial t} + h^2\frac{\partial^2}{\partial s^2} + \dots,$$

$$h^2\Delta = \frac{\partial^2}{\partial t^2} - \frac{h}{R} \cdot \frac{\partial}{\partial t} + h^2\left(\frac{\partial^2}{\partial s^2} - \frac{t}{R^2} \cdot \frac{\partial}{\partial t}\right) + \dots$$

Using the last formula (4.7) we can obtain the decomposition of the biharmonic operator in powers of h

$$h^4 \Delta\Delta = \frac{\partial^4}{\partial t^4} - \frac{2h}{R} \cdot \frac{\partial^3}{\partial t^3} + \cdots \tag{4.8}$$

3. We construct the boundary layer type integrals by starting from the equations which the functions $\omega_{(k)}$ and $\phi_{(k)}$ must satisfy. We first turn to the equations (3.10) for determining the functions $\omega_{(k)}$ and construct the rotational boundary layer.

Let $D = \| d_{ik} \|$ be a diagonal matrix and $A = \| a_{ik} \|$ a symmetric codiagonal matrix

$$d_{ii} = \frac{1}{4i-1}, \quad d_{ik} = 0, \quad i \neq k, \quad i, k = 1, 2, 3, \cdots, \frac{N+1}{2} = M,$$
$$a_{ii} = \frac{2}{(4i-3)(4i-1)(4i+1)}, \quad a_{ii+1} = -\frac{1}{(4i-1)(4i+1)(4i+3)}, \tag{4.9}$$
$$a_{ii+k} = 0, \quad k > 1.$$

Then (3.10) may be written as

$$\left(D - \frac{Eh\Delta}{2(1+\nu)G} A\right)\omega = 0, \tag{4.10}$$

where ω denotes the vector

$$\omega = (\omega_{(1)}, \omega_{(3)}, \cdots, \omega_{(N)}). \tag{4.11}$$

If in (4.10) we expand the Laplace operator in powers of h in accordance with (4.7) and use the small parameter method, setting

$$\omega = h^a \left(\overset{(0)}{\omega} + h \overset{(1)}{\omega} + h^2 \overset{(2)}{\omega} + \cdots\right) \tag{4.12}$$

(a — is an as-yet-undefined integer) we obtain a recursive system of ordinary linear differential equations with constant coefficients. It is required of the solutions of these equations that they have the boundary layer nature, i.e., they approach zero together with their derivatives as $t \to +\infty$. Therefore, to construct these solutions, we use the fundamental solutions of the homogeneous equations, which correspond to negative roots of the characteristic equation, and the particular solutions (of the boundary layer type) of the inhomogeneous

equations, which can be constructed by the method of undetermined coefficients [3].

Thus, in the s-th approximation (s = 0, 1, 2, ...) we obtain

$$\overset{(s)}{\omega} = \sum_{i=1}^{M} \left[\overset{(s)}{\Omega_i} + \overset{(s)}{C_i}(t) \right] \exp\left(- \sqrt{\frac{2(1+\nu)G}{E}} \lambda_i t \right), \tag{4.13}$$

where

$$\overset{(0)}{C_i} = 0,$$

$$\lambda_1 < \lambda_2 < \ldots < \lambda_M \tag{4.14}$$

are positive roots of the equation

$$|D - \lambda^2 A| = 0; \tag{4.15}$$

$\overset{(s)}{\Omega_1}$ is a nonzero vector satisfying the equation

$$(D - \lambda_i^2 A) \overset{(s)}{\Omega_i} = 0; \tag{4.16}$$

and, finally, $\overset{(s)}{C_1}(t)$ is a vector whose components are polynomials in t of order no higher than s.

After finding ω, we can use (3.8), (3.9) to obtain the expansions of $h\,\tau\overset{(k)}{_{\alpha\beta}}$ and $\tau\overset{(k)}{_{\alpha}}$ in powers of h. After some transformations using (4.16), we have (only the first terms of these expansions are written out below)

$$\tau_{11} = (\tau_{11}^{(1)},\ \tau_{11}^{(2)},\ \ldots,\ \tau_{11}^{(N)}) =$$
$$= 2h^{1+a}\sqrt{\frac{E}{2(1+\nu)G}} \sum_{i=1}^{M} \frac{1}{\lambda_i} \cdot \frac{d\overset{(0)}{\Omega_i}}{ds} \exp\left(- \sqrt{\frac{2(1+\nu)G}{E}} \lambda_i t \right) + \ldots$$

$$\tau_{12} = (\tau_{12}^{(1)},\ \tau_{12}^{(2)},\ \ldots,\ \tau_{12}^{(N)}) =$$
$$= h^a \sum_{i=1}^{M} \overset{(0)}{\Omega_i} \exp\left(- \sqrt{\frac{2(1+\nu)G}{E}} \lambda_i t \right) + \ldots,$$

$$\tau_{22} = (\tau_{22}^{(1)},\ \tau_{22}^{(2)},\ \ldots,\ \tau_{22}^{(N)}) =$$
$$- 2h^{1+a}\sqrt{\frac{E}{2(1+\nu)G}} \sum_{i=1}^{M} \frac{1}{\lambda_i} \cdot \frac{d\overset{(0)}{\Omega_i}}{ds} \exp\left(- \sqrt{\frac{2(1+\nu)G}{E}} \lambda_i t \right) + \tag{4.17}$$

$$\tau_1 = (\tau_1^{(1)},\ \tau_1^{(2)},\ \ldots,\ \tau_1^{(N)}) =$$
$$= - h^a \sum_{i=1}^{M} \frac{d\overset{(0)}{\Omega_i}}{ds} \exp\left(- \sqrt{\frac{2(1+\nu)G}{E}} \lambda_i t \right) + \ldots$$

$$\tau_2 = (\tau_2^{(1)},\ \tau_2^{(2)},\ \ldots,\ \tau_2^{(N)}) =$$
$$= - h^{a-1} \sqrt{\frac{2(1+\nu)G}{E}} \sum_{i=1}^{M} \overset{(0)}{\Omega_i} \lambda_i \exp\left(- \sqrt{\frac{2(1+\nu)G}{E}} \lambda_i t \right) + \ldots$$

4. Turning to the construction of the boundary layer type
integrals of the potential stress state, we note that $\Delta u = 0$ implies
$u = 0$, since this equation does not contain the small parameter h
and its boundary layer is equal to zero. Therefore, from (3.14) and
(3.17_1) we have for the boundary layers $\phi_{(1)}$ and w

$$\Phi_{(1)}=0, \quad w=\tfrac{h}{35}\left(\tfrac{v_z(1+v)}{E_z}-\tfrac{1}{G}\right)\Phi_{(3)}, \tag{4.18}$$

where $\phi_{(3)}$ is a boundary layer type function which will be defined
later. From (4.18) and (3.18_1) we have

$$t_s^{(1)}=0, \quad t_{s3}^{(1)}=\tfrac{E}{E_s}\cdot\tfrac{v_z h^3}{35}e^r_s e^s_3\nabla_s\nabla_t\Phi_{(3)}. \tag{4.19}$$

Now we turn to (3.17_2) and using matrix symbolization rewrite
it in the form of the single equation

$$\left[(1-v^2)ID-\left(\tfrac{E}{G}-2v_z(1+v)\tfrac{E}{E_s}\right)h^2\Delta IA+\right.$$
$$\left.+\tfrac{E}{E_s}\left(1-\tfrac{E}{E_s}v_z^2\right)h^4\Delta\Delta B\right]\Phi=0, \tag{4.20}$$

where

$$\Phi=(\Phi_{(3)},\ \Phi_{(5)},\ \ldots,\ \Phi_{(N)}): \tag{4.21}$$

A and D are the matrices (4.9) introduced previously; I is a diagonal
matrix of M-th order, all elements of which on the principal diagonal
equal unity except for the first, which equals zero; $B = \| b_{1k} \|$
is a symmetric matrix of (M - 1)st order whose elements are the numbers

$$b_{ii}=\tfrac{6}{(4i-5)(4i-3)(4i-1)(4i+1)(4i+3)} \quad (i=2,\ 3,\ \ldots,\ M-1).$$
$$b_{MM}=\tfrac{6}{(2N-3)(2N-1)(2N+1)(2N+3)(2N+5)}+$$
$$+\tfrac{E}{E_s}v_z^2\left(1-\tfrac{E}{E_s}v_z^2\right)^{-1}\tfrac{1}{(2N+1)^2(2N+3)^2(2N+5)}. \tag{4.22}$$
$$b_{i i+1}=-\tfrac{4}{(4i-3)(4i-1)(4i+1)(4i+3)(4i+5)},$$
$$b_{i i+2}=\tfrac{1}{(4i-1)(4i+1)(4i+3)(4i+5)(4i+7)}, \tag{4.22}$$
$$b_{i i+k}=0,\ k>2 \quad (i=2,\ 3,\ \ldots,\ M).$$

The boundary layer type integral of (4.20) is constructed just as the integral of (4.10) was constructed above. With the aid of the expansions (4.7), (4.8), the operator in the left side of (4.20) is expanded in powers of h, after which the following series

$$\phi = h^b \left(\overset{(0)}{\phi} + h \overset{(1)}{\phi} + h^2 \overset{(2)}{\phi} + \ldots \right) \tag{4.23}$$

(b is an integer) is substituted into (4.20), and the coefficients of all powers of h are equated to zero. We than obtain a recursive sequence of linear ordinary differential equations with constant coefficients whose solutions of the boundary layer type have the form

$$\overset{(s)}{\phi} = \sum_{i=1}^{N-1} \left(\overset{(s)}{\varphi_i} + \overset{(s)}{D_i}(t) \right) \exp(-\mu_i t),$$
$$\overset{(0)}{D}(t) = 0, \tag{4.24}$$

where $\phi_1 \exp(-\mu_1 t)$ are the boundary layer type solutions of the homogeneous equations; $\overset{(s)}{D_1}(t) \exp(-\mu_1 t)$ are particular solutions of the boundary layer type of the corresponding inhomogeneous equations; $-\mu_1$ are the roots of the characteristic equation

$$|B^\circ(\mu)| = \left| (1-\nu^2) ID - \left(\frac{E}{U} - 2\nu_s(1+\nu)\frac{E}{E_s} \right) \mu^2 IA + \right.$$
$$\left. + \frac{E}{E_s}\left(1 - \frac{E}{E_s}\nu_s^2\right)\mu^4 B \right| = 0, \tag{4.25}$$

having negative real parts, and $\overset{(s)}{\phi_1}$ is a nonzero vector satisfying the equation

$$B^\circ(-\mu_i)\varphi_i = 0. \tag{4.26}$$

On the basis of the positive definiteness of the plate potential energy, we can show that the characteristic equation (4.25) has N - 1 roots with negative real parts.

Substituting the value found for ϕ into (4.18), (4.19) and (3.18₂), (3.4), we obtain expansions in powers of h of all the quantities characterizing the boundary layer type potential stress state (only terms with the lowest power of h are shown in the following formulas)

FTD-HC-23-361-69

23

$$w = \frac{h^{1+\delta}}{3S}\left(\frac{\nu_s(1+\nu)}{E_s} - \frac{1}{\sigma}\right)\sum_{i=1}^{N-1}\varphi_i^{(0)}\exp(-\mu_i t) + \dots$$

$$f_{11}^{(0)} = \frac{E}{E_s}\nu_s\frac{h^{1+\delta}}{3S}\cdot\frac{1}{R}\sum_{i=1}^{N-1}\varphi_i^{(0)}\exp(-\mu_i t) + \dots$$

$$f_{12}^{(0)} = \frac{E}{E_s}\nu_s\frac{h^{1+\delta}}{3S}\sum_{i=1}^{N-1}\frac{d\varphi_i^{(0)}}{ds}\mu_i\exp(-\mu_i t) + \dots$$

$$f_{22}^{(0)} = \frac{E}{E_s}\nu_s\frac{h^{\delta}}{3S}\sum_{i=1}^{N-1}\mu_i^2\varphi_i^{(0)}\exp(-\mu_i t) + \dots$$

$$f_{\cdot}^{(0)} = 0,$$

$$t_1 = (t_1^{(0)}, t_1^{(0)}, \dots, t_1^{(N)}) =$$
$$= -h^{\delta-1}\sum_{i=1}^{N-1}\mu_i\varphi_i^{(0)}\exp(-\mu_i t) + \dots$$

$$t_2 = (t_2^{(0)}, t_2^{(0)}, \dots, t_2^{(N)}) =$$
$$= h^{\delta}\sum_{i=1}^{N-1}\frac{d\varphi_i^{(0)}}{ds}\exp(-\mu_i t) + \dots$$

$$t_{11} = (t_{11}^{(0)}, t_{11}^{(0)}, \dots, t_{11}^{(N)}) =$$
$$= h^{\delta}\sum_{i=1}^{N-1}\varphi_i^{(0)}\exp(-\mu_i t) + \dots$$

$$ID t_{12} = ID(t_{12}^{(0)}, t_{12}^{(0)}, \dots, t_{12}^{(N)}) =$$
$$= -\frac{E}{E_s}\nu_s h^{\delta+1}\sum_{i=1}^{N-1}\mu_i IA\frac{d\varphi_i}{ds}\exp(-\mu_i t) -$$
$$- h^{\delta+1}(1-\nu)\sum_{i=1}^{N-1}\frac{1}{\mu_i}ID\frac{d\varphi_i}{ds}\exp(-\mu_i t) + \dots$$

$$ID t_{22} = ID(t_{22}^{(0)}, t_{22}^{(0)}, \dots, t_{22}^{(N)}) =$$
$$= h^{\delta}\left(\nu ID - \frac{E}{E_s}\nu_s\cdot\frac{\partial}{\partial t}IA\right)\sum_{i=1}^{N-1}\varphi_i^{(0)}\exp(-\mu_i t) + \dots,$$

$$(4 \cdot 27)$$

where $\overset{(0)}{\phi_1}(3)$ is the first component of the vector $\overset{(0)}{\phi_1}$.

5. The boundary layer type integrals are defined in a quite small vicinity of Γ, but by using the boundary layer decay property they may be extended into the entire plate median plane region with only small errors being introduced.

At the boundary Γ (for t = 0),the rotational boundary layer has $M = \frac{N + 1}{2}$ degrees of freedom (equal to the number of positive roots of the characteristic equation (4.15)),while the potential boundary layer has N - 1 degrees of freedom (equal to the number of roots with negative real part of the characteristic equation (4.25)). Thus,it is easy to see that the integrals of the regular part of the asymptotic solution together with the integrals of the boundary layer type will have sufficient disposable constants of integration to satisfy all the problem boundary conditions.

The disposable constants of integration are determined sequentially at each stage of all three iteration processes with the aid of the procedure for superposing boundary conditions [4]. The regular part of the asymptotic solution and the boundary layers are substituted into the problem boundary conditions and then the integers a and b (which appear in (4.12), (4.23)) are selected in a suitable fashion. After this, in each of the resulting equalities,we equate terms with the same powers of h in the left and right sides. From the relations thus obtained,we can determine sequentially the constants of integration in (4.13) and (4.24) and establish the boundary conditions for the inegrals of (4.2).

We shall consider some boundary condition cases as examples.

a) Static Boundary Conditions

Let us assume that the right sides of the static boundary conditions (2.9) may be expanded into series in powers of the small parameter h as follows

$$\sigma_{aa}^{(h)} = h^{-2}\left(\overset{(0)}{\sigma_{aa}^{(h)}} + h\overset{(1)}{\sigma_{aa}^{(h)}} + \ldots\right),$$
$$\sigma_{as}^{(h)} = h^{-2}\left(\overset{(0)}{\sigma_{as}^{(h)}} + h\overset{(1)}{\sigma_{as}^{(h)}} + \ldots\right),$$
$$\sigma_{a}^{(h)} = h^{-2}\left(\overset{(0)}{\sigma_{a}^{(h)}} + h\overset{(1)}{\sigma_{a}^{(h)}} + \ldots\right) \quad (k = 1, 3, \ldots, N).$$

(4.28)

The corresponding expansions of the boundary forces and moments (as we see from (1.10), (1.8)) begin with the zero power of h.

Substituting (4.28) into the right sides of (2.9) and expressing the left sides in accordance with (4.1), (4.2), (4.17), (4.27), in terms of the regular terms and the boundary layer, we obtain

$$
\left(\overset{(0)}{\sigma_{\varphi}^{(1)}} + h\overset{(1)}{\sigma_{\varphi}^{(1)}} + \ldots\right) n^{\circ} n^{3} + h^{p+2}\frac{E\nu_{s}}{E_{s}} \cdot \frac{1}{36R} \sum_{i=1}^{N-1} \overset{(0)}{\varphi_{i}^{(3)}} P_{i} + \ldots
$$

$$
\ldots + 2h^{p+3}\sqrt{\frac{E}{2(1+\nu)G}} \sum_{i=1}^{M} \frac{1}{\kappa_{i}} \cdot \frac{d\overset{(0)}{\Omega_{i}^{(1)}}}{ds} + \ldots = \overset{(0)}{\sigma_{nn}^{(1)}} + h\overset{(1)}{\sigma_{nn}^{(1)}} + \ldots
$$

$$
\left(\overset{(0)}{\tau_{\kappa}^{(1)}} + h\overset{(1)}{\tau_{\kappa}^{(1)}} + \ldots\right) n^{\circ} + h^{p+2} \sum_{i=1}^{M} \frac{d\overset{(0)}{\Omega_{i}^{(1)}}}{ds} + \ldots = \overset{(0)}{\sigma_{n}^{(1)}} + h\overset{(1)}{\sigma_{n}^{(1)}} + \ldots,
$$

$$
\left(\overset{(0)}{\sigma_{\varphi}^{(1)}} + h\overset{(1)}{\sigma_{\varphi}^{(1)}} + \ldots\right) n^{\circ} s^{3} + h^{p+3}\frac{E\nu_{s}}{E_{s}} \cdot \frac{1}{36} \sum_{i=1}^{N-1} \frac{d\overset{(3)}{\varphi_{i}}}{ds} P_{i} + \ldots
$$

$$
\ldots + h^{p+2} \sum_{i=1}^{M} \overset{(0)}{\Omega_{i}^{(1)}} + \ldots = \overset{(0)}{\sigma_{ns}^{(1)}} + h\overset{(1)}{\sigma_{ns}^{(1)}} + \ldots,
$$

(4.29)

$$
\left(\overset{(2)}{\sigma_{\varphi 3}} + h\overset{(3)}{\sigma_{\varphi 3}} + \ldots\right) n^{\circ} n^{3} + h^{p} \sum_{i=1}^{N-1} \overset{(0)}{\varphi_{i}} + \ldots
$$

$$
\ldots + 2h^{p+1}\sqrt{\frac{E}{2(1+\nu)G}} \sum_{i=1}^{M} \frac{1}{\kappa_{i}} l \frac{d\overset{(0)}{\Omega_{i}}}{ds} + \ldots = h^{-2}\left(\overset{(0)}{\sigma_{nn}} + h\overset{(1)}{\sigma_{nn}} + \ldots\right),
$$

$$
\left(\overset{(2)}{\tau_{\kappa}} + h\overset{(3)}{\tau_{\kappa}} + \ldots\right) n^{\circ} + h^{p-1} \sum_{i=1}^{N-1} \mu_{i}\varphi_{i} + \ldots
$$

$$
\ldots + h^{p} \sum_{i=1}^{M} l \frac{d\overset{(0)}{\Omega_{i}}}{ds} + \ldots = h^{-2}\left(\overset{(0)}{\sigma_{n}} + h\overset{(1)}{\sigma_{n}} + \ldots\right),
$$

$$
\left(\overset{(2)}{\sigma_{\varphi 3}} + h\overset{(3)}{\sigma_{\varphi 3}} + \ldots\right) n^{\circ} s^{3} + h^{p} \sum_{i=1}^{M} l\overset{(0)}{\Omega_{i}} + \ldots
$$

$$
\ldots - \frac{E\nu_{s}}{E_{s}} h^{p+1} \sum_{i=1}^{N-1} \mu_{i} l A D^{-1} \frac{d\overset{(0)}{\varphi_{i}}}{ds} -
$$

$$
- (1-\nu) h^{p+1} \sum_{i=1}^{N-1} \frac{1}{\mu_{i}} \cdot \frac{d\overset{(0)}{\varphi_{i}}}{ds} + \ldots = h^{-2}\left(\overset{(0)}{\sigma_{ns}} + h\overset{(1)}{\sigma_{ns}} + \ldots\right)
$$

The last three relations represent the boundary conditions in matrix form and utilize notations similar to the following

$$
\overset{(s)}{\sigma_{\varphi}} = \left(\overset{(s)}{\sigma_{\varphi}^{(3)}}, \overset{(s)}{\sigma_{\varphi}^{(5)}}, \ldots, \overset{(s)}{\sigma_{\varphi}^{(N)}}\right).
$$

It is not difficult to see that the integers a and b should be selected so that

$$a = b = -2$$

(for other values of a and b the resulting system of boundary relations will either be inconsistent or $\overset{(k)}{\Omega}_i$ and $\overset{(k)}{\varphi}_i$ vanish entirely). Equating coefficients on the left and right of like powers of h in the third and sixth equation (4.29),we obtain a sequence of boundary relations from which $\overset{(k)}{\Omega}_i$ are fully defined. In the zero approximation these will be the equations

$$\sum_{i=1}^{N} \overset{(0)}{\Omega}_i^{(1)} = \overset{(0)}{\sigma}_{ss}^{(1)} - \overset{(0)}{\sigma}_{s3}^{(1)} n^* s',$$

$$\sum_{i=1}^{N} l_i \overset{(0)}{\Omega}_i = \overset{(0)}{\sigma}_{ss}.$$

(4.30)

Similarly, the fourth and fifth equations (4.29) define the sequence of boundary relations from which $\overset{(n)}{\varphi}_i$ are found. In the zero approximation these will be the equations

$$\sum_{i=1}^{N-1} \overset{(0)}{\varphi}_i = \overset{(0)}{\sigma}_{sn}, \quad \sum_{i=1}^{N-1} p_i \overset{(0)}{\varphi}_i = 0.$$

The first two equations (4.29) define the boundary conditions for the biharmonic problems (4.2). In the zero approximation,we obtain the relations

$$\overset{(0)}{\sigma}_{s3}^{(1)} n^* n^* = \overset{(0)}{\sigma}_{nn}^{(1)},$$

$$\overset{(0)}{\sigma}_{s}^{(1)} n^* + \sum_{i=1}^{N} \frac{d \overset{(0)}{\Omega}_i^{(1)}}{ds} = \overset{(0)}{\sigma}_n^{(1)},$$

which in view of the first equation (4.30) coincide with the Kirchhoff static boundary conditions.

Outside some vicinity of the boundary Γ the plate stress state
is defined by the regular part of the asymptotic solution, since the
boundary layer within the region is infinitely small in comparison
with any power of h. In the immediate vicinity of the boundary, as
we see from (4.17), (4.27), the boundary layer stresses τ_{12}, τ_1, $t_{22}^{(1)}$, t_2, t_{11}, t_{21}
have the same order, while the stresses τ_2 and t_1 are of lower order
by one (relative to h) than the basic stress state defined by the
regular part of the asymptotic solution. This implies that the
stresses (1.5), tangential and normal to the median plane, which are
neglected in classical plate theory, are quantities of the same
order as the tangential stresses (1.4). Therefore, the error of the
Kirchhoff hypothesis near the boundary may be arbitrarily large for
sufficiently small h. A similar result was obtained in [2] on the
basis of Lur'ye's symbolical method.

Let us further assume that $\tau_{22}^{(1)} = 0$, and a $\sigma_{22}^{(1)}$ and $\sigma_z^{(1)}$ are
connected by the relation

$$\sigma_z^{(1)} - \frac{\partial \tau_{22}^{(1)}}{\partial s} = 0,$$

i.e., the system of edge restraints is statically equivalent to zero
on any small segment of the edge. Then in the zero approximation the
principal stress state disappears, and only the boundary layer remains.
However, in the first approximation the principal stress state will
still be, generally speaking, nonzero. Thus, the stress state due to
the system of edge loads, which are statically equivalent to zero
on any small segment of the edge, encompasses the entire plate region.
This contradicts the Saint Venant principle in the classical formula-
tion, but corresponds to the Mises modification of this principle, in
accordance with which the Saint Venant principle must be related not
with the stress decay at infinity but with the relative order at
infinity of the stresses due to the various systems of loads acting
on a small segment of the body boundary [11, 12].

b) Completely Clamped Edge

In this case, we set a = -1, b = -2. Omitting the detailed arguments, we write the zero approximation boundary conditions

$$-\frac{1}{E_s}\left(1-\frac{E}{E_s}v_z^2\right)\sum_{i=1}^{N-1}\mu_i^3 B\varphi_i^{(0)}+\left(\frac{1}{G}-\frac{v_z(1+v)}{E_s}\right)\sum_{i=1}^{N-1}\mu_i B\varphi_i^{(0)}=0,$$

$$\frac{1}{E_s}\left(1-\frac{E}{E_s}v_z^2\right)\sum_{i=1}^{N-1}\mu_i^2 B\varphi_i^{(0)}+\frac{v_z(1+v)}{E_s}\sum_{i=1}^{N-1}TA\varphi_i^{(0)}=-\frac{v_z}{E_s}IA\sigma_z^{(0)},$$

$$\sqrt{\frac{2(1+v)G}{E}}\sum_{i=1}^{M}\lambda_i\left(A\Omega_i^{(0)}\right)^{(1)}=-s^*\left(A\sigma_z^{(0)}\right)^{(1)}-\frac{1}{105}\sum_{i=1}^{N-1}\frac{d\varphi_i^{(0)(3)}}{ds},$$

$$\sqrt{\frac{2(1+v)G}{E}}\sum_{i=1}^{M}\lambda_i J\left(A\Omega_i^{(0)}\right)-\sum_{i=1}^{N-1}IA\frac{d\varphi_i^{(0)}}{ds}-s^*J\left(A\sigma_z^{(0)}\right),$$

$$\frac{\partial w}{\partial x}n^*=0,\quad w^{(0)}=0,$$

$$\sigma_n^{(0)}=\left(\sigma_n^{(0)(1)},\ \sigma_n^{(0)(2)},\ \ldots,\ \sigma_n^{(0)(N)}\right)=\left(\sigma_n^{(0)(1)},0,\ldots,0\right),$$

$$\sigma_s^{(0)}=\left(\sigma_{s(1)}^{(0)},\ \sigma_{s(2)}^{(0)},\ \ldots,\ \sigma_{s(N)}^{(0)}\right)=\left(\sigma_{s(1)}^{(0)},\ 0,\ldots,\ 0\right).$$

The first four equations are used to determine the constants of integration in $\varphi_i^{(0)}, \Omega_i^{(0)}$. The boundary conditions of the biharmonic problem are the same as in classical plate theory.

Near the boundary, the tangential and normal stresses (1.5) are of the same order (relative to h) as the stresses (1.4). However, their numerical values may be small since they depend on the factor v_z.

c) Freely Supported Edge

Here two versions are possible: 1) the stresses σ_{nn}, σ_{ns} and normal deflection u_3 equal zero and 2) $\sigma_{nn} = 0$, $u_3 = 0$ and the displacement u_s tangential to the boundary of the median plane equals zero.

In the first version, we set $a = b = 2$, in the second $a = -1$, $b = -2$. The basic stress state in the zero approximation is determined from classical plate bending theory. The boundary layer stresses are of the same order (in terms of h) as the basic stress state. Just as in the clamped case, the numerical values of the potential boundary layer stresses may be large by virtue of the fact that they depend on the factor ν_z.

6.   The linear ordinary differential equations, to the solution of which the boundary layer construction reduces, and their boundary conditions are independent of plate geometry, and therefore may be integrated once and for all. For practical computation purposes, these equations need only be solved for small N, since the boundary layers $\Psi_{(k)}, \Phi_{(k)}$ decay rapidly for large k, and their effect on the basic stress state diminishes rapidly, although in the sense of asymptotic behavior they are of the same order.

The study of plate bending problems with various support conditions (clamped, free) shows that the effect of the potential boundary layer on the basic stress state in the first and second approximations is expressed (by means of the Poisson ratio ν_z) in accounting for the deformations of the transverse fibers in determining the deformations of the fibers parallel to the median plane. Therefore, accounting for the potential boundary layer introduces into the first and second approximations of the basic stress state only slight corrections, which vanish entirely if Poisson's ratio ν_z vanishes. For example, for a circular plate of radius a which is clamped along the edge and loaded by the uniform pressure p, in the first approximation, we have for the deflection function (r is the distance from the center of the circle)

$$w = \frac{1-\nu^2}{Eh^3} \cdot \frac{3p}{128}(r^2 - a^2)\,[(r^2 - a^2) + ahC],$$

where C is a constant. The second term in the square brackets is the correction to classical theory which appears as a result of accounting for the potential boundary layer. For an isotropic plate $\nu = 0.3; \ C \approx 0.05.$

The corrections to the basic stress state introduced by the rotational boundary layer are more significant and in certain cases they should be considered. The integrals (4-13) of (4.10), subject to the corresponding boundary conditions, show good internal convergence with increase of N. Therefore, Reissner's plate theory, which includes the first equation (3·10), may be applied successfully for determining the first correction to the basic stress state given by classical theory. A similar conclusion concerning Reissner's theory is presented in [13], in which the problem of a strip clamped along the edges is examined with account for edge effects.

We note that with increase of the ratio E/G the boundary layer decays more slowly and its effect on the basic stress state increases. Therefore, ignoring the edge effects may lead to considerable error for strongly anisotropic plates, for which the ratio E/G is large.

REFERENCES

1. Ponyatovskiy, V. V., "On the theory of plates of moderate thickness," PMM, (Prikladnaya matematika i mekhanika), Vol. 26, No. 2, 1962.

2. Aksentyan, O.K., and I. I. Vorovich, "Stress state of a plate of small thickness," PMM, Vol. 27, No. 6, 1963.

3. Vishik, M. I., and L. A. Lyusternik, "Regular degeneration and the boundary layer for linear differential equations with a small parameter," UMN, (Uspekhi matematicheskikh nauk), Vol. 12, No. 5 (77), 1957.

4. Gol'denveyzer, A. L., "Some mathematical problems of linear theory of thin elastic shells," UMN, Vol. 15, No. 5 (95), 1960.

5. Reissner, E. Some Problems of Shell Theory. Elastic Shells (Russian translation), Moscow, Foreign Literature Press, 1962.

6. Kagan, V. F., Osnovy teorii poverkhnostey (Fundamentals of Surface Theory), Part 1, Moscow-Leningrad, GITTL (Gosudarstvennoye izdatel'stvo tekhnicheskoy i teoreticheskoy literatury), 1947.

7. Reissner, E., On the theory of bending of elastic plates. J. math. a. phys., Vol. 23, 1944.

8. Reissner, E., On bending of elastic plates. Quart. appl. math., Vol. 5, No. 1, 1947.

9. Ambartsumyan, S. A., "On the theory of anisotropic plate bending," IAN (Izvestiya akademii Nauk) SSSR, OTN, (Otdeleniye tekhniches-kikh nauk), No. 5., 1958.

10. Ambartsumyan, S. A., "On the theory of bending of anisotropic plates and hollow shells," PMM, Vol. 24, No. 2, 1960

11. Mises, R., On Saint-Venant's principle. Bull. Amer. math. soc., 51, 555, 1945.

12. Belonosov, S. M., Osnovnyye ploskiye staticheskiye zadachi teorii uprugosti dlya odnosvyaznykh i dvusvyaznykh oblastey (Basic Planar Static Problems of Elasticity Theory for Singly and Doubly Connected Regions), Novosibirsk, Izd. SO AN SSSR, 1962.

13. Nigul, U.K., "On the approximate account for edge effects of the Saint Venant type in static plate edge problems", PMM, Vol. 28, No. 1, 1964.

SOME QUESTIONS OF UNCOUPLING AND DISCRETIZATION OF SHELL THEORY EQUATIONS

L.A. Rozin

In plate and shell theory,it is of interest to construct problem
solution methods which can be ascribed definite physical relevance.
This is because physical considerations are often useful in construct-
ing computational algorithms. Moreover, this approach makes possible
a more profound and simpler analysis of the various assumptions and
simplifications.

Some techniques were indicated in[1, 2] for decoupling the
operators of the differential equations of shell theory and these
techniques were used to construct solution schemes having definite
physical relevance. In particular,it was possible to reduce the
problem to the calculation of a crossed bar system. It was found
that this sort of system is not a crossed bar system in the usual
sense. Its individual bars do not bend relative to the normal to
the shell middle surface. Their twist takes place with a rigidity
proportional to the moment of inertia, additional forces and moments
acting on the bars appear, the calculation result does not depend
on the relative width of the bars and so on. The resulting bar
system differs in this aspect from the conventional crossed bar
system. The latter sometimes appears inthose studies where an attempt
is made to construct computational schemes not on the basis of the
fundamental mathematical formulation of the problem,but by means of

33

unconvincing and at times erroneous arguments based on "engineering" intuition.

In the present paper, we develop the basic propositions presented in [1, 2]. The general equations of shell theory are transformed with the aid of a decoupling method. Here our objective is to transform the equations of shell theory so that they will be as similar as possible to the equations of crossed bar systems. In the transformation process, we clarify the degree to which this may be done. We found that this technique makes it possible to transform the equations of shell theory to the equations for a four-layer crossed bar system. The two inner layers of this system do not differ, at least in principle, from the conventional crossed bar system, and in many problems they are the primary load-carrying portion of the shell. The outer layers arise as a result of the difference in principle between the equations of shell theory and those for the bar systems. However, even these layers may be treated in an arbitrary sense as bar systems, at least from the viewpoint of constructing computational algorithms. By a slight extension of the concept of the crossed bar system, we are able to account for the effect of Poisson's ratio comparatively simply. The familiar differences (different order of the equations) in the formulation of the boundary conditions for the considered bar systems and the equations of shell theory are indicated.

The mathematical decoupling technique reduces the problem to the solution of a system of specific integral equations. Discretization of these equations onto a grid leads to the calculation of the crossed bar systems mentioned above. We can thus connect the questions of analysis of the bar system and solution of the integral equations of the decoupling method. On the one hand, we can use the analysis and approximate methods for solving integral equations and carry them over to the bar system. On the other hand, we can use the effective methods for calculating bar systems for approximate solution of the integral equations of the decoupling method.

In the following, we use the notations of [3] without further explanation.

1. By analogy with [1] we decouple the operators of the system of differential equations of equilibrium shell theory along the lines of principal curvature of the middle surface. Then, setting $b_1 = C_1(s_2) A_2$ and $b_2 = C_2(s_1) A_1$ where $C_1(s_2)$, $C_2(s_1)$ are arbitrary functions, we have

$$L_{1b_1}(T_{1b}, M_{1b}, T_{12b}, M_{12b}) = K_{1b_1}(p_{1b}, p_{2b}, p_{nb},$$
$$q_{1b}^{(1)}, q_{2b}^{(1)}, q_{nb}^{(1)}, m_{1b}^{(1)}, m_{2b}^{(1)}),$$

$$T_{12b} + \frac{M_{12b}}{R_1} = - m_{nb}^{(1)} \quad (i = 1, 2, 3, 4); \tag{1.1}$$

$$L_{1b_2}(T_{2b}, M_{2b}, T_{21b}, M_{21b}) =$$
$$= K_{1b_2}(0, 0, 0, q_{1b}^{(2)}, q_{2b}^{(2)}, q_{nb}^{(2)}, m_{1b}^{(2)}, m_{2b}^{(2)}),$$

$$T_{21b} + \frac{M_{21b}}{R_2} = - m_{nb}^{(2)} \quad (i = 1, 2, 3, 4). \tag{1.2}$$

Here the internal forces (moments), the components of the external load p_1, p_2, p_3 and the interaction functions [1] q_1, q_2, q_3, m_1, m_2, m_n, are multiplied by b_1, b_2, respectively. This is denoted by the subscript b and by the superscripts 1, 2 for the interaction functions. The external load components p_1, p_2, p_n, in (1.1) could also be partially applied to (1.2). The conventional differential operators appearing in (1.1), (1.2) have the form

$$L_{1s_k}(z_1, \ldots, z_4) = \frac{\partial z_1}{\partial s_k} + \frac{1}{A_k} \cdot \frac{\partial A_k}{\partial s_{3-k}}\left(z_3 + \frac{z_4}{R_k}\right) + \frac{1}{R_k} \cdot \frac{\partial z_2}{\partial s_k},$$

$$L_{3-k s_k}(z_1, \ldots, z_4) = \frac{\partial z_2}{\partial s_k} - \frac{1}{A_k} \cdot \frac{\partial A_k}{\partial s_{3-k}} z_1,$$

$$L_{2s_k}(z_1, \ldots, z_4) = \frac{\partial^2 z_3}{\partial s_k^2} + \frac{\partial}{\partial s_k}\left(\frac{z_4}{A_k} \cdot \frac{\partial A_k}{\partial s_{3-k}}\right) - \frac{z_1}{R_k},$$

$$L_{4s_k}(z_1, \ldots, z_4) = \frac{\partial z_4}{\partial s_k} - \frac{z_3}{A_k} \cdot \frac{\partial A_k}{\partial s_{3-k}} \quad (k = 1, 2); \tag{1.3}$$

$$K_{1s_k}(z_1, \ldots, z_6) = - z_1 + (-1)^k z_{3+k} - \frac{z_{6+k}}{R_k},$$

$$K_{3-k s_k}(z_1, \ldots, z_6) = - z_2 + (-1)^k z_{6-k},$$

$$K_{2s_k}(z_1, \ldots, z_8) = - z_3 + (-1)^k z_6 - \frac{\partial z_{6+k}}{\partial s_k},$$

$$K_{4s_k}(z_1, \ldots, z_9) = z_{9-k} \quad (k = 1, 2). \tag{1.4}$$

Using some elasticity relation, for example the Balabukh-Novozhilov law, we set

$$T_{1b} = T_{1b}^0 + \Phi_1, \quad M_{1b} = M_{1b}^0 + \Phi_3,$$
$$T_{12b} = T_{12b}^0 + \Phi_2, \quad M_{12b} = M_{12b}^0 + \Phi_4,$$
$$T_{2b} = T_{2b}^0 + \Psi_1, \quad M_{2b} = M_{2b}^0 + \Psi_3,$$
$$T_{21b} = T_{21b}^0 + \Psi_2, \quad M_{21b} = M_{21b}^0 + \Psi_4,$$

$$(1 \cdot 5)$$

where

$$T_{kb}^0 = B_k \varepsilon_k; \quad M_{kb}^0 = D_k \varkappa_k; \quad T_{kib}^0 = L_k \omega_k;$$
$$M_{kib}^0 = D_{ok} \tau_k \quad (k=1, 2; \ t=2, 1);$$

$$(1 \cdot 6)$$

$$\Phi_1 = \nu B_1 \varepsilon_2, \quad \Phi_2 = \nu D_1 \varkappa_2, \quad \Phi_3 = L_1 \omega_2 + \frac{D_{o1}}{R_2} \tau_2,$$

$$\Phi_4 = \frac{D_{o1}}{R_1} \omega_2,$$

$$(1 \cdot 7)$$

$$\Psi_1 = \nu B_2 \varepsilon_1, \quad \Psi_2 = \nu D_2 \varkappa_1, \quad \Psi_3 = L_2 \omega_1 + \frac{D_{o2}}{R_1} \tau_1, \quad \Psi_4 = \frac{D_{o2}}{R_2} \omega_1$$

and B_k, D_k, $L_k \left(1 + \frac{h^2}{6R_{3-k}^2}\right) \approx L_k$, $D_{ok} = D_k(1-\nu)$ $(k=1, 2)$ — are the corresponding stiffnesses, multiplied by b_1 for k = 1 and b_2 for k = 2. We substitute (1·5) into (1·1), (1·2) and rewrite them as follows

$$L_{ki_1}(T_{1b}^0, M_{1b}^0, T_{12b}^0, M_{12b}^0) = K_{ki_1}(p_{1b}, p_{bb}, p_{nb}, q_{1b}^{(1)}, q_{2b}^{(1)}, q_{nb}^{(1)}, m_{1b}^{(1)}, m_{2b}^{(1)}) + K_{ki_1}(0, 0, 0, f_{1b}^{(1)}, f_{2b}^{(1)}, f_{nb}^{(1)}, 0, n_{2b}^{(1)});$$

$$(1 \cdot 8)$$

$$L_{ki_1}(\Phi_1, \Phi_2, \Phi_3, \Phi_4) = K_{ki_1}(0, 0, 0, -f_{1b}^{(1)}, -f_{2b}^{(1)}, -f_{nb}^{(1)}, 0, -n_{2b}^{(1)}) \quad (i=1, 2, 3, 4);$$

$$(1 \cdot 9)$$

$$L_{ki_1}(T_{2b}^0, M_{2b}^0, T_{21b}^0, M_{21b}^0) =$$
$$= K_{ki_1}(0, 0, 0, q_{1b}^{(2)}, q_{2b}^{(2)}, q_{nb}^{(2)}, m_{1b}^{(2)}, m_{2b}^{(2)}) +$$
$$+ K_{ki_1}(0, 0, 0, f_{1b}^{(2)}, f_{2b}^{(2)}, f_{nb}^{(2)}, n_{1b}^{(2)}, 0);$$

$$(1 \cdot 10)$$

$$L_{ki_1}(\Psi_1, \Psi_2, \Psi_3, \Psi_4) =$$
$$= K_{ki_1}(0, 0, 0, -f_{1b}^{(2)}, -f_{2b}^{(2)}, -f_{nb}^{(2)}, -n_{1b}^{(2)}, 0)$$
$$(i=1, 2, 3, 4),$$

$$(1 \cdot 11)$$

where we have introduced the additional interaction functions $f_{1b}^{(k)}$, $f_{2b}^{(k)}$, $f_{nb}^{(k)}$ $(k=1, 2)$, $n_{2b}^{(1)}$, $n_{1b}^{(2)}$. Here we have omitted the last equations (1·1), (1·2), which are not required in the following since the corresponding equation in shell theory is satisfied identically. Equations (1·8) — (1·11) transform to the differential equations of shell theory if we exclude the thirteen interaction functions introduced above

$$q_1, \; q_2, \; q_a, \; m_1, \; m_2, \; f^{(k)}_{10}, \; f^{(k)}_{20}, \; f^{(k)}_{ab} \; (k=1, \, 2), \; n^{(1)}_{22}, \; n^{(2)}_{11}.$$

We denote the operators which are formed in the left sides of (1.8), (1.10), after converting therein to displacements and rotations using (1.6), as follows

$$L^{\bullet}_{i k_2}\left(u^{(k)}_1, \, u^{(k)}_2, \, w^{(k)}, \, \vartheta^{(k)}_{3-k}\right) \; \binom{i=1, \, 2, \, 3, \, 4;}{k=1, \, 2}.$$

(1.12)

Then if we follow the idea of the decoupling method [1] and seek the interaction functions on the basis of the requirement for equivalence (1.8), (1.9), (1.10), (1.11) (where the left sides of (1.8), (1.10) are replaced by (1.12)) with the basic equations of shell theory, then this requirement takes the form of the conditions

$$u^{(t)}_1 = u^{(k)}_1, \; w^{(1)} = w^{(2)}, \; \vartheta^{(t)}_k = -\frac{\partial w^{(k)}}{\partial \alpha_k} + \frac{u^{(k)}_k}{R_k}$$

$$(k=1, \, 2; \; t=2, \, 1);$$

(1.13)

$$\frac{\Phi_1}{\nu B_2} = \frac{T^{\bullet}_{20}}{B_2}, \quad \frac{\Phi_2}{\nu D_2} = \frac{M^{\bullet}_{20}}{D_2}, \quad \frac{\Phi_4 R_1}{D_{01}} = \frac{T^{\bullet}_{210}}{L_2},$$

$$\frac{R_2}{D_{02}}\Phi_3 - \frac{L_1 R_1 R_2}{D^2_{01}}\Phi_4 = \frac{M^{\bullet}_{210}}{D_{02}};$$

(1.14)

$$\frac{\Psi_1}{\nu B_1} = \frac{T^{\bullet}_{10}}{B_1}, \quad \frac{\Psi_2}{\nu D_2} = \frac{M^{\bullet}_{10}}{D_1}, \quad \frac{\Psi_4 R_2}{D_{02}} = \frac{T^{\bullet}_{120}}{L_1},$$

$$\frac{R_1}{D_{01}}\Psi_3 - \frac{L_2 R_1 R_2}{D^2_{02}}\Psi_4 = \frac{M^{\bullet}_{120}}{D_{01}}.$$

(1.15)

where (1.14), (1.15) follows from (1.6) and (1.7). In other words, for complete equivalence of the decoupled and original equations it is necessary that the interaction functions be selected so that the conditions (1.13), (1.14), (1.15) are satisified.

Here we have used the elasticity law in the Balabukh-Novozhilov form with the assumption $L_k\left(1 + \frac{h^2}{6R^2_{2-k}}\right) \approx L_k,$ which is not essential and has been adopted only for convenience of exposition. Other elasticity laws may also be used, for example, that used in [4] and [8]. Then the following changes occur in (1.6), (1.7)

$$M^{\bullet}_{120} = \frac{D_{01}}{2}\tau_1, \quad M^{\bullet}_{210} = \frac{D_{02}}{2}\tau_2,$$

(1.16)

$$\Phi_4 = \frac{D_{01}}{2}\tau_2, \quad \Psi_4 = \frac{D_{02}}{2}\tau_1, \quad \Phi_3 = L_1\vartheta_2, \quad \Psi_3 = L_2\vartheta_1.$$

In (1.14), (1-15) the last two equalities are replaced by

$$\frac{\phi_3}{L_1} = \frac{T_{240}^0}{L_2}, \quad \frac{\phi_4}{D_{44}} = \frac{M_{210}^0}{D_{44}}.$$

$$\frac{\Psi_3}{L_2} = \frac{T_{120}^0}{L_1}, \quad \frac{\Psi_4}{D_{44}} = \frac{M_{120}^0}{D_{44}}.$$
(1.17)

In the case of the Love elasticity law (1.6), (1.7) will become

$$\phi_3 = L_1 \phi_2, \quad \phi_4 = \frac{D_{44}}{L_1 R_1} \phi_3.$$

$$\Psi_3 = L_2 \Psi_1, \quad \Psi_4 = \frac{D_{44}}{L_2 R_2} \Psi_2.$$
(1.18)

Here the functions Φ_3, Φ_4 and Ψ_3, Ψ_4 are already related. Then the
four interaction functions in (1.9) are defined only by the three
functions ϕ_1 and consequently only three of them will be independent.
Similar arguments apply to (1.11). As a result, the adopted decoupling
of the governing equations, and the Love elasticity relation leads to
eleven interaction functions in place of thirteen as in the case of the
other elasticity laws. The number of conditions (1.14), (1.15) also
decreases to six. In place of the last two conditions in (1.14) and
(1.15), we have one condition each of the form

$$\frac{\phi_3}{L_1} = \frac{T_{240}^0}{L_2}, \quad \frac{\Psi_3}{L_2} = \frac{T_{120}^0}{L_1}.$$
(1.19)

2. Now we turn to the mechanical analysis of the solution of
shell theory problems by the decoupling method on the basis of the
decoupled equations and the conditions (1.13), (1.14), (1.15). In
the left sides of (1.8), (1.9), (1.10), (1.11) there appear the
operators L_{1s_k} $(z_1, \ldots, z_4)$ (k = 1, 2), which are the operators of
the equilibrium equations of curvilinear bars of width b_1 and b_2 if
the arguments z_i (i = 1, 2, 3, 4) are given the meaning, respectively,
of normal force, bending moment, tangential force, and torsional
moment in the bar. The axes of these bars coincide with the lines
α_2 = const and α_1 = const, and the unit vectors $\vec{e}_2$, $\vec{e}_n$ and $\vec{e}_1$, $\vec{e}_n$
coincide with the principal axes of inertia of their cross section
(Figure 1). Here there are no bending moments relative to the unit
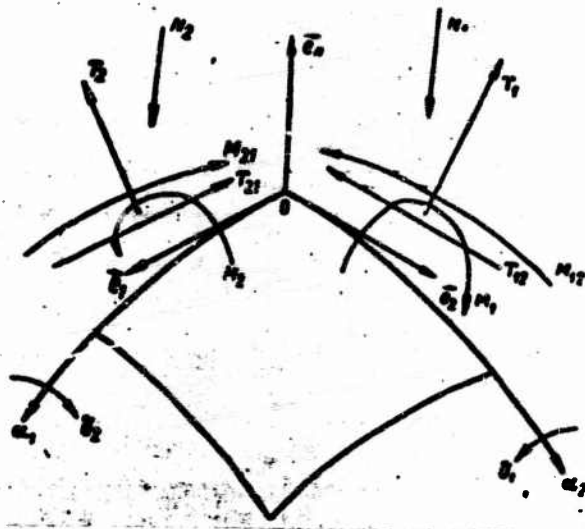vector $\vec{e}_n$ and equilibrium of the moments about $\vec{e}_n$ is satisfied by

Figure 1.

virtue of the external distributed moments $m_{\text{nb}}^{(k)}$ $(k = 1, 2)$ which, as noted above, are not essential.

Now let us turn to the operators L_{1s_k} $(k = 1, 2)$ in (1.8), (1.10). The forces and moments here are connected with the deformations by (1.6). Conversion from forces (moments) to displacements (rotations) using (1.6) permits obtaining the operators (1.12). We see from (1.6) and (1.8), (1.10) that the difference between (1.12) and the conventional bar operators is that [1] bending of the bars takes place only relative to $\vec{e}_2$ or $\vec{e}_1$ [2]. In the $\vec{e}_1$, $\vec{e}_2$ plane there is only pure shear; moreover, the section form coefficient in shear equals unity [3]. Torsion takes place without bending relative to $\vec{e}_n$ with stiffness proportional to the bar moment of inertia [4]. The Poisson ratio appears in the corresponding stiffnesses. Comparing these specific properties of the operators $L_{1s_k}^{*}$ $(k - 1, 2)$ with the properties of the conventional bar operators, we can write for the transformation $L_{1s_k}^{*}$ $(k = 1, 2)$ the Maxwell-Mohr formulas of the following type

$$\Delta_{ij}^1 = \int\limits_{s_b} \frac{T_{bki}^0 T_{bkj}^0}{B_b}\, ds_k + \int\limits_{s_D} \frac{M_{bki}^0 M_{bkj}^0}{D_b}\, ds_k +$$
$$+ \int\limits_{s_k} \frac{T_{bki}^0 T_{bkj}^0}{L_k}\, ds_k + \int\limits_{s_k} \frac{n M_{bki}^0 M_{bkj}^0}{D_{bk}}\, ds_k. \qquad (2 \cdot 1)$$

where, respectively, k = 1, 2; t = 2, 1; n = 1, and in the case of
the elasticity law of [4], [8] n = 2. Here quantities with sub—
scripts i and j denote the forces (moments) from the action of which
and corresponding to which we seek the generalized displacement values.
Expression (2·1) follows from the fact that the connection between
the forces (moments) and the deformations is taken in the form (1·6)
or (1·16). In fact, considering (1.6) and examining for definiteness
the case k = 1 we can rewrite (2·1) in the form

$$\Delta_{ij}^1 = \int\limits_{s_1} \left(e_{1i} T_{b0j}^0 + \varkappa_{1i} M_{1bj}^0 + \omega_{1i} T_{12bj}^0 + \tau_{1i} M_{12bj}^0 \right) ds_1.$$

Substituting herein in place of the deformations their expressions in
terms of displacement and rotation, and integrating the resulting
integral by parts with use of the fact that the forces (moments)
with subscript j satisfy the equilibrium equations (1·8) with the
right sides $\bar{q}_{1bj}^{(1)}, \bar{q}_{2bj}^{(1)}, \bar{q}_{nbj}^{(1)}, \bar{m}_{2bj}^{(1)}$, to which the generalized displace-
ment in question corresponds , we obtain

$$\Delta_{ij}^k = \int\limits_{s_k} \left(u_{1i}^{(1)} \bar{q}_{1bj}^{(1)} + u_{2i}^{(1)} \bar{q}_{2bj}^{(1)} + w_i^{(1)} \bar{q}_{nbj}^{(1)} - \vartheta_{2i}^{(1)} m_{2bj}^{(1)} \right) ds_1 + \left[u_{1i}^{(1)} T_{1bj}^0 \right] +$$
$$+ \left[u_{2i}^{(1)} T_{12bj}^0 \right] + \left[w_i^{(1)} \left(N_{1bj}^0 - m_{1bj}^{(1)} \right) \right] + \left[\vartheta_{1i}^{(1)} M_{1bj}^0 \right] + \left[\vartheta_{2i}^{(1)} M_{12bj}^0 \right].$$

Here the square brackets denote nonintegral terms which arise as
a result of integration by parts, and the quantity N_{1bj}^0 is the
transverse shearing force. The brackets represent the work of all the
concentrated loads corresponding to the state k on the corresponding
linear and angular displacements of the state i. In turn, the inte-
gral is the work of the distributed loads. Thus, Δ_{ij}^k in (2·1) is
the generalized displacement, understood in the usual sense.

We shall term these bars, with left sides of the equilibrium
equations the same as the left sides of (1.8), (1·10), with the

elasticity law in the form (1.6) and no bending relative to the unit vector $\vec{e}_n$, P bars. Hereafter, we denote the P bars located along s_1 and s_2 by P_1 and P_2, respectively.

Now let us consider the operators $K_{u_k}(z_1, \ldots, z_8)$ $(k=1, 2)$ in the right sides of (1.8) - (1.11). Taking (1.4) into account, we can conclude that K_{u_k} $(k=1, 2)$ are the operators in the right sides of the equations for conventional bars relative to the distributed loads $z_1, \ldots z_8$. In K_{1s_1} the quantities z_1, z_2, z_3 and z_4, z_5, z_6 are the projections of the distributed running forces on the unit vectors $\vec{e}_1, \vec{e}_2, \vec{e}_n$, and z_7, z_8, are the projections of the distributed running moments on the unit vectors $\vec{e}_2$, $\vec{e}_1$. In K_{1s_2} the quantities z_4, z_5, z_6, z_7, z_8 are nonzero. They have the same significance as the corresponding loads in K_{1s_1}, except that they act in the opposite direction.

Let us assume that the quantities $f_{1b}^{(k)}$, $f_{2b}^{(k)}$, $f_{nb}^{(k)}$ $(k=1, 2)$ and $n_{1b}^{(2)}$, $n_{2b}^{(1)}$ may be dropped in (1.8), (1.10). Then we find the five interaction functions q_1, q_2, q_n, m_1, m_2, for the equations (1.8), (1.10) with the aid of the five conditions (1.13). Here the equations (1.8), (1.10), and the elasticity law (1.6) describe the behavior of two continuous families of bars P_1 and P_2 positioned along the coordinate lines s_1 and s_2. The bars P_1 are loaded by the external loading and unknown running loads, while the bars P_2 are loaded by unknown running loads of opposite sign. There is the following connection between the magnitudes of these running loads.

$$\frac{q_{1b}^{(1)}}{b_1} = \frac{q_{1b}^{(2)}}{b_2}, \quad \frac{q_{2b}^{(1)}}{b_1} = \frac{q_{2b}^{(2)}}{b_2}, \quad \frac{q_{nb}^{(1)}}{b_1} = \frac{q_{nb}^{(2)}}{b_2},$$
$$\frac{m_{1b}^{(1)}}{b_1} = \frac{m_{1b}^{(2)}}{b_2}, \quad \frac{m_{2b}^{(1)}}{b_1} = \frac{m_{2b}^{(2)}}{b_2}. \tag{2.2}$$

The unknown running loads in (2.2), which may be termed the interaction loads between P_1 and P_2, are defined from the conditions (1.13). The latter express the equality of the displacements and rotations (twist) of the considered families of P bars. A similar situation holds in the crossed bar system. Therefore, we shall call this system the crossed and continuous P bar system and denote it by

$\left\{ P_1, P_2 \right\}$.   On the basis of the properties of the P bars, we can conclude that the algorithms for the calculation of such a system do not differ in any fundamental way from the algorithms for calculating the conventional continuous and crossed bar system.

Reduction of the mathematical formulation of the shell theory problem to the equations of the crossed and continuous P bar system is possible in those cases when the quantities $f_{1b}^{(k)},\ f_{2b}^{(k)},\ f_{2b}^{(k)}\ (k=1,\ 2),\ \kappa_{1b}^{(2)},\ \kappa_{2b}^{(1)}$ may be dropped in (1.8), (1.10). This can be done in several problems. However, in the general case we must consider all the equations and take into account all the interaction functions.

Let us consider the general case. We first turn to the equations (1.9), which do not differ in any way from the equilibrium equations for the P_1 bars relative to $\Phi_l\ (l=1,\ 2,\ 3,\ 4)$. Let ϕ_1 be found by solving (1.9), then the displacements and corresponding rotations may be found as follows. From ϕ_1 and (1.14) we find the forces (moments) just like $T_{2b}^0,\ M_{2b}^0,\ T_{21b}^0,\ M_{21b}^0$.   Then with the aid of the elasticity law (1.6) we find the corresponding displacements and rotation from (2.1), just as for the P_2 bars. Therefore, we can consider that (1.9) together with (1.6) and (1.14) describe the behavior of an equivalent continuous bar-type system for which the internal forces (moments) are found from (1.9) and (1.14). In turn, the displacements (rotation) are found from the forces (moments) just as in the P_2 bar system. To determine the static quantities of such a system we must invert the operators L_{1b_1} in (1.9) with respect to s_1, just as for the P_1 bars, while to find its kinematic constants we must invert the operators (1.6) with respect to s_2 just as for the P_2 bar system. This is the basic feature of the system described by (1.9), (1.14), and (1.6). At the same time it is advisable to consider it as a bar system, since in determining the internal forces (moments) and displacements (rotations) in this system we must invert the operators just as for the P_1 and P_2 bars We term such a system a continuous family of P_{21} bars, and we abritrarily consider its bars positioned along s_2.

Now let us consider the system of equations (1.8), (1.6) for the continuous family of P_1 bars, and the sytem of equations (1.9), (1.14), (1.6) for the continuous family of P_{21} bars. In

accordance with the right sides of (1.8), (1.9) equal and opposite interaction loads $f_{1b}^{(1)}$, $f_{2b}^{(1)}$, $f_{nb}^{(1)}$, $n_{2b}^{(1)}$, act between P_1 and P_{21}. Suppose P_1 and P_{21} form a continuous crossed bar system $\{P_1, P_{21}\}$ with the interaction loads indicated above. Denoting the displacements and roations for the P_1 bars by $u_1^{(1)}$, $u_2^{(1)}$, $w^{(1)}$, $\vartheta_2^{(1)}$ and those for the P_{21} bars by $u_1^{(21)}$, $u_2^{(21)}$, $w^{(21)}$, $\vartheta_1^{(21)}$, we determine the interaction loads in the crossed system $\{P_1, P_{21}\}$ from the conditions

$$u_1^{(21)} = u_1^{(1)}, \quad u_2^{(21)} = u_2^{(1)}, \quad w^{(21)} = w^{(1)},$$
$$\vartheta_1^{(21)} = -\frac{\partial w^{(1)}}{\partial s_1} + \frac{f^{P}}{A}. \tag{2.3}$$

Thus, we take the crossed system $\{P_1, P_{21}\}$ to be a system consisting of the elements P_1 and P_{21} between which there act the interaction boads $f_{1b}^{(1)}$, $f_{2b}^{(1)}$, $f_{nb}^{(1)}$, $n_{2b}^{(1)}$, determined from the conditions (2.3).

We can introduce similarly, the concept of a continuous family of P_{12} bars along s_1, whose behavior is described by (1.11), (1.15), (1.6). Moreover, we shall consider that (1.10), (1.5) for the continuous family of P_2 bars and (1.11), (1.15), (1.6) for the continuous family of P_{12} bars describe the behavior of the continuous crossed bar system $\{P_2, P_{12}\}$ with the interaction loads $f_{1b}^{(2)}$, $f_{2b}^{(2)}$, $f_{nb}^{(2)}$, $n_{1b}^{(2)}$. These loads are found from the conditions

$$u_1^{(12)} = u_1^{(2)}, \quad u_2^{(12)} = u_2^{(2)}, \quad w^{(12)} = w^{(2)},$$
$$\vartheta_2^{(12)} = -\frac{\partial w^{(2)}}{\partial s_2} + \frac{f^{P}}{A}. \tag{2.4}$$

where the displacements and rotations of the P_2 and P_{12} bars are denoted by $u_1^{(2)}$, $u_2^{(2)}$, $w^{(2)}$, $\vartheta_1^{(2)}$ and $u_1^{(12)}$, $u_2^{(12)}$, $w^{(12)}$, $\vartheta_2^{(12)}$. respectively.

Now let us consider a four-layer continuous system of bars which are crossed at each layer. Suppose the 1-st (upper) and 4th (lower) layers consitute, respectively, P_{21} and P_{12} systems, and the middle pair of layers of a crossed P bar system (Figure 2). Thirteen interaction loads act between the four families of bars P_{21}, P_1, P_2, P_{12},
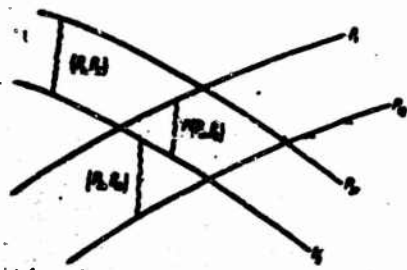
Figure 2.

which constitute this four-layer system. Five of these loads which appear in (2.2) for the $\{P_1, P_2\}$ system are found from the conditions (1.13), while the remaining eight are found from the conditions (2.3), (2.4). Let us show that the equations describing the behavior of such a four-layer bar system, which we denote by P_{4c}, coincide with the uncoupled shell theory equations presented above and that the conditions (2.3), (2.4) are equivalent to the conditions (1.14), (1.15). In fact, the equilibrium equations of the P_{4c} four-layer bar system are by definition the same as the uncoupled equilibrium equations of shell theory written in the form (1.8),— (1.11). In both cases the forces (moments) with the zero superscript in (1.8), (1.10), are related with the the deformations by the equations (1.6). It would appear that the only difference is that for the uncoupled equations of shell theory, the conditions (1.13), (1.14), (1.15), must be satisfied, while in P_{4c} the conditions (1.13), (2.3), (2.4) must be satisfied. However, in actuality these conditions are equivalent. We denote the forces (moments) in the P_{21} system, obtained in accordance with (1.14) from ϕ_1, as follows: $T^{\circ}_{20}(P_{21})$, $M^{\circ}_{20}(P_{21})$, $T^{\circ}_{210}(P_{21})$, $M^{\circ}_{210}(P_{21})$. Correspondingly, in the P_{12} system the analogous quantities will be $T^{\circ}_{10}(P_{12})$, $M^{\circ}_{10}(P_{12})$, $T^{\circ}_{120}(P_{12})$, $M^{\circ}_{120}(P_{12})$. The displacements and rotations corresponding to these quantities must satisfy (2.3), (2.4). In the right sides of these equalities there appear the displacements and rotations of the P_2, P_1, bars, which in turn are connected with one another by (1.13). Thus, on the basis of (1.13)

$$u_2^{(21)} = u_1^{(2)}, \quad u_2^{(21)} = u_2^{(2)}, \quad w^{(21)} = w^{(2)}, \quad \vartheta_1^{(21)} = \vartheta_1^{(2)},$$

$$(2.5)$$

$$u_1^{(12)} = u_1^{(1)}, \quad u_2^{(12)} = u_2^{(1)}, \quad w^{(12)} = w^{(1)}, \quad \vartheta_2^{(12)} = \vartheta_2^{(1)}.$$

$$(2.6)$$

Since in accordance with (2.5) the displacements and rotations are equal in P_{21} and P_2, on the basis of (1.6) the corresponding internal forces (moments) in P_{21} and P_2 are equal, i.e.,

$$T_{2b}^o(P_{21}) = T_{2b}^o, \quad M_{2b}^o(P_{21}) = M_{2b}^o, \quad T_{21b}^o(P_{21}) = T_{21b}^o,$$
$$M_{21b}^o(P_{21}) = M_{21b}^o.$$

(2.7)

Similarly, for P_{12} and P_1 (2-6) yield

$$T_{1b}^o(P_{12}) = T_{1b}^o, \quad M_{1b}^o(P_{12}) = M_{1b}^o, \quad T_{12b}^o(P_{12}) = T_{12b}^o,$$
$$M_{12b}^o(P_{12}) = M_{12b}^o.$$

(2.8)

By definition the left sides of (2.7), (2.8) are connected with Φ_1 and ψ_1 by (1.14), (1.15). Consequently, the right sides of (2.7) (2.8) are connected with c Φ_1, ψ_1 by (1.14), (1.15). Thus, if the equalities (2.3), (2.4), (1.13) are satisfied , (1.14) and (1.15) are automatically satisfied. The equations are conditions defining the interaction loads for both P_{4c} and the uncoupled equations of shell theory are identical. Moreover, since the uncoupled equations and the conditions (1.13), (1.14), (1.15) are equivalent to the governing equations of shell theory, the equations of the four-layer bar system will be equivalent to them.

This four-layer bar system is quite reminescent of the conventional bar system. The main difference from the latter is the nature of the bars P_{21} and P_{12}. However, in spite of this none of the operators which must be inverted in the calculation of such a system differ in any way from the operators for P bars. Therefore,the basic nature of the algorithms is the same in both cases.

3. Now let us formulate the boundary conditions for this four-layer bar system, equivalent to the boundary conditions of shell theory. For simplicity,we consider that the shell edges coincide with the coordinate lines.

Let the boundary conditions, four at each shell edge, be given in terms of displacements. To invert the operators (1.12) with respect to the displacements and rotations in P_1 and P_2 we need five conditions at each edge, since these operators are tenth order. The

missing fifth condition with respect to the rotation is obtained from
the given shell edge displacements by differentiating these displace-
ments along the edge. Consider the operators L_{1s_k} (k = 1, 2) in
(1.9), (1.11) for the P_{21} and P_{12} systems. Since ϕ_1 and ψ_1 appear
here as forces (moments), to invert L_{1s_k} (k = 1, 2) we need to

know the five quantities $\phi_i^\bullet, \ \psi_i^\bullet, \ \left(\frac{\partial \phi_2}{\partial s_1}\right)^\bullet, \ \left(\frac{\partial \psi_2}{\partial s_2}\right)^\bullet \ (i=1, 2, 3, 4).$

at the corresponding edges. Generally speaking, these quantities
do not appear in the boundary conditions of shell theory. They must
be considered additional edge interaction functions or additional
edge loads, analogous to the thirteen distributed interaction loads.
They are defined with the aid of (1.14), (1.15) at the corresponding
shell edges. The reason is that at the edges the conditions (1.14),
(1.15) cannot be satisfied by the distributed interaction loads,
just as in the case of a cantilever bar end loads must be applied
at the tip in order to satisfy certain static conditions there.
In the present case, when the displacements at the shell edge are
given, by inverting the operators (1.12) we can obtain the forces
(moments) with zero superscript in F_1 and P_2. Then we use (1.14),
(1.15) to calculate the quantites $\phi_i^\bullet, \ \psi_i^\bullet, \ \left(\frac{\partial \phi_2}{\partial s_1}\right)^\bullet, \ \left(\frac{\partial \psi_2}{\partial s_2}\right)^\bullet \ (i=1, 2, 3, 4)$
at the corresponding edges.

Consider the case in which forces (moments) are given at one of
the boundaries, for example $\alpha_1 = \alpha_1^0 = $ const, while the condition
at the remaining edges are given in terms of displacements. We
transform the boundary conditions of shell theory for $\alpha_1 = \alpha_1^0 =$ const
as follows

$$T_{1b} = Q_{11b}^\circ, \quad T_{12b} + \frac{M_{12b}}{R_2} = Q_{12b}^\circ,$$
$$N_{1b} + \frac{\partial M_{12b}}{\partial s_2} - \frac{M_{12b}}{b_1} \cdot \frac{\partial b_1}{\partial s_2} = Q_{1mb}^\circ, \quad M_{1b} = M_{11b}^\circ, \tag{3.1}$$

where the given values are on the right. Noting that

$$M_{12b} = -\frac{M_{21b}}{b_2} b_1, \quad \frac{\partial}{\partial s_2}(M_{21b}) = m_{1b}^{(2)} + \frac{M_{2b}}{b_1} \cdot \frac{\partial b_1}{\partial s_1}, \tag{3.2}$$

and substituting (3.2) into (3.1), we obtain

$$T^{\circ}_{1b} = Q^{\circ}_{11b} - \Phi^{\circ}_1,$$

$$T^{\circ}_{12b} = Q^{\circ}_{12b} - \Phi^{\circ}_3 - \frac{M^{\circ}_{21b} b_1}{R_2 b_2} - \frac{\Psi_4 b_3}{R_2 b_2},$$

$$N^{\circ}_{1b} = Q^{\circ}_{13b} - \Phi^{\circ}_N - m^{(1)}_{1b} - \frac{M^{\circ}_{2b} + \Psi_2}{b_3} \cdot \frac{\partial b_1}{\partial s_1} +$$

$$+ \frac{(M^{\circ}_{21b} + \Psi_4) b_1}{b_3^2} \cdot \frac{\partial b_3}{\partial s_3},$$

$$M^{\circ}_{1b} = M^{\circ}_{11b} - \Phi^{\circ}_2,$$

$$M^{\circ}_{12b} = M^{\circ}_{31b} \frac{b_1}{b_3} + \Psi_4 \frac{b_1}{b_3} - \Phi^{\circ}_4.$$

(3.3)

Here, on the basis of the corresponding uncoupled equilibrium equation [1]

$$\frac{\partial M_{1b}}{\partial s_1} + M_{12b} \frac{1}{A_1} \cdot \frac{\partial A_1}{\partial s_2} - N_{1b} = - m^{(1)}_{1b},$$

in which the transverse shearing force $N_{1b} = N^{\circ}_{1b} + \Phi^{\circ}_N$ appears, we can take

$$\Phi^{\circ}_N = \left(\frac{\partial \Phi_2}{\partial s_1}\right)^{\circ} + \frac{\Phi^{\circ}_4}{b_3} \cdot \frac{\partial b_3}{\partial s_3}.$$

(3.4)

Then at the boundary we will also have

$$\frac{\partial M^{\circ}_{1b}}{\partial s_1} = N^{\circ}_{1b} - m^{(1)}_{1b} - \frac{M^{\circ}_{21b}}{b_3} \cdot \frac{b_1}{b_2} \cdot \frac{\partial b_2}{\partial s_3}.$$

The expressions for the forces (moments) with zero superscript for the edge $\alpha_2 = \alpha_2^0 =$ const are written similarly to (3.3). Expressions (3.3) are the boundary conditions at the loaded edge $\alpha_1 = \alpha_1^0$ for the P_1 bars. In the right sides of (3.3) there appear Φ_i, $\left(\frac{\partial \Phi_2}{\partial s_1}\right)^{\circ}$, Ψ_2, Ψ_4 and the moments in P_2 for $\alpha_1 = \alpha_1^0$. This situation indicates that the boundary conditions at the loaded edge $\alpha_1 = \alpha_1^0$ for P_1 may be established after determining M^0_{2b}, M^0_{21b} in P_2 for $\alpha_1 = \alpha_1^0$. In the present case, we first invert the operators corresponding to P_2. This yields Φ^*_1, and $\left(\frac{\partial \Phi_2}{\partial s_1}\right)^{\circ}$ and M^0_{2b}, M^0_{21b} for $\alpha_1 = \alpha_1^0$. Then we find Φ_1, Ψ_1 in terms of the five as yet undetermined quantities Ψ^*_1, $\left(\frac{\partial \Psi_2}{\partial s_3}\right)^{\circ}$. After this we establish the boundary conditions (3.3) and make the calculation of the P_1 bars. Finally, the quantities

Ψ_1^* , $(\frac{\partial \Psi_2}{\partial s_2})^*$ are found at the boundary $\alpha_2 = \alpha_2^0 = $const with the aid of the conditions (1.15).

Assume a shell has two neighboring loaded edges while the boundary conditions at the other two edges are given in terms of displacements. Moreover, we consider that the concentrated normal force Q_n^* acts at the intersection of the loaded edges. In shell theory the following condition is taken for the corner point

$$[(\cos^2 \gamma - \sin^2 \gamma) M_{12}] = Q_n^*,$$

where the square brackets denote the jump of the quantity in the brackets with transition from one of the loaded edges to the other in the counterclockwise direction. Here γ is the angle between the unit vector $\vec{e}_1$ and the tranjectory direction, measured counterclockwise. This immediately implies that at the corner

$$M_{120}^0 = \pm \frac{Q_n^* b_1}{2} - \Phi_4,$$

$$M_{21b}^0 = \pm \frac{Q_n^* b_2}{2} - \Psi_4, \qquad (3.5)$$

Moreover, since the loading on the loaded edges is given, at the corner we know the moments appearing in the boundary conditions (3.3), and the analogous conditions for $\alpha_2 = \alpha_2^0 = $ const for the extreme P_1 and P_2 bars positioned along the loaded edges. We take the quantities $\Phi_i^*, \Psi_i^*, \left(\frac{\partial \Phi_2}{\partial s_1}\right)^*, \left(\frac{\partial \Psi_2}{\partial s_2}\right)^*$ as the edge interaction function at the loaded edges. Then in accordance with the boundary conditions of the type (3.3) we can analyze the extreme P_1 and P_2 bars. Moreover, by inverting the operators (1.9), (1.11) we find the quantities Φ_1, Ψ_1. After this we can establish the boundary conditions the type (3.3) for all the P_1 and P_2 bars. Calculation of the P_1 and P_2 bars makes it possible to determine the internal forces (moments) with zero superscript and write with the aid of (1.14), (1.15) the ten equations for finding the quantities $\Phi_i^*, \Psi_i^*, \left(\frac{\partial \Phi_2}{\partial s_1}\right)^*, \left(\frac{\partial \Psi_2}{\partial s_2}\right)^*$.

Other boundary conditions and also the existence of an oblique edge may be examined similarly. In the case of the oblique edge, additional edge interaction loads appear, acting between the bar systems which converge at the edge. This is the only problem complication

which appears for the oblique edge. The shell support scheme in which the families of bars under consideration may not be in equilibrium under the influence of external loads and support reactions presents a problem for this technique. For example, this sort of case includes the shell with two opposite free (or loaded edges) which coincide with the lines of curvature. In this case we note the technique of [2] which makes it possible to turn to consideration of the conventional edge conditions. Thus, in all cases the edge conditions adopted in shell theory together with the corresponding relations for the four-layer P_{4c} bar system make it possible to formulate the boundary conditions for the bars forming P_{4c}. Therefore, P_{4c} becomes completely equivalent to the shell within the framework of general shell theory [3].

4. There are thirteen interaction loads in the P_{4c} system. The number may be reduced to nine and in the case of the Love elasticity relation to seven by a slight generalization of the concept of the crossed and continuous P bar system. We rewrite the uncoupled system of equations (1.8)—(1.11) in the form

$$
\begin{aligned}
L_{u_i}(T_{1b}, M_{1b}, T_{12b}^0, M_{12b}^0) = \\
= K_{u_i}(P_{1b}, P_{2b}, P_{n3}, q_{1b}^{(1)}, q_{2b}^{(1)}, q_{nb}^{(1)}, m_{1b}^{(1)}, m_{2b}^{(1)}) + \\
+ K_{u_i}(0, 0, 0, f_{1b}^{(1)}, f_{2b}^{(1)}, f_{nb}^{(1)}, 0, n_{2b}^{(1)});
\end{aligned}
\tag{4.1}
$$

$$
\begin{aligned}
L_{u_i}(0, 0, \Phi_3, \Phi_4) = \\
= K_{u_i}(0, 0, 0, -f_{1b}^{(1)}, -f_{2b}^{(1)}, -f_{nb}^{(1)}, 0, -n_{2b}^{(1)}) \\
(l = 1, 2, 3, 4);
\end{aligned}
\tag{4.2}
$$

$$
\begin{aligned}
L_{u_i}(T_{2b}, M_{2b}, T_{21b}^0, M_{21b}^0) = \\
= K_{u_i}(0, 0, 0, q_{1b}^{(2)}, q_{2b}^{(2)}, q_{nb}^{(2)}, m_{1b}^{(2)}, m_{2b}^{(2)}) + \\
+ K_{u_i}(0, 0, 0, f_{1b}^{(2)}, f_{2b}^{(2)}, f_{nb}^{(2)}, n_{1b}^{(2)}, 0);
\end{aligned}
\tag{4.3}
$$

$$
\begin{aligned}
L_{u_i}(0, 0, \Psi_3, \Psi_4) = \\
= K_{u_i}(0, 0, 0, -f_{1b}^{(2)}, -f_{2b}^{(2)}, -f_{nb}^{(2)}, -n_{1b}^{(2)}, 0) \\
(l = 1, 2, 3, 4).
\end{aligned}
\tag{4.4}
$$

Here only two of the four interaction functions in (4.2) are independent, since they are all related by the two equations which follow

from (4.2). A similar situation exists in (4.4). Thus, in (4.1)—(4.4) there are nine independent interaction functions which must satisfy the five conditions (1.13) and four of the conditions (1.14), (1.15), in which Φ_3, Φ_4, Ψ_3, Ψ_4, figure.

Let us examine the mechanical meaning of the uncoupled equations (4.1)—(4.4). We first consider the equations (4.1), (4.3), dropping therein the interaction functions which appear in (4.2), (4.4). They do not differ at all from the equilibrium equations of the P bars if we take $T_{1b}, M_{1b}, T_{2b}, M_{2b}$, to mean, respectively, the normal forces and bending moments in the bars. However, in this case we have in place of (1.6)

$$\varepsilon_k = \frac{1}{1-\nu^2}\left(\frac{T_{kb}}{B_k} - \nu\frac{T_{tb}}{B_t}\right), \quad \varkappa_k = \frac{1}{1-\nu^2}\left(\frac{M_{kb}}{D_k} - \nu\frac{M_{tb}}{D_t}\right),$$
$$\omega_k = \frac{T_{kib}^s}{L_k}, \quad \tau_k = \frac{M_{kib}^s}{D_{wk}} \quad (k=1, 2; t=2, 1).$$

(4.5)

Hence we see that the difference between the crossed and continuous bar system described by the equilibrium equations (4.1), (4.3) with the elasticity law (4.5), and the crossed and continuous P bar system lies in the first two relations (4.5). If we call this the P_ν system and denote it by $P_{1\nu}$, $P_{2\nu}$, this difference between P_ν and P reduces to the fact that we can no longer consider separately the families of $P_{1\nu}$ and $P_{2\nu}$ bars positioned along s_1 and s_2, respectively. The deformations, displacements and rotations in $P_{1\nu}$ depend on the T_{2b}, M_{2b}, acting in $P_{2\nu}$ and vice versa. Thus, in this case we must consider the P_ν crossed system as a whole. Obviously, for $\nu = 0$ this connection between $P_{1\nu}$ and $P_{2\nu}$ disappears and the P_ν system transitions to P.

The necessity for considering P_ν as a whole has little effect on its analysis and calculation in the spirit of the bar system. In fact, in the statically determinate case the equilibrium equations (4.1), (4.3) for $P_{1\nu}$ and $P_{2\nu}$ may be integrated independently. Moreover, for the $P_{1\nu}$, $P_{2\nu}$ bars we can write formulas analogous to (2.1) for finding the generalized displacements from the given deformations

$$\Delta_{ij}^b = \int_{s_b} \frac{1}{1-\nu^2} \left(\frac{T_{kbi}}{B_k} - \nu \frac{T_{lbi}}{B_l} \right) T_{kbj} ds_k +$$

$$+ \int_{s_b} \frac{1}{1-\nu^2} \left(\frac{M_{kbi}}{D_k} - \nu \frac{M_{lbi}}{D_l} \right) M_{kbj} ds_k +$$

$$+ \int_{s_b} \frac{T^0_{kbi} T^0_{kbj}}{L_k} ds_k + \int_{s_b} \frac{M^0_{kbi} M^0_{kbj}}{D_{ak}} ds_k \quad (k=1, 2; \; l=2, 1).$$

$$(4.6)$$

Finally, the five interaction loads (2.2) in P_ν are found from the five conditions (1.13), which express the equality of the displacements and rotations for the $P_{1\nu}$ and the $P_{2\nu}$ systems.

In the general case with account for all nine interaction functions we can by analogy with P_{4c}, consider the four-layer bar system $P_{4c\nu}$ which is continuous and crossed at every layer. This system is formed sequentially by the families of bars $P_{21\nu}$, $P_{1\nu}$, $P_{2\nu}$, $P_{12\nu}$, The nature of the $P_{21\nu}$ and $tP_{12\nu}$ bars is the same as that of P_{21} and P_{12}, except that in this case the quantities Φ_1, Φ_2, Ψ_1, Ψ_2, are missing. From the equation (4.2), (4.4), we can find Φ_3, Φ_4 and Ψ_3, Ψ_4, and then these values are used to find the quantities T^0_{21b} $(P_{21\nu})$ M^0_{21b} $(P_{21\nu})$ and T^0_{12b} $(P_{12\nu})$, M^0_{12b} $(P_{12\nu})$, in accordance with (1.14) and with (1.15). We define the displacements and rotations in $P_{21\nu}$ as follows

$$u_2^{(21\nu)} = u_2^{(1\nu)}, \quad w^{(21\nu)} = w^{(1\nu)},$$

$$\frac{\partial u_1^{(21\nu)}}{\partial s_2} - \frac{1}{A_2} \cdot \frac{\partial A_2}{\partial s_1} u_2^{(1\nu)} = \frac{T^0_{21b}(P_{21\nu})}{L_2},$$

$$\frac{\partial \vartheta_1^{(21\nu)}}{\partial s_2} + \frac{1}{A_2} \cdot \frac{\partial A_2}{\partial s_1} \left(\frac{\partial w^{(1\nu)}}{\partial s_2} - \frac{u_2^{(1\nu)}}{R_2} \right) = \frac{M^0_{21b}(P_{21\nu})}{D_{a2}}, \quad (4.7)$$

where the indices (21 ν) and (1ν) denote, respectively, displacements and rotations in the $P_{21\nu}$ and $P_{1\nu}$ systems. We proceed similarly in the $P_{12\nu}$ system, setting therein

$$u_1^{(12\nu)} = u_1^{(2\nu)}, \quad w^{(12\nu)} = w^{(2\nu)},$$

$$\frac{\partial u_2^{(12\nu)}}{\partial s_1} - \frac{1}{A_1} \cdot \frac{\partial A_1}{\partial s_2} u_1^{(2\nu)} = \frac{T^0_{12b}(P_{12\nu})}{L_1},$$

$$\frac{\partial \vartheta_2^{(12\nu)}}{\partial s_1} + \frac{1}{A_1} \cdot \frac{\partial A_1}{\partial s_2} \left(\frac{\partial w^{(2\nu)}}{\partial s_1} - \frac{u_1^{(2\nu)}}{R_1} \right) = \frac{M^0_{12b}(P_{12\nu})}{D_{a1}}$$

$$(4.8)$$

In this case the four conditions of equality of the corresponding displacements and rotations for each of the $P_{21\nu}$, $P_{1\nu}$, and $P_{2\nu}$, $P_{12\nu}$ systems

$$u_1^{(21\nu)} = u_1^{(1\nu)}, \quad \vartheta_1^{21\nu} = -\frac{\partial w^{(1\nu)}}{\partial s_1} + \frac{u_1^{(1\nu)}}{R_1},$$

$$u_2^{(12\nu)} = u_2^{(2\nu)}, \quad \vartheta_2^{(12\nu)} = -\frac{\partial w^{(2\nu)}}{\partial s_2} + \frac{u_2^{(2\nu)}}{R_2},$$

$$(4.9)$$

and also the five conditions (1.13) for $P_{1\nu}$ and $P_{2\nu}$ yield all the necessary equations for finding the nine interaction loads. In fact, all these conditions will be equivalent to (1.13) and the four conditions (1.14), (1.15) with Φ_3, Φ_4, Ψ_3, Ψ_4. This in turn leads to the uncoupled equations (4.1)—(4.4) together with (4.5), describing the behavior of $P_{4c\nu}$, becoming completely equivalent to the equations of shell theory.

The boundary conditions in $P_{4c\nu}$ are formulated similarly to those in P_{4c}, with the exception that Φ_1, Φ_2, Ψ_1, Ψ_2, are missing in $P_{4c\nu}$.

5. The four-layer P_{4c} system consists of the bar system P_{21}, P_1, P_2, P_{12}. It is not difficult to see that as a rule P_{21}, P_{12}, are relatively compliant systems and the crossed P bar system forms the basis of P_{4c}. This applies even more to the $P_{4c\nu}$ system, in which P_ν forms the basis. However, the technique for calculating the P system does not differ from that for calculating the conventional crossed bar systems. Nor is this difference essential in the case of the P_ν system. In general neglect of Φ_4, Ψ_4, in (1.5) and in all the succeeding formulas does not lead to a large error. Moreover, if we use the elasticity law in the Love form, the difference between P_{4c} and P will be due to ν and Φ_3, Ψ_3 while the difference between $P_{4c\nu}$ and P_ν will be due only to Φ_3, Ψ_3, which are proportional to the shear deformation components. Sometimes P_{4c} and $P_{4c\nu}$ degenerate into P and P_ν. For example, this occurs in plate bending, axisymmetric deformation of shells of revolution and so on. In many cases the transition from P_{4c} and $P_{4c\nu}$ to P and P_ν may be accomplished approximately. Moreover, in general in calculating P_{4c} and $P_{4c\nu}$ we examine the iteration process with consideration of only the P and P_ν systems at each step.

6. In the uncoupling method the conditions (1.13), (1.14), (1.15) or (1.13), (2.3), (2.4) lead to a system of integral equations of the Fredholm type of the first kind in terms of the interaction functions (interaction loads). They are obtained by inverting the operators (1.8)—(1.12) and equating the corresponding quantities in accordance with (1.13), (1.14), (1.15) or (1.13), (2.3), (2.4). A peculiarity of these integral equations is that the unknown functions of two variables appear in these equations as single integrals of each variable separately. Moreover, in the case of certain boundary conditions they may contain nonintegral terms with values of the unknown functions at the edges. In the general case the number of such equations for the P_{4c} system is thirteen, and for the P_{4cv} system the number is nine. In those cases in which additional interaction loads do not occur, the number decreases to five and in several concrete problems the number may be even less. Thus, the problem of calculating the continuous and crossed bar systems obtained above reduces to the solution of the corresponding integral equations of the uncoupling method.

Now let us consider the discrete bar systems. We can use the following technique to discretize the integral equations of the uncoupling method. We form a grid on the shell middle surface using the lines of principal curvature. We specify on the grid lines the unknown distributed interaction loads as depending on n unknown parameters, where n is the number of nodes of the grid being used. Then we determine these n parameters from the conditions for satisfaction of the integral equations or the conditions (1.13), (1.14) (1.15) or (1.13), (2.3), (2.4) only at the grid nodes (colocation method for integral equations). This approximate method for solving the problem may be treated in a certain sense as the calculation of a crossed bar system with distributed unknown interaction loads. However, it is of interest to go directly to the calculation of the discrete bar system with concentrated interaction loads at the nodes. We shall show how this may be done, using as an example the bending of a plate.

In the case of bending of a flat plate, we shall dwell in greater detail on the discretization and peculiarities of the numerical solution of the integral equations of the uncoupling method. The uncoupled plate equations may be transformed to the equations for the continuous and crossed P bar system

$$
\begin{cases}
D\dfrac{\partial^4 \bar w^{(1)}}{\partial x^4} = p_n + q_n + \dfrac{\partial \bar m_1}{\partial x}, \\
D\dfrac{\partial^2 \vartheta^{(1)}}{\partial x^2} = \bar m_2;
\end{cases}
\tag{6.1}
$$

$$
\begin{cases}
D\dfrac{\partial^4 \bar w^{(2)}}{\partial y^4} = -q_n + \dfrac{\partial \bar m_1}{\partial y}, \\
D\dfrac{\partial^2 \vartheta^{(2)}}{\partial y^2} = \bar m_1,
\end{cases}
\tag{6.2}
$$

where the subscript b is dropped, since we have assumed $b_1 = b_2 = 1$ and

$$
\bar m_k = \frac{m^{(k)}}{1 - v} \quad (k = 1, 2).
$$

In this case the conditions (1·13) will be

$$
w^{(1)} = w^{(2)}, \quad \vartheta_2^{(1)} = -\frac{\partial w^{(2)}}{\partial y}, \quad \vartheta_1^{(2)} = -\frac{\partial w^{(1)}}{\partial x}
\tag{6.3}
$$

and the problem reduces to a system of three integral equations in q_n, $\bar m_1$, $\bar m_2$. For simplicity of analysis, we consider a rectangular plate which is clamped along the contour, and we take approximately $\bar m_1 = \bar m_2 = 0$. Then, solving the first ordinary differential equations (6-1), (6-2), satisfying the clamping boundary conditions and satisfying the first conditions (6.3), we obtain

$$
\int_a^b \int_c^d \left[\delta(t' - y) K_1(x, t) + \delta(t - x) K_2(y, t') \right] q_n(t, t')\, dt\, dt' =
$$
$$
= -\int_a^b \int_c^d \delta(t' - y) K_1(x, t) p_n(t, t')\, dt\, dt' = -F(x, y),
\tag{6.4}
$$
$$
a \leqslant x \leqslant b; \quad c \leqslant y \leqslant d,
$$

where δ is the delta function, $K_1(x, t)$, $K_2(y, t')$ are the deflection influence functions for the clamped P bars. Let us break down the region in question by a grid of straight lines. If we use the idea of the colocation method and equate the left and right sides of (6.4)

at the grid nodes, and specify q_n (x, y) to within undetermined parameters on the straight grid lines, we obtain a system of algebraic equations. The same equations are obtained when calculating the discrete and crossed system of P bars, defined on the grid lines, with distributed interaction loads. We can proceed differently. We replace the integral in the left side of (6.4) using the formulas for mechanical quadrature. We consider that the grid nodes coincide with the nodes of the quadrature formulas, and we equate the left and right sides of (6.4) at these same points. Then we obtain a system of algebraic equations of the form

$$\sum_{k=2}^{a-1} A_k^{(x)} K_1(x_i, x_k) q_a(x_k, y_j) +$$
$$+ \sum_{k=2}^{a-1} A_k^{(y)} K_2(y_j, y_k) q_a(x_i, y_k) = -F(x_i, y_j) + \rho_{ij}$$

(6.5)

where factors $A_k^{(x)}$, $A_k^{(y)}$ result from the quadrature formulas and ρ_{ij} are the overall error of the quadrature formulas. Setting $\rho_{ij} = 0$, we obtain the equations for the approximate values of of the $\bar{q}_n(x_i, y_i)$. Taking account of the physical meaning influence functions, we note that for $\rho_{ij} = 0$ and $A_{k_1}^{(x)} = A_{k_2}^{(y)} = 1$ the equations (6.5) also hold for the discrete P bar system described by the first equations (6.1), (6.2) with the concentrated excess unknowns at the nodes $q_{nc}^*(x_i, y_j)$. Hence, using a uniform grid spacing and quadrature formulas such that $A_{k_1}^{(x)} = A_{k_2}^{(y)} = A$, we obtain

$$\bar{q}_a(x_i, y_j) = \frac{q_{nc}(x_i, y_j)}{A}$$

This relates the approximate solution of the integral equations of the uncoupling method and the calculation of bar systems by the method of forces. The uncoupling method and the method of forces in structural mechanics, which are similar in form, become similar in essence. These arguments make it possible in constructing the approximate solution of the integral equation (6.4) to calculate the corresponding discrete P bar system with concentrated interaction loads at the nodes rather than calculating the system (6.5) directly.

In so doing, we can use many effective techniques of **structural** mechanics to construct the approximate solution of the integral equations in question. On the other hand, conversely, analysis of the integral equations may be useful in calculating high-order crossed bar systems.

The difficulties in the numerical solution of integral equations of the first kind are well known [5,6]. They are associated with the fact that the operator in (6.4) overrides the strongly oscillating solution and the zero is a condensation point of its eigenvalue spectrum. A similar situation occurs in calculating crossed bar systems of both the P and conventional types. There this leads to poorconditioning of the system of algebraic equations of the method of forces. The various approaches to the solution of equations of the type (6.4) reduce to the introduction in one form or another of additional information on the sought solution in the original mathematical formulation of the problem. For example, Tikhonov [5, 6] considered the sought solution to be sufficiently smooth and proposed to screen out the oscillations in the numerical solution of (6.4) by minimization of a smoothing functional. In our case we can write

$$M^\alpha = \int_a^b \int_c^d A q_\mu q_\mu \, dx \, dy + 2 \int_a^b \int_c^d q_\mu F \, dx \, dy + \alpha \Omega;$$

(6.6)

$$\Omega = \int_a^b \int_c^d \left[\varphi_1(x, y) \left(\frac{\partial q_\mu}{\partial x} \right)^2 + \varphi_2(x, y) \left(\frac{\partial q_\mu}{\partial y} \right)^2 + \varphi_3(x, y) q_\mu^2 \right] dx \, dy,$$

$$\varphi_i(x, y) > 0 \quad (i = 1, 2, 3),$$

(6.7)

where A is the operator of (6.4) and α is the parameter. Since the operator A is positive, the solution of (6.4) minimizes the functional M^0 (a = 0). The role of the regulating functional Ω consists in smoothing the approximate solution. The parameter α is selected so that the function which minimizes (6.6) will be close to the solution of (6.4), but at the same time the influence of Ω will not disappear. The Euler equation and the natural boundary conditions for the functional M^α have the form

$$\int_a^b K_1(x, t)\, q_a(t, y)\, dt + \int_c^d K_2(y, t')\, q_a(x, t')\, dt' +$$
$$+ F(x, y) = a\left\{\frac{\partial}{\partial x}\left[\varphi_1(x, y)\frac{\partial q_a}{\partial x}\right] + \right.$$
$$\left. + \frac{\partial}{\partial y}\left[\varphi_2(x, y)\frac{\partial q_a}{\partial y}\right] - \varphi_3(x, y)\, q_a\right\}.$$
$$\frac{\partial q_a}{\partial x} = 0 \quad \text{for,} \quad x=a,\ x=b; \quad \frac{\partial q_a}{\partial y} = 0 \quad \text{for } y=c,\ y=d. \tag{6.8}$$

The physical meaning of the left side of (6.8) makes it possible to conclude that in this case a filler material has appeared between the two continuous crossed systems of P bars and that the displacement law for this filler is defined by the left side of (6.8).

We can proceed similarly in calculating the bar systems. In this case we minimize the corresponding quadratic form rather than the functional $M^{\underline{\alpha}}$. For example, for a girder framework we can take in place of Ω the sum of the squares of the differences of the excess knowns at neighboring nodes of the grid in both directions, and the sum of the squares of the values of the unknown quantities themselves, multiplied by some positive weighting functions of the integer argument (of the grid nodes).

Other techniques may be used for the approximate solution of these problems of integral equations and bar systems by using additional information on the sought solution. It is often convenient to write the additional conditions in the form of inequalities and seek a solution which will satisfy these inequalities while at the same time satisfying with the maximal possible accuracy the basic problem formulation. Moreover, we can formulate overdefined problems, in which we introduce the required additional information into the basic problem formulations by means of redundant equations. The solution of the overdefined problems may be constructed using the method of least squares or in the Chebyshev approximation sense. In many cases the methods developed in linear programming [7] are effective in solving the problems mentioned above.

We can point out still another effere technique for calculating
the crossed bar system within the framewo. of quadratic programming.
We write in place of the system of equati s of the method of forces
a system of inequalities in the form

$$|Ax - F| < \alpha F \qquad (6.9)$$

and we seek a minimum of the smoothing quadratic form Ω_h, equal, for
example, to the sum of the squares of the differences of the excess
unkowns at neighboring nodes in both directions, and the sum of the
squares of the values of the unknwns themselves, multiplied by some
positive weighting functions of an integer argument (of the framework
nodes), under the condition that the inequalities (6.9) be satisfied.
We assume the function Ω_h to be convex. In the problems being
considered the quantity α, which characterizes the maximal acceptable
error in the equations of the method of forces in each specific
case, may be estimated quite accurately. Algorithms for the solution
of this problem formulation in quadratic programming theory are
known. Similar arguments may be applied to the integral equations of
the uncoupling method.

REFERENCES

1. Rozin, L. A., "The uncoupling method in shell theory," PMM,
    Vol. 25, No. 5, 1961.

2. Rozin, L. A., "On the analysis of structures by the uncoupling
    method," Information bulletin of Legidep (Leningrad Branch of
    the All-Union State Planning Institute "Gidroenergoproyekt").
    No. 21, 1961.

3. Novozhilov, V. V., Teoriya tonkikh obolochek (Thin Shell
    Theory), Moscow, State United Press of the Shipbuilding Industry.
    1962.

4. Reissner, E., A new derivation of the equations for the defor-
    mation of elastic shells. Amer. j. math., Vol. 63, No. 1,
    1941, pp. 177-184.

5. Tikhonov, A. N., "On the solution of incorrectly posed problems
    and the regularization method." DAN SSSR, (Doklady Akedemii
    Nauk SSSR) Vol. 51, No. 3., L963.

6. Tikhonov, A. N., "On the regularization of incorrectly posed problems. DAN SSSR, Vol. 153, No. 1, 1963.

7. Kantorovich, L. V., "On some new approaches to computational methods and reduction of observations," Siberskiy Matematicheskiy Zhurnal, Vol. III, No. 5, 1962.

Received 28 March 1964

ON THE DETERMINATION OF THE MOMENTLESS STRESS STATE
IN COVERINGS WITH POLYGONAL PLANFORM

V. Ya. Pavilaynen

Shells which cover a space with nonrectangular planform find
application in the construction of pavilions, trade centers, and
other structures. Here the most efficient shells are those in which
the midsurface has positive Gaussian curvature, since these shells
provide a stress state which is nearly moment-free under the primary
design loads (dead weight, snow). In this case a considerable portion
of the shell, with the exception of small regions near the edge,
operates in uniform compression and this permits effective use of the
material in reinforced concrete designs.

It is advisable to perform the calculation of these coverings on
the basis of the equations of momentless shell theory in Cartesian
coordinates, first derived by Pucher [1] and valid for shells of
arbitrary rise. In formulating the boundary conditions, it is usually
assumed that the elements of the shell supporting contour have
stiffness only in the shell plane and that the entire load is trans-
mitted by means of tangential forces. As a rule these forces increase
with approach to the corners of the covering and may, in particular,
increase without limit in absolute magnitude [2].

This fact indicates that under certain conditions the momentless
nature of the stress state is significantly disrupted near the shell

support contour and also at the shell corners. However, in many cases all the momentless forces in the shell may remain finite, and this has been the subject of several studies, including [3]. The interest in this question is explained by the fact that the determination of the contour forces, and also the stress state in the corner area, where there is a marked increase of the tangential stresses, is the most critical part of the design and controls the choice of the optimal constructional version.

In the present paper we suggest a method for calculating coverings with nonrectangular planform which differs from that of [3]. The Pucher system of equations is generalized to the case of an oblique Cartesian coordinate system. We examine several cases of the application of the resulting equations to the analysis of coverings which have an arbitrary parallelogram planform, and also the questions of direct determination of the tangential forces at the shell corners.

§ 1. Equilibrium Equations of Momentless
Shell Theory in Oblique Cartesian
Coordinates

The shell midsurface is given by

$$z = z(x, y), \tag{1.1}$$
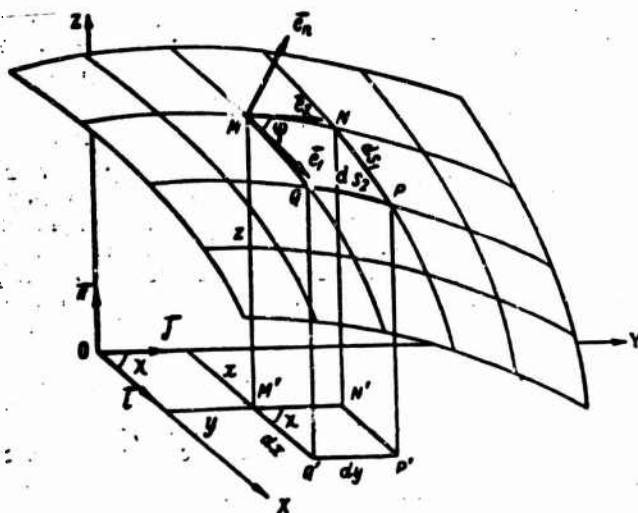
Figure 1.

where x, y, z are oblique Cartesian coordinates (Figure 1). The
X and Y axes of this system lie in the horizontal plane of the shell
planform and form the angle χ with one another. The Z axis is directed
upward along the vertical, and the unit vectors $\vec{i}, \vec{j}, \vec{k}$ are connected
by the relations

$$\vec{i} \cdot \vec{j} = \cos \chi,$$
$$\vec{i} \cdot \vec{k} = \vec{j} \cdot \vec{k} = 0:$$

$$(1.2)$$

$$[\vec{i}, \vec{j}] = \sin \chi \vec{k},$$
$$[\vec{j}, \vec{k}] = \frac{1}{\sin \chi} \vec{i} - \operatorname{ctg} \chi \vec{j},$$
$$[\vec{k}, \vec{i}] = \frac{1}{\sin \chi} \vec{j} - \operatorname{ctg} \chi \vec{i}.$$

$$(1.3)$$

In the general case, in which the shell planform is an arbitrary
polygon, it is advisable to select the angle χ and direct the X and
Y axes so that they are parallel to two adjacent sides of the shell
planform contour. The x and y coordinate lines on the midsurface
will be the curves formed by intersection with planes parallel to
the planes XOZ and YOZ, respectively. Generally speaking, such a
system is not orthogonal.

In fact, taking the parameters x and y as curvilinear Gaussian
coordinates of the surface, we write (1.1) in vector form

$$\vec{r}(x, y) = x\vec{i} + y\vec{j} + z(x, y)\vec{k}.$$

$$(1.4)$$

The vectors tangent to the coordinate lines will be

$$\frac{\partial \vec{r}}{\partial x} = \vec{r}_x = \vec{i} + \frac{\partial z}{\partial x} \vec{k},$$
$$\frac{\partial \vec{r}}{\partial y} = \vec{r}_y = \vec{j} + \frac{\partial z}{\partial y} \vec{k},$$

$$(1.5)$$

and the corresponding unit vectors are

$$\vec{e}_1 = \frac{1}{A_1} \vec{r}_x = \frac{1}{\sqrt{1 + \left(\frac{\partial z}{\partial x}\right)^2}} \left(\vec{i} + \frac{\partial z}{\partial x} \vec{k}\right),$$
$$\vec{e}_2 = \frac{1}{A_2} \vec{r}_y = \frac{1}{\sqrt{1 + \left(\frac{\partial z}{\partial y}\right)^2}} \left(\vec{j} + \frac{\partial z}{\partial y} \vec{k}\right).$$

$$(1.6)$$

Here A_1, A_2 are the Lamé parameters

$$A_1 = |\vec{r}_x| = \sqrt{1 + \left(\frac{\partial z}{\partial x}\right)^2},$$

$$A_2 = |\vec{r}_y| = \sqrt{1 + \left(\frac{\partial z}{\partial y}\right)^2}. \tag{1.7}$$

With account for (1·2) we find

$$\vec{e}_1 \cdot \vec{e}_2 = \frac{1}{\sqrt{1 + \left(\frac{\partial z}{\partial x}\right)^2} \sqrt{1 + \left(\frac{\partial z}{\partial y}\right)^2}} \left(\cos \chi + \frac{\partial z}{\partial x} \cdot \frac{\partial z}{\partial y}\right) = \cos \psi, \tag{1.8}$$

where ψ is the angle between the coordinate lines on the surface (see Figure 1). It follows from (1·8) that in the general case $\cos \psi \neq 0$ and, consequently, the coordinate line grid on the surface is not orthogonal. The unit vector normal to the surface, defined by the formula

$$\vec{e}_n = \frac{1}{\sin \psi} \left[\vec{e}_1, \vec{e}_2\right]$$

will be, on the basis of (1·3) and (1·8),

$$\vec{e}_n = \frac{1}{\sqrt{\sin^2 \chi + \left(\frac{\partial z}{\partial x}\right)^2 + \left(\frac{\partial z}{\partial y}\right)^2 - 2\cos\chi \frac{\partial z}{\partial x} \cdot \frac{\partial z}{\partial y}}} \times$$
$$\times \left[\left(-\frac{1}{\sin\chi} \cdot \frac{\partial z}{\partial x} + \operatorname{ctg}\chi \frac{\partial z}{\partial y}\right)\vec{i} + \right.$$
$$\left. + \left(-\frac{1}{\sin\chi} \cdot \frac{\partial z}{\partial y} + \operatorname{ctg}\chi \frac{\partial z}{\partial x}\right)\vec{j} + \sin\chi \vec{k}\right]. \tag{1.9}$$

Let us consider the conditions for momentless equilibrium of a small element cut from the shell by two nearby planes parallel to the XOZ plane and by two nearby planes parallel to the YOZ plane (see Figure 1). The sides of this element are

$$ds_1 = \sqrt{1 + \left(\frac{\partial z}{\partial x}\right)^2} \, dx,$$

$$ds_2 = \sqrt{1 + \left(\frac{\partial z}{\partial y}\right)^2} \, dy, \tag{1.10}$$

and its projection on the XOY plane is a parallelogram with sides dx and dy and the included angle χ.

We denote the force vector acting on the unit arc length MN by $-\vec{T}_x$ and the force vector acting on the unit arc length MQ by $-\vec{T}_y$, where

$$\vec{T}_x = T_{xx}\vec{i} + T_{xy}\vec{j} + T_{xz}\vec{k},$$
$$\vec{T}_y = T_{yx}\vec{i} + T_{yy}\vec{j} + T_{yz}\vec{k}. \qquad (1.11)$$

Then the force acting on the entire arc MN equals

$$-\vec{T}_x ds_2 = -\vec{T}_x \sqrt{1 + \left(\frac{\partial z}{\partial y}\right)^2}\, dy = -\vec{S}_x dy, \qquad (1.12)_1$$

and on the arc MQ
$$-\vec{T}_y ds_1 = -\vec{T}_y \sqrt{1 + \left(\frac{\partial z}{\partial x}\right)^2}\, dx = -\vec{S}_y dx. \qquad (1\;12)_2$$

On the opposite sides PQ and NP the following forces act

$$\vec{T}_x ds_2 + \frac{\partial \vec{T}_x ds_2}{\partial x}\, dx = \left(\vec{S}_x + \frac{\partial \vec{S}_x}{\partial x}\, dx\right) dy, \qquad (1.13)$$
$$\vec{T}_y ds_1 + \frac{\partial \vec{T}_y ds_1}{\partial y}\, dy = \left(\vec{S}_y + \frac{\partial \vec{S}_y}{\partial y}\, dy\right) dx.$$

In (1.12), (1.13) we have introduced the new forces $\vec{S}_x$ and $\vec{S}_y$, whose decompositions along the $\vec{i}, \vec{j}, \vec{k}$ axes have the form

$$\vec{S}_x = S_{xx}\vec{i} + S_{xy}\vec{j} + S_{xz}\vec{k},$$
$$\vec{S}_y = S_{yx}\vec{i} + S_{yy}\vec{j} + S_{yz}\vec{k}, \qquad (1.14)$$

and from (1.11) and (1.12) we have the obvious relations

$$S_{xx} = T_{xx}\sqrt{1 + \left(\frac{\partial z}{\partial y}\right)^2}, \quad S_{yx} = T_{yx}\sqrt{1 + \left(\frac{\partial z}{\partial x}\right)^2},$$
$$S_{xy} = T_{xy}\sqrt{1 + \left(\frac{\partial z}{\partial y}\right)^2}, \quad S_{yy} = T_{yy}\sqrt{1 + \left(\frac{\partial z}{\partial x}\right)^2}, \qquad (1.15)$$
$$S_{xz} = T_{xz}\sqrt{1 + \left(\frac{\partial z}{\partial y}\right)^2}, \quad S_{yz} = T_{yz}\sqrt{1 + \left(\frac{\partial z}{\partial x}\right)^2}.$$

We denote the external force vector acting on the shell element in question by

$$d\vec{P}=\left[q_x(x,\ y)\vec{i}+q_y(x,\ y)\vec{j}+q_z(x,\ y)\vec{k}\right]d\Omega,$$

where $d\Omega=\sin\chi\,dx\,dy$ is the area of the parallelogram M'N'P'Q' (see Figure 1) and q_x, q_y, q_z are the load intensities, given in the XOY coordinate plane.

The condition for vanishing of the principal vector of the external and internal forces applied to the element is expressed by the equation

$$\frac{\partial\vec{S}_x}{\partial x}+\frac{\partial\vec{S}_y}{\partial y}+\left(q_x\vec{i}+q_y\vec{j}+q_z\vec{k}\right)\sin\chi=0, \tag{1.16}$$

which is projected onto the coordinate axes with account for (1.14) and (1.2) to yield

$$\left(\frac{\partial S_{xx}}{\partial x}+\frac{\partial S_{yx}}{\partial y}\right)+\left(\frac{\partial S_{xy}}{\partial x}+\frac{\partial S_{yy}}{\partial y}\right)\cos\chi+q_x\sin\chi=0,$$
$$\left(\frac{\partial S_{xx}}{\partial x}+\frac{\partial S_{yx}}{\partial y}\right)\cos\chi+\left(\frac{\partial S_{xy}}{\partial x}+\frac{\partial S_{yy}}{\partial y}\right)+q_y\sin\chi=0,$$
$$\frac{\partial S_{xz}}{\partial x}+\frac{\partial S_{yz}}{\partial y}+q_z\sin\chi=0. \tag{1.17}$$

Consider the first two equations (1.17). Since in all the arguments it is assumed that the angle $\chi\neq0,\pi$ (otherwise the problem formulation loses meaning), these equations may be solved for the expressions in the parentheses. As a result (1.17) is written as

$$\frac{\partial S_{xx}}{\partial x}+\frac{\partial S_{yx}}{\partial y}=-\frac{q_x}{\sin\chi}+q_y\operatorname{ctg}\chi,$$
$$\frac{\partial S_{xy}}{\partial x}+\frac{\partial S_{yy}}{\partial y}=-\frac{q_y}{\sin\chi}+q_x\operatorname{ctg}\chi,$$
$$\frac{\partial S_{xz}}{\partial x}+\frac{\partial S_{yz}}{\partial y}=-q_z\sin\chi. \tag{1.18}$$

Now let us find the condition for vanishing of the principal moment of all the forces acting on the isolated middle surface element. We take as the reference point the center of gravity of the element(see Figure 1),and we note that the radius vectors of the points of application of the internal forces on its edges are characterized by the relations

$$d\vec{s}_1=dx\vec{i}+dz\vec{k}=\left(\vec{i}+\frac{\partial z}{\partial x}\vec{k}\right)dx,$$
$$d\vec{s}_2=dy\vec{j}+dz\vec{k}=\left(\vec{j}+\frac{\partial z}{\partial y}\vec{k}\right)dy. \tag{1.19}$$

Then, retaining terms of no higher than second order of smallness, the sought equality is written in the form

$$\left[\vec{S}_x dy, \left(\vec{i}+\frac{\partial z}{\partial x}\vec{k}\right)dx\right]+\left[\vec{S}_y dx, \left(\vec{j}+\frac{\partial z}{\partial y}\vec{k}\right)dy\right]=0. \tag{1.20}$$

Projecting (1.20) onto the coordinate axes and considering (1.14) (1.3), $\sin \chi \neq 0$, we find

$$S_{yz}+S_{zz}\cos\chi=\left(S_{yy}\frac{\partial z}{\partial y}+S_{x_y}\frac{\partial z}{\partial x}\right)+\left(S_{zx}\frac{\partial z}{\partial x}+S_{yz}\frac{\partial z}{\partial y}\right)\cos\chi, \tag{1.21}$$
$$S_{yz}\cos\chi+S_{xz}=\left(S_{zx}\frac{\partial z}{\partial x}+S_{yz}\frac{\partial z}{\partial y}\right)+\left(S_{y_z}\frac{\partial z}{\partial y}+S_{xy}\frac{\partial z}{\partial x}\right)\cos\chi,$$
$$S_{xy}=S_{yx}.$$

From the first two equations (1.21) we have

$$S_{xz}=S_{xx}\frac{\partial z}{\partial x}+S_{yx}\frac{\partial z}{\partial y},$$
$$S_{yz}=S_{yy}\frac{\partial z}{\partial y}+S_{xy}\frac{\partial z}{\partial x}. \tag{1.22}$$

Equalities (1.22) show that the internal forces on the shell which is in the momentless stress state do not have components normal to the midsurface. To see this we examine the decompositions of the vectors $\vec{T}_x$, $\vec{T}_y$, along the directions $\vec{e}_1$, $\vec{e}_2$, $\vec{e}_n$:

$$\vec{T}_x=T_1\vec{e}_1+T_{12}\vec{e}_2+T_{1n}\vec{e}_n, \tag{1.23}$$
$$\vec{T}_y=T_{21}\vec{e}_1+T_2\vec{e}_2+T_{2n}\vec{e}_n.$$

Projecting $\vec{T}_x$ on the direction $\vec{e}_n$ and taking account of (1.9) and (1.11), we have

$$\vec{T}_x\cdot\vec{e}_n=T_{1n}=\frac{\sin\chi}{\sqrt{\sin^2\chi+\left(\frac{\partial z}{\partial x}\right)^2+\left(\frac{\partial z}{\partial y}\right)^2-2\cos\chi\frac{\partial z}{\partial x}\cdot\frac{\partial z}{\partial y}}}\times$$
$$\times\left[-T_{xx}\frac{\partial z}{\partial x}-T_{xy}\frac{\partial z}{\partial y}+T_{xz}\right]=0,$$

since the expression in the square brackets vanishes in view of (1.15) and (1.22)$_1$.

We obtain similarly

$$\vec{T}_y \cdot \vec{e}_1 = T_{2s} = 0.$$

Now let us find the coefficients T_1, T_{12}, T_{21}, T_2, i.e., the components of the vectors $\vec{T}_x$ and $\vec{T}_y$ along the coordinate directions. We project $\vec{T}_x$ onto the directions $\vec{e}_1$ and $\vec{e}_2$:

$$\vec{T}_x \cdot \vec{e}_1 = T_1 + T_2 \cos \varphi =$$
$$= \frac{1}{\sqrt{1+\left(\frac{\partial z}{\partial x}\right)}}\left(T_{xx} + \cos \chi T_{xy} + \frac{\partial z}{\partial x} T_{xz}\right).$$

$$\vec{T}_x \cdot \vec{e}_2 = T_1 \cos \varphi + T_{12} =$$
$$= \frac{1}{\sqrt{1+\left(\frac{\partial z}{\partial y}\right)^2}}\left(T_{xx} \cos \chi + T_{xy} + \frac{\partial z}{\partial y} T_{xz}\right). \tag{1.24}$$

Transforming the numerator in the right side of $(1.24)_1$ with account for (1.15) and $(1.22)_1$, we obtain the expression

$$T_{xx} + \cos \chi T_{xy} + \frac{\partial z}{\partial x} T_{xz} = \frac{1}{\sqrt{1+\left(\frac{\partial z}{\partial y}\right)^2}}\left[S_{xx} + \cos \chi S_{xy} + \right.$$
$$+ \frac{\partial z}{\partial x}\left(S_{xx}\frac{\partial z}{\partial x} + S_{xy}\frac{\partial z}{\partial y}\right)\right] =$$
$$= \frac{1}{\sqrt{1+\left(\frac{\partial z}{\partial y}\right)^2}}\left\{\left[1+\left(\frac{\partial z}{\partial x}\right)^2\right]S_{xx} + \left(\cos \chi + \frac{\partial z}{\partial x}\cdot\frac{\partial z}{\partial y}\right)S_{xy}\right\}.$$

which we substitute into $(1.24)_1$ to find

$$T_1 + T_{12}\cos \varphi = \sqrt{\frac{1+\left(\frac{\partial z}{\partial x}\right)^2}{1+\left(\frac{\partial z}{\partial y}\right)^2}}\, S_{xx} + \cos \varphi S_{xy}. \tag{$1.25)_1$}$$

Equality $(1.24)_2$ is reduced in the same way to the form

$$T_1 \cos \varphi + T_{12} = \cos \varphi \sqrt{\frac{1+\left(\frac{\partial z}{\partial x}\right)^2}{1+\left(\frac{\partial z}{\partial y}\right)^2}}\, S_{xx} + S_{xy}, \tag{$1.25)_2$}$$

Hence

$$T_1 = \sqrt{\frac{1 + \left(\frac{\partial z}{\partial x}\right)^2}{1 + \left(\frac{\partial z}{\partial y}\right)^2}}\, S_{xx}, \quad T_{12} = S_{xy}. \tag{1.26}$$

The coefficients T_{21} and T_2 are found by entirely analogous arguments as a result of which we have

$$T_2 = \sqrt{\frac{1 + \left(\frac{\partial z}{\partial y}\right)^2}{1 + \left(\frac{\partial z}{\partial x}\right)^2}}\, S_{yy}, \quad T_{21} = S_{..} \tag{1.27}$$

Formulas (1.26) and (1.27), first derived by Pucher [1], define all the tangential forces in the momentless shell and, in particular, establish the pairing law for the tangential stresses T_{12} and T_{21} in the adopted coordinate system.

To derive the resolving equation of the problem, we substitute S_{xz} and S_{yz} in accordance with (1.22) and $(1.21)_3$ into $(1.18)_3$ which takes the form

$$S_{xx}\frac{\partial^2 z}{\partial x^2} + 2S_{xy}\frac{\partial^2 z}{\partial x \partial y} + S_{yy}\frac{\partial^2 z}{\partial y^2} = q_x\left(\frac{1}{\sin\chi}\cdot\frac{\partial z}{\partial x} - \operatorname{ctg}\chi\frac{\partial z}{\partial y}\right)$$
$$+ q_y\left(\frac{1}{\sin\chi}\cdot\frac{\partial z}{\partial y} - \operatorname{ctg}\chi\frac{\partial z}{\partial x}\right) - q_z\sin\chi. \tag{1.28}$$

The first two equations (1.18) will be satisfied identically if we introduce the stress function F, associated with the forces S_{xx}, S_{xy}, S_{yy} by the formulas

$$S_{xx} = \frac{\partial^2 F}{\partial y^2} - \int_{x_0}^{x}\left[\frac{q_x}{\sin\chi} - q_y\operatorname{ctg}\chi\right]dx,$$
$$S_{yy} = \frac{\partial^2 F}{\partial x^2} - \int_{y_0}^{y}\left[\frac{q_y}{\sin\chi} - q_x\operatorname{ctg}\chi\right]dy, \tag{1.29}$$
$$S_{xy} = S_{yx} = -\frac{\partial^2 F}{\partial x \partial y}$$

and (1.28) takes the final form

$$\frac{\partial^2 z}{\partial y^2}\cdot\frac{\partial^2 F}{\partial x^2}-2\frac{\partial^2 z}{\partial x\partial y}\frac{\partial^2 F}{\partial x\partial y}+\frac{\partial^2 z}{\partial x^2}\cdot\frac{\partial^2 F}{\partial y^2}=-q_z\sin\chi$$
$$+\frac{\partial}{\partial x}\left[\frac{\partial z}{\partial x}\int_{x_0}^{x}\left(\frac{q_x}{\sin\chi}-q_y\,\mathrm{ctg}\,\chi\right)dx\right]+$$
$$+\frac{\partial}{\partial y}\left[\frac{\partial z}{\partial y}\int_{y_0}^{y}\left(\frac{q_y}{\sin\chi}-q_x\,\mathrm{ctg}\,\chi\right)dy\right]$$

(1.30)

and is identical to the familiar Pucher equation [1], differing from
the latter only in the form of the right side. Thus (1.30) may be
considered a generalization of the Pucher equation to the oblique
Cartesian coordinate system.

§. 2. Some Analysis Problems

It is convenient to use the relations obtained in the preceding
section for the analysis of shells whose planform is arbitrary. In
this case we refer the surface to the oblique Cartesian coordinate
system and find the solution of (1.30).

The use of this equation makes it possible to determine directly
the tangential forces at the corners of coverings with polygonal
planform, which is of definite practical interest. We shall demon-
strate this on the example of a paraboloid of revolution having an
equilateral triangle planform. We first consider the XYZ system of
rectangular Cartesian coordinates in which the equation of the shell
midsurface has the form (Figure 2)

$$z=h-\frac{h}{4a^2}(x^2+y^2),$$

(2.1)

and the load is distributed uniformly in the planform plane, i.e.,

$$q_z=-q_0=\mathrm{const.}$$

Then the problem reduces to integration of the Poisson equation

$$\frac{\partial^2 F}{\partial x^2}+\frac{\partial^2 F}{\partial y^2}=-\frac{2q_0a^2}{h},$$

(2.2)

whose solution, by analogy with the problem of torsion of a prismatic
bar, may be obtained in closed form [2].

$$F = -\frac{q_0 a^2}{h}\left[\frac{1}{6a}(x^3 - 3xy^2) - \frac{2}{3}a^2 + \frac{1}{2}(x^2 + y^2)\right].$$ (2.3)

Differentiating (2.3), we find the forces S_{xx}, S_{yy}, S_{xy}:

$$S_{xx} = -\frac{q_0 a^2}{h}\left(1 - \frac{x}{a}\right),$$
$$S_{yy} = -\frac{q_0 a^2}{h}\left(1 + \frac{x}{a}\right),$$ (2.4)
$$S_{xy} = -\frac{q_0 a^2}{h}\cdot\frac{y}{a}.$$
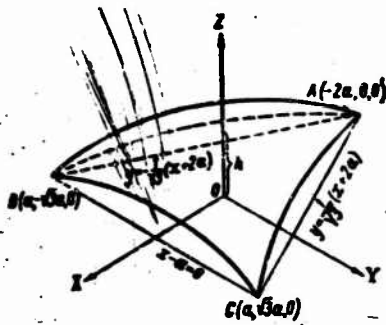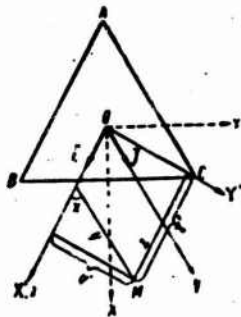
Figure 2.   Figure 3

At the boundary $y = \frac{1}{\sqrt{3}}(x + 2a)$ the forces normal and tangential
to the contour are found from the formulas

$$S'_{yy} = S_{xx}\sin^2\alpha + S_{yy}\cos^2\alpha - S_{xy}\sin 2\alpha,$$
$$S'_{xy} = \frac{1}{2}(S_{yy} - S_{xx})\sin 2\alpha + S_{xy}\cos 2\alpha,$$ (2.5)

where α is the angle between the tangent to the contour and the X
axis. Substituting (2.4) into these equalities and setting $\alpha = \frac{\pi}{6}$,
we obtain

$$S'_{yy} = 0, \quad S'_{xy} = \frac{2}{\sqrt{3}}\cdot\frac{q_0 a^2}{h}\left(\frac{1}{2} + \frac{x}{a}\right).$$

In particular, at the shell corners

$$S'_{xy} = -\frac{q a^2 \sqrt{3}}{h} \quad \text{for } x = -2a,$$
$$S'_{xy} = \frac{q a^2 \sqrt{3}}{h} \quad \text{for } x = a.$$

(2.6)

We note that the same values of S_{xy} may be obtained if in $(2.4)_3$ we set $y = \pm \sqrt{3}a$.

Thus, in the general case, in order to determine the tangential forces at the shell corners we must have, first, the solution of the differential equation (2.2) and, second, the subsequent scaling of the forces.

Let us show that all this may be avoided if we use (1.30). We return to the example in question. In the shell planform plane we introduce the oblique Cartesian coordinate system xOy (Figure 3), which may be obtained from the basic coordinate system by rotating the system XOY through the angle $\frac{\pi}{6}$ clockwise and a further rotation of the Y' axis through the same angle. Let us find the equation of the surface (2.1) in this coordinate system.

The expression $x^2 + y^2$ is invariant to the first axis of rotation; therefore, (2.1) remains unchanged in the X'OY' system. In the second transformation the coordinates of any point M in the X'OY' and xOy systems will be connected by the relations

$$x' = x + y \cos \chi,$$
$$y' = y \sin \chi.$$

(2.7)

Substituting (2.7) into (2.1), we obtain

$$z = h - \frac{h}{4a^2}(x^2 + y^2 + 2xy \cos \chi),$$

(2.8)

or for $\chi = \frac{\pi}{3}$,

$$z = h - \frac{h}{4a^2}(x^2 + y^2 + xy).$$

(2.9)

71

This is then the equation of the surface in question in the xOy coordinate system (see Figure 3). Hence, we have

$$\frac{\partial^2 z}{\partial x^2} = \frac{\partial^2 z}{\partial y^2} = -\frac{h}{2a^2}, \quad \frac{\partial^2 z}{\partial x \partial y} = -\frac{h}{4a^2},$$

and (1.30) takes the form

$$\frac{\partial^2 F}{\partial x^2} - \frac{\partial^2 F}{\partial x \partial y} + \frac{\partial^2 F}{\partial y^2} = -\frac{2q_0 a^2}{h}\sin\chi = -\frac{q_0 a^2 \sqrt{3}}{h}. \tag{2.10}$$

As we would expect, in the new coordinate system the twist of the surface element, characterized by the quantity $\frac{\partial^2 z}{\partial x \partial y}$ is nonzero, since one of the families of coordinate lines no longer coincides with the lines of translation. This ensures retention in (1.30) of the term containing $\frac{\partial^2 F}{\partial x \partial y}$ and in the final analysis assures equilibration of the vertical load in the corner zones by the tangential forces alone. For the boundary condition version adopted

$$S_{xx} = \frac{\partial^2 F}{\partial y^2}\Big|_{x=-\frac{2}{\sqrt{3}}a} = 0, \quad S_{yy} = \frac{\partial^2 F}{\partial x^2}\Big|_{y=-\frac{2}{\sqrt{3}}a} = 0. \tag{2.11}$$

Using (2.11), we find the tangential forces at the point $\left(-\frac{2}{\sqrt{3}}a, -\frac{2}{\sqrt{3}}a\right)$ directly from (2.10)

$$S_{xy} = -\frac{\partial^2 F}{\partial x \partial y} = -\frac{q_0 a^2 \sqrt{3}}{h} \tag{2.12}$$

which completes the solution of the posed problem.

Now let the original surface (2.1) have an arbitrary polygonal planform. By selecting the angle χ and the direction of the coordinate axes, by analogy with the preceding example, we write (1.30) in the form

$$\frac{\partial^2 F}{\partial x^2} - 2\cos\chi\frac{\partial^2 F}{\partial x \partial y} + \frac{\partial^2 F}{\partial y^2} = -\frac{2q_0 a^2}{h}\sin\chi. \tag{2.13}$$

where the value of the angle χ depends only on the choice of the shell planform corner at which the shearing force is determined. Assuming that edge conditions analogous to (2.11) are satisfied on the adjacent edges, we obtain the formula for the force S_{xy} at the corner point

$$S_{xy} = -\frac{\partial^2 F}{\partial x \partial y} = -\frac{q\varphi^2}{h} \operatorname{tg} \chi.$$

(2.14)

This formula shows that if the paraboloid of revolution has a polygonal planform the tangential force at the corner points is proportional to $\operatorname{tg}\chi$ and has a singularity only at the point $\chi = \frac{\pi}{2}$, while this force remains finite for all other values of the angle χ in the intervals

$$0 < \chi < \frac{\pi}{2}, \quad \frac{\pi}{2} < \chi < \pi$$

Moreover, (2.14) implies that S_{xy} changes sign as the angle χ passes through the singular point. For example, if the surface (2.1) has a regular hexagonal planform, i.e., $\chi = \frac{2}{3}\pi$, then we obtain

$$S_{xy} = \frac{q\varphi^2 \sqrt{3}}{h}.$$

In conclusion we note that in certain cases the forces in the shell with oblique planform may be obtained by simple scaling, without solving the differential equations, if we know the solution for the corresponding shell in the rectangular Cartesian coordinate system. We shall clarify this by an example.

Let the shell midsurface be a surface of translation whose equation is

$$z(x, y) = f_1(x) + f_2(y).$$

(2.15)

and the lines of translation $z_1 = f_1(x)$ and $z_2 = f_2(y)$ are located in mutually perpendicular vertical planes. In the case of a load which is uniformly distributed over the shell planform, the Pucher equation will have the form

$$\frac{d^2 f_2}{dy^2} \cdot \frac{\partial^2 F}{\partial x^2} + \frac{d^2 f_1}{dx^2} \cdot \frac{\partial^2 F}{\partial y^2} = q_0.$$

(2.16)

Now let us assume that the solution of (2.16) is known and examine another surface of translation with nonrectangular planform, whose lines of translation are located in vertical planes which form the

arbitrary angle χ with one another, and are also described in these planes by the equations $z_1 = f_1 (x)$ and $z_2 = f_2 (y)$. For the same load $q_z = -q_0$, the equation (1.30) for such a surface takes the form

$$\frac{d^2 f_2}{dy^2} \cdot \frac{\partial^2 F}{\partial x^2} + \frac{d^2 f_1}{dx^2} \cdot \frac{\partial^2 F}{\partial y^2} = q_0 \sin \chi.$$

from which it becomes quite clear that for the same boundary conditions all the internal forces in the corresponding sections of the second shell may be obtained by simple multiplication of the known forces for the first shell by the constant sin χ. For example, the case of a cylindrical surface having a parallelogram planform immediately reduces to the analogous surface with rectangular planform.

Figure 4

Consider still another example. Let the equation of the shell midsurface expressed in oblique Cartesian coordinates have the form

$$z = h - \frac{h}{4a^2}(x^2 + y^2).$$

For $q_z = -q_0$ the equation (1.30) for such a surface will be

$$\frac{\partial^2 F}{\partial x^2} + \frac{\partial^2 F}{\partial y^2} = -\frac{2q_0 a^2}{h} \sin \chi.$$

and on the basis of (2.3) the corresponding function

$$F = -\frac{q_0 a^2}{h} \left[\frac{1}{6a}(x^3 - 3xy^2) - \frac{2}{3} a^2 + \frac{1}{2}(x^2 + y^2) \right] \sin \chi.$$

vanishes on the triangular contour (Figure 4). Thus, by multiplying (2.4) by sin χ we obtain the solution in closed form for the surface of translation which is analogous to an elliptical paraboloid and has the indicated triangular planform.
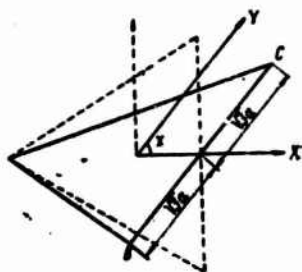
REFERENCES

1. Pucher, A., Über Spannungszustand in gekrümmten Flächen.
    (State of stress in curved srufaces) Beton u. Eisen, 33, Issue
    19, 1934.

2. Novozhilov, V. V., Teoriya tonkikh obolochek (Thin Shell Theory)
    2-nd edition, Leningrad, Sudpromgiz (State All-Union Publishing
    House of the Shipbuilding Industry), 1962.

3. Chernykh, K. F., "On the calculation of momentless coverings with
    polygonal planform," IAN SSSR, OTN, Mechanics and machine design,
    No. 4., 1963.

Received 5 April 1964

SOME CASES OF TORSION OF BARS WITH
VARYING ELASTIC MODULI

S. G. Lekhnitskiy

The problem of torsion of an elastic bar of constant cross
section in the classical formulation, i.e., under the assumption
that the deformations are small and the material obeys the generalized
Hooke's law, is known to reduce to the determination of a stress
function which satisfies in the region of the cross section a
second-order linear equation and takes a constant value on the con-
tour. For a homogeneous bar this equation has constant coefficients
which depend on the modulus of elasticity [1, page 149]. However,
if the elastic moduli are continuous functions of the coordinates
we obtain for the stress function a second-order differential equation
with variable coefficients, and the question of finding an effective
solution for the torsion problem becomes much more complex. It
appears that this problem has been solved only for a bar in the
form of a solid or hollow circular cylinder having cylindrical aniso-
tropy, with elastic moduli which are constant along the length [2]
[1, pages 203-205].

In the present article we consider several cases of bars with
variable moduli for which an effective solution of the torsion problem
may be obtained elementarily, using the same methods used in solving

the corresponding problems for the homogeneous isotropic bar. These
cases are, first, an orthotropic bar of rectangular section with
shear moduli given in the form of exponential and power-law functions
of the single coordinate y and, second, a tubular bar having
cylindrical anisotropy in which the moduli depend on the distance
r from the center of the section and vary along the length.

§ 1. General Torsion Theory Equations for
a Bar with Rectilinear Anisotropy

Consider an elastic bar of arbitrary constant cross section
having rectilinear anisotropy. We use the x, y, z coordinate system,
aligning the xy plane with the plane of one of the ends and directing
the z axis parallel to the generator (Figure 1). Forces which reduce
to the twisting moments M are distributed over the ends.
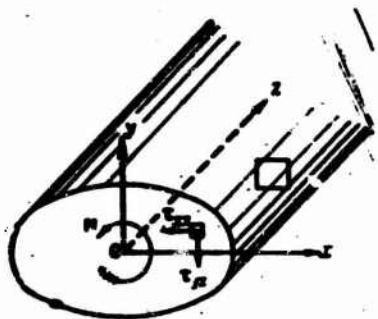
We make the following assump-
tions:

Figure 1

1. The bar material obeys
the generalized Hooke's law and
experiences small deformations
under the influence of the load.

2. At each point there is
a plane of elastic symmetry normal
to the bar centerline, and conse-
quently the number of independent
coefficients appearing in the
equation of the generalized Hooke's law is 13.

3. The deformation coefficients a_{ij} are continuous differenti-
able functions of the two coordinates x and y,but do not very along
the length of the bar. Thus, we shall consider only "continuous
inhomogeneity" and exclude from consideration bars composed of
different materials (composite bars), in which the elastic properties
vary abruptly from point to point.

We shall use the conventional notations of elasticity theory.

The basis of Saint Venant torsion theory is that four of the six stress components vanish

$$\sigma_x = \sigma_y = \sigma_z = \tau_{xy} = 0,$$

(1.1)

while the other two, as implied by the equilibrium equations, are expressed in terms of the stress function $\psi(x,y)$

$$\tau_{xz} = \frac{\partial \psi}{\partial y}, \quad \tau_{yz} = -\frac{\partial \psi}{\partial x}.$$

(1.2)

In view of (1.1), we write the equations expressing the generalized Hooke's law as follows

$$\begin{aligned}
\varepsilon_x &= 0, \quad \gamma_{yz} = a_{44}\tau_{yz} + a_{45}\tau_{xz}, \\
\varepsilon_y &= 0, \quad \gamma_{xz} = a_{45}\tau_{yz} + a_{55}\tau_{xz}, \\
\varepsilon_z &= 0, \quad \gamma_{xy} = 0,
\end{aligned}$$

(1.3)

where

$$\varepsilon_x = \frac{\partial u}{\partial x}, \ \ldots, \ \gamma_{yz} = \frac{\partial v}{\partial z} + \frac{\partial w}{\partial y}, \ \ldots,$$

(1.4)

u, v, w are the projections of the displacement on the directions of the x, y, z axes.

From these equations, we obtain the expressions for the displacements

$$\begin{aligned}
u &= -\theta yz + \beta z - \gamma y + u_0, \\
v &= \theta xz + \gamma x - \alpha z + v_0, \\
w &= \tau(x, y) + \alpha y - \beta x + w_0,
\end{aligned}$$

(1.5)

and the equations which the "torsion function" ϕ and the stress function must satisfy

$$\begin{aligned}
\frac{\partial \phi}{\partial x} &= \theta y + a_{55}\frac{\partial \psi}{\partial y} - a_{45}\frac{\partial \psi}{\partial x}, \\
\frac{\partial \phi}{\partial y} &= -\theta x + a_{44}\frac{\partial \psi}{\partial y} - a_{45}\frac{\partial \psi}{\partial x}.
\end{aligned}$$

(1.6)

Excluding ϕ from (1.6), we obtain a second-order equation with variable coefficients for the stress function

$$\frac{\partial}{\partial x}\left(a_{44}\frac{\partial\psi}{\partial x}-a_{45}\frac{\partial\psi}{\partial y}\right)+\frac{\partial}{\partial y}\left(a_{55}\frac{\partial\psi}{\partial y}-a_{45}\frac{\partial\psi}{\partial x}\right)=-2\theta.$$

(1.7)

The boundary condition for ψ is derived just as in the case of the homogeneous bar and reduces to the following: the stress function takes constant values on every contour bounding the section; in particular, in the case of a singly connected region $\psi = 0$ on the contour.

The constant θ , the relative rotation, or twist, is proportional to the torsional moment

$$\theta=\frac{M}{C}.$$

(1.8)

In the case of a singly connected cross section region S the stiffness C is

$$C=\frac{2}{\theta}\iint_S \psi\,dx\,dy.$$

(1.9)

The constants $a, b, \gamma, u_0, v_0, w_0,$ which express the "rigid" displacements, are determined from the conditions at the restrained end of the bar. We consider the end $z = 0$ free and the end $z = \underline{l}$ restrained, and we find all six constants by requiring that a small area in the $z = \underline{l}$ plane ($\underline{l}$ is the bar length) be stationary.

§ 2. Orthotropic Rectangular Bar

In the case of an orthotropic bar, the number of independent coefficients a_{ij} reduces to nine. If the bar is orthotropic and the coordinate axes are directed normal to the planes of elastic symmetry, in (1.3), (1.6) and (1.7) we must set

$$a_{45}=0,\; a_{44}=\frac{1}{G_1},\; a_{55}=\frac{1}{G_2},.$$

(2.1)

where $G_1(x, y)$, $G_2(x, y)$ are the shear moduli for the planes of elastic symmetry parallel to yz and xz. We obtain the simpler equation for the stress function in place of (1.7)

$$\frac{\partial}{\partial x}\left(\frac{1}{G_1}\cdot\frac{\partial\psi}{\partial x}\right)+\frac{\partial}{\partial y}\left(\frac{1}{G_2}\cdot\frac{\partial\psi}{\partial y}\right)=-2\theta, \qquad (2.2)$$

which becomes in the case of a homogeneous bar an equation of the elliptic type with constant coefficients and, in particular, the Poission equation for a homogeneous isotropic bar.
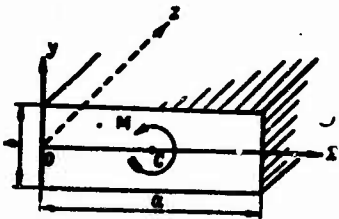
Figure 2.

Consider torsion of an orthotropic bar of rectangular section with sides a and b. We assume that the planes of elastic symmetry at every point are parallel to the planes bounding the bar. Directing the axes as shown in Figure 2, we restrict ourselves to study of the cases when G_1 and G_2 depend only on the single coordinate y. In these cases it is possible to use for the solution the same series method as is used for the isotropic and homogeneous orthotropic bars.

The boundary conditions reduce to

$$\psi=0 \text{ for } x=0, \ x=a, \ y=\pm\frac{b}{2}. \qquad (2.3)$$

We expand the right side of (2.2) into a Fourier sine series on the interval (0, a) and obtain

$$-2\theta=-\frac{8\theta}{\pi}\sum_{k=1,3,5,\dots}^{\infty}\frac{1}{k}\sin\frac{k\pi x}{a}. \qquad (2.4)$$

We seek the expression for ψ in the form of the series

$$\psi=\sum_{k=1,3,5,\dots}^{\infty} Y_k(y)\sin\frac{k\pi x}{a}. \qquad (2.5)$$

It will satisfy the conditions on both sides $x = 0$, $x = a$. Substituting (2.4) and (2.5) into (2.2), we obtain

$$Y_k'' + G_2\left(\frac{1}{G_1}\right)' Y_k' - \left(\frac{k\pi}{a}\right)^2 \frac{G_2}{G_1} Y_k = -\frac{m\,G_2}{a^2}$$
$$(k = 1, 3, 5, \tag{2.6}$$

Denoting by Y_{k0} the particular solution of the inhomogeneous equation (2.6) and by Y_{k1} and Y_{k2} the linearly independent solutions of the corresponding homogeneous equation, we obtain the general expression for the function ψ

$$\psi = \sum_{k=1,3,5\ldots} (A_k Y_{k1} + B_k Y_{k2} + Y_{k0}) \sin \frac{k\pi x}{a}. \tag{2.7}$$

The constants A_k, B_k for each value of k are found from the conditions on the sides $y = \pm \frac{b}{2}$ and are expressed in terms of σ , which in turn is found from (1.8)-(1.9).

It is obvious that the particular solutions Y_{k1}, Y_{k2} cannot be found in explicit form for arbitrary G_1 and G_2. The solution of the inhomogeneous equation for Y_{k0} is found from one of the known solutions of the homogeneous equation with the aid of quadratures.

Let us analyze further two cases of the representation of G_1 and G_2 in which the particular solutions of the homogeneous equation corresponding to (2.6) are found simply: these solutions are expressed either in terms of elementrary functions or Bessel functions.

§ 3. Rectangular Bar with Shear Moduli
Given in the Form of Exponential
Functions

Let the shear moduli of the bar shown in Figure 2 be given as follows

$$G_1 = g_1 e^{-\frac{n\pi y}{b}}, \quad G_2 = g_2 e^{-\frac{n\pi y}{b}}, \tag{3.1}$$

where n is any real number: positive, negative, whole, fractional or zero, and g_1, g_2 are constants having the dimension of the shear modulus, i.e., kg /cm^2.

Substituting (3.1) into the equation for Y_k, we obtain a second-order inhomogeneous equation with constant coefficients

$$Y_k'' + \frac{n\pi}{b} Y_k' - \left(\frac{k\pi}{a}\right)^2 g_0 Y_k = -\frac{80\, g_1}{\pi k} e^{-\frac{n\pi y}{b}}. \tag{3.2}$$

Here

$$g_0 = \frac{g_2}{g_1} = \frac{G_2}{G_1} \tag{3.3}$$

is the ratio of the shear moduli, a constant.

Equation (3.2) is easily solved. We denote: c = a:b (ratio of the sides of the section),

$$s_k = 0{,}5\left(\sqrt{n^2 + \frac{4k^2}{c^2} g_0} - n\right),$$
$$t_k = 0{,}5\left(\sqrt{n^2 + \frac{4k^2}{c^2} g_0} + n\right). \tag{3.4}$$

In the following, we shall drop the subscript k in these quantities for simplicity of writing, i.e., we write s, t in place of s_k, t_k. The general integral of (3.2) is

$$Y_k = A_k e^{\frac{s\pi y}{b}} + B_k e^{-\frac{t\pi y}{b}} + \frac{80\, g_1 a^2}{\pi^3 k^3} e^{-\frac{n\pi y}{b}}. \tag{3.5}$$

Determining A_k and B_k from the conditions

$$Y_k\left(\frac{b}{2}\right) = Y_k\left(-\frac{b}{2}\right) = 0, \tag{3.6}$$

we obtain the final expressions for the stress function and the stress components

$$\psi = \frac{80\, g_1 a^2}{\pi^3} \times$$

$$\times \sum \frac{1}{k^3}\left[\frac{\mathrm{sh}\,(n-(t\frac{\pi}{2}\, e^{\frac{s\pi y}{b}} - \mathrm{sh}\,(n+s)\frac{\pi}{2}\, e^{-\frac{t\pi y}{b}}}{\mathrm{sh}\,(s+t)\frac{\pi}{2}} + e^{-\frac{n\pi y}{b}}\right]\sin\frac{k\pi x}{a}; \ (3.7) \tag{3.7}$$

$$\tau_{xz} = \frac{80\, g_1 ac}{\pi^2} \times$$

$$\times \sum \frac{1}{k^3}\left[\frac{s\,\mathrm{sh}\,(n-t)\frac{\pi}{2}\, e^{\frac{s\pi y}{b}} + t\,\mathrm{sh}\,(n+s)\frac{\pi}{2}\, e^{-\frac{t\pi y}{b}}}{\mathrm{sh}\,(s+t)\frac{\pi}{2}} - n e^{-\frac{n\pi y}{b}}\right]\sin\frac{k\pi x}{a};$$

FTD-HC-23-361-69

82

$$\tau_{yz} = -\frac{M g_1 c}{a^2} \times$$

$$\times \sum \frac{1}{k^2} \left[\frac{sh(n-t)\frac{\pi}{2} e^{\frac{k\pi y}{b}} - sh(n+s)\frac{\pi}{2} e^{\frac{k\pi y}{b}}}{sh(s+t)\frac{\pi}{2}} + e^{-\frac{k\pi y}{b}} \right] \cos \frac{k\pi x}{a}. \tag{3.8}$$

Here and in all the following formulas the symbol Σ denotes for simplicity summation over odd k from 1 to ∞, as in (2.7).

The expression for the stiffness, found from (1.9), has the form

$$C = \frac{64 g_1 c^4 b}{a^3} \times$$

$$\times \sum \frac{1}{k^4} \left[\frac{c}{k^2 g_0} \cdot \frac{t\, sh(n-t)\frac{\pi}{2} sh\frac{s\pi}{2} - s\, sh(n+t)\frac{\pi}{2} sh\frac{t\pi}{2}}{sh(s+t)\frac{\pi}{2}} + \frac{1}{n} sh \frac{n\pi}{2} \right]. \tag{3.9}$$

We know that the maximal stress in a homogeneous isotropic bar for a > b is found at the points $x = \frac{a}{2}, y = \pm\frac{b}{2}$, i.e., at the mid points of the long sides of the rectangle. The question of the location of the most highly stressed points in the present case can be only resolved by specifying numerical values of n.

In a particular case we obtain from (3.7)-(3.9) formulas for the homogeneous orthotropic rectangular bar. Specifically, setting n = 0 we obtain

$$s = t = \frac{b}{c} \sqrt{\frac{G_2}{G_1}}. \tag{3.10}$$

Then (3.7) and (3.9) become the familiar expressions [1, pages 157-158]

$$\phi = \frac{32 G_1 c^2}{\pi^3} \sum \frac{1}{k^3} \left(1 - \frac{ch \frac{s\pi y}{b}}{ch \frac{s\pi}{2}} \right) \sin \frac{k\pi x}{a}. \tag{3.11}$$

$$C = \frac{32 G_1 c^4 b}{\pi^4} \sum \frac{1}{k^4} \left(1 - \frac{2c}{k\pi} \sqrt{\frac{G_1}{G_2}} \, \text{th} \, \frac{\pi \pi}{2}\right). \tag{3.12}$$

§ 4. Rectangular Bar with Shear Moduli Given in the Form of Power-Law Functions

It is not difficult to obtain the solution in those cases in which the shear moduli are represented by power-law functions of the distance, namely,

$$G_1 = g_1 \left(\frac{y + y_0}{b}\right)^{-m}, \quad G_2 = g_2 \left(\frac{y + y_0}{b}\right)^{-n}. \tag{4.1}$$

Here m and n are any real numbers — positive, negative, whole, fractional or zero, equal or unequal; g_1, g_2 are constants having the dimension of the shear modulus; and y_0 is a positive constant with the dimension of length. Since by definition the shear moduli cannot be negative and imaginary or complex numbers, we shall consider that the bracketed expressions in (4.1) are always positive within the rectangle, or at most vanish at the side y = -b/2, i.e., we assume that y_0 > b/2.

Equation (2.6) will have the form

$$Y_k'' + \frac{n}{y + y_0} Y_k' - \left(\frac{k\pi}{a}\right)^2 g_0 b^{n-m}(y + y_0)^{m-n} Y_k = -\frac{32 g_2 b^n}{\pi k}(y + y_0)^{-n}$$
$$(g_0 = g_2 : g_1). \tag{4.2}$$

We introduce the new variable

$$\eta = y + y_0 \tag{4.3}$$

and denote by primes derivatives with respect to η, rather than with respect to y. Then we obtain in place of (4.2)

$$Y_k'' + \frac{n}{\eta} Y_k' - \left(\frac{k\pi}{a}\right)^2 g_0 b^{n-m} \eta^{m-n} Y_k = -\frac{32 g_2 b^n}{\pi k} \eta^{-n}. \tag{4.4}$$

The integral of this equation is expressed in terms of Bessel functions (of imaginary argument) [3, pages 52, 53, 47].

We introduce the notations (the sign of the expression for N is selected so that $N \geq 0$)

$$\alpha = \frac{n-1}{2}, \quad \beta = \frac{2+m-n}{2}, \quad N = \pm \frac{n-1}{2+m-n}, \quad \gamma = \frac{k\pi}{a} \cdot \frac{\sqrt{\xi_0}}{\beta}. \qquad (4.5)$$

Then for noninteger N the particular linearly independent solutions of the homogeneous equation corresponding to (4.4) will be

$$Y_{k1} = \eta^{-\alpha} I_N (\gamma \eta^\beta), \quad Y_{k2} = \eta^{-\alpha} I_{-N} (\gamma \eta^\beta). \qquad (4.6)$$

where I_N is the Bessel function of the first kind J_N of the purely imaginary argument $i\gamma\eta^\beta$. For integer N we must substitute $K_N(\gamma\eta^\beta)$ (the Macdonald function), in place of $I_{-N}(\gamma\eta^\beta)$.

We find the particular solution of the second-order inhomogeneous equation (4.4) for the known Y_{k1}; this solution will have the form

$$Y_{k0} = -\frac{\omega \xi_0 \nu}{\alpha \delta} Y_{k1} \int \left(Y_{k1}^{-2} \eta^{-n} \int Y_{k1} \, d\eta \right) d\eta. \qquad (4.7)$$

For N not equal to an integer or zero, we obtain the following expression for the stress function

$$\psi = \sum \left[A_k \eta^{-\alpha} I_N (\gamma \eta^\beta) + B_k \eta^{-\alpha} I_{-N}(\gamma \eta^\beta) + Y_{k0} \right] \sin \frac{k\pi x}{a}. \qquad (4.8)$$

For integer or zero N

$$\psi = \sum \left[A_k \eta^{-\alpha} I_N (\gamma \eta^\beta) + B_k \eta^{-\alpha} K_N (\gamma \eta^\beta) + Y_{k0} \right] \sin \frac{k\pi x}{a}. \qquad (4.9)$$

We find the final expressions for ψ after determining the constants A_k and B_k from the conditions at the sides $y = \pm \frac{b}{2}$, but in view of their complexity we shall not write them out here. Nor shall we write out the formulas for the stiffness, which are obtained from (1.9) after determining A_k and B_k (which, just as Y_{k0}, will be proportional to the constant ψ).

§ 5. Particular Cases of Power-Law
Dependence

We shall consider the most typical cases of power-law dependence of the shear modulus on $y + y_0$.

Equation (4.4) and the expression for ψ are simplified somewhat when the shear moduli are proportional to the same power of $y + y_0$,

$$G_1 = g_1 \left(\frac{y + y_0}{b} \right)^{-n}, \quad G_2 = g_2 \left(\frac{y + y_0}{b} \right)^{-n}. \tag{5.1}$$

Then $(m = n)$

$$\frac{G_2}{G_1} = \frac{g_2}{g_1} = g_0 = \text{const},$$

$$\alpha = \frac{n-1}{2}, \quad \beta = 1, \quad N = \pm \frac{n-1}{2}, \quad \tau = \frac{k\pi}{a} \sqrt{g_0}. \tag{5.2}$$

We write the expressions for the stress function for four particular cases of this sort.

1. Linear dependence

$$G_1 = g_1 \left(\frac{y + y_0}{b} \right), \quad G_2 = g_2 \left(\frac{y + y_0}{b} \right),$$

$$n = -1, \quad \alpha = -1, \quad N = 1; \tag{5.3}$$

$$\tag{5.4}$$

$$\phi = \sum \left[A_k \eta I_1(\tau\eta) + B_k \eta K_1(\tau\eta) + Y_{k0} \right] \sin \frac{k\pi x}{a}.$$

2. Inverse proportionality

$$G_1 = g_1 \left(\frac{b}{y + y_0} \right), \quad G_2 = g_2 \left(\frac{b}{y + y_0} \right),$$

$$n = 1, \quad \alpha = 0, \quad N = 0; \tag{5.5}$$

$$\tag{5.6}$$

$$\phi = \sum \left[A_k I_0(\tau\eta) + B_k K_0(\tau\eta) + Y_{k0} \right] \sin \frac{k\pi x}{a}.$$

3. Moduli proportional to distance squared

$$G_1 = g_1 \left(\frac{y + y_0}{b} \right)^2, \quad G_2 = g_2 \left(\frac{y + y_0}{b} \right)^2,$$

$$n = -2, \quad \alpha = -\frac{3}{2}, \quad N = \frac{3}{2}. \tag{5.7}$$

In this case the formula for ψ contains Bessel functions of order $\pm\frac{3}{2}$, which are known to be expressible in terms of the elementary functions. We obtain finally

$$\psi = \sum [A_k(\sh \tau\eta - \tau\eta \ch \tau\eta) + B_k(\ch \tau\eta - \tau\eta \sh \tau\eta) + Y_{k0}]\sin\frac{k\pi x}{c}. \tag{5.8}$$

4. Moduli inversely proportional to the square of the distance $y + y_0$:

$$G_1 = g_1\left(\frac{b}{y+y_0}\right)^2, \quad G_2 = g_2\left(\frac{b}{y+y_0}\right)^2,$$
$$n = 2, \quad a = \frac{1}{2}, \quad N = \frac{1}{2}; \tag{5.9}$$

$$\psi = \sum (A_k\eta^{-1}\sh\tau\eta + B_k\eta^{-1}\ch\tau\eta + Y_{k0})\sin\frac{k\pi x}{c}. \tag{5.10}$$

We shall not write out the particular solutions for Y_{k0} since they are quite complex; they are found using (4.7) with the aid of two quadratures from expressions containing Bessel functions, or in cases three and four using hyperbolic functions.

We note another particular case in which the stresses are expressed in terms of elementary (power-law) functions.

Let

$$G_1 = g_1\left(\frac{b}{y+y_0}\right)^{n-2}, \quad G_2 = g_2\left(\frac{b}{y+y_0}\right)^n,$$
$$m = n - 2, \tag{5.11}$$

where n is any real number, in particular zero. The equation (4.4) becomes the Euler equation

$$Y_k'' + \frac{n}{\eta} Y_k' - \left(\frac{k\pi}{c}\right)^2 \frac{g_0}{\eta^2} Y_k = -\frac{q_0 g_2 b^n}{n b} \eta^{-n}. \tag{5.12}$$

The expression for the stress function is written as

$$\tag{5.13}$$

$$\psi = \frac{q_0 g_2 b^n}{n} \sum (A_k\eta^\nu + B_k\eta^{-\nu} + \eta^{2-n}) \frac{\sin\frac{k\pi x}{c}}{b\left[n-2+\left(\frac{k\pi}{c}\right)^2 g_0\right]}.$$

Here

$$\lambda = 0.5\left[\sqrt{(n-1)^2+4\left(\frac{kx}{c}\right)^2}-(n-1)\right],$$
$$\mu = 0.5\left[\sqrt{(n-1)^2+4\left(\frac{kx}{c}\right)^2}+(n-1)\right]$$

(5.14)

(the subscripts k for λ and μ are dropped).

These examples of the rectangular bar with variable elastic
moduli do not by any means include all possible solutions of the
problem. However, they show that there are a large number of function-
al dependences of the moduli on the y ccordinate for which the
torsion problem is solved nearly as simply as for the homogeneous
isotropic bar. In addition to the exponential and power-law functions
we could cite many others, but we shall not do tnis here; rather we
shall consider a different sort of case, which seems to us to be
of no less interest.

§ 6.   Torsion of Tubular Bar with
Cylindrical Anisotropy

In conclusion,we shall present the results of a study for a
bar having anisotropy of a different kind, namely cylindrical, and
we shall indicate how the elastic moduli must depend on the coordinates
in order that the qualivative stress distribution pattern be the
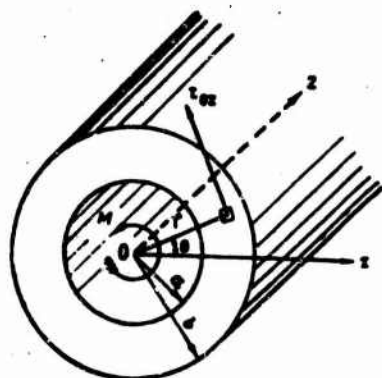same as for the corresponding isotropic homogeneous bar.

Figure   3

Consider a bar in the form
of a hollow circular cylinder whose
material obeys the generalized
Hooke's law and has cylindrical
anisotropy with an axis of aniso-
tropy coinciding with the geometric
z axis; we consider the deforma-
tion coefficients a_{ij} to be con-
tinuous functions of the coordinates.
One end of the bar is restrained,
while forces which reduce to the

torsional moment M act on the other end.   We use a cylindrical
coordinate system (Figure 3).

The stress distribution in the homogeneous isotropic bar is
characterized by the single stress component $\tau_{\theta z}$, which depends only
on r. We shall clarify the conditions which the variable deformation
coefficients must satisfy in order that only one $\tau_{\theta z}$ of the six
stress components in the twisted bar be nonzero, and we shall find
this component.

We shall not consider the most general anisotropy case, rather
we shall assume that 1). the relative elongations ε_r, ε_θ, ε_z,
are independent of $\tau_{\theta z}$, i.e., $a_{14} = a_{24} = a_{34} = 0$ and 2). The
coefficients a_{44}, a_{45}, a_{46} are given in the form of products of
functions of z alone by functions of r alone, i.e.,

$$a_{44} = Z_{44}(z)\,b_{44}(r), \quad a_{45} = Z_{45}(z)\,b_{45}(r), \quad a_{46} = Z_{46}(z)\,b_{46}(r). \tag{6.1}$$

The remaining coefficients a_{ij} may be any functions of the
cylindrical coordinates r and z and also of the angle θ. These
assumptions are quite general, although they obviously do not include
all possible cases.

Setting

$$\varepsilon_r = \varepsilon_\theta = \varepsilon_z = \tau_{rz} = \tau_{r\theta} = 0, \quad \tau_{\theta z} = \tau_{\theta z}(r).$$

$$\tag{6.2}$$

we write the generalized Hooke's law equations

$$
\begin{aligned}
\varepsilon_r &= 0, & \tau_{\theta z} &= a_{44}\tau_{\theta z},\\
\varepsilon_\theta &= 0, & \tau_{rz} &= a_{45}\tau_{\theta z},\\
\varepsilon_z &= 0, & \tau_{r\theta} &= a_{46}\tau_{\theta z}.
\end{aligned}
\tag{6.3}
$$

Expressing the deformation coefficients in terms of the
displacement projections u_r, u_θ, w along the directions r, θ, z and
considering the displacements to be functions only of r and z, we
obtain from (6.3)

$$Z_{44}=1, \quad u_r=0, \quad w \doteq \int b_{44} \tau_{44} dr + w_0,$$

(6.4)

and the equations relating u_θ and $\tau_{\theta z}$

$$\frac{\partial}{\partial z}\left(\frac{u_\theta}{r}\right)=\overline{Z_{44}}\frac{b_{44}\tau_{\theta z}}{r},$$
$$\frac{\partial}{\partial r}\left(\frac{u_\theta}{r}\right)=Z_{44}\frac{b_{44}\tau_{44}}{r}.$$

(6.5)

These equations for u_θ will be compatible only if

$$Z_{44}=Z(z), \quad Z_{44}=\int Z dz + a$$

(6.6)

(a is a constant, $Z(z)$ is an arbitrary continuous function).
Consequently,

$$a_{44}=Z(z)\,b_{44}(r), \quad a_{44}=b_{44}(r), \quad a_{44}=\left(\int Z dz + a\right)b_{44}(r).$$

(6.7)

Excluding the displacements from (6.5), we obtain the equations
for $\tau_{\theta z}$

$$\frac{d}{dr}\left(\frac{b_{44}\tau_{44}}{r}\right)-\frac{b_{44}\tau_{44}}{r}=0.$$

(6.8)

Introducing the function

$$f(r)=e^{\int \frac{b_{44}}{b_{44}}dr}.$$

(6.9)

we write the final expressions for the stress and displacements as
follows

$$\tau_{44}=\vartheta\frac{rf(r)}{b_{44}};$$

(6.10)

$$u_r=0,$$
$$u_\theta=\vartheta\left(\int Z dz + a\right)rf(r)+\omega r,$$
$$w=\vartheta\int\frac{r b_{44} f(r)}{b_{44}}dr + w_0.$$

(6.11)

Thus, we find that if the deformation coefficients are given by
(6.7) the stress and displacements are defined by (6.10) and (6.11).
We find the constants ω and w_0 from the conditions at the
restrained end $z = \underline{1}$ and the constant ϑ from the formula

90

$$\Phi = \frac{M}{2\pi \int_0^a \frac{r^3 f(r)}{b_{44}} dr} \tag{6.12}$$

(the stress $\tau_{\theta z}$ in any cross section reduces to the torsional moment M).

In particular, for the orthotropic bar (with planes of elastic symmetry normal to the axis, radial and orthogonal to the first two) we have

$$a_{45} = a_{46} = 0, \ b_{45} = b_{46} = 0. \tag{6.13}$$

If the shear modulus for the radial planes of elastic symmetry (i.e., those passing through the geometric axis z) is given in the form of the function

$$G_1 = \frac{1}{a_{44}} = \frac{1}{Z(z) b_{44}(r)}. \tag{6.14}$$

where Z and b_{44} are arbitrary continuous functions of z and r, then the stress $\tau_{\theta z}$ is found from the formula

$$\tau = \Phi \frac{r}{b_{44}(r)}. \tag{6.15}$$

where

$$\Phi = \frac{M}{2\pi \int_0^a \frac{r^3}{b_{44}} dr}. \tag{6.16}$$

The corresponding displacements will be

$$\begin{gathered} u_r = w = 0, \\ u_\theta = \Phi r \left(\int Z \, dz + \omega_0 \right). \end{gathered} \tag{6.17}$$

Hence, after determining ω_0 from the condition at the restrained end $u_\theta = 0$ we find the total twist angle

$$\Phi = \frac{1}{r} (u_\theta)_{r=a} = -\Phi \int_0^l Z \, dz. \tag{6.18}$$

For example, if the shear modulus is given by the formula

$$G_1 = \frac{1}{z^n b_{44}(r)} \qquad (n > 0). \tag{6.19}$$

we obtain

$$\frac{1+\varkappa}{1+\varkappa'}\varphi = -\varepsilon \varphi$$

(6.20)

As for the stress, it is independent of z in both cases considered here; we obtain the same stress for any representation of the function $Z(z)$ and it is found from (6.10), (6.12) or (6.15), (6.16). Thus, the factor $Z(z)$ affects only the deformation of the bar in torsion (more precisely, the displacement u_θ and the total twist angle).

REFERENCES

1. Lekhnitskiy, S. G., Teoriya uprugosti anizotropnogo tela (Elasticity Theory for an Anisotropic Body), Moscow-Leningrad, GITTL (State Press for Technical and Theoretical Literature), 1960.

2. Voigt, W., Ueber die Elastizitätsverhaltnisse cylindrisch aufgebauter Körper. (Elasticity of cylindrical-shaped bodies) Nachrichten v. d. Königl. Gesellschaft der Wissenschaften und der Georg-Augustin Universität zu Göttingen, Nr. 16, 1886.

3. Kuz'min, R. O., Besselevy funktsii (Bessel Functions), Moscow, ONTI (Ob'yedineniye nauchno-tekhnicheskikh izdatel'stv), 1935.

CYLINDRICAL SHELL AND PLATE SUBJECTED TO
A MOVING HEAT SOURCE

K. Kh. Kozhakhmetov
and
R. M. Finkel'shteyn

We consider thin circular cylindrical shells of radius R and a
semi-infinite flat plate under the influence of a moving heat source.
The temperature is distributed linearly through the thickness of
the shells and plate.

NOTATIONS

κ — thermal conductivity

K_0 — heat transfer coefficient

c — specific heat

ρ — material density

h — shell and plate thickness

v — source motion velocity

$Q = \int\limits_{-h/2}^{h/2} q\,dz$ — heat source density per unit middle surface area

$z_{\bullet} = \frac{1}{Q} \int\limits_{-h/2}^{h/2} zq\,dz$ — coordinate of source "center of gravity"

q — specific output of heat sources

z — coordinate along normal to middle surface

$\zeta = \frac{z}{R}$ — dimensionless coordinate in the direction of the generators

t — time

$\tau = F_0 = \frac{at}{R^2}$ — dimensionless time

F_0 — Fourier criterion

$\chi = \frac{a R t}{s}$ — dimensionless distance traveled by source

δ — Dirac function

$$\beta^2 = \frac{2 K_0 R^2}{c \rho a R}; \quad \tau^2 = \frac{12 R^2}{h^2} + 3 \beta^2;$$

T_0 — middle surface temperature

K — temperature gradient through shell thickness

$T^* = \frac{x c \rho h}{q R}$ — dimensionless middle surface temperature

$K^* = \frac{x c \rho h^2}{3 q R}$ — dimensionless temperature gradient through shell thickness

$$m = \frac{a R}{s}, \quad n^2 = \left(\frac{2i}{m}\right)^2, \quad p^2 = \left(\frac{2i}{m}\right)^2,$$

$$n_1^2 = \left(\sqrt{\beta^2 + \frac{m^2}{4}} + \frac{m}{2}\right)^2, \quad n_2^2 = \left(\sqrt{\beta^2 + \frac{m^2}{4}} - \frac{m}{2}\right)^2$$

$$m_1^2 = \left(\sqrt{\tau^2 + \frac{m^2}{4}} + \frac{m}{2}\right)^2,$$

$$m_2^2 = \left(\sqrt{\tau^2 + \frac{m^2}{4}} - \frac{m}{2}\right)^2.$$

$\text{erf}(z) = \frac{2}{\sqrt{\pi}} \int_0^z e^{-y^2} dy$ — Gauss function

u — longitudinal component of displacement vector

w — normal component of displacement vector

$u^* = \frac{u}{h}$ — dimensionless longitudinal component of displacement vector

$w^* = \frac{w}{h}$ — dimensionless normal component of displacement vector

α — thermal expansion coefficient

E — Young's modulus

ν — Poisson's ratio

$$A^* = \frac{12 R^2 (1 - \nu)}{h^2}, \quad B = \frac{12 \nu \alpha q R^4 (1 + \nu)}{x c \rho h^4},$$

$$C = \frac{3 \alpha q R^2 (1 + \nu)}{x c \rho h^2}, \quad D = \frac{12 \gamma x^2 (1 - \nu^2)}{E h^2};$$

$$D_1 = \frac{Eh}{1-\nu^2} \quad \text{— compressional stiffness}$$

$$a = \frac{\pi R}{2l_0}, \quad l_0 = \frac{l}{R}, \quad D_2 = \frac{Eh^3}{12(1-\nu^2)} \text{— cylindrical stiffness}$$

$$T_1, T_2 \text{ — forces}$$

$$M_1, M_2 \text{ — bending moments}$$

I.   Semi-Infinite Shell

§ 1.   Temperature Field

We assume that the temperature of the medium is zero, and the heat transfer coefficients from the outer and inner sides of the shell are the same.   Then for a linear distribution of the heat through the shell thickness

$$T(x, z, t) = T_0(x, t) + zK(x, t) \tag{1.1}$$

we have for T_0 and K the independent equations[1]

$$\frac{\partial T_0}{\partial t} - \varkappa \frac{\partial^2 T_0}{\partial x^2} + \frac{2K_0}{c\rho h} T_0 = \frac{Q}{c\rho h},$$

$$\frac{\partial K}{\partial t} - \varkappa \frac{\partial^2 K}{\partial x^2} + \left(\frac{12\varkappa}{h^2} + \frac{6K_0}{c\rho h} \right) K = \frac{12}{c\rho h^2} Qz_0, \tag{1.2}$$

or

$$\frac{\partial T^\bullet}{\partial \tau} - \frac{\partial^2 T^\bullet}{\partial \xi^2} + \beta^2 T^\bullet = \delta(\xi - \chi),$$

$$\frac{\partial K^\bullet}{\partial \tau} - \frac{\partial^2 K^\bullet}{\partial \xi^2} + \gamma^2 K^\bullet = \delta(\xi - \chi). \tag{1.3}$$

The initial and boundary conditions for (1.2) are

$$T_0 = K = 0 \text{ for } t = 0,$$
$$T_0 = K = 0 \text{ for } x = 0 \text{ and for } x = \infty.$$

Then these conditions for (1.3) take the form

$$T^\bullet = K^\bullet = 0 \text{ for } \tau = 0,$$
$$T^\bullet = K^\bullet = 0 \text{ for } \xi = 0 \text{ and for } \xi = \infty. \tag{1.4}$$

We apply the Fourier sine transformation to the new (1.3)

$$\theta(\alpha, \tau) = \sqrt{\frac{2}{\pi}} \int_0^\infty T^\bullet(\xi, \tau) \sin \alpha \xi \, d\xi. \tag{1.5}$$

Then this equation takes the form

$$\frac{d\theta}{d\tau} + (\alpha^2 + \beta^2)\theta = \sqrt{\frac{2}{\pi}}\sin\alpha\pi\tau;$$

(1.6)

$$\theta|_{\tau=0} = 0,$$

(1.7)

whose solution will be

$$\theta(\alpha, \tau) = \frac{\sqrt{2}\left[(\alpha^2 + \beta^2)\sin\alpha\eta - \alpha\pi\cos\alpha\eta\right]}{\sqrt{\pi}\left[(\alpha^2 + \beta^2)^2 + \alpha^2\pi^2\right]} + \frac{\sqrt{2}\,\alpha\pi e^{-(\alpha^2 + \beta^2)\tau}}{\sqrt{\pi}\left[(\alpha^2 + \beta^2)^2 + \alpha^2\pi^2\right]}.$$

(1.8)

and after transformation we have

$$T^\circ(\xi, \tau) = \frac{2}{\pi}\int_0^\infty \frac{(\alpha^2 + \beta^2)\sin\alpha\eta\,\sin\alpha\xi}{(\alpha^2 + \beta^2)^2 + \alpha^2\pi^2}\,d\alpha -$$

$$-\frac{2\pi}{\pi}\int_0^\infty \frac{\alpha\sin\alpha\xi\cos\alpha\eta}{(\alpha^2 + \beta^2)^2 + \alpha^2\pi^2}\,d\alpha + \frac{2\pi}{\pi}\int_0^\infty \frac{\alpha e^{-(\alpha^2 + \beta^2)\tau}\sin\alpha\xi}{(\alpha^2 + \beta^2)^2 + \alpha^2\pi^2}\,d\alpha.$$

(1.9)

Calculating the integrals in (1.9), we obtain

$$T^\circ(\xi, \tau) = \frac{-e^{-\gamma\tau - \frac{\xi^2}{4\tau}}}{2m\sqrt{1 + \pi^2}}\left\{\exp\left(n_1\sqrt{\tau} - \frac{\xi}{2\sqrt{\tau}}\right)^2 \times\right.$$

$$\times\left[1 - \text{erf}\left(n_1\sqrt{\tau} - \frac{\xi}{2\sqrt{\tau}}\right)\right] - \exp\left(n_1\sqrt{\tau} + \frac{\xi}{2\sqrt{\tau}}\right)^2 \times$$

$$\times\left[1 - \text{erf}\left(n_1\sqrt{\tau} + \frac{\xi}{2\sqrt{\tau}}\right)\right] - \exp\left(n_2\sqrt{\tau} - \frac{\xi}{2\sqrt{\tau}}\right)^2 \times$$

$$\times\left[1 - \text{erf}\left(n_2\sqrt{\tau} - \frac{\xi}{2\sqrt{\tau}}\right)\right] + \exp\left(n_2\sqrt{\tau} + \frac{\xi}{2\sqrt{\tau}}\right)^2 \times$$

$$\left.\times\left[1 - \text{erf}\left(n_2\sqrt{\tau} + \frac{\xi}{2\sqrt{\tau}}\right)\right]\right\} +$$

$$\left|\begin{array}{ll} \frac{e^{-n_2\xi}}{m\sqrt{1 + \pi^2}}(\text{sh}\,n_2\chi + \text{ch}\,n_1\chi) + \frac{e^{-n_1\xi}}{m\sqrt{1 + \pi^2}}(\text{sh}\,n_2\chi - \text{ch}\,n_2\chi) & \\ & \text{for } 0 < \chi < \xi, \\ -\frac{1}{m\sqrt{1 + \pi^2}}\,e^{-2n_1\xi} & \text{for } 0 < \chi = \xi, \\ \frac{2}{m\sqrt{1 + \pi^2}}\,e^{-n_2\chi}\,\text{sh}\,n_2\xi & \text{for } 0 < \xi < \chi. \end{array}\right.$$

(1.10)

Since the second equation of (1.3) differs from the first only by a constant factor, we can immediately write

$$K^\circ(\xi, \tau) = -\frac{e^{-\gamma\tau - \frac{\xi^2}{4\tau}}}{2m\sqrt{1 + \pi^2}}\left\{\exp\left(m_1\sqrt{\tau} - \frac{\xi}{2\sqrt{\tau}}\right)^2 \times\right.$$

$$\times\left[1 - \text{erf}\left(m_1\sqrt{\tau} - \frac{\xi}{2\sqrt{\tau}}\right)\right] - \exp\left(m_1\sqrt{\tau} + \frac{\xi}{2\sqrt{\tau}}\right)^2 \times$$

$$\times\left[1 - \text{erf}\left(m_1\sqrt{\tau} + \frac{\xi}{2\sqrt{\tau}}\right)\right] - \exp\left(m_2\sqrt{\tau} - \frac{\xi}{2\sqrt{\tau}}\right)^2 \times$$

(1.11)

$$\times\left[1 - \text{erf}\left(m_2\sqrt{\tau} - \frac{\xi}{2\sqrt{\tau}}\right)\right] + \exp\left(m_2\sqrt{\tau} + \frac{\xi}{2\sqrt{\tau}}\right)^2 \times$$

$$\left.\times\left[1 - \text{erf}\left(m_2\sqrt{\tau} + \frac{\xi}{2\sqrt{\tau}}\right)\right]\right\} +$$

(Equation continued from preceding page)

$$+ \begin{cases} \dfrac{e^{-m_1 \xi}}{m\sqrt{1+\rho^2}}(\mathrm{sh}\, m_1\chi + \mathrm{ch}\, m_1\chi) + \dfrac{e^{-m_2 \xi}}{m\sqrt{1+\rho^2}}(\mathrm{sh}\, m_2\chi - \mathrm{ch}\, m_2\chi) \\ \qquad\qquad\qquad\qquad\qquad \text{for } 0 < \chi < \xi, \\[4pt] -\dfrac{1}{m\sqrt{1+\rho^2}} e^{-2m_1 \xi} \qquad\quad \text{for } 0 < \chi = \xi, \\[4pt] \dfrac{2}{m\sqrt{1+\rho^2}} e^{-m_1\chi}\,\mathrm{sh}\, m_1\xi \qquad \text{for } 0 < \xi < \chi. \end{cases}$$

$$(1.11)$$

It is not difficult to see that (1.10) and (1.11) satisfy the initial and boundary conditions.

Now let us find the displacement field. We shall consider separately the quasistatic case (dropping all the inertial terms), and the case in which only the inertia of the normal component of the displacement vector is taken into account.

§ 2. Displacement Field (Quasistatic Case)

In the quasistatic case, the thermoelastic equations in terms of displacement for this problem have the form

$$\frac{\partial^4 w^*}{\partial \xi^4} + A^4 w^* = -BT^* - C\frac{\partial^2 K^*}{\partial \xi^2};$$

$$(2.1)$$

$$\frac{\partial u^*}{\partial \xi} + v w^* = \frac{CR}{3\lambda}T^*.$$

$$(2.2)$$

Let the shell be pin-ended. Then the solution of (2.1) must satisfy the conditions

$$w^*(\xi, 0) = w^*(0, \tau) = \frac{\partial^2 w^*(0, \tau)}{\partial \xi^2} = w^*(\infty, \tau) = 0.$$

$$(2.3)$$

Applying the Fourier sine transformation to (2.1) under the conditions (2.3)

$$\bar{w}^*(x, \tau) = \sqrt{\frac{2}{\pi}} \int_0^{\infty} w^*(\xi, \tau)\sin x\xi\, d\xi,$$

$$(2.4)$$

we obtain

$$\bar{w}^* = \frac{\sqrt{\frac{2}{\pi}} B\,[(\alpha^2 + \beta^2)\sin \alpha\chi - \alpha m \cos \alpha\chi]}{(\alpha^4 + A^4)\,[(\alpha^2 + \beta^2)^2 + \alpha^2 m^2]} -$$
$$- \frac{\sqrt{\frac{2}{\pi}}\,\alpha m B e^{-(\alpha^2 + \beta^2)\tau}}{(\alpha^4 + A^4)\,[(\alpha^2 + \beta^2)^2 + \alpha^2 m^2]} +$$
$$+ \frac{\sqrt{\frac{2}{\pi}} C\alpha^2\,[(\alpha^2 + \gamma^2)\sin \alpha\chi - \alpha m \cos \alpha\chi]}{(\alpha^4 + A^4)\,[(\alpha^2 + \gamma^2)^2 + \alpha^2 m^2]} -$$
$$- \frac{\sqrt{\frac{2}{\pi}} C\alpha m^2 e^{-(\alpha^2 + \gamma^2)\tau}}{(\alpha^4 + A^4)\,[(\alpha^2 + \gamma^2)^2 + \alpha^2 m^2]} \qquad (2.5)$$

and, inverting (2.5), we obtain

$$w^*(\xi, \tau) = - \frac{2B}{\pi} \int \frac{(\alpha^2 + \beta^2)\sin \alpha\chi - \alpha m \cos \alpha\chi}{(\alpha^4 + A^4)\,[(\alpha^2 + \beta^2)^2 + \alpha^2 m^2]} \sin \alpha\xi\,d\alpha +$$
$$+ \frac{2C}{\pi} \int \frac{\alpha^2\,[(\alpha^2 + \gamma^2)\sin \alpha\chi - \alpha m \cos \alpha\chi]}{(\alpha^4 + A^4)\,[(\alpha^2 + \gamma^2)^2 + \alpha^2 m^2]} \sin \alpha\xi\,d\alpha -$$
$$- \frac{2mB}{\pi} \int \frac{\alpha e^{-(\alpha^2 + \beta^2)\tau} \sin \alpha\xi}{(\alpha^4 + A^4)\,[(\alpha^2 + \beta^2)^2 + \alpha^2 m^2]}\,d\alpha + \qquad (2.6)$$
$$+ \frac{2mC}{\pi} \int \frac{\alpha^2 e^{-(\alpha^2 + \gamma^2)\tau} \sin \alpha\xi}{(\alpha^4 + A^4)\,[(\alpha^2 + \gamma^2)^2 + \alpha^2 m^2]}\,d\alpha.$$

We obtain from (2.2), taking account of (1.10) and (2.6),

$$\frac{\partial w^*}{\partial \xi} = \frac{2\nu B}{\pi} \int \frac{(\alpha^2 + \beta^2)\sin \alpha\chi - \alpha m \cos \alpha\chi}{(\alpha^4 + A^4)\,[(\alpha^2 + \beta^2)^2 + \alpha^2 m^2]} \sin \alpha\xi\,d\alpha -$$
$$- \frac{2\nu C}{\pi} \int \frac{\alpha^2\,[(\alpha^2 + \gamma^2)\sin \alpha\chi - \alpha m \cos \alpha\chi]}{(\alpha^4 + A^4)\,[(\alpha^2 + \gamma^2)^2 + \alpha^2 m^2]} \sin \alpha\xi\,d\alpha +$$
$$+ \frac{2\nu m B}{\pi} \int \frac{\alpha e^{-(\alpha^2 + \beta^2)\tau} \sin \alpha\xi}{(\alpha^4 + A^4)\,[(\alpha^2 + \beta^2)^2 + \alpha^2 m^2]}\,d\alpha -$$
$$- \frac{2\nu m C}{\pi} \int \frac{\alpha^2 e^{-(\alpha^2 + \gamma^2)\tau} \sin \alpha\xi}{(\alpha^4 + A^4)\,[(\alpha^2 + \gamma^2)^2 + \alpha^2 m^2]}\,d\alpha -$$
$$- \frac{CRe^{-p\tau - \frac{\pi^2}{4\tau}}}{6 k m \sqrt{1 + n^2}} \left\{ \exp\left(n_1\sqrt{\tau} - \frac{\xi}{2\sqrt{\tau}}\right)^2 \left[1 - \operatorname{erf}\left(n_1\sqrt{\tau} - \frac{\xi}{2\sqrt{\tau}}\right)\right] - \right.$$
$$- \exp\left(n_1\sqrt{\tau} + \frac{\xi}{2\sqrt{\tau}}\right)^2 \left[1 - \operatorname{erf}\left(n_1\sqrt{\tau} + \frac{\xi}{2\sqrt{\tau}}\right)\right] -$$
$$- \exp\left(n_2\sqrt{\tau} - \frac{\xi}{2\sqrt{\tau}}\right)^2 \left[1 - \operatorname{erf}\left(n_2\sqrt{\tau} - \frac{\xi}{2\sqrt{\tau}}\right)\right] +$$
$$\left. + \exp\left(n_2\sqrt{\tau} + \frac{\xi}{2\sqrt{\tau}}\right)^2 \left[1 - \operatorname{erf}\left(n_2\sqrt{\tau} + \frac{\xi}{2\sqrt{\tau}}\right)\right] \right\} +$$
$$+ \begin{cases} \dfrac{CR}{3 k m \sqrt{1 + n^2}} \left[e^{-n_2(\xi - \chi)} - e^{-n_2(\xi + \chi)}\right] & \text{for } 0 < \chi < \xi, \\[2mm] -\dfrac{CR}{3 k m \sqrt{1 + n^2}} e^{-2n_2\xi} & \text{for } 0 < \chi = \xi, \qquad (2.7) \\[2mm] \dfrac{CR}{3 k m \sqrt{1 + n^2}} e^{-n_2\chi} \operatorname{sh} n_2\xi & \text{for } 0 < \xi < \chi. \end{cases}$$

The integrals in (2.6) and (2.7) break down into a series of tabulated integrals. The calculations of these integrals follow.

$$I_1 = \int_0^\infty \frac{(\alpha^2 + \beta^2)\sin\alpha\xi\sin\alpha\chi}{(\alpha^4 + A^4)[(\alpha^2 + \beta^2)^2 + \alpha^2 m^2]}\,d\alpha = \int_0^\infty \frac{(L_1\alpha^2 + L_2)\sin\alpha\xi\sin\alpha\chi}{\alpha^4 + A^4}\,d\alpha +$$

$$+ L_3\int_0^\infty \frac{\sin\alpha\xi\sin\alpha\chi}{\alpha^2 + n_1^2}\,d\alpha + L_4\int_0^\infty \frac{\sin\alpha\xi\sin\alpha\chi}{\alpha^2 + n_2^2}\,d\alpha =$$

$$= \begin{cases}
\dfrac{\pi}{4\sqrt{2}A}\Big\{\exp\Big(-\dfrac{A(\xi-\chi)}{\sqrt{2}}\Big)\Big[\Big(L_1 + \dfrac{L_2}{A^2}\Big)\cos\dfrac{A(\xi-\chi)}{\sqrt{2}} + \\
\quad + \Big(\dfrac{L_2}{A^2} - L_1\Big)\sin\dfrac{A(\xi-\chi)}{\sqrt{2}}\Big] - \exp\Big(-\dfrac{A(\xi+\chi)}{\sqrt{2}}\Big)\times \\
\quad \times\Big[\Big(L_1 + \dfrac{L_2}{A^2}\Big)\cos\dfrac{A(\xi+\chi)}{\sqrt{2}} + \Big(\dfrac{L_2}{A^2} - L_1\Big)\sin\dfrac{A(\xi+\chi)}{\sqrt{2}}\Big]\Big\} + \\
\quad + 2L_3 e^{-n_1\xi}\operatorname{sh} n_1\chi + 2L_4 e^{-n_2\xi}\operatorname{sh} n_2\chi \quad \text{for } \xi > \chi, \\[2mm]
\dfrac{\pi}{4\sqrt{2}A}\Big\{\exp\Big(\dfrac{A(\xi-\chi)}{\sqrt{2}}\Big)\Big[\Big(L_1 + \dfrac{L_2}{A^2}\Big)\cos\dfrac{A(\xi-\chi)}{\sqrt{2}} + \\
\quad + \Big(L_1 - \dfrac{L_2}{A^2}\Big)\sin\dfrac{A(\xi-\chi)}{\sqrt{2}}\Big] - \exp\Big(-\dfrac{A(\xi+\chi)}{\sqrt{2}}\Big)\times \\
\quad \times\Big[\Big(L_1 + \dfrac{L_2}{A^2}\Big)\cos\dfrac{A(\xi+\chi)}{\sqrt{2}} + \Big(\dfrac{L_2}{A^2} - L_1\Big)\sin\dfrac{A(\xi+\chi)}{\sqrt{2}}\Big]\Big\} + \\
\quad + 2L_3 e^{-n_1\chi}\operatorname{sh} n_1\xi + 2L_4 e^{-n_2\chi}\operatorname{sh} n_2\xi \quad \text{for } \xi \leqslant \chi;
\end{cases}$$

$$I_2 = \int_0^\infty \frac{\alpha\sin\alpha\xi\cos\alpha\chi}{(\alpha^4 + A^4)[(\alpha^2 + \beta^2)^2 + \alpha^2 m^2]}\,d\alpha = \int_0^\infty \frac{\alpha(L_5\alpha^2 + L_6)\sin\alpha\xi\cos\alpha\chi}{\alpha^4 + A^4}\,d\alpha +$$

$$+ L_7\int_0^\infty \frac{\alpha\sin\alpha\xi\cos\alpha\chi}{\alpha^2 + n_1^2}\,d\alpha + L_8\int_0^\infty \frac{\alpha\sin\alpha\xi\cos\alpha\chi}{\alpha^2 + n_2^2}\,d\alpha =$$

$$= \begin{cases}
\dfrac{\pi}{4}\Big\{\exp\Big(-\dfrac{A(\xi-\chi)}{\sqrt{2}}\Big)\Big[L_5\cos\dfrac{A(\xi-\chi)}{\sqrt{2}} + \dfrac{L_6}{A^2}\sin\dfrac{A(\xi-\chi)}{\sqrt{2}}\Big] + \\
\quad + \exp\Big(-\dfrac{A(\xi+\chi)}{\sqrt{2}}\Big)\Big[L_5\cos\dfrac{A(\xi+\chi)}{\sqrt{2}} + \dfrac{L_6}{A^2}\sin\dfrac{A(\xi+\chi)}{\sqrt{2}}\Big]\Big\} + \\
\quad + \dfrac{\pi}{2}\big(L_7 e^{-n_1\xi}\operatorname{ch} n_1\chi + L_8 e^{-n_2\xi}\operatorname{ch} n_2\chi\big) \quad \text{for } \xi > \chi, \\[2mm]
\dfrac{\pi}{4}\Big\{\exp\Big(\dfrac{A(\xi-\chi)}{\sqrt{2}}\Big)\Big[L_5\cos\dfrac{A(\xi-\chi)}{\sqrt{2}} - \dfrac{L_6}{A^2}\sin\dfrac{A(\xi-\chi)}{\sqrt{2}}\Big] + \\
\quad + \exp\Big(-\dfrac{A(\xi+\chi)}{\sqrt{2}}\Big)\Big[L_5\cos\dfrac{A(\xi+\chi)}{\sqrt{2}} - \dfrac{L_6}{A^2}\sin\dfrac{A(\xi+\chi)}{\sqrt{2}}\Big]\Big\} - \\
\quad - \dfrac{\pi}{2}\big(L_7 e^{-n_1\chi}\operatorname{sh} n_1\xi + L_8 e^{-n_2\chi}\operatorname{sh} n_2\xi\big) \quad \text{for } \xi \leqslant \chi;
\end{cases}$$

$$I_3 = \int_0^\infty \frac{\alpha^2(\alpha^2 + \gamma^2)\sin\alpha\xi\sin\alpha\chi}{(\alpha^4 + A^4)[(\alpha^2 + \gamma^2)^2 + \alpha^2 m^2]}\,d\alpha = \int_0^\infty \frac{(L_9\alpha^2 + L_{10})\sin\alpha\xi\sin\alpha\chi}{\alpha^4 + A^4}\,d\alpha +$$

$$+ L_{11}\int_0^\infty \frac{\sin\alpha\xi\sin\alpha\chi}{\alpha^2 + n_1^2}\,d\alpha + L_{12}\int_0^\infty \frac{\sin\alpha\xi\sin\alpha\chi}{\alpha^2 + n_2^2}\,d\alpha =$$

(Equation continued on next page)

99

(Equation continued from preceding page)

$$
= \begin{cases}
\begin{aligned}
&\frac{\pi}{4\sqrt{2}A}\left\{\exp\left(-\frac{A(\xi-\chi)}{\sqrt{2}}\right)\left[\left(L_\theta+\frac{L_{10}}{A^2}\right)\cos\frac{A(\xi-\chi)}{\sqrt{2}}+\right.\right.\\
&\left.+\left(\frac{L_{10}}{A^4}-L_\theta\right)\sin\frac{A(\xi-\chi)}{\sqrt{2}}\right]-\exp\left(-\frac{A(\xi+\chi)}{\sqrt{2}}\right)\times\\
&\times\left.\left[\left(L_\theta+\frac{L_{10}}{A^2}\right)\cos\frac{A(\xi+\chi)}{\sqrt{2}}+\left(\frac{L_{10}}{A^4}-L_\theta\right)\sin\frac{A(\xi-\chi)}{\sqrt{2}}\right]\right\}+\\
&+2L_{11}e^{-m_1\xi}\operatorname{sh}m_1\chi+2L_{12}e^{-m_1\xi}\operatorname{sh}m_2\chi \quad \text{for}\,\xi>\chi.\\[6pt]
&\frac{\pi}{4\sqrt{2}A}\left\{\exp\left(\frac{A(\xi-\chi)}{\sqrt{2}}\right)\left[L_\theta+\frac{L_{10}}{A^2}\right]\cos\frac{A(\xi-\chi)}{\sqrt{2}}+\right.\\
&\left.+\left(L_\theta-\frac{L_{10}}{A^2}\right)\sin\frac{A(\xi-\chi)}{\sqrt{2}}\right]-\exp\left(-\frac{A(\xi+\chi)}{\sqrt{2}}\right)\times\\
&\times\left.\left[\left(L_\theta+\frac{L_{12}}{A^2}\right)\cos\frac{A(\xi+\chi)}{\sqrt{2}}+\left(\frac{L_{10}}{A^4}-L_\theta\right)\sin\frac{A(\xi+\chi)}{\sqrt{2}}\right]\right\}+\\
&+2L_{11}e^{-m_1\chi}\operatorname{sh}m_1\xi+2L_{12}e^{-m_2\chi}\operatorname{sh}m_2\xi \quad \text{for}\,\xi<\chi;
\end{aligned}
\end{cases}
$$

$$
J_4=\int_0^\infty\frac{a^4\sin a\xi\cos a\chi}{(a^4+A^4)[(a^2+\gamma^2)^2+a^2m_1^4]}\,da=\int_0^\infty\frac{a(L_{13}a^2+L_{14})\sin a\xi\cos a\chi}{a^4+A^4}\,da+
$$

$$
+L_{15}\int_0^\infty\frac{a\sin a\xi\cos a\chi}{a^2+m_1^2}\,da+L_{16}\int_0^\infty\frac{a\sin a\xi\cos a\chi}{a^2+m_2^2}\,da=
$$

$$
= \begin{cases}
\begin{aligned}
&\frac{\pi}{4}\left\{\exp\left(-\frac{A(\xi-\chi)}{\sqrt{2}}\right)\left[L_{13}\cos\frac{A(\xi-\chi)}{\sqrt{2}}+\frac{L_{14}}{A^2}\sin\frac{A(\xi-\chi)}{\sqrt{2}}\right]+\right.\\
&\left.+\exp\left(-\frac{A(\xi+\chi)}{\sqrt{2}}\right)\left[L_{13}\cos\frac{A(\xi+\chi)}{\sqrt{2}}+\frac{L_{14}}{A^2}\sin\frac{A(\xi+\chi)}{\sqrt{2}}\right]\right\}+\\
&+\frac{\pi}{2}\left(L_{15}e^{-m_1\xi}\operatorname{ch}m_1\chi+L_{16}e^{-m_2\xi}\operatorname{ch}m_2\chi\right) \quad \text{for}\,\xi>\chi.\\[6pt]
&\frac{\pi}{4}\left\{\exp\left(\frac{A(\xi-\chi)}{\sqrt{2}}\right)\left[L_{13}\cos\frac{A(\xi-\chi)}{\sqrt{2}}-\frac{L_{14}}{A^2}\sin\frac{A(\xi-\chi)}{\sqrt{2}}\right]+\right.\\
&\left.+\exp\left(-\frac{A(\xi+\chi)}{\sqrt{2}}\right)\left[L_{13}\cos\frac{A(\xi+\chi)}{\sqrt{2}}+\frac{L_{14}}{A^2}\sin\frac{A(\xi+\chi)}{\sqrt{2}}\right]\right\}+\\
&+\frac{\pi}{2}\left(L_{15}e^{-m_1\chi}\operatorname{sh}m_1\xi+L_{16}e^{-m_2\chi}\operatorname{sh}m_2\xi\right) \quad \text{for}\,\xi<\chi.
\end{aligned}
\end{cases}
$$

Here the notations are:

$$
L_1=-\frac{A^4-n_1^2n_2^2+\gamma^2(n_1^2+n_2^2)}{(A^4-n_1^2n_2^2)+A^4(n_1^2+n_2^2)^2},\quad
L_2=\frac{A^4(n_1^2+n_2^2)-\gamma^2(A^4-n_1^2n_2^2)}{(A^4-n_1^2n_2^2)^2+A^4(n_1^2+n_2^2)^2},
$$

$$
L_3=\frac{L_2+n_2^2L_1}{n_1^2-n_2^2},\quad L_4=-\frac{L_2+n_1^2L_1}{n_1^2-n_2^2},
$$

$$
L_5=-\frac{n_1^2+n_2^2}{(A^4-n_1^2n_2^2)^2+A^4(n_1^2+n_2^2)^2},\quad
L_6=\frac{n_1^2n_2^2-A^4}{(A^4-n_1^2n_2^2)^2+A^4(n_1^2+n_2^2)^2} \quad (2.8)
$$

(Equation continued from preceding page)

$$L_7 = \frac{L_5 m_2^2 + L_6}{m_1^2 - m_2^2}, \quad L_8 = -\frac{L_6 + L_5 m_1^2}{m_1^2 - m_2^2}.$$

$$L_9 = \frac{A^4(m_1^2 + m_2^2) - \tau^2(A^4 - m_1^2 m_2^2)}{(A^4 - m_1^2 m_2^2)^2 + A^4(m_1^2 + m_2^2)^2}, \quad L_{10} = \frac{A^4\left[(A^4 - m_1^2 m_2^2) + \tau^2(m_1^2 + m_2^2)\right]}{(A^4 - m_1^2 m_2^2)^2 + A^4(m_1^2 + m_2^2)^2}, \qquad (2.8)$$

$$L_{11} = \frac{L_{10} + L_9 m_2^2 - 1}{m_1^2 - m_2^2}, \quad L_{12} = \frac{1 - L_{10} - L_9 m_1^2}{m_1^2 - m_2^2}.$$

$$L_{13} = \frac{m_1^2 m_2^2 - A^4}{(A^4 - m_1^2 m_2^2)^2 + A^4(m_1^2 + m_2^2)^2}, \quad L_{14} = \frac{A^4(m_1^2 + m_2^2)}{(A^4 - m_1^2 m_2^2)^2 + A^4(m_1^2 + m_2^2)^2},$$

$$L_{15} = \frac{L_{13} + L_{13} m_2^2}{m_1^2 - m_2^2}, \quad L_{16} = -\frac{L_{14} - L_{13} m_1^2}{m_1^2 - m_2^2}.$$

NOTE: In specific cases the calculation of these integrals is simplified considerably. The quantity $n^2 = \frac{4V^2}{m^4}$ even for large values of the heat transfer coefficient and small source velocities is much smaller than one.

For example, for a steel shell of thickness h = 1 cm and source velocity V = 10 m/hr

$$\kappa = 45 \cdot 10^{-3}\left[\frac{m^2}{hr}\right], \quad C = 0.11\left[\frac{kcal}{kg/deg}\right] \quad \rho = 7900\left[\frac{kg}{m^3}\right]$$

$$n^2 = 0.00035\,\dot{K}_0.$$

for $\dot{K}_0 = 35 \; kcal/m^2 \cdot hr \cdot deg$

$$n^2 \ll 1.$$

For these same values

$$p^2 = \frac{4V n^2}{h^4 \omega^4} \approx 10,$$

and only for velocities of the order of 300 m/hr is $p^2 \approx 0.01$, i.e., also small in comparison with one.

For $n^2 \ll 1$

$$n_1^2 \approx m^2, \quad n_2^2 = \frac{\mu}{m^2}, \quad n_1^2 \pm n_2^2 \approx m^2.$$

<div align="right">(a)</div>

If in this case $P^2 \ll 1$, then

$$m_1^2 = m^2, \quad m_2^2 = \frac{\gamma^2}{m^2}, \quad m_1^2 \pm m_2^2 \approx m^2$$

<div align="right">(b)</div>

and for $P^2 \gg 1$

$$m_1^2 = \tau(\tau + m), \quad m_2^2 = \tau(\gamma - m),$$
$$m_1^2 + m_2^2 = 2\gamma^2, \quad m_1^2 - m_2^2 = 2\tau m.$$

<div align="right">(c)</div>

The constants L_i from (2.8) are simplified correspondingly. We denote

$$\varphi_1(\xi, \tau) = \frac{1}{2} \exp\left[-\frac{A(\xi - \chi)}{\sqrt{2}}\right] \times$$
$$\times \left\{\left[m(L_4 B - L_{13}C) + \frac{1}{\sqrt{2}A}(L_6 C - L_1 B) + \frac{1}{\sqrt{2}A^2}(L_{10}C - L_2 B)\right] \times \right.$$
$$\times \cos\frac{A(\xi - \chi)}{\sqrt{2}} + \left[\frac{m}{A^2}(L_6 B - L_{11}C) + \frac{1}{\sqrt{2}A}(L_1 B - L_9 C) + \right.$$
$$\left. + \frac{1}{\sqrt{2}A^2}(L_{10}C - L_2 B)\right] \sin\frac{A(\xi - \chi)}{\sqrt{2}}\right\} \quad \text{for } \xi > \chi;$$

$$\varphi_2(\xi, \tau) = \frac{1}{2} \exp\left[-\frac{A(\xi + \chi)}{\sqrt{2}}\right] \times$$
$$\times \left\{\left[\frac{1}{\sqrt{2}A}(L_1 B - L_9 C) + \frac{1}{\sqrt{2}A^2}(L_2 B - L_{10}C) + m(L_4 B - L_{13}C)\right] \times \right.$$
$$\times \cos\frac{A(\xi + \chi)}{\sqrt{2}} + \left[\frac{1}{\sqrt{2}A}(L_9 C - L_1 B) + \frac{1}{\sqrt{2}A^2}(L_2 B - L_{10}C) + \right.$$
$$\left. + \frac{m}{A^2}(L_6 B - L_{11}C)\right] \sin\frac{A(\xi + \chi)}{\sqrt{2}}\right\} \quad \text{for } \xi > \chi;$$

$$\varphi_3(\xi, \tau) = e^{-n_1\xi}\left(\frac{4}{\pi} L_5 \, \text{sh} \, n_1\chi - mL_7 \, \text{ch} \, n_1\chi\right) +$$
$$+ e^{-n_2\xi}\left(\frac{4}{\pi} L_4 \, \text{sh} \, n_2\chi - mL_8 \, \text{ch} \, n_2\chi\right) \quad \text{for } \xi > \chi;$$

$$\varphi_4(\xi, \tau) = e^{-m_1\xi}\left(\frac{4}{\pi} L_{11} \, \text{sh} \, m_1\chi - mL_{13} \, \text{ch} \, m_1\chi\right) +$$
$$+ e^{-m_2\xi}\left(\frac{4}{\pi} L_{12} \, \text{sh} \, m_2\chi - mL_{16} \, \text{ch} \, m_2\chi\right) \quad \text{for } \xi > \chi;$$

$$\varphi_5(\xi, \tau) = \frac{1}{2} \exp\left[\frac{A(\xi - \chi)}{\sqrt{2}}\right] \times$$
$$\times \left\{\left[\frac{1}{\sqrt{2}A}(L_9 C - L_1 B) + \frac{1}{\sqrt{2}A^2}(L_{10}C - L_2 B) + m(L_5 B - L_{13}C)\right] \times \right.$$
$$\times \cos\frac{A(\xi - \chi)}{\sqrt{2}} + \left[\frac{1}{\sqrt{2}A}(L_9 C - L_1 B) + \frac{1}{\sqrt{2}A^2}(L_2 B - L_{10}C) + \right.$$
$$\left. + \frac{m}{A^2}(L_{14}C - L_6 B)\right] \sin\frac{A(\xi - \chi)}{\sqrt{2}}\right\} \quad \text{for } \xi < \chi;$$

FTD-HC-23-361-69

(Equation continued from preceding page)

$$\varphi_6(\xi, \tau) = \tfrac{1}{2}\exp\left[-\tfrac{A(\xi+\chi)}{\sqrt{2}}\right] \times$$

$$\times\left\{\left[\tfrac{1}{\sqrt{2}A}(L_1 B - L_3 C) + \tfrac{1}{\sqrt{2}A^2}(L_5 B - L_{10}C) + m(L_6 B - L_{15}C)\right] \times\right.$$

$$\times \cos\tfrac{A(\xi+\chi)}{\sqrt{2}} + \left[\tfrac{1}{\sqrt{2}A}(L_3 C - L_1 B) + \tfrac{1}{\sqrt{2}A^2}(L_9 B - L_{10}C) +\right.$$

$$\left.\left. + \tfrac{m}{A}(L_6 B - L_{16}C)\right]\sin\tfrac{A(\xi+\chi)}{\sqrt{2}}\right\} \quad \text{for } \xi \leqslant \chi;$$

$$\varphi_7(\xi, \tau) = e^{-n_1 z}\left(\tfrac{A}{n}L_3 + L_7 m\right)\operatorname{sh} n_1\xi +$$

$$+ e^{-n_2 z}\left(\tfrac{A}{n}L_4 + L_8 m\right)\operatorname{sh} n_2\xi \quad \text{for } \xi \leqslant \chi;$$

$$\varphi_8(\xi, \tau) = e^{-m_1 z}\left(\tfrac{A}{n}L_{11} - L_{16}m\right)\operatorname{sh} m_1\xi +$$

$$+ e^{-m_2 z}\left(\tfrac{A}{n}L_{12} - L_{16}m\right)\operatorname{sh} m_2\xi \quad \text{for } \xi \leqslant \chi;$$

$$f_1(\xi, \tau) = \tfrac{e^{-\tau-\frac{\xi}{n}}}{4}\left\{L_1\exp\left(n_1\sqrt{\tau} - \tfrac{\xi}{2\sqrt{\tau}}\right)^2 \times\right.$$

$$\times\left[1 - \operatorname{erf}\left(n_1\sqrt{\tau} - \tfrac{\xi}{2\sqrt{\tau}}\right)\right] - L_1\exp\left(n_1\sqrt{\tau} + \tfrac{\xi}{2\sqrt{\tau}}\right)^2 \times$$

$$\times\left[1 - \operatorname{erf}\left(n_1\sqrt{\tau} + \tfrac{\xi}{2\sqrt{\tau}}\right)\right] + L_2\exp\left(n_2\sqrt{\tau} - \tfrac{\xi}{2\sqrt{\tau}}\right)^2 \times$$

$$\times\left[1 - \operatorname{erf}\left(n_2\sqrt{\tau} - \tfrac{\xi}{2\sqrt{\tau}}\right)\right] - L_2\exp\left(n_2\sqrt{\tau} + \tfrac{\xi}{2\sqrt{\tau}}\right)^2 \times$$

$$\times\left.\left[1 - \operatorname{erf}\left(n_2\sqrt{\tau} + \tfrac{\xi}{2\sqrt{\tau}}\right)\right]\right\};$$

$$f_2(\xi, \tau) = \tfrac{e^{-\tau-\frac{\xi}{n}}}{4}\left\{L_{11}\exp\left(m_1\sqrt{\tau} - \tfrac{\xi}{2\sqrt{\tau}}\right)^2 \times\right.$$

$$\times\left[1 - \operatorname{erf}\left(m_1\sqrt{\tau} - \tfrac{\xi}{2\sqrt{\tau}}\right)\right] - L_{11}\exp\left(m_1\sqrt{\tau} + \tfrac{\xi}{2\sqrt{\tau}}\right)^2 \times$$

$$\times\left[1 - \operatorname{erf}\left(m_1\sqrt{\tau} + \tfrac{\xi}{2\sqrt{\tau}}\right)\right] + L_{12}\exp\left(m_2\sqrt{\tau} - \tfrac{\xi}{2\sqrt{\tau}}\right)^2 \times$$

$$\times\left[1 - \operatorname{erf}\left(m_2\sqrt{\tau} - \tfrac{\xi}{2\sqrt{\tau}}\right)\right] - L_{12}\exp\left(m_2\sqrt{\tau} + \tfrac{\xi}{2\sqrt{\tau}}\right)^2 \times$$

$$\times\left.\left[1 - \operatorname{erf}\left(m_2\sqrt{\tau} + \tfrac{\xi}{2\sqrt{\tau}}\right)\right]\right\};$$

$$f_3(\xi, \tau) = \tfrac{e^{-\tau-\frac{\xi}{n}}}{8}\left\{\left(L_5 - \tfrac{L_6}{LA^2}\right)\left[\exp\left(A\sqrt{k\tau} - \tfrac{\xi}{2\sqrt{\tau}}\right)^2 \times\right.\right.$$

$$\left.\times\operatorname{erfc}\left(A\sqrt{k\tau} - \tfrac{\xi}{2\sqrt{\tau}}\right) - \exp\left(A\sqrt{k\tau} + \tfrac{\xi}{2\sqrt{\tau}}\right)^2\operatorname{erfc}\left(A\sqrt{k\tau} + \tfrac{\xi}{2\sqrt{\tau}}\right)\right] +$$

$$+ \left(L_5 + \tfrac{L_6}{A^2i}\right)\left[\exp\left(-A\sqrt{k\tau} - \tfrac{\xi}{2\sqrt{\tau}}\right)^2\operatorname{erfc}\left(-A\sqrt{k\tau} - \tfrac{\xi}{2\sqrt{\tau}}\right) -\right.$$

$$\left.\left. - \exp\left(-A\sqrt{k\tau} + \tfrac{\xi}{2\sqrt{\tau}}\right)^2\operatorname{erfc}\left(-A\sqrt{k\tau} + \tfrac{\xi}{2\sqrt{\tau}}\right)\right]\right\};$$

$$f_4(\xi, \tau) = \tfrac{e^{-\tau-\frac{\xi}{n}}}{8}\left\{\left(L_{15} - \tfrac{L_{16}}{LA^2}\right)\left[\exp\left(A\sqrt{k\tau} - \tfrac{\xi}{2\sqrt{\tau}}\right)^2 \times\right.\right.$$

$$\left.\times\operatorname{erfc}\left(A\sqrt{k\tau} - \tfrac{\xi}{2\sqrt{\tau}}\right) - \exp\left(A\sqrt{k\tau} + \tfrac{\xi}{2\sqrt{\tau}}\right)^2\operatorname{erfc}\left(A\sqrt{k\tau} + \tfrac{\xi}{2\sqrt{\tau}}\right)\right] +$$

$$+ \left(L_{15} + \tfrac{L_{16}}{LA^2}\right)\left[\exp\left(-A\sqrt{k\tau} - \tfrac{\xi}{2\sqrt{\tau}}\right)^2\operatorname{erfc}\left(-A\sqrt{k\tau} - \tfrac{\xi}{2\sqrt{\tau}}\right) -\right.$$

$$\left.\left. - \exp\left(-A\sqrt{k\tau} + \tfrac{\xi}{2\sqrt{\tau}}\right)^2\operatorname{erfc}\left(-A\sqrt{k\tau} + \tfrac{\xi}{2\sqrt{\tau}}\right)\right]\right\}.$$

Then we have the following expressions for w^* and $\dfrac{\partial w^*}{\partial \xi}$

$$w^*(\xi, \tau) = -\frac{mB}{2} f_1(\xi, \tau) + \frac{mC}{2} f_2(\xi, \tau) - \frac{2mB}{\pi} f_3(\tau, \xi) + $$
$$+ \frac{2mC}{\pi} f_4(\xi, \tau) + $$
$$+ \begin{cases} \varphi_1(\xi, \tau) + \varphi_2(\xi, \tau) - B\varphi_3(\xi, \tau) + C\varphi_4(\xi, \tau) & \text{for } \xi > \chi, \\ \varphi_5(\xi, \tau) + \varphi_6(\xi, \tau) - B\varphi_7(\xi, \tau) + C\varphi_8(\xi, \tau) & \text{for } \xi < \chi; \end{cases}$$

$$\frac{\partial w^*(\xi, \tau)}{\partial \xi} = -\frac{CRe^{-n_1 \cdots \frac{\xi}{R}}}{6\hbar m \sqrt{1+n^2}} \Big\{ \exp\Big(n_1 \sqrt{\tau} - \frac{\xi}{2\sqrt{\tau}}\Big)^2 \times$$

$$\times \Big[1 - \operatorname{erf}\Big(n_1 \sqrt{\tau} - \frac{\xi}{2\sqrt{\tau}}\Big)\Big] - \exp\Big(n_1 \sqrt{\tau} + \frac{\xi}{2\sqrt{\tau}}\Big)^2 \times$$

$$\times \Big[1 - \operatorname{erf}\Big(n_1 \sqrt{\tau} + \frac{\xi}{2\sqrt{\tau}}\Big)\Big] - \exp\Big(n_2 \sqrt{\tau} - \frac{\xi}{2\sqrt{\tau}}\Big)^2 \times$$

$$\times \Big[1 - \operatorname{erf}\Big(n_2 \sqrt{\tau} - \frac{\xi}{2\sqrt{\tau}}\Big)\Big] + \exp\Big(n_2 \sqrt{\tau} + \frac{\xi}{2\sqrt{\tau}}\Big)^2 \times$$

$$\times \Big[1 - \operatorname{erf}\Big(n_2 \sqrt{\tau} + \frac{\xi}{2\sqrt{\tau}}\Big)\Big]\Big\} - \frac{vmB}{2}\Big(f_1 + \frac{4}{\pi} f_3\Big) + \frac{vmC}{2}\Big(f_2 + \frac{4}{\pi} f_4\Big)$$

$$+ \begin{cases} \varphi_1 + \varphi_2 - B\varphi_3 + C\varphi_4 + \dfrac{CR}{6\hbar m \sqrt{1+n^2}} \times \\ \quad \times [e^{-n_1(\xi - \tau)} - e^{-n_2(\xi + \tau)}] & \text{for } \xi > \chi, \\ \varphi_5 + \varphi_6 - B\varphi_7 + C\varphi_8 + \dfrac{CR}{6\hbar m \sqrt{1+n^2}} \times \\ \quad \times e^{-n_1 \xi} \operatorname{sh} n_1 \xi & \text{for } \xi < \chi. \end{cases}$$

(2.9)

(2.10)

The forces and moments are calculated from

$$T_1(\xi, \tau) = \frac{D_1 h}{R}\Big(\frac{\partial w^*}{\partial \xi} + v w^* - \frac{Ch}{3R} T^*\Big),$$
$$T_2(\xi, \tau) = \frac{D_1 h}{R}\Big(v\frac{\partial w^*}{\partial \xi} + w^* - \frac{Ch}{3R} T^*\Big),$$
$$N_1(\xi, \tau) = -\frac{D_2 h}{R^2}\Big(\frac{\partial^3 w^*}{\partial \xi^3} + C\frac{\partial K^*}{\partial \xi}\Big),$$
$$M_1(\xi, \tau) = -\frac{D_2 h}{R^2}\Big(\frac{\partial^2 w^*}{\partial \xi^2} + CK^*\Big),$$
$$M_2(\xi, \tau) = -\frac{D_2 h}{R^2}\Big(v\frac{\partial^2 w^*}{\partial \xi^2} + CK^*\Big)$$

(2.11)

§ 3. Displacement Field (with account for
       inertia of normal component of the
       displacement vector)

In the case of the displacement field (with account for the normal component of the inertia forces), the thermoelasticity equations in terms of displacements will be

$$\frac{\partial^4 w^*}{\partial \xi^4} + A^4 w^* = -BT^* - C\frac{\partial^2 K^*}{\partial \xi^2} - D\frac{\partial^2 w^*}{\partial t^2},$$
$$\frac{\partial u^*}{\partial \xi} + v w^* = \frac{CR}{3h} T^*.$$

(3.1)

Applying the transformation (2.4) to the first equation under the conditions (2.3), we obtain

$$D\frac{d^2\bar{w}^0}{d\tau^2}+(a^4+A^4)\bar{w}^0=-\frac{\sqrt{\frac{2}{\pi}}B[(a^2+\beta^2)\sin\eta\chi-am\cos a\chi]}{(a^2+\beta^2)^2+a^2m^2}-$$
$$-\frac{\sqrt{\frac{2}{\pi}}Bame^{-(a^2+\beta^2)\tau}}{(a^2+\beta^2)^2+a^2m^2}-\frac{\sqrt{\frac{2}{\pi}}Ca^2[(a^2+\gamma^2)\sin a\chi-am\cos a\chi]}{(a^2+\gamma^2)^2+a^2m^2}+$$
$$+\frac{\sqrt{\frac{2}{\pi}}Ca^2me^{-(a^2+\gamma^2)\tau}}{(a^2+\gamma^2)^2+a^2m^2}; \qquad (3.2)$$

$$\bar{w}^0(a,0)=\frac{d\bar{w}^0(a,0)}{d\tau}=0. \qquad (3.3)$$

Solving (3.2) under the conditions (3.3) and then inverting the result, we obtain

$$w^0(\xi,\tau)=\frac{2}{\pi}\int_0^{\infty}\left\{-Bam\frac{(a^2+\beta^2)\sin\eta\tau-\eta\cos\eta\tau+\eta e^{-(a^2+\beta^2)\tau}}{D\eta[(a^2+\beta^2)^2+\eta^2][(a^2+\beta^2)^2+a^2m^2]}-\right.$$
$$-\frac{B}{D\eta[(a^2+\beta^2)^2+a^2m^2][\eta^2-a^2m^2]}\left[(a^2+\beta^2)(\eta\sin a\chi-2am\cos\eta\tau)-\right.$$
$$\left.-am\eta(\cos a\chi-2\cos\eta\tau)\right]+Ca^2m\frac{(a^2+\gamma^2)\sin\eta\tau-\eta\cos\eta\tau+\eta e^{-(a^2+\gamma^2)\tau}}{D\eta[(a^2+\gamma^2)^2+\eta^2][(a^2+\gamma^2)^2+a^2m^2]}+ \qquad (3.4)$$
$$+\frac{Ca^2}{D\eta[(a^2+\gamma^2)^2+a^2m^2][\eta^2-a^2m^2]}\left[(a^2+\gamma^2)(\eta\sin a\chi-\right.$$
$$\left.\left.-2ma\cos\eta\tau)-ma\eta(\cos a\chi-2\cos\eta\tau)\right]\right\}\sin a\xi\,da.$$

From the second expression of (3.1) with account for (3.4) and (1.10), we have

$$\frac{dw^0}{d\xi}=-\frac{CRe^{-p\tau-\frac{\xi^2}{4\tau}}}{6\hbar m\sqrt{1+m^2}}\left\{\exp\left(n_1\sqrt{\tau}-\frac{\xi}{2\sqrt{\tau}}\right)^2\mathrm{erfc}\left(n_1\sqrt{\tau}-\frac{\xi}{2\sqrt{\tau}}\right)-\right.$$
$$-\exp\left(n_1\sqrt{\tau}+\frac{\xi}{2\sqrt{\tau}}\right)^2\mathrm{erfc}\left(n_1\sqrt{\tau}+\frac{\xi}{2\sqrt{\tau}}\right)-$$
$$-\exp\left(n_2\sqrt{\tau}-\frac{\xi}{2\sqrt{\tau}}\right)^2\mathrm{erfc}\left(n_2\sqrt{\tau}-\frac{\xi}{2\sqrt{\tau}}\right)+$$
$$\left.+\exp\left(n_2\sqrt{\tau}+\frac{\xi}{2\sqrt{\tau}}\right)^2\mathrm{erfc}\left(n_2\sqrt{\tau}+\frac{\xi}{2\sqrt{\tau}}\right)\right\}+$$
$$+\frac{2\tau}{\pi}\int_0^{\infty}\left\{Bam\frac{(a^2+\beta^2)\sin\eta\tau-\eta\cos\eta\tau+\eta e^{-(a^2+\beta^2)\tau}}{D\eta[(a^2+\beta^2)^2+\eta^2][(a^2+\beta^2)^2+a^2m^2]}+\right.$$
$$+\frac{B}{D\eta[(a^2+\beta^2)^2+a^2m^2][\eta^2-a^2m^2]}\left[(a^2+\beta^2)(\eta\sin a\chi-2am\cos\eta\tau)-\right. \qquad (3.5)$$
$$\left.-am\eta(\cos a\chi-2\cos\eta)\right]-Ca^2m\frac{(a^2+\gamma^2)\sin\eta\tau-\eta\cos\eta\tau+\eta e^{-(a^2+\gamma^2)\tau}}{D\eta[(a^2+\gamma^2)^2+\eta^2][(a^2+\gamma^2)^2+a^2m^2]}-$$
$$-\frac{Ca^2}{D\eta[(a^2+\gamma^2)^2+a^2m^2][\eta^2-a^2m^2]}\left[(a^2+\gamma^2)(\eta\cos a\chi-2ma\cos\eta\tau)-\right.$$
$$\left.\left.-ma\eta(\cos a\eta-2\cos\eta\tau)\right]\right\}\sin a\xi\,da+$$

$$+\begin{cases}\dfrac{CR}{3\hbar m\sqrt{1+m^2}}\left[e^{-n_i(\xi-\chi)}-e^{-n_i(\xi+\chi)}\right] & \text{for } 0<\chi<\xi,\\[2ex] -\dfrac{CR}{3\hbar m\sqrt{1+m^2}}e^{-2n_i\xi} & \text{for } 0<\chi=\xi, \quad (3.5\\[2ex] \dfrac{CR}{3\hbar m\sqrt{1+m^2}}e^{-n_i\chi}\,\mathrm{sh}\,n_i\xi & \text{for } 0<\xi<\chi.\end{cases}$$

In (3.4) and (3.5) we have used the notation

$$\tau_r^2 = \frac{\pi^4 + A^4}{D}.$$
(3.6)

for simplicity.

II.   Shells of Finite Length

§ 4.   Temperature Field

In the case of a shell of finite length, we solve (1.3) under the conditions

$$T^{\bullet}(\xi, 0) = T^{\bullet}(0, \tau) = T^{\bullet}(l_0, \tau) = 0,$$
(4.1)

$$K^{\bullet}(\xi, 0) = K^{\bullet}(0, \tau) = K^{\bullet}(l_0, \tau) = 0.$$
(4.2)

Applying the finite Fourier sine transformation

$$\theta(n, \tau) = \int_0^l T^{\bullet} \sin \frac{n\pi\xi}{l_0} d\xi,$$
(4.3)

to the first equation (1.3) under the conditions (1.4), we have

$$\frac{d\theta}{d\tau} + \left(\beta^2 + \frac{n^2\pi^2}{l_0^2}\right)\theta = \sin \alpha\tau,$$
(4.4)

$$\theta(n, 0) = 0.$$
(4.5)

We solve this equation under the condition (4.5) and invert the result.   Then

$$T^{\bullet}(\xi, \tau) =$$
$$-\frac{2}{l_0}\sum_{n=1}^{\infty}\frac{\left\{\left(\beta^2 + \frac{n^2\pi^2}{l_0^2}\right)\sin \alpha n\tau - \alpha n \cos \alpha n\tau + n\alpha \exp\left[-\left(\beta^2 + \frac{n^2\pi^2}{l_0^2}\right)\right]\right\} \sin \frac{n\pi\xi}{l_0}}{\left(\beta^2 + \frac{n^2\pi^2}{l_0^2}\right)^2 + \alpha^2 n^2}$$
(4.6)

We obtain similarly

$$K^{\bullet}(\xi, \tau) =$$
$$-\frac{2}{l_0}\sum_{n=1}^{\infty}\frac{\left\{\left(\tau^2 + \frac{n^2\pi^2}{l_0^2}\right)\sin \alpha n\tau - \alpha n \cos \alpha n\tau + n\alpha \exp\left[-\left(\tau^2 + \frac{n^2\pi^2}{l_0^2}\right)\right]\right\} \sin \frac{n\pi\xi}{l_0}}{\left(\tau^2 + \frac{n^2\pi^2}{l_0^2}\right)^2 + \alpha^2 n^2}.$$
(4.7)

§ 5. Displacement Field (quasistatic case)

We solve (2.1) under the conditions

$$w^\circ(0, \tau) = w^\circ(l_0, \tau) = \frac{\partial^2 w^\circ(0, \tau)}{\partial \xi^2} = \frac{\partial^2 w^\circ(l_0, \tau)}{\partial \xi^2} = 0. \tag{5.1}$$

We apply the finite Fourier sine transformation

$$\overline{w}^\circ(n, \tau) = \int_0^{l_0} w^\circ \sin \frac{n\pi\xi}{l_0}\, d\xi \tag{5.2}$$

to (2.1) under the conditions (5.1) and after inverting the result we have

$$w^\circ(\xi, \tau) = \frac{2\beta}{l_0} \sum_{n=1}^{\infty} \frac{1}{\beta^4 + \frac{n^4\pi^4}{l_0^4}} \left\{ \frac{n\alpha \exp\left[-\left(\beta^2 + \frac{n^2\pi^2}{l_0^2}\right)\tau\right]}{\left(\beta^2 + \frac{n^2\pi^2}{l_0^2}\right)^2 + n^2\alpha^2} + \right.$$

$$\left. + \frac{n\alpha \cos \alpha n\tau - \left(\beta^2 + \frac{n^2\pi^2}{l_0^2}\right)\sin \alpha n\tau}{\left(\beta^2 + \frac{n^2\pi^2}{l_0^2}\right)^2 + n^2\alpha^2} \right\} \sin \frac{n\pi\xi}{l_0} +$$

$$+ \frac{3C\alpha^2}{l_0} \sum_{n=1}^{\infty} \frac{1}{\gamma^4 + \frac{n^4\pi^4}{l_0^4}} \left\{ \frac{n\alpha \exp\left[-\left(\gamma^2 + \frac{n^2\pi^2}{l_0^2}\right)\tau\right]}{\left(\gamma^2 + \frac{n^2\pi^2}{l_0^2}\right)^2 + \alpha^2 n^2} + \right. \tag{5.3}$$

$$\left. + \frac{\left(\gamma^2 + \frac{n^2\pi^2}{l_0^2}\right)\sin \alpha n\tau - n\alpha \cos \alpha n\tau}{\left(\gamma^2 + \frac{n^2\pi^2}{l_0^2}\right)^2 + \alpha^2 n^2} \right\} \sin \frac{n\pi\xi}{l_0}.$$

From (2.2) with account for (4.6) and (5.3), we have

$$\frac{\partial w^\circ}{\partial \xi} = \frac{2CR}{3hl_0} \sum_{n=1}^{\infty} \left\{ \frac{\left(\beta^2 + \frac{n^2\pi^2}{l_0^2}\right)\sin \alpha n\tau - \alpha n \cos \alpha n\tau}{\left(\beta^2 + \frac{n^2\pi^2}{l_0^2}\right)^2 + \alpha^2 n^2} + \right.$$

$$\left. + \frac{\alpha n \exp\left[-\left(\beta^2 + \frac{n^2\pi^2}{l_0^2}\right)\tau\right]}{\left(\beta^2 + \frac{n^2\pi^2}{l_0^2}\right)^2 + \alpha^2 n^2} \right\} \sin \frac{n\pi\xi}{l_0} - \tag{5.4}$$

(Equation continued on next page)

(Equation continued from preceding page)

$$-\frac{2\nu B}{l_0}\sum_{n=1}^{\infty}\frac{1}{A^4+\frac{n^4\pi^4}{l_0^4}}\left\{\frac{na\exp\left[-\left(\beta^2+\frac{n^2\pi^2}{l_0^2}\right)\tau\right]+na\cos an\tau}{\left(\beta^2+\frac{n^2\pi^2}{l_0^2}\right)^2+a^2n^2}\right.$$

$$\left.-\frac{\left(\beta^2+\frac{n^2\pi^2}{l_0^2}\right)\sin an\tau}{\left(\beta^2+\frac{n^2\pi^2}{l_0^2}\right)^2+a^2n^2}\right\}\sin\frac{n\pi\xi}{l_0}- \tag{5.4}$$

$$-\frac{2\nu C\pi^2}{l_0^2}\sum_{n=1}^{\infty}\frac{1}{A^4+\frac{n^4\pi^4}{l_0^4}}\left\{\frac{na\exp\left[-\left(\gamma^2+\frac{n^2\pi^2}{l_0^2}\right)\tau\right]}{\left(\gamma^2+\frac{n^2\pi^2}{l_0^2}\right)^2+a^2n^2}+\right.$$

$$\left.+\frac{\left(\gamma^2+\frac{n^2\pi^2}{l_0^2}\right)\sin an\tau-an\cos an\tau}{\left(\gamma^2+\frac{n^2\pi^2}{l_0^2}\right)^2+a^2n^2}\right\}\sin\frac{n\pi\xi}{l_0}.$$

§ 6. Displacements with Account for Inertia of the Normal Component of the Displacement Vector

In this case we solve (3.1) under the conditions

$$w^*(0,t)=w^*(0,\tau)=w^*(l_0,\tau)=\frac{\partial^2 w^*(0,\tau)}{\partial\xi^2}=\frac{\partial^2 w^*(l_0,\tau)}{\partial\xi^2}=0. \tag{6.1}$$

We apply the finite Fourier sine transformation (5.2) to the first equation of (3.1) under the condition (6.1) and obtain

$$D\frac{d^2\bar{w}^*}{dt^2}+\left(A^4+\frac{n^4\pi^4}{l_0^4}\right)\bar{w}^*=$$

$$=\frac{-B\left[\left(\beta^2+\frac{n^2\pi^2}{l_0^2}\right)\sin an\tau-an\cos an\tau\right]}{\left(\beta^2+\frac{n^2\pi^2}{l_0^2}\right)^2+a^2n^2}-\frac{Bna\exp\left[-\left(\beta^2+\frac{n^2\pi^2}{l_0^2}\right)\tau\right]}{\left(\beta^2+\frac{n^2\pi^2}{l_0^2}\right)^2+a^2n^2}-$$

$$-\frac{C\frac{n^2\pi^2}{l_0^2}\left[\left(\gamma^2+\frac{n^2\pi^2}{l_0^2}\right)\sin an\tau-an\cos an\tau\right]}{\left(\gamma^2+\frac{n^2\pi^2}{l_0^2}\right)^2+a^2n^2}+ \tag{6.2}$$

$$+\frac{C\frac{n^2\pi^2}{l_0^2}a\exp\left[-\left(\gamma^2+\frac{n^2\pi^2}{l_0^2}\right)\tau\right]}{\left(\gamma^2+\frac{n^2\pi^2}{l_0^2}\right)^2+a^2n^2};$$

$$\ddot{w}^\circ(n,\,0)=\frac{d\bar{w}^\circ(n,\,0)}{dt}=0. \tag{6.3}$$

Solving (6.2) under the conditions (6.3) and inverting the result, we obtain

$$w^\circ(\xi,\tau)=\frac{2}{l_0}\sum_{n=1}^{\infty}\left\{-Ban\frac{\left(\beta^2+\frac{n^2\pi^2}{l_0^2}\right)\sin\zeta\tau-\zeta\cos\zeta\tau+\zeta e^{-\left(\beta^2+\frac{n^2\pi^2}{l_0^2}\right)\tau}}{D\zeta\left[\left(\beta^2+\frac{n^2\pi^2}{l_0^2}\right)^2+\zeta^2\right]\left[\left(\beta^2+\frac{n^2\pi^2}{l_0^2}\right)^2+a^2n^2\right]}-\right.$$

$$-\frac{B}{D\zeta\left[\left(\beta^2+\frac{n^2\pi^2}{l_0^2}\right)^2+a^2n^2\right]\left[\zeta^2-a^2n^2\right]}\left[\left(\beta^2+\frac{n^2\pi^2}{l_0^2}\right)(\zeta\sin an\tau-\right.$$

$$\left.-2an\cos\zeta\tau)-an^2(\cos an\tau-2\cos\zeta\tau)\right]+$$

$$+Cn^2a\frac{\left(\gamma^2+\frac{n^2\pi^2}{l_0^2}\right)\sin\zeta\tau-\zeta\cos\zeta\tau+\zeta e^{-\left(\gamma^2+\frac{n^2\pi^2}{l_0^2}\right)\tau}}{D\zeta\left[\left(\gamma^2+\frac{n^2\pi^2}{l_0^2}\right)^2+\zeta^2\right]\left[\left(\gamma^2+\frac{n^2\pi^2}{l_0^2}\right)^2+a^2n^2\right]}+$$

$$+\frac{Cn^2}{D\zeta\left[\left(\gamma^2+\frac{n^2\pi^2}{l_0^2}\right)^2+a^2n^2\right]\left[\zeta^2-a^2n^2\right]}\left[\left(\gamma^2+\frac{n^2\pi^2}{l_0^2}\right)(\zeta\sin an\tau-\right. \tag{6.4}$$

$$\left.\left.-2an\cos\zeta\tau)-an^2(\cos an\tau-2\cos\zeta\tau)\right]\right\}\sin\frac{n\pi\xi}{l_0},$$

where

$$\zeta^2=\frac{(Al_0)^4+(n\pi)^4}{Dl_0^4}. \tag{6.5}$$

From the second expression (3.1) with account for (4.6) and (6.4) we have

$$\frac{\partial w^\circ}{\partial\xi}=\frac{2CR}{3hl_0}\sum_{n=1}^{\infty}\left\{\frac{\left(\beta^2+\frac{n^2\pi^2}{l_0^2}\right)\sin an\tau-an\cos an\tau}{\left(\beta^2+\frac{n^2\pi^2}{l_0^2}\right)^2+a^2n^2}+\right.$$

$$\left.+\frac{an\exp\left[-\left(\beta^2+\frac{n^2\pi^2}{l_0^2}\right)\tau\right]}{\left(\beta^2+\frac{n^2\pi^2}{l_0^2}\right)^2+a^2n^2}\right\}\sin\frac{n\pi\xi}{l_0}+ \tag{6.6}$$

(Equation continuted on next page)

109

(Equation continued from preceding page)

$$+\frac{2\nu}{l_0}\sum_{a=1}^{\cdot}\left\{Ban\frac{\left(\beta^2+\frac{n^2\pi^2}{l_0^2}\right)\sin\zeta\tau-\zeta\cos\zeta\tau+\zeta e^{-\left(\beta^2+\frac{n^2\pi^2}{l_0^2}\right)\tau}}{D\zeta\left[\left(\beta^2+\frac{n^2\pi^2}{l_0^2}\right)^2+\tau^2\right]\left[\left(\beta^2+\frac{n^2\pi^2}{l_0^2}\right)^2+a^2n^2\right]}+\right.$$

$$+\frac{B}{D\zeta\left[\left(\beta^2+\frac{n^2\pi^2}{l_0^2}\right)^2+a^2n^2\right]\left[\zeta^2-a^2n^2\right]}\times$$

$$\times\left[\left(\beta^2+\frac{n^2\pi^2}{l_0^2}\right)(\zeta\sin an\tau-2an\cos\zeta\tau)-an\zeta(\cos an\tau-\right.$$

$$\left.-2\cos\zeta\tau)\right]-Cn^2a\frac{\left(\gamma^2+\frac{n^2\pi^2}{l_0^2}\right)\sin\zeta\tau-\zeta\cos\zeta\tau+\zeta e^{-\left(\gamma^2+\frac{n^2\pi^2}{l_0^2}\right)\tau}}{D\zeta\left[\left(\gamma^2+\frac{n^2\pi^2}{l_0^2}\right)^2+\zeta^2\right]\left[\left(\gamma^2+\frac{n^2\pi^2}{l_0^2}\right)^2+a^2n^2\right]}+$$

$$+\frac{Cn^2}{D\zeta\left[\left(\gamma^2+\frac{n^2\pi^2}{l_0^2}\right)+a^2n^2\right]\left[\zeta^2-a^2n^2\right]}\left[\left(\gamma^2+\frac{n^2\pi^2}{l_0^2}\right)(\zeta\sin an\tau-\right.$$

$$\left.\left.-2an\cos\zeta\tau)-an\zeta(\cos an\tau-2\cos\zeta\tau)\right]\right\}\sin\frac{n\pi\xi}{l_0}. \qquad (6.6)$$

III. Flat Plate

The temperature field for the flat plate has the same form as for the semi-infinite cylindrical shell. The temperature field for the latter was found above in (1.10), (1.11). In the case of the flat plate, we must set in (1.10) and (1.11)

$$\xi=\frac{x}{h}, \ \tau=\frac{\nu t}{h^2}, \ \chi=\frac{\nu h\tau}{\varkappa}, \ m=\frac{\nu h}{\varkappa}, \ \beta^2=\frac{2K_0h}{c\gamma\varkappa},$$
$$\gamma^2=3(4+\beta^2). \qquad (7.1)$$

We also note that in the case of the plate

$$T^\circ=\frac{\varkappa c\rho}{q h^2}T_0, \ K^\circ=\frac{\varkappa c\rho}{3qh}K. \qquad (7.2)$$

For the quasistatic case the tangential and normal components of the displacement vector will satisfy the very simple equations

$$\frac{\partial u^{\circ}}{\partial \xi} = \frac{aqh^2(1+\nu)}{\kappa c \rho} \cdot \frac{\partial T^{\circ}}{\partial \xi},$$

$$\frac{\partial w^{\circ}}{\partial \xi} = -\frac{3aqh^2(1+\nu)}{\kappa c \rho} \cdot \frac{\partial K^{\circ}}{\partial \xi}. \tag{7.3}$$

If we assume that the ends of the plate are also freely supported, then we have

$$\frac{\partial u^{\circ}}{\partial \xi} = -\frac{aqh^2(1+\nu)}{2\kappa c \rho m \sqrt{1+n^2}} e^{-p^2\tau - \frac{\xi^2}{4\tau}} \left\{ \exp\left(n_1\sqrt{\tau} - \frac{\xi}{2\sqrt{\tau}}\right)^2 \times \right.$$

$$\times \left[1 - \operatorname{erf}\left(n_1\sqrt{\tau} - \frac{\xi}{2\sqrt{\tau}}\right)\right] - \exp\left(n_1\sqrt{\tau} + \frac{\xi}{2\sqrt{\tau}}\right)^2 \times$$

$$\times \left[1 - \operatorname{erf}\left(n_1\sqrt{\tau} + \frac{\xi}{2\sqrt{\tau}}\right)\right] - \exp\left(n_2\sqrt{\tau} - \frac{\xi}{2\sqrt{\tau}}\right)^2 \times$$

$$\times \left[1 - \operatorname{erf}\left(n_2\sqrt{\tau} - \frac{\xi}{2\sqrt{\tau}}\right)\right] + \exp\left(n_2\sqrt{\tau} + \frac{\xi}{2\sqrt{\tau}}\right)^2 \times$$

$$\times \left[1 - \operatorname{erf}\left(n_2\sqrt{\tau} + \frac{\xi}{2\sqrt{\tau}}\right)\right] \right\} +$$

$$+ \frac{aqh^2(1+\nu)}{\kappa c \rho} \begin{cases} \frac{1}{m\sqrt{1+n^2}}\left[e^{-n_1(\xi-\chi)} - e^{-n_2(\xi+\chi)}\right] & \text{for } \xi > \chi, \\ \frac{2}{m\sqrt{1+n^2}} e^{-n_1\chi} \operatorname{sh} n_2\xi & \text{for } \xi < \chi; \end{cases} \tag{7.4}$$

$$\frac{\partial w^{\circ}}{\partial \xi} = \frac{3aqh^2(1+\nu)}{2\kappa c \rho m \sqrt{1+p^2}} e^{-p^2\tau - \frac{\xi^2}{4\tau}} \left\{ \exp\left(m_1\sqrt{\tau} - \frac{\xi}{2\sqrt{\tau}}\right)^2 \times \right.$$

$$\times \left[1 - \operatorname{erf}\left(m_1\sqrt{\tau} - \frac{\xi}{2\sqrt{\tau}}\right)\right] - \exp\left(m_1\sqrt{\tau} + \frac{\xi}{2\sqrt{\tau}}\right)^2 \times$$

$$\times \left[1 - \operatorname{erf}\left(m_1\sqrt{\tau} + \frac{\xi}{2\sqrt{\tau}}\right)\right] - \exp\left(m_2\sqrt{\tau} - \frac{\xi}{2\sqrt{\tau}}\right)^2 \times$$

$$\times \left[1 - \operatorname{erf}\left(m_2\sqrt{\tau} - \frac{\xi}{2\sqrt{\tau}}\right)\right] + \exp\left(m_2\sqrt{\tau} + \frac{\xi}{2\sqrt{\tau}}\right)^2 \times$$

$$\times \left[1 - \operatorname{erf}\left(m_2\sqrt{\tau} + \frac{\xi}{2\sqrt{\tau}}\right)\right] \right\} + \tag{7.5}$$

$$+ \frac{3aqh^2(1+\nu)}{\kappa c \rho} \begin{cases} \frac{1}{m\sqrt{1+p^2}}\left[e^{-m_1(\xi-\chi)} - e^{-m_2(\xi+\chi)}\right] & \text{for } \xi > \chi \\ \frac{2}{m\sqrt{1+p^2}} e^{-m_1\chi} \operatorname{sh} m_2\xi & \text{for } \xi < \chi \end{cases}$$

If we now consider the inertia of the normal component of the displacement vector, the components of the displacement vector will be defined from the equations

$$\frac{\partial^2 u^{\circ}}{\partial \xi^2} = \frac{aqh^2(1+\nu)}{\kappa c \rho} \cdot \frac{\partial T^{\circ}}{\partial \xi},$$

$$\frac{\partial^2 w^{\circ}}{\partial \xi^2} = -\frac{3aqh^2(1+\nu)}{\kappa c \rho} \cdot \frac{\partial K^{\circ}}{\partial \xi} - \frac{12p^2(1-\nu^2)}{Eh^3} \cdot \frac{\partial^2 w^{\circ}}{\partial \tau^2} + \tag{7.6}$$

$$+ \frac{p^2(1-\nu^2)}{Eh^3} \cdot \frac{\partial^2 w^{\circ}}{\partial \tau^2 \partial \xi^2}.$$

We see that the first equation here coincides with the first equation (7.3). As for the second equation, applying to it the Fourier sine transformation, as in the case of the cylindrical shell, for hinged-free edge fastening we have

$$
w^{\bullet}(\xi, \tau) = \frac{6\alpha q m h^{3}(1+\nu)}{\pi c \rho \pi} \int_{0}^{\infty} \frac{p}{+[(p^{2}+\tau^{2})^{2}+p^{2}m^{2}]} \times
$$

$$
\times \left[\frac{(p^{2}+\tau^{2})\sin\psi\tau - \psi\cos\psi\tau + \psi e^{-(p^{2}+\tau^{2})\tau}}{(p^{2}+\tau^{2})^{2}+\psi^{2}} + \right.
$$

$$
\left. + \frac{(p^{2}+\tau^{2})(pm\sin\psi\tau - \psi\sin p\tau) + pm\psi(\cos p\tau - \cos\psi\tau)}{pm(p^{2}m^{2}-\psi^{2})} \right] \sin p\xi \, dp. \tag{7.7}
$$

Here we have denoted for convenience

$$
\psi^{2} = \frac{Eh^{3}}{c\pi^{2}(1-\nu^{2})} \cdot \frac{p^{4}}{12h^{2}+p^{2}}. \tag{7.8}
$$

The forces and moments are expressed as follows in terms of the displacement components and the temperature

$$
T_{1}(\xi, \tau) = D_{1}\frac{\partial w^{\bullet}}{\partial \xi} - \frac{12(1+\nu)\,\alpha q D_{2}}{\pi c \rho} T^{\bullet},
$$

$$
T_{2}(\xi, \tau) = D_{1}\nu\frac{\partial w^{\bullet}}{\partial \xi} - \frac{12(1+\nu)\,\alpha q D_{2}}{\pi c \rho} T^{\bullet},
$$

$$
M_{1}(\xi, \tau) = -\frac{D_{2}}{h}\cdot\frac{\partial^{2}w^{\bullet}}{\partial \xi^{2}} - \frac{D_{2}\alpha q h(1+\nu)}{4\pi \rho c} K^{\bullet},
$$

$$
M_{2}(\xi, \tau) = -\frac{D_{2}\nu}{h}\cdot\frac{\partial^{2}w^{\bullet}}{\partial \xi^{2}} - \frac{D_{2}\tau q h(1+\nu)}{4\pi c \rho} K^{\bullet}, \tag{7.9}
$$

$$
N_{1}(\xi, \tau) = -\frac{D_{2}}{h^{2}}\cdot\frac{\partial^{3}w^{\bullet}}{\partial \xi^{3}} - \frac{3D_{2}q\alpha(1+\nu)}{\pi c \rho}\cdot\frac{\partial K^{\bullet}}{\partial \xi}.
$$

Received 8 March 1964.

INTEGRALS OF THE EQUATIONS OF AXISYMMETRIC
VIBRATIONS OF SHELLS OF REVOLUTION

P. Ye. Tovstik

The asymptotic method for integrating equations with small
parameters in the higher derivatives is employed to integrate the
system of equations of small axisymmetric vibrations of a thin elastic
shell of revolution. In some frequency range the resolvent equation
has a reversal point. In this article we consider the case in
which the coefficient of the second derivative in the resolvent
has a simple root (simple reversal point),and we find the Stokes
multipliers relating the integrals of the resolvent to the right
and left of the reversal point. Moreover, the integrals in the im-
mediate vicinity of the reversal point are calculated. As an example,
we examine the problem of the natural vibration frequencies of a
shell with clamped edges.

The present article is an extension of the study initiated by
Alumyae [1] for a conical shell.

§ 1. Equations of the Vibrations of a
Shell of Revolution

After separation of variables,the system of equations of small
axisymmetric vibrations of an elastic shell of revolution has the
form [2]

$$\frac{d}{ds}\left(\frac{1}{B}\cdot\frac{d(Bu)}{ds}\right)+\left(\lambda+\frac{1-\sigma}{R_1R_2}\right)u-\left(\frac{1}{R_1}+\frac{\sigma}{R_2}\right)\frac{dw}{ds}-$$
$$-\frac{d}{ds}\left(\frac{1}{R_1}+\frac{1}{R_2}\right)w=0,$$
$$\left(\frac{1}{R_2}+\frac{\sigma}{R_1}\right)\frac{du}{ds}+\left(\frac{\sigma}{R_1}+\frac{1}{R_2}\right)\frac{B'}{B}u+\left(\lambda-\frac{1}{R_1^2}-\frac{2\sigma}{R_1R_2}-\right.$$
$$\left.-\frac{1}{R_2^2}\right)w-\frac{h^2}{12}\cdot\frac{1}{B}\cdot\frac{d}{ds}\left(B\frac{d}{ds}\left(\frac{1}{B}\cdot\frac{d}{ds}\left(B\frac{dw}{ds}\right)\right)\right)=0. \tag{1.1}$$

Here s is the meridian (generator) arc length; u and w are the
projections of the middle surface displacements on the direction of
the normal and meridian; B = B(s) denotes the distance from the
middle surface points to the axis of revolution and is assumed to be
a holomorphic function of s; R_1 and R_2 are the principal radii of
curvature, and

$$\frac{1}{R_1}=-\frac{B''}{\sqrt{1-B'^2}},\quad \frac{1}{R_2}=\frac{1}{B}\sqrt{1-B'^2}. \tag{1.2}$$

$\lambda=(1-\sigma^2)\frac{\rho p^2}{E}$,   where σ is Poisson's ratio; ρ,density; p,the
vibration frequency; E,Young's modulus.

The shell thickness is denoted by h, which we assume small in
comparison with the characteristic radius of curvature. We introduce
the small parameter μ by the formula

$$\mu^4=\frac{1}{12}h^2. \tag{1.3}$$

Excluding u from (1.1),we find

$$-\mu^4\left(a_1\frac{d^6w}{ds^6}+a_2\frac{d^5w}{ds^5}+\ldots\right)+b_3\frac{d^3w}{ds^3}+b_1\frac{dw}{ds}+b_0w=0. \tag{1.4}$$

Without loss of generality we can consider that $a_0=a_0(s)\equiv 1$
Then

$$b_2=b_2(s,\lambda)=\lambda-(1-\sigma^2)(R_2(s))^{-2}. \tag{1.5}$$

§ 2. Integrals of (1.4)

Assume the function $b_2(s)$ does not vanish in the interval
$s_1 < s < s_2$. Assume B(s) also does not vanish in this interval
(thereby we exclude from consideration shells in the form of a dome).
Then we can construct asymptotic series for the four integrals of
(1.4) which have a large variability index [3, 4].

$$\omega_i(s) = \sum_{k=0}^{\infty} \rho^k y_{ik}(s) \exp\left\{\frac{1}{\rho}\int_{s_0}^{s} \omega(t)\, dt\right\}, \qquad i = 1, 2, 3, 4, \tag{2.1}$$

where $\omega(s)$ satisfies the equation

$$\omega^4 - b_2 \omega^2 = 0, \tag{2.2}$$

and the functions $y_{ik}(s)$ are determined sequentially in quadratures;
s_0 is an arbitrary point.

After making the necessary calculations, we find the approximate
expressions for the integrals (2.1)

$$\omega_i^{\pm}(s) = (y_0(s) + O(\rho))\, W_i^{\pm}(z), \qquad i = 1, 2, 3, 4. \tag{2.3}$$

Here the indices "+" and "−" correspond to $b_2 > 0$ and $b_2 < 0$. In
the case $b_2 > 0$, we have

$$W_1^+ = e^{-z}, \quad W_2^+ = e^{z}, \quad W_3^+ = \cos z, \quad W_4^+ = \sin z, \tag{2.4}$$

and for $b_2 < 0$

$$W_1^- = e^{z_1}\cos z_1, \quad W_2^- = e^{z_1}\sin z_1, \quad W_3^- = e^{-z_1}\cos z_1, $$
$$W_4^- = e^{-z_1}\sin z_1. \tag{2.5}$$

Here

$$z = \frac{1}{\rho}\int_{s_0}^{s} |b_2(t)|^{\frac{1}{2}}\, dt, \quad z_1 = \frac{z}{\sqrt{2}}, \quad y_0(s) = (B(s))^{-\frac{1}{2}}|b_2(s)|^{-\frac{3}{8}}. \tag{2.6}$$

To the integrals (2.3) we must add two other integrals $w_5(s,\mu)$ and $w_6(s,\mu)$, corresponding to the zero roots of (2.2) with an error on the order of μ^4, and coinciding with the integrals of the momentless equation

$$b_2\frac{d^2w}{ds^2}+b_1\frac{dw}{ds}+b_0w=0. \qquad (2.7)$$

Numerical integration methods must be used to find the integrals of this equation.

Now assume the function $b_2(s)$ vanishes at the points α_j, $s_1 < \alpha_1 < \alpha_2 < \ldots < \alpha_n \leqslant s_2$. Then the integrals (2.3) no longer hold throughout the interval (s_1, s_2), since the form of the integrals changes with passage through the points $s = \alpha_j$ and $y_6(\alpha_j) = \infty$. Nevertheless, in each of the intervals $\alpha_j + \varepsilon < s < \alpha_{j+1} - \varepsilon$ the functions (2.3) are integrals of (2.1). The question arises of the connection between these integrals for neighboring intervals and also the question of the behavior of the integrals in the immediate vicinity of the points α_j.

The points α_j are termed reversal points and the coefficients expressing the connection between the integrals for neighboring intervals are termed Stokes multipliers. If $\dot{b}_2(\alpha_j) \neq 0$, the point α_j is termed a simple reversal point.

We shall show that the hypothesis of the existence of isolated roots of the equation $b_2(s, \lambda) = 0$ is general. In fact, it is not difficult to show that $R_2(s) = $ const only for two types of shells — cylindrical and spherical, and in all the remaining cases $R_2(s)$ is not an identical constant, and in accordance with (1.5) there are values of λ (and consequently of the frequency p) for which the function b_2 will vanish for certain α_j for the interval (s_1, s_2).

Assume $\alpha_0 = \alpha_0(\lambda)$ is a simple reversal point. Moreover, $b_2(\alpha_0) > 0$ and in the interval (s_1, s_2) there are no other reversal points (the case $\dot{b}_2(\alpha_0) < 0$ reduces to the preceding case by the replacement $s' = -s$).

Starting from the form of the coefficients of (1.1), we show that $b_1(\alpha_0)=2b_2'(\alpha_0)$, which implies that the momentless equation (2.7) has a single regular solution and a single solution with a singularity for $s = \alpha_0$. As the fifth and sixth integrals of (1.4), we take the integrals having near $s = \alpha_0$ the expansions

$$\varpi_5(s)=1+c_{11}(s-\alpha_0)+c_{12}(s-\alpha_0)^2+\ldots+O(r^4),$$
$$\varpi_6(s)=\gamma(\alpha_0)\varpi_5(s)\ln|s-\alpha_0|+\frac{1}{s-\alpha_0}+c_{21}(s-\alpha_0)+\ldots+$$
$$+O(r^4(s-\alpha_0)^{-3}),$$

(2.8)

where

$$\gamma(s)=\frac{1}{b_2(s)}\left(-b_2''(s)+b_1'(s)-b_0(s)\right)=\frac{1}{b_2}\left\{\frac{(1-s^2)B''}{B}\left[\left(\frac{2}{R_1}+\right.\right.\right.$$
$$+\frac{1}{R_2}\right)\left(\frac{1}{R_2}\right)'-\frac{1}{R_2}\left(\frac{1}{R_1}\right)'\right]+\frac{(1-s^2)B''}{BR_2}\left(\frac{1}{R_1}+\frac{s}{R_2}\right)-\lambda\left(\frac{1}{R_1}+\frac{s}{R_2}\right)^2\right\}.$$

(2.9)

and c_{ij} are expressed in terms of the coefficients of the expansions of $b_2(s)$, $b_1(s)$ and $b_0(s)$ into series in powers of $s - \alpha_0$.

§ 3. Reference Equation

The results of [1] could be used to establish the connection between the integrals of (1.4) to the right and left of the reversal point. However, the reference equation introduced in [1] is inconvenient for studying the behavior of these integrals in the immediate vicinity of the reversal point. Therefore, we introduce into consideration the equation

$$-r^4\left(\frac{d^4v}{d\xi^4}+\gamma_0\frac{d^3v}{d\xi^3}\right)+\xi\frac{d^2v}{d\xi^2}+(2+\gamma_0\xi)\frac{dv}{d\xi}=0, \quad (3.1)$$

(3.1)

where $\gamma_0=\gamma(\alpha_0)$ is found from (2.9).

Employing the Laplace transformation, we represent the integrals of (3.1) in the form of the contour integrals

$$v_j(\xi)=\int_{C_j}\left(1+\frac{\gamma_0}{t}\right)\exp\left\{\xi t-\frac{r^4 t^3}{3}\right\}dt, \quad j=1, 2, \ldots, 6,$$

(3.2)

where the contours of integration must be selected so that the increment of the function

$$f(t) = (t + \gamma_0)^2 \exp\left\{\xi t - \frac{\mu^4 t^5}{5}\right\}$$

is zero when t covers the entire contour. The function f(t) vanishes for t $= -\gamma_0$ and also for $t = \infty \cdot e^{\frac{2\pi i}{5}}$, $k \doteq 0, 1, \ldots, 4.$

Following [1],we take contours of integration which yield real solutions (Figure)

$$
\begin{aligned}
&C_1 = A_3 a_2 a_0 A_0 + A_4 a_4 a_0 A_0, \quad C_2 = A_2 a_2 a_1 A_1 + A_3 a_3 a_1 A_1, \\
&C_3 = A_2 a_2 a_2 A_2, \quad C_4 = A_4 a_0 a_0 a_1 A_1, \quad C_5 = a_0 a_1 a_2 a_3 a_1 a_0, \\
&C_6 = F\gamma_0 a_3 a_1 A_1 + F a_0 a_3 a_1 A_1,
\end{aligned}
\tag{3.3}
$$

where the points a_j are located on a circle of radius ε for the points A_j recede to infinity.
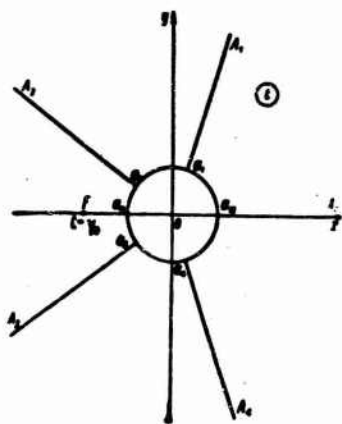
Figure

To calculate the integrals v_j $(j = 1, 2, 3, 4)$ and $|\xi| \gg \mu^{\frac{4}{5}}$, we use the method of steepest descent and find the asymptotic expansions of these integrals [1]. The expressions for $\xi < 0$ are shown on the left; those for $\xi > 0$ are on the right; the relative error of the formulas presented below is of order $\mu \xi^{-\frac{4}{3}}$:

$$
\begin{aligned}
de^{-\zeta} \cos\left(\zeta_1 + \frac{3\pi}{8}\right) &\leftarrow v_1(\xi) \rightarrow d e^{\zeta}, \\
de^{\zeta} \cos\left(\zeta_1 + \frac{\pi}{8}\right) &\leftarrow v_2(\xi) \rightarrow \frac{d}{\sqrt{2}}(\cos\zeta - \sin\zeta), \\
de^{\zeta} \sin\left(\zeta_1 + \frac{\pi}{8}\right) &\leftarrow i^{-1} v_3(\xi) \rightarrow \frac{d}{2} e^{-\zeta}, \\
de^{-\zeta} \sin\left(\zeta_1 + \frac{3\pi}{8}\right) &\leftarrow i^{-1} v_4(\xi) \rightarrow \frac{d}{\sqrt{2}}(\cos\zeta + \sin\zeta) + i v_3(\xi)
\end{aligned}
\tag{3.4}
$$

FTD-HC-23-361-69   118

where

$$d = \sqrt{2\pi} \, \mu^{-\frac{1}{3}} |\xi|^{-\frac{3}{4}},$$

$$\zeta = \frac{4}{5} \xi^{\frac{5}{4}} \mu^{-1},$$

$$\zeta_1 = \frac{2\sqrt{2}}{5} (-\xi)^{\frac{5}{4}} \mu^{-1}.$$

The integral $v_5 (\xi)$ is a constant

$$v_5(\xi) = -2\pi \gamma_0 i. \qquad (3.5)$$

For $\xi < 0$ the integral $v_6(\xi)$ coincides with the integral

$$v_6^{(0)}(\xi) = \int_{\zeta_1} \left(1 + \frac{\gamma_0}{t}\right) e^{it} dt = 2\left(\frac{1}{\xi} + \gamma_0 \ln |\zeta \gamma_0| + \dots\right). \qquad (3.6)$$

to within $\mu^4 \xi^{-6}$. However, if $\xi > 0$ the integral (3.6) diverges. We represent the contour of integration C_6 in the form $C_6 = C_6' + C_2$, where $C_6' = Fa_* a_2 A_2 = Fa_* a_3 A_3$. Then for $\xi > 0$ we have

$$v_6(\xi) = v_2(\xi) + \int_{C_6'} \left(1 + \frac{\gamma_0}{t}\right) e^{it} dt + O(\mu^4 \xi^{-6}), \qquad (3.7)$$

and the integral along the contour C'_6 has the same expansion (3.6) into a series in ξ.

We seek the integrals of the basic equation (1.4) in the form

$$\widetilde{w}_j(s) = \widetilde{y}_0(s) v_j [\xi(s)], \quad j = 1, 2, \dots, 6, \qquad (3.8)$$

where the functions $\widetilde{y}_0(s)$ and $\xi(s)$ are selected so that the highest order terms in the expansion of the left side of (1.4) into a series in μ will vanish

$$\xi(s) = \left\{\frac{5}{4} \int_{s_0}^{s} (b_2(t))^{\frac{1}{4}} dt\right\}^{\frac{4}{5}} =$$

$$= (b_2'(a_0))^{\frac{1}{4}} (s - a_0)\left(1 + \frac{b_2''(a_0)}{18 b_2'(a_0)} (s - a_0) + \dots\right). \qquad (3.9)$$

$$\widetilde{y}_0(s) = \sqrt{\frac{\mu}{2\pi B}} \left(\frac{d\xi}{ds}\right)^{-\frac{3}{2}}. \qquad (3.10)$$

The integrals $\tilde{w}_j(s)$, $j = 1, 2, 3, 4$, are expressed linearly in terms of the integrals (2.3), which with account for (3.4) yields the connection between the integrals (2.3) to the left and right of the reversal point.

The integrals $\tilde{w}_5(s)$ and $\tilde{w}_6(s)$ may be considered as integrals of (1.4) only for $|s - a_0| \ll 1$. For $|s - a_0| > 1$ the behavior of these integrals of (1.4) and (3.1) is significantly different. The integral $w_5(s)$ of (1.4), which has the expansion (2.8) near $s = \alpha_0$, corresponds to the integral $v_5(\xi)$, of (3.1).

The representation of the integral $\tilde{w}_6(s)$ for $s < 0$ and $s > 0$ with account for (3.8), (3.6) and (3.7) makes it possible to construct the sixth integral of (1.4), since $\tilde{w}_0(s)$ is a good approximation of the integral of (1.4) for $|s - a_0| \ll 1$, and these formulas are applicable in the intervals $|s - a_0| \gg \mu^{\frac{4}{7}}$.

The following expressions yield the connection between the integrals (2.3) and (2.8) of (1.4) to the left and right of the reversal point, where in (2.6) we take $s_0 = \alpha_0$. These expressions may be used for $|s - a_0| \gg \mu^{\frac{4}{7}}$:

$$w_1^- \cos \frac{3\pi}{8} + w_2^- \sin \frac{3\pi}{8} \leftarrow \tilde{w}_1 \rightarrow w_3^+,$$

$$w_3^- \cos \frac{\pi}{8} + w_4^- \sin \frac{\pi}{8} \leftarrow \tilde{w}_2 \rightarrow \frac{1}{\sqrt{2}}(w_3^+ - w_4^+),$$

$$w_3^- \sin \frac{\pi}{8} - w_4^- \cos \frac{\pi}{8} \leftarrow t^{-1}\tilde{w}_3 \rightarrow \frac{1}{2}w_1^+,$$

$$w_1^- \sin \frac{3\pi}{8} - w_2^- \cos \frac{3\pi}{8} \leftarrow t^{-1}\tilde{w}_4 \rightarrow \frac{1}{\sqrt{2}}(w_3^+ + w_4^+) + \mu^{\frac{1}{2}}aw_6, \qquad (3.11)$$

$$w_6 \leftarrow \tilde{w}_6 \rightarrow w_6 + \mu^{-\frac{1}{2}}b(w_3^+ - w_4^+),$$

where

$$a = -\sqrt{\frac{2\pi}{B(a_0)}}\, \tau_0 |b_2'(a_0)|^{-\frac{3}{10}}, \quad b = \frac{1}{2}\sqrt{\pi}\,(b_2'(a_0)\, B(a_0))^{\frac{1}{2}}. \qquad (3.12)$$

§ 4. Behavior of the Integrals Near the Reversal Point

As noted above, the formulas (3.11) are not suitable for $|s-a_0| < \rho^{\frac{4}{7}}$. In order to examine this interval of the variable we again turn to (3.2). The idea for their calculation consists in the expansion of $e^{i\epsilon} = \sum_{k=0}^{\infty} \frac{1}{k!} (\xi \eta)^k$ and subsequent term by term integration.

As a result, we obtain

$$v_1(\xi) = \sum_{k=0}^{\infty} a_k \left(1 - \cos \frac{2(k+1)\pi}{5}\right) \eta^k,$$

$$v_2(\xi) = \sum_{k=0}^{\infty} a_k \left(\cos \frac{2(k+1)\pi}{5} - \cos \frac{4(k+1)\pi}{5}\right) \eta^k,$$

$$\Gamma^{-1} v_3(\xi) = \sum_{k=0}^{\infty} a_k \sin \frac{4(k+1)\pi}{5} \eta^k - \frac{2\pi\eta_0}{5},$$

$$\Gamma^{-1} v_4(\xi) = \sum_{k=0}^{\infty} a_k \sin \frac{2(k+1)\pi}{5} \eta^k + \frac{4\pi\eta_0}{5},$$

$$v_5(\xi) = \sum_{k=0}^{\infty} a_k \cos \frac{2(k+1)\pi}{5} \eta^k + 2\eta_0 - \frac{2}{5}\left(C + \ln\left|\frac{\rho^4 \eta_0^5}{5}\right|\right) + \quad (4.1)$$

$$+ O\left(\rho^{\frac{4}{7}}\right).$$

where

$$\eta = \rho^{-\frac{4}{5}} \xi, \quad a_k = \frac{2 \cdot 5^{\frac{k-4}{5}} \Gamma\left(\frac{k+1}{5}\right)}{k!}\left(\rho^{-\frac{4}{5}} + \frac{\eta_0^5}{k+1}\right); \quad (4.2)$$

C is the Euler constant; $\Gamma(z)$ is the gamma function.

In view of the rapid decay of the coefficients a_k, the series (4.1) are suitable for calculating the functions $v_j(\xi)$ for $|\xi| < \rho^{\frac{4}{5}}$ (or for $|\eta| < 1$) or even in a broader region.

To obtain the functions $\widetilde{v}_j(s)$, we must use (3.8)-(3.10). In view of the fact that $|s-a_0| < \rho^{\frac{4}{7}}$, the right sides of (3.9 and (3.10) may be approximated by the first terms in their expansion into Taylor series

$$\xi(s)=(b_2'(a_0))^{\frac{1}{3}}(s-a_0), \quad \tilde{y}_0(s)=\sqrt{\frac{\mu}{2\pi B(a_0)}}\,(b_2'(a_0))^{-\frac{3}{10}}.$$

$$(4.3)$$

We see from (4.1)-(4.3) that

$$\widetilde{w}_j(a_0)=O\left(\mu^{-\frac{3}{10}}\right), \quad \widetilde{w}_j^{(n)}(s_0)=O\left(\mu^{-\frac{3}{10}-\frac{4n}{3}}\right).$$

$$(4.4)$$

§ 5. Frequency Equation for Shell with Clamped Edges

Assume that in the interval (s_1, s_2) the radius of curvature $R_2(s)$ increases $(R_2'(s)>0)$. Then by virtue of (1.5) in this interval there will be a single (simple) reversal point $a_0=a_0(\lambda)$, if $\Lambda_1 < \lambda < \Lambda_2$, where $\Lambda_1=(1-\sigma^2)(R_2(s_2))^{-2}$, $\Lambda_2=(1-\sigma^2)(R_2(s_1))^{-2}$. However, if λ is outside this interval there are no reversal points

Let the shell edges be clamped, i.e.,

$$u=0, \; w=0, \; \frac{dw}{ds}=0 \quad \text{for } s=s_1, \; s=s_2. \quad (5.1)$$

In order to satisfy the conditions (5.1), we need the expressions for the integrals $u_j(s)$, corresponding to the integrals $w_j(s)$. On the basis of (1.1) the asymptotic expressions for the integrals $u_j(s)$ with large variability index are

$$u_j^{\pm}(s)=(u_0(s)+O(\mu))\,U_j^{\pm}(z), \quad j=1, 2, 3, 4,$$

$$(5.2)$$

where

$$u_0(s)=\mu\,|b_2(s)|^{-\frac{1}{4}}\left(\frac{1}{R_1}+\frac{\sigma}{R_2}\right)y_0(s), \quad U_j^{\pm}(z)=\int W_j^{\pm}(z)\,dz, \quad (5.3)$$

and $W_j^{\pm}(z)$ are determined from (2.4) and (2.5). The integral $u_5(s)$ is regular while $u_6(s)$ has a logarithmic singularity as $\mu\to0$ at $s = a_0$. With passage through the reversal point the integrals $u_j(s)$ are transformed using the same formulas (3.11).

We take the general solution of (1.1) in the form

$$u(s)=\sum_{j=1}^{6} C_{j}\widetilde{u}_{j}(s), \quad w(s)=\sum_{j=1}^{6} C_{j}\widetilde{w}_{j}(s). \tag{5.4}$$

Using the boundary conditions (5.1), we obtain the frequency equation $\Delta(\lambda, \mu)=0$ in the form of equality to zero of a sixth order determinant. Let us consider various cases.

For $\lambda < A_1$ we have $b_2 < 0$ for all s; there are no reversal points in the interval (s_1, s_2), and the integrals with large variability index have the nature of nondegenerate edge effect functions. In this case

$$\Delta(\lambda, \mu)=u_1^{(0)}(s_1, \lambda)u_2^{(0)}(s_2, \lambda)-u_2^{(0)}(s_2, \lambda)u_1^{(0)}(s_1, \lambda)+O(\mu)=0. \tag{5.5}$$

Here and in the following the superscript (0) means that these solutions are taken for $\mu = 0$. We see from (5.5) that the natural vibration frequencies may be determined from the momentless equations to within quantites of order μ.

Now let $A_1 \lesssim \lambda < A_3$. In this case there is a reversal point within the interval of integration and the natural frequencies are found from the equation

$$\sqrt{2}ab\, u_1^{(0)}(s_1)\, u_2^{(0)}(s_2)\cos\frac{\varphi}{\mu}+(u_2^{(0)}(s_2)\dot{u}_1^{(0)}(s_1)-$$
$$-u_1^{(0)}(s_1)u_2^{(0)}(s_2))\sin\frac{\varphi}{\mu}+O\left(\mu^{\frac{1}{2}}\right)=0,$$

$$\tag{5.6}$$

where

$$\varphi(\lambda)=\int_{a(\lambda)}^{s_2}(b_2(t, \lambda))^{\frac{1}{4}}dt, \tag{5.7}$$

a (λ) and b(λ) are found from (3.12), and the functions $u_1^{(0)}$ and $u_2^{(0)}$ also depend on λ.

Finally, let $\lambda > A_4$. In this case $b_2(s) > 0$, and again there are no reversal points within the integration. In this case the frequency equation breaks down into two equations: the momentless

equation, coinciding in form with (5.5), and the equation depending on functions with a large variability index

$$\cos \frac{\eta_1}{\mu} + O(\mu) = 0,$$

(5.8)

where

$$\varphi_1(\lambda) = \int_{\lambda_1}^{t_0} (b_2(t, \lambda))^{\frac{1}{4}} dt.$$

(5.9)

Equations (5.5), (5.6) and (5.8) are applicable if $|\lambda - \Lambda_1| \gg \mu^{\frac{4}{3}}, |\lambda - \Lambda_2| \gg \mu^{\frac{4}{3}}$. In order to solve (5.5), it is necessary to know the integrals of (1.1) for $h = 0$. In the general case they can be constructed only by numerical integration methods. These integrals also appear in (5.6). However, certain conclusions on the distribution density of the natural frequencies can be made even without knowing the functions $u_1^{(0)}$ and $u_2^{(0)}$.

We write (5.6) in the form

$$\text{tg} \frac{\varphi(\lambda)}{\mu} = \psi(\lambda).$$

(5.10)

In view of the fact that for small μ the argument of the tangent in (5.10) changes very rapidly with variation of λ, to within the order μ, we can consider that $\psi(\lambda)$ remains constant in the interval between the neighboring roots λ_n and λ_{n+1} of (5.10). Then the distance $\Delta\lambda$ between neighboring roots is

$$\Delta\lambda = \frac{\pi\mu}{\varphi'(\lambda)} + O(\mu^2),$$

(5.11)

or, introducing the root distribution density $n(\lambda)$, the reciprocal distance between roots, we find

$$n(\lambda) = \frac{1}{\pi\mu} \varphi'(\lambda) = \frac{1}{4\pi\mu} \int_{t_0(\lambda)}^{t_1} (b_2(t, \lambda))^{-\frac{3}{4}} dt.$$

(5.12)

Similarly, for $\lambda > \Lambda_2$ the density $n(\lambda)$ is

(5.13)

$$n(\lambda) = \frac{1}{\pi\mu} \varphi'_1(\lambda) = \frac{1}{4\pi\mu} \int_{\lambda_1}^{t_0} (b_2(t, \lambda))^{-\frac{3}{4}} dt.$$

We see from an examination of (5.12) and (5.13) that near $\lambda = \Lambda$ the density $n(\lambda)$ increases rapidly and reaches a maximal value for $\lambda = \lambda_o$. $\Lambda_1 < \lambda_o \leqslant \Lambda_2$. For $\lambda > \Lambda_2$ the density $n(\lambda)$ decreases.

REFERENCES

1. Alumyae, N., "On the fundamental system of integrals of the equation for small axisymmetric steady state vibrations of an elastic conical shell of revolution," IAN Estonian SSR, Physico-Mathematical and Technical Sciences Series, No. 1., 196?

2. Gol'denveyzer, A. L., Teoriya tonkikh uprugikh obolochek (Theory of Thin Elastic Shells), Moscow, Fizmatgiz, 1953

3. Noaillon, P., Asymptotic developments in differential equations with variable parameter, Memoires de la Societe de Liege, IX, 1912.

4. Zimin, V. I., "On application of the asymptotic integration method to the solution of an equation of shell theory," IAN Uzbek SSSR, Physico-Mathematical Sciences Series, No. 4, 1957.

REGULAR INTEGRALS CF THE EQUATIONS FOR
## AXISYMMETRIC VIBRATIONS OF A DOME

P.Ye Tovstik

It is known [1, 2] that the general solution of the system of
equations of free axisymmetric vibrations of a thin elastic shell of
revolution is made up of two integrals of the momentless equations
and four integrals with a large variability index. The asymptotic ex-
pressions for these four integrals may be found easily in intervals
which do not contain either so-called reversal points or singular
points of the shell vibration equations. The behavior of the inte-
grals in the vicinity of a simple reversal point is examined in [2, 3].
The equations for the vibrations of a shell in the form of a dome
have a regular singular point at the shell apex.

In the present study, we construct the regular integrals with
large variability index at the dome apex, and find their asymptotic
expressions far from the apex of the dome. We need to know these in-
tegrals in order to determine the natural vibration frequency of the
dome.

§ 1

Let the shell be formed by revolution of the curve $y = f(B)$
(Figure) about the y-axis, where $f(B)$ is an even function which is
holomorphic near $B = 0$ and $f(0) = 0$, $f''(0) = R$, R is the shell radi-
us of curvature at the apex of the dome $(B = 0)$. Small axisymmetric
vibrations of such a shell are described by the system of equations[4].
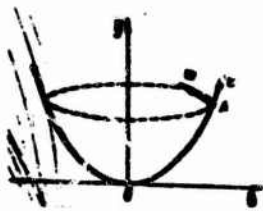
$$L_1[u, w] = \frac{d}{ds}\left(\frac{1}{B} \cdot \frac{d}{ds}(Bu)\right) + \left(\lambda + \frac{1-\sigma}{R_1 R_2}\right)u -$$
$$- \left(\frac{1}{R_1} + \frac{\sigma}{R_2}\right)\frac{dw}{ds} - \frac{d}{ds}\left(\frac{1}{R_1} + \frac{1}{R_2}\right)w = 0,$$
$$L_2[u, w; \mu] = \left(\frac{1}{R_1} + \frac{\sigma}{R_2}\right)\frac{du}{ds} + \left(\frac{\sigma}{R_1} + \frac{1}{R_2}\right)\frac{B'}{B}u +$$
$$+ \left(\lambda - \frac{1}{R_1^2} - \frac{2\sigma}{R_1 R_2} - \frac{1}{R_2^2}\right)w - \mu^4 \frac{1}{B} \cdot \frac{d}{ds}\left(B\frac{d}{ds}\left(\frac{1}{B} \cdot \frac{d}{ds}\left(B\frac{dw}{ds}\right)\right)\right) = 0. \qquad (1.1)$$

Here s is the arc length of the generator OA; u(s) and w(s) are the projections of the displacement of the middle surface points in the direction of the generator and the normal; $\lambda = (1 - \sigma^2)E^{-1}\rho\omega^2$ (σ is the Poisson ratio; E, Young's modulus; ρ, density; ω, the vibration frequency); μ is a small parameter where $\mu^4 = h^2/12$ (h is the shell thickness, which is assumed small in comparison with the radius (R). We call the system obtained from (1.1) for $\mu = 0$ momentless or degenerate.

$R_1(s)$ and $R_2(s)$ are the principal radii of curvature, which are even functions of s; B(s) is an odd function. Near s = 0, these functions have the following expansions into series in powers of s

$$R_1(s) = R + a_2 s^2 + \ldots, \quad R_2(s) = R + b_2 s^2 + \ldots,$$
$$B(s) = s - \frac{s^3}{6R^2} + c_5 s^5 + \ldots \qquad (1.2)$$

For s = 0, certain of the coefficients in (1.1) become infinite. Our task is to construct solutions of (1.1) which are regular for s = 0. Here we shall assume that $\lambda \neq (1 - \sigma^2)R^{-2}$. In the case, $\lambda = (1 - \sigma^2)R^{-2}$, the momentless system (1.1) has no regular solutions, and this case requires special study (in this case the dome apex coincides with the reversal point).

§ 2

It is not difficult to see by direct substitution that the degenerate system (1.1) has the solution $u_0(s)$, $\omega_0(s)$ of the form

$$u_0(s) = \sum_{k=0}^{\infty} u_{2k+1}^{(0)} s^{2k+1}, \quad \omega_0(s) = \sum_{k=0}^{\infty} \omega_{2k}^{(0)} s^{2k}, \qquad (2.1)$$

where $\omega_0^{(0)} = 1$ and the coefficients $u_j(0)$, $\omega_j(0)$ are determined sequentially from linear equations.

We seek the regular solution of (1.1) in the form

$$u(s) = \sum_{n=0}^{\infty} \mu^{4n} u_n(s), \quad w(s) = \sum_{n=0}^{\infty} \mu^{4n} w_n(s). \tag{2.2}$$

Then the functions $u_n(s)$ and $w_n(s)$ will satisfy the equations

$$L_1[u_n, w_n] = 0, \quad L_2[u_n, w_n; 0] = \frac{1}{B} \cdot \frac{d}{ds}\left(B\frac{d}{ds}\left(\frac{1}{B}\cdot\frac{d}{ds}\left(B\frac{dw_{n-1}}{ds}\right)\right)\right). \tag{2.3}$$
$$n = 1, 2, \ldots$$

For uniqueness of selection of u_n, ω_n, we require, in addition to their regularity at $s = 0$, that $w_n(0) = 0$. It is not difficult to show by induction that all $w_n(s)$ are even functions, and then the right side of the second equation (2.3) is a regular function of s. Expanding $u_n(s)$ and $w_n(s)$ into series in powers of s cf the form (2.1), we show that there is a unique regular solution of (2.3) satisfying the condition $w_n(0) = 0$.

Thus, we have shown the existence of a regular solution of (1.1) which differs by a magnitude of order μ^4 from the regular solution of the degenerate system. Numerical integration must be used for the actual construction of the solution (2.1) for values of s which are not close to zero.

§ 3

We shall construct two regular integrals of (1.1) which have a large variability index.

We replace the first equation (1.1) by

$$\frac{1}{B} \cdot \frac{d}{ds}(BL_1) = 0 \tag{3.1}$$

and introduce the new unknown function v(s) by the formula

$$v = \frac{1}{B} \cdot \frac{d}{ds}(Bu) \qquad \left(u = \frac{1}{B}\int_0^s B \, ds\right). \tag{3.2}$$

Then (1.1) takes the form

$$\Delta v + \left(\lambda + \frac{1-\sigma}{R_1 R_2}\right)v + \frac{d}{ds}\left(\frac{1-\sigma}{R_1 R_2}\right)u - \left(\frac{1}{R_1} + \frac{\sigma}{R_2}\right)\Delta w -$$
$$- \frac{d}{ds}\left(\frac{2}{R_1} + \frac{1+\sigma}{R_2}\right)\frac{dw}{ds} - \frac{1}{B} \cdot \frac{d}{ds}\left(B\frac{d}{ds}\left(\frac{1}{R_1} + \frac{1}{R_2}\right)\right)w = 0,$$
$$\left(\frac{1}{R_1} + \frac{\sigma}{R_2}\right)v + (1-\sigma)\left(\frac{1}{R_2} - \frac{1}{R_1}\right)\frac{B'}{B}u + \tag{3.3}$$
$$+ \left(\lambda - \frac{1}{R_1^2} - \frac{2\sigma}{R_1 R_2} - \frac{1}{R_2^2}\right)w - \mu^4 \Delta\Delta w = 0,$$

where the operator Δ is

$$\Delta z = \frac{1}{B} \cdot \frac{d}{ds}\left(B\frac{dz}{ds}\right). \tag{3.4}$$

We seek the solution of (3.3) in the form

$$v(s) = \sum_{n=0}^{\infty} \mu^{2n} B_{2n}(s) V(s) + \mu \sum_{n=0}^{\infty} \mu^{2n+1} B_{2n+1}(s) \frac{dV}{ds},$$

$$w(s) = \sum_{n=0}^{\infty} \mu^{2n} C_{2n}(s) V(s) + \mu \sum_{n=0}^{\infty} \mu^{2n+1} C_{2n+1}(s) \frac{dV}{ds}, \tag{3.5}$$

where V(s) is the solution of the equation

$$\tag{3.6}$$

and the functions p(s), $B_n(s)$ and $C_n(s)$ are to be determined (we limit ourselves to finding p, B_0 and C_0). In evaluating the order of the individual terms in (3.3), we assume that the functions p, B_n and C_n are of order unity in comparison with μ and $d^n V/ds^n = 0(\mu^{-n}V)$. We substitute (3.5) into (3.3) and equate coefficients of like powers of μ to zero. The higher order terms yield

$$-B_0 p + \left(\frac{1}{R_1} + \frac{\sigma}{R_2}\right) C_0 p = 0,$$

$$\left(\frac{1}{R_1} + \frac{\sigma}{R_2}\right) B_0 + \left(\lambda - \frac{1}{R_1^2} - \frac{2\sigma}{R_1 R_2} - \frac{1}{R_2^2}\right) C_0 - p^2 C_0 = 0, \tag{3.7}$$

and we thus have

$$p_{1,2} = \pm\left(\lambda - \frac{1-\sigma^2}{R_2^2(s)}\right)^{\frac{1}{2}}, \quad B_0 = \left(\frac{1}{R_1} + \frac{\sigma}{R_2}\right) C_0. \tag{3.8}$$

The coefficients of dV/ds in the first equation (3.3) and of $\mu^2(dV/ds)$ in the second equation yield

$$-B_1 p + \left(\frac{1}{R_1} + \frac{\sigma}{R_2}\right) C_1 p + 2\frac{dB_0}{ds} - 2\left(\frac{1}{R_1} + \frac{\sigma}{R_2}\right)\frac{dC_0}{ds} -$$

$$- \frac{d}{ds}\left(\frac{2}{R_1} + \frac{1+\sigma}{R_2}\right) C_0 = 0,$$

$$\left(\frac{1}{R_1} + \frac{\sigma}{R_2}\right) B_1 - \left(\frac{1}{R_1} + \frac{\sigma}{R_2}\right)^2 C_1 + \frac{(1-\sigma)B}{pB}\left(\frac{1}{R_1} - \frac{1}{R_2}\right) B_0 +$$

$$+ 2\frac{dp}{ds} C_0 + 4p\frac{dC_0}{ds} = 0. \tag{3.9}$$

From compatibility of (3.9) with respect to the unknowns $B_1(s)$ and $C_1(s)$, we find

$$-\frac{d}{ds}\left(\frac{1-\sigma^2}{R_2^2(s)}\right) C_0 + 4\left(\lambda - \frac{1-\sigma^2}{R_2^2(s)}\right)\frac{dC_0}{ds} = 0, \tag{3.10}$$

and we have

$$C_0(s) = \left|\lambda - \frac{1-\sigma^2}{R_2^2(s)}\right|^{-\frac{1}{4}}. \tag{3.11}$$

For $\lambda = (1 - \sigma^2)(R_2(s))^{-2}$, the quantity $C_0(s)$ becomes infinite. Therefore, the solution construction is good from the dome apex up

to and including the first root s_0 of the equation $\lambda - (1 - \sigma^2)(R_2(s))^{-2} = 0$. Here s_0 is a reversal point. If $R_2(s_0) \neq 0$, we can use the results of [2, 3] to construct the corresponding integrals to the right of the reversal point.

§ 4

Now let us integrate (3.6). We use the reference equation method [5]. We seek the solution in the form

$$V(s) = \sum_{n=0}^{\infty} \mu^{2n} D_{2n}(s) J_0[z(s)] + \sum_{n=0}^{\infty} \mu^{2n+1} D_{2n+1}(s) \frac{dJ_0}{dz}, \qquad (4.1)$$

where $J_0(z)$ is the Bessel function of zero order. We substitute (4.1) into (3.6) and equate coefficients of like powers of μ to zero. Then we obtain

$$\left(\frac{dz}{ds}\right)^2 - \mu^{-2} p(s) = 0, \quad z = \pm \mu^{-1} \int_0^s (p(t))^{\frac{1}{2}} dt;$$

$$D_0 \frac{d^2 z}{ds^2} + 2 \frac{dD_0}{ds} \cdot \frac{dz}{ds} + \frac{D_0}{B} \cdot \frac{dB}{ds} \cdot \frac{dz}{ds} - \frac{D_0}{z} \left(\frac{dz}{ds}\right)^2 = 0, \qquad (4.2)$$

$$D_0(s) = \left(\frac{z}{B \frac{dz}{ds}}\right)^{\frac{1}{2}}. \qquad (4.3)$$

To clarify the behavior of these solutions for $s \gg \mu R$, we use the asymptotic formula for the function $J_0(z)$ [6]

$$J_0(z) = \left(\frac{2}{\pi z}\right)^{\frac{1}{2}} \left\{\cos\left(z - \frac{\pi}{4}\right) + O(z^{-1})\right\}. \qquad (4.4)$$

§ 5

Using the analysis of § 3 and § 4, we present the final expressions, having a relative error of order μ, for the two real solutions $w_1(s)$ and $w_2(s)$ of the system (1.1) which are regular at $s = 0$.

Let $\lambda - (1 - \sigma^2)(R_2(s))^{-2} > 0$. For $s = O(\mu R)$ we have

$$w_1(s) = \psi(s) J_0(\mu^{-1} \xi(s)), \quad w_2(s) = \psi(s) I_0(\mu^{-1} \xi(s)), \qquad (5.1)$$

where

$$\xi(s) = \int_0^s \left|\lambda - \frac{1 - \sigma^2}{R_2^2(t)}\right|^{\frac{1}{4}} dt, \quad \psi(s) = \left(\frac{\pi \xi(s)}{2\mu B(s)}\right)^{\frac{1}{2}} \left|\lambda - \frac{1 - \sigma^2}{R_2^2(s)}\right|^{-\frac{3}{8}}. \qquad (5.2)$$

For $s \gg \mu R$ the solutions (5.1) have an asymptotic representation of the form

$$w_1(s) = \eta(s)\left[\cos\left(\frac{\xi(s)}{\mu} - \frac{\pi}{4}\right) + O\left(\frac{\mu}{\xi}\right)\right], \quad w_2(s) =$$
$$= \frac{1}{2}\eta(s)e^{\frac{\xi(s)}{\mu}}\left(1 + O\left(\frac{\mu}{\xi}\right)\right). \tag{5.3}$$

where

$$\eta(s) = (B(s))^{-\frac{1}{2}}\left|\lambda - \frac{1-\sigma^2}{R_2^2(s)}\right|^{-\frac{3}{8}}. \tag{5.4}$$

Now let $\lambda - (1 - \sigma^2)(R_2(s))^{-2} < 0$. For $s = O(\mu R)$

$$w_1(s) = \phi(s)\operatorname{Re}\left\{J_0\left(\mu^{-1}\xi(s)e^{\frac{i\pi}{4}}\right)\right\}, \quad w_2(s) = \phi(s)\operatorname{Im}\left\{J_0\left(\mu^{-1}\xi(s)e^{\frac{i\pi}{4}}\right)\right\} \tag{5.5}$$

where Re z and Im z denote, respectively, the real and imaginary parts of the complex number z.

For $s \gg \mu R$

$$w_1(s) = \frac{1}{2}\eta(s)e^{\frac{\xi(s)}{\mu\sqrt{2}}}\left[\cos\left(\frac{\xi(s)}{\mu\sqrt{2}} - \frac{\pi}{8}\right) + O\left(\frac{\mu}{\xi}\right)\right],$$
$$w_2(s) = -\frac{1}{2}\eta(s)e^{\frac{\xi(s)}{\mu\sqrt{2}}}\left[\sin\left(\frac{\xi(s)}{\mu\sqrt{2}} - \frac{\pi}{8}\right) + O\left(\frac{\mu}{\xi}\right)\right]. \tag{5.6}$$

Using (5.2) and (5.4) it is not difficult to show that the solutions (5.3) and (5.6) are linear combinations of the solutions constructed in [2] far from the dome apex.

We use (3.2), (3.6) and (3.8) to find the corresponding integrals $u_1(s)$ and $u_2(s)$. To within a relative error of order μ, we obtain

$$u_i(s) = \left(\frac{1}{R_1} + \frac{\sigma}{R_2}\right)\phi(s)\left(\frac{dz_i}{ds}\right)^{-1}J_1(z_i(s)), \quad i = 1, 2 \tag{5.7}$$

(the subscripts $i = 1, 2$ correspond to different signs in (3.8)). It is not difficult to obtain formulas similar to (5.1)–(5.6) for the functions u_1 and u_2 by use of (5.7). We simply note that

$$z_i(s) = O(\mu w_i(s)), \quad i = 1, 2.$$

REFERENCES

1. Zimin, V. I., "On the application of asymptotic integration to the solution of a particular equation of shell theory." IAN Uzbek SSR, Physics and Mathematical Sciences Series, No. 4, 1957.

2. Tovstik, P. Ye., "Integral equations for axisymmetric vibrations of a shell of revolution." In the present collection.

3. Alumyae, N. "On the fundamental system of integrals for the equation of small axisymmetric steady state vibrations of an elastic, conical shell of revolution," IAN Estonian SSR, Physico-Mathematical and Technical Sciences Series, No. 1, 1960.

4. Gol'denveyzer, A. L. Teoriya tonkikh uprugikh obolochek (Theory of Thin Elastic Shells), Moscow, GITTL, 1953.

5. Dorodnitsyn, A. A., "Asymptotic eigenvalue distribution laws for some special forms of second order differential equations." UMN, Vol. 7, No. 6, 1952.

6. Gradshteyn I. S., I. M. Ryzhik, Tablitsy integralov, summ, ryadov i proizvedeniy (Tables of Integrals, Sums, Series and Products). Moscow, Fizmatgiz, 1962.

Received 31 March 1964

SHELLS OF REVOLUTION WITH A SMALL CENTRAL OPENING
SUBJECTED TO SYMMETRIC AND ANTISYMMETRIC LOADING

V.I. Kruglyakova

This article presents a unified method for determining the stresses near a small central opening in shells of revolution subjected to symmetric and antisymmetric loads. Primary emphasis is placed on reducing the solution to a form convenient for practical application. In particular, the edge stiffness coefficients are obtained.

In most studies on this question (see § 10 of the present paper) symmetric deformation of a shallow shell is examined. In contrast to these studies, the proposed method contains a simplification involving replacement of $\sin \theta$ by θ only in the equation coefficients. The trigonometric multipliers are retained in the expressions for the stresses and displacements. Comparison of the resulting solution with a specially constructed more exact solution has shown its acceptability for a wide range of values of the angle θ_0; corresponding to the edge of the opening in the shell. The region of values of the basic parameters $(h/R, \theta_0)$, in which the suggested Bessel solution may be replaced by the much simpler familiar Geckeler solution, is determined. A brief review of the studies known to the author is presented.

The basic relations and notations used here are described in [1, 2].

§ 1. Basic Relations for Shells of Revolution
Formed by Rotation of Second Order Curves

In studying shells of revolution, we usually take the angles θ and φ (Figure 1) as the curvilinear coordinates.

Among the shells of positive Gaussian curvature, those most frequently encountered are the shells whose middle surfaces are formed by rotating second order curves about their axes of symmetry. For these shells the principal radii of curvature

$$R_1 = \frac{R_0}{(1+\gamma\sin^2\theta)^{3/2}}, \quad R_2 = \frac{R_0}{(1+\gamma\sin^2\theta)^{1/2}} \tag{1.1}$$

are independent of the angle φ . Here $\gamma = 0$ corresponds to a sphere; $\gamma = -1$ is a paraboloid; $\gamma > -1$ are ellipsoids; $\gamma < -1$ are hyperboloids, and the parameter R_0 is the value of the radii of curvature for $\theta = 0$.
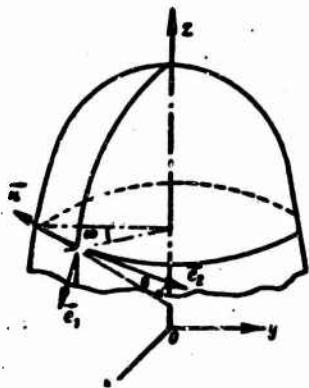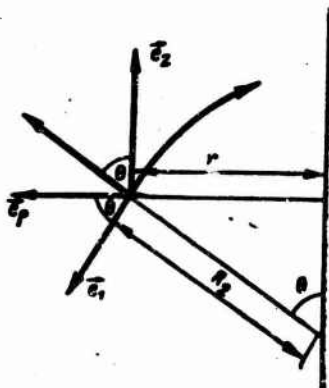

Figure 1.   Figure 2.

The Codazzi-Gauss relations are written as

$$\frac{dR_2\sin\theta}{d\theta} = \frac{dr}{d\theta} = R_1\cos\theta \qquad (r = R_2\sin\theta). \tag{1.2}$$

In shells of revolution, it is often convenient to introduce, in place of the usual unit vectors $\vec{e}_1$ and $\vec{n}$ (Figure 2), the unit vectors of the horizontal and vertical directions

$$\vec{e}_r = \cos\theta\,\vec{e}_1 + \sin\theta\,\vec{n}, \quad \vec{e}_1 = \cos\theta\,\vec{e}_r - \sin\theta\,\vec{e}_z, $$
$$\vec{e}_z = -\sin\theta\,\vec{e}_1 + \cos\theta\,\vec{n}, \quad \vec{n} = \sin\theta\,\vec{e}_r + \cos\theta\,\vec{e}_z. \tag{1.3}$$

Resolving the displacement vector

$$\vec{U} = u\vec{e}_1 + v\vec{e}_2 + w\vec{n} = u_r\vec{e}_r + v\vec{e}_2 + u_z\vec{e}_z.$$

along these directions, we obtain the expressions for its components

$$u_r = \cos\theta\,u + \sin\theta\,w, \quad u = \cos\theta\,u_r - \sin\theta\,u_z, $$
$$u_z = -\sin\theta\,u + \cos\theta\,w, \quad w = \sin\theta\,u_r + \cos\theta\,u_z. \tag{1.4}$$

We have for the rotation angle of the tangent to the meridian

$$\theta = -\frac{1}{R_1}\left(\frac{\partial w}{\partial s} - u\right) = -\frac{1}{R_1}\left(\sin\theta\frac{\partial u_\rho}{\partial s} + \cos\theta\frac{\partial u_z}{\partial s}\right) \qquad (1.5)$$

and for the deformation components

$$\varepsilon_1 = \frac{1}{R_1}\left(\frac{\partial u}{\partial s} + w\right) = \frac{1}{R_1\cos\theta}\cdot\frac{\partial u_\rho}{\partial s} + \text{tg}\,\theta\,\vartheta,$$

$$\varepsilon_2 = \frac{1}{R_2\sin\theta}\left(\frac{\partial v}{\partial \gamma} + u_z\right), \quad \tau_1 = \frac{1}{R_1}\cdot\frac{\partial v}{\partial s}, \qquad (1.6)$$

$$\tau_3 = -\frac{1}{r^2}\left(\sin\theta\frac{\partial u_\rho}{\partial s} + \cos\theta\frac{\partial u_z}{\partial s} - \sin\theta\frac{\partial v}{\partial \gamma}\right) + \frac{1}{r}\cos\theta\,\vartheta.$$
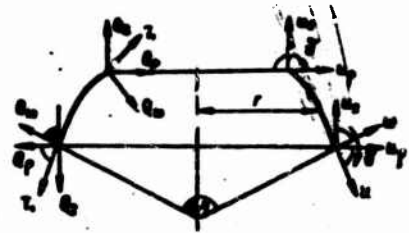
Figure 3.

Figure 4.

The stresses which arise on the lateral surfaces of the shell are reduced to forces and moments, whose positive directions are shown in Figure 3. Here T_1 are meridional forces and T_2 are circumferential forces; M_1, M_2 are the meridional and circumferential bending moments. In place of the meridional T_1 and shearing Q_{1n} forces, we often consider the horizontal Q_ρ and vertical Q_z forces (Figure 4)

$$Q_\rho = \cos\theta\,T_1 + \sin\theta\,Q_{1n},$$
$$Q_z = \sin\theta\,T_1 - \cos\theta\,Q_{1n}. \qquad (1.7)$$

The catenary stresses (uniform across the shell thickness) are found from the formulas

$$\sigma_{T_1} = \frac{T_1}{h}, \quad \sigma_{T_2} = \frac{T_2}{h}, \qquad (1.8)$$

and the bending stresses are found from

$$\sigma_{M_1} = \frac{6M_1}{h^2}, \quad \sigma_{M_2} = \frac{6M_2}{h^2}. \qquad (1.9)$$

The maximal stresses, occurring in the extreme fibers of the shell, are determined by the maximum of the quantities

$$|\sigma_1| = \left|\frac{T_1}{h} \pm \frac{6M_1}{h^2}\right|,$$
$$|\sigma_2| = \left|\frac{T_2}{h} \pm \frac{6M_2}{h^2}\right|. \qquad (1.10)$$

where the upper signs correspond to the stresses on the outer shell surface, and the lower are for the inner surface.

The forces and moments are related with the deformations by Hooke's law

$$T_1 = \frac{Eh}{1-\nu^2}(\varkappa_1 + \nu\varkappa_2), \quad M_1 = \frac{Eh^3}{12(1-\nu^2)}(\varkappa_1 + \nu\varkappa_2),$$
$$T_2 = \frac{Eh}{1-\nu^2}(\varkappa_2 + \nu\varkappa_1), \quad M_2 = \frac{Eh^3}{12(1-\nu^2)}(\varkappa_2 + \nu\varkappa_1),$$

$$(1.11)$$

ν is the Poisson coefficient.

We consider the complex displacements [1]

$$\tilde{u} = u + i\bar{u}, \quad \tilde{w} = w + i\bar{w},$$

$$(1.12)$$

whose real parts are the conventional displacements, while the imaginary parts are the stress functions $\bar{u}, \bar{w}$, and the complex forces

$$\widetilde{T}_1 = T_1 - iEhc\varkappa_2,$$
$$\widetilde{T}_2 = T_2 - iEhc\varkappa_1$$
$$\left(c = \frac{h}{\sqrt{12(1-\nu^2)}}\right)$$

$$(1.13)$$

It is not difficult to see that

$$T_1 = \mathrm{Re}\,\widetilde{T}_1, \quad T_2 = \mathrm{Re}\,\widetilde{T}_2,$$
$$M_1 = -c\,\mathrm{Im}\,\{\widetilde{T}_2 + \nu\widetilde{T}_1\},$$
$$M_2 = -c\,\mathrm{Im}\,\{\widetilde{T}_1 + \nu\widetilde{T}_2\}.$$

$$(1.14)$$

The complex forces $\tilde{T}_1$ and $\tilde{T}_2$ are defined in terms of the basic Novozhilov complex function $\tilde{T} = \tilde{T}_1 + \tilde{T}_2$, which is the solution of the system of differential equations

$$G\{\widetilde{U}\} - \left[1 - ic\left(\frac{1}{R_1} - \frac{1}{R_2}\right)\frac{1}{\sin^2\theta}\right]\frac{\partial^2 \widetilde{T}}{\partial\varphi^2} = f(\theta, \varphi),$$
$$-icG\{\widetilde{T}\} + \widetilde{T} + \left(\frac{1}{R_1} - \frac{1}{R_2}\right)\frac{1}{\sin^2\theta}\widetilde{U} = R_2 q_n,$$

$$(1.15)$$

where

$$G = \frac{1}{R_1 R_2 \sin\theta} \cdot \frac{\partial}{\partial\theta}\left(\frac{R_2^2 \sin\theta}{R_1} \cdot \frac{\partial}{\partial\theta}\right) + \frac{1}{R_2 \sin^2\theta} \cdot \frac{\partial^2}{\partial\varphi^2},$$
$$f(\theta, \varphi) = \frac{1}{R_1 R_2 \sin\theta}\left\{\frac{\partial}{\partial\theta}\left[(q_n \cos\theta - q_1 \sin\theta)R_2^2 \sin^2\theta\right] + \frac{\partial q_2}{\partial\varphi}R_1 R_2^2 \sin^2\theta\right\}.$$

$$(1.16)$$

The basic forces are determined from the functions $\tilde{T}$ and $\tilde{U}$ found from this system

$$\widetilde{T}_1 = \frac{\widetilde{U}}{R_2 \sin^2\theta} + ic\frac{\mathrm{ctg}\,\theta}{R_1} \cdot \frac{\partial\widetilde{T}}{\partial\theta},$$
$$\widetilde{T}_2 = -\frac{\widetilde{U}}{R_2 \sin^2\theta} + \widetilde{T} - ic\frac{\mathrm{ctg}\,\theta}{R_1} \cdot \frac{\partial\widetilde{T}}{\partial\theta}.$$

$$(1.17)$$

The following expressions are obtained for the complex boundary values [2]

$$\widetilde{Q}_i = Q_i - iEhc\,\varkappa_i = \cos\theta\,\widetilde{T}_1 + ic\frac{\sin\theta}{R_1}\cdot\frac{\partial\widetilde{T}}{\partial\theta},$$

$$\widetilde{Q}_i = Q_i + iEhc\,\varkappa_i = \sin\theta\,\widetilde{T}_1 - ic\frac{\cos\theta}{R_1}\cdot\frac{\partial\widetilde{T}}{\partial\theta}, \qquad (1.18)$$

$$\widetilde{M}_1 = M_1 + iEhc\,\iota_2 = ic\{\widetilde{T}_2 - \nu\widetilde{T}_1\}, \quad \widetilde{Q}_{12} = \widetilde{S}.$$

Using the resulting forces, the complex displacements are found from the relations of the complex Hooke's law, which takes the following form for shells of revolution

$$\frac{\widetilde{u}}{R} + \widetilde{w} \cdots \frac{1}{\sin\theta}\cdot\frac{\partial\widetilde{u}}{\partial\theta} + R_1\,\mathrm{tg}\theta\,\widetilde{u} = \frac{R_1}{Eh}\left\{\widetilde{T}_1 - \nu\widetilde{T}_2 + \frac{i}{c}M_2^{\bullet}\right\},$$

$$\frac{\partial\widetilde{w}}{\partial\varphi} + \cos\theta\,\widetilde{u} + \sin\theta\,\widetilde{w} = \frac{\partial\widetilde{v}}{\partial\varphi} + \widetilde{u}_r = \frac{r}{Eh}\left\{\widetilde{T}_2 - \nu\widetilde{T}_1 + \frac{i}{c}M_1^{\bullet}\right\},$$

$$\frac{R_2\sin\theta}{R_1}\cdot\frac{\partial}{\partial\theta}\left(\frac{\widetilde{v}}{R_2\sin\theta}\right) + \frac{1}{R_2\sin\theta}\cdot\frac{\partial\widetilde{u}}{\partial\varphi} = \frac{1}{Eh}\left\{2(1+\nu)\widetilde{S} - \frac{i}{c}2H^{\bullet}\right\},$$

$$-\frac{1}{R_1}\cdot\frac{\partial}{\partial\theta}\left[\frac{1}{R_1}\left(\frac{\partial\widetilde{w}}{\partial\theta} - \widetilde{u}\right)\right] = \frac{1}{R_1}\cdot\frac{\partial\widetilde{v}}{\partial\theta} = \frac{i}{Ehc}\{\widetilde{T}_2 - \widetilde{T}_2^{\bullet}\}, \qquad (1.19)$$

$$-\frac{1}{(R_2\sin\theta)^2}\cdot\frac{\partial}{\partial\varphi}\left(\frac{\partial\widetilde{w}}{\partial\varphi} - \sin\theta\,\widetilde{v}\right) - \frac{\cos\theta}{R_1R_2\sin\theta}\left(\frac{\partial\widetilde{w}}{\partial\theta} - \widetilde{u}\right) =$$
$$= \frac{i}{Ehc}(\widetilde{T}_1 - \widetilde{T}_1^{\bullet}),$$

$$-\frac{1}{R_1}\cdot\frac{\partial}{\partial\theta}\left[\frac{1}{R_2\sin\theta}\left(\frac{\partial\widetilde{w}}{\partial\varphi} - \sin\theta\,\widetilde{v}\right)\right] + \frac{1}{R_1R_2\sin\theta}\left(\frac{\partial\widetilde{u}}{\partial\varphi} - \cos\theta\,\widetilde{v}\right) =$$
$$= -\frac{i}{Ehc}(\widetilde{S} - S^{\bullet})$$

Here the starred quantities $T_1^{\bullet}$, $T_2^{\bullet}$, $M_1^{\bullet}$, M_2, $S^{\bullet}$, $H^{\bullet}$ are a static system of functions which is the particular solution of the nonhomogeneous system of equilibrium equations. For the majority of problems of practical interest the momentless solution, i.e., the solution of the system

$$\frac{\partial R_2\sin\theta\,T_1^{\bullet}}{\partial\theta} + R_1\frac{\partial S^{\bullet}}{\partial\varphi} - R_1\cos\theta\,T_2^{\bullet} = -R_1R_2\sin\theta\,q_1,$$

$$R_1\frac{\partial T_2^{\bullet}}{\partial\varphi} + \frac{1}{R_2\sin\theta}\frac{\partial R_2^2\sin^2\theta\,\partial S^{\bullet}}{\partial\theta} = -R_1R_2\sin\theta\,q_2, \qquad (1.20)$$

$$\frac{T_1^{\bullet}}{R_1} + \frac{T_2^{\bullet}}{R_2} = q_n$$

$$(M_1^{\bullet} = M_2^{\bullet} = H^{\bullet} = 0).$$

may be taken as the particular solution

§ 2. Symmetric Case

In the symmetric loading case all the quantities of the preceding section are independent of the angle φ and the system of equations (1.15) for the basic complex function $\widetilde{T}$ reduces to a single second-order differential equation

$$\frac{d\tilde{T}}{d\theta} + \left[\left(2\frac{R_1}{R_2} - 1\right)ctg\,\theta - \frac{1}{R_1}\cdot\frac{dR_1}{d\theta}\right]\frac{d\tilde{T}}{d\theta} + i\frac{R_1^2}{cR_2}\tilde{T} = i\frac{R_1^2}{cR_2}F(\theta).\qquad(2.1)$$

where

$$F(\theta) = R_2 q_n - \left(\frac{1}{R_1} - \frac{1}{R_2}\right)\frac{U}{\sin^2\theta}$$

and q_n is the normal component of the surface load.

The function U, the axial vertical force acting on a parallel circle, may be easily calculated

$$U = -\frac{R_2\sin\theta}{2\pi}F_z^0.\qquad(2.2)$$

Here F_z is the axial component of the principal vector of the edge loads applied to the parallel circle and

$$F_z^0 = (F_z)_0.$$

We take the momentless solution $T^* = T_1^* + T_2^*$ as the particular solution of (2.1) and write the homogeneous equation with account for (1.1) in the form

$$\frac{d\tilde{T}^0}{d\theta} + \frac{1 + 2\gamma\sin^2\theta}{1 + \gamma\sin^2\theta}\cdot\frac{\cos\theta}{\sin\theta}\cdot\frac{d\tilde{T}^0}{d\theta} + i\frac{R_0}{c(1 + \gamma\sin^2\theta)^{3/2}}\tilde{T}^0 = 0.\qquad(2.3)$$

The question of the integration of this equation will be examined later in application to specific forms of shells of revolution (sphere and ellipsoid). After the function $\tilde{T}^0$ is found, we determine the complex forces from (1.17)

$$\tilde{T}_1 = T_1^* + ic\frac{ctg\,\theta}{R_1}\cdot\frac{d\tilde{T}^0}{d\theta},$$
$$\tilde{T}_2 = T_2^* + \tilde{T}^0 - ic\frac{ctg\,\theta}{R_1}\cdot\frac{d\tilde{T}^0}{d\theta}.\qquad(2.4)$$

We note that finding the momentless forces T_1^*, T_2^* from (1.20) usually does not present any difficulty for particular forms of loading.

In the symmetric case, we obtain for the complex boundary conditions (1.18)

$$\tilde{Q}_\gamma = Q_\gamma + i\frac{c}{R_1}\cdot\frac{1}{\sin\theta}\cdot\frac{d\tilde{T}^0}{d\theta}$$
$$(Q_\gamma = \cos\theta\,T_1^*),$$
$$\tilde{M}_1 = ic\left\{T_2^* - \nu T_1^* + \tilde{T}^0 - ic(1 + \nu)\frac{ctg\,\theta}{R_1}\cdot\frac{d\tilde{T}^0}{d\theta}\right\}.\qquad(2.5)$$

We also write out the expressions which will be needed later for the radial displacement u_ρ and the edge rotation angle ϑ, using for this purpose the system in terms of complex displacements (1.19)

$$a_\varphi = a_\varphi^* + \frac{R_2 \sin \theta}{Eh}\left\{\operatorname{Re}\widetilde{T}^\circ + (1+\nu)\frac{c}{R_1}\operatorname{ctg}\theta\operatorname{Im}\frac{d\widetilde{T}^\circ}{d\theta}\right\}, \qquad (2.6)$$

$$\theta = \theta^\circ - \frac{1}{Eh}\cdot\frac{R_2}{R_1}\operatorname{Re}\frac{d\widetilde{T}^\circ}{d\theta},$$

where

$$a_\varphi^* = \frac{R_2 \sin \theta}{Eh}(T_2^\circ - \nu\, T_1^\circ),$$

$$\theta^\circ = -\frac{1}{Eh}\cdot\frac{R_2}{R_1}\cdot\frac{dT^\circ}{d\theta} \qquad (2.7)$$

$$(T^\circ = T_1^\circ + T_2^\circ).$$

§ 3. Antisymmetric Case (wind load)

The antisymmetric case is that in which both the unknown and given quantities have the following dependence on the angle φ:

$$(a,\, w,\, a_\varphi,\, a_x,\, \theta) = (a_{.1},\, w_{.1},\, u_{\varphi.1},\, u_{x.1},\, \theta_{.1})\begin{matrix}\cos\varphi \\ \sin\varphi\end{matrix},$$

$$v = v_{.1}\begin{matrix}\sin\varphi \\ \cos\varphi\end{matrix},$$

$$(a_\varphi,\, a_x,\, x_1,\, x_2) = (a_{2.1},\, a_{2.1},\, x_{1.1},\, x_{2.1})\begin{matrix}\cos\varphi \\ \sin\varphi\end{matrix},$$

$$(T_1,\, T_2,\, M_1,\, M_2,\, Q_\varphi,\, Q_x) = (T_{1.1},\, T_{2.1},\, M_{1.1},\, M_{2.1},\, Q_{\varphi.1},\, Q_{x.1})\begin{matrix}\cos\varphi \\ \sin\varphi\end{matrix}. \qquad (3.1)$$

$$(q_1,\, q_n) = (q_{1.1},\, q_{n.1})\begin{matrix}\cos\varphi \\ \sin\varphi\end{matrix},$$

$$q_2 = q_{2.1}\begin{matrix}\sin\varphi \\ \cos\varphi\end{matrix},$$

where the upper functions apply to the first antisymmetric case and the lower apply to the second case. For definiteness we shall consider the first case in the following.

Upon substituting (3.1) into the relations of § 1 and simplifying the trigonometric factors, we obtain relations which depend only on the angle θ for the quantities of interest to us. Just as in the symmetric case, the problem reduces to the integration of a single ordinary differential equation in the complex function

$$\widetilde{T}_{.1} = \widetilde{T}_{1.1} + \widetilde{T}_{2.1},$$

$$\frac{d^2\widetilde{T}_{.1}}{d\theta^2} + \left[\left(2\frac{R_1}{R_2} - 1\right)\operatorname{ctg}\theta - \frac{1}{R_1}\cdot\frac{dR_1}{d\theta}\right]\frac{d\widetilde{T}_{.1}}{d\theta} + \qquad (3.2)$$

$$+ \frac{R_1}{R_2}\left(1 - 2\frac{R_1}{R_2}\right)\frac{1}{\sin^2\theta}\widetilde{T}_{.1} + i\frac{R_1^2}{cR_2}\widetilde{T}_{.1} = i\frac{R_1^2}{cR_2}F(\theta),$$

where

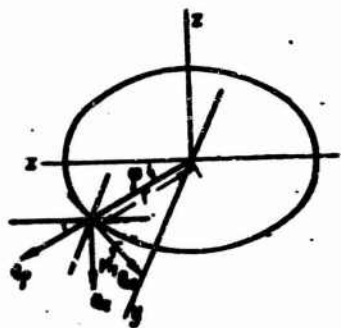$$F(\theta) = R_2 q_{n.1} - \left(\frac{1}{R_1} - \frac{1}{R_2}\right)\frac{w}{\sin^2\theta}.$$

$$W = \frac{1}{R_2 \sin \theta} \left\{ \frac{1}{z} \begin{matrix} B_y^0 \\ -B_x^0 \end{matrix} + \right.$$
$$+ \frac{1}{z} \begin{matrix} F_x^0 \\ F_y^0 \end{matrix} \int_0^\theta R_1 \sin \theta \, d\theta +$$
$$+ \left. \int_0^\theta \Phi(\theta) R_1 \sin \theta \, d\theta \right\}, \quad (\qquad (3.3)$$

Figure 5.

$$\Phi(\theta) = (q_{n,1} \cos \theta - q_{1,1} \sin \theta)$$
$$\times R_2^2 \sin \theta - \int_0^\theta (q_{n,1} \sin \theta + q_{1,1} \cos \theta - q_{2,1}) R_1 R_2 \sin \theta \, d\theta, \quad (3.4)$$

The components of the principal vector and of the principal moment
of the forces and moments applied to the parallel section of the shell
(Figure 5) have the form

$$B_x = \begin{cases} 0 \\ -\pi r (M_{1,1} + r Q_{n,1}) \end{cases}, \quad B_x^0 = (B_x)_{\lambda},$$
$$B_y = \begin{cases} \pi r (M_{1,1} + r Q_{n,1}) \\ 0 \end{cases}, \quad B_y^0 = (B_y)_{\lambda},$$
$$F_x = \begin{cases} \pi r (Q_{n,1} - T_{12,1}) \\ 0 \end{cases}, \quad F_x^0 = (F_x)_{\lambda}, \qquad (3.5)$$
$$F_y = \begin{cases} 0 \\ \pi r (Q_{n,1} + T_{12,1}) \end{cases}, \quad F_y^0 = (F_y)_{\lambda}.$$

For the shell class in question (1.1) the basic equation is writ-
ten in the form

$$\frac{d^2 \tilde{T}_{,1}}{d\theta^2} + \frac{1 + 2\gamma \sin^2 \theta}{1 + \gamma \sin^2 \theta} \cdot \frac{\cos \theta}{\sin \theta} \cdot \frac{d\tilde{T}_{,1}}{d\theta} - \frac{1}{\sin^2 \theta} \cdot \frac{1 - \gamma \sin^4 \theta}{(1 + \gamma \sin^2 \theta)} \tilde{T}_{,1} \cdot$$
$$\cdot \, L \, i \frac{R_0}{e(1 + \gamma \sin^2 \theta)^{3/2}} \tilde{T}_{,1} = i \frac{R_0}{e(1 + \gamma \sin^2 \theta)^{3/2}} F(\theta). \qquad (3.6)$$

If we take the momentless solution as the particular solution, then
in accordance with (1.17) the complex forces are written as

$$\tilde{T}_{1,1} = T_{1,1}^0 + ic \left\{ \frac{\text{ctg}\,\theta}{R_1} \cdot \frac{d\tilde{T}_{,1}^0}{d\theta} - \frac{1}{R_2 \sin^2 \theta} \tilde{T}_{,1}^0 \right\},$$
$$\tilde{T}_{2,1} = T_{2,1}^0 + \tilde{T}_{,1}^0 - ic \left\{ \frac{\text{ctg}\,\theta}{R_1} \cdot \frac{d\tilde{T}_{,1}^0}{d\theta} - \frac{1}{R_2 \sin^2 \theta} \tilde{T}_{,1}^0 \right\}, \qquad (3.7)$$

where $\overset{\sim 0}{T}_{,1}$ is the general solution of the homogeneous equation (3.6)
and

$$T_{1,1}^0 = \frac{W}{R_2 \sin^2 \theta},$$
$$T_{2,1}^0 = R_2 q_{n,1} - \frac{W}{R_1 \sin^2 \theta}. \qquad (3.8)$$

We obtain the expressions for the edge conditions (1.18)

$$Q_{t,1} = Q'_{t,1} - \frac{c}{R_1} \cdot \frac{1}{\sin\theta} \left\{ \text{Im} \frac{d\widetilde{T}^0_{,1}}{d\theta} - \frac{R_1}{R_2} \text{ctg}\,\theta\,\text{Im}\,\widetilde{T}^0_{,1} \right\},$$

$$Q'_{n,1} = \cos\theta\,T^0_{1,1},$$

$$\overline{M_{1,1}} = -c \left\{ \text{Im}\,\widetilde{T}^0_{,1} - c(1+\nu) \left[\frac{\text{ctg}\,\theta}{R_1} \text{Re} \frac{d\widetilde{T}^0_{,1}}{d\theta} - \right. \right. \tag{3.9}$$

$$\left. \left. - \frac{1}{R_2 \sin^2\theta} \text{Re}\,\widetilde{T}^0_{,1} \right] \right\}.$$

The functions χ and $(r\gamma)$ in the antisymmetric case play the role of the quantities u_ρ and θ of the symmetric case. The first of these functions is the elastic rotation of the tangent to the meridian, and $(r\gamma)$ is the relative elongation of the edge.

$$\chi = \chi^\circ + \frac{1}{Eh} \left\{ \text{ctg}\,\theta\,\text{Re}\,\widetilde{T}^0_{,1} - \text{Re} \frac{d\widetilde{T}^0_{,1}}{d\theta} \right\},$$

$$r\gamma = r\gamma^\circ + \frac{R_2 \sin\theta}{Eh} \left\{ \text{Re}\,\widetilde{T}^0_{,1} + \right. \tag{3.10}$$

$$\left. + (1+\nu)c \left[\frac{\text{ctg}\,\theta}{R_1} \text{Im} \frac{d\widetilde{T}^0_{,1}}{d\theta} - \frac{1}{R_2 \sin^2\theta} \text{Im}\,\widetilde{T}^0_{,1} \right] \right\},$$

where

$$r\gamma^\circ = \frac{R_2 \sin\theta}{Eh} (T^\circ_{2,1} - \nu T^\circ_{1,1}),$$

$$\chi^\circ = \frac{1}{Eh} \left\{ - \frac{R_2^2 \sin\theta}{R_1} \cdot \frac{d}{d\theta} \left(\frac{T^\circ_{,1}}{R_2 \sin\theta} \right) + \right. \tag{3.11}$$

$$\left. + (1+\nu) \left[- \frac{1}{k_1 R_2 \sin^2\theta} \cdot \frac{d R_2 \sin\theta\,W}{d\theta} + R_2(q_{n,1}\,\text{ctg}\,\theta - 2q_{1,1}) \right] \right\}$$

We note that the quantities θ^* in (2.6) and χ^* in (3.10) may be neglected within the limits of shell theory accuracy [2].

§ 4. On the Solution of the Reference Equation

To find the solutions of the homogeneous equations (2.3) and (3.6) we use the method of reference equations [3], which involves the use of simpler known equations with the same singularities in the coefficients as the equation in question, in order to find the solution.

In our case we take as the reference equation the Bessel equation

$$\frac{d^2 y}{d\psi^2} + \frac{1}{\psi} \cdot \frac{dy}{d\psi} - \left(i + \frac{n^2}{\psi^2}\right) y = 0. \tag{4.1}$$

Its fundamental solution [4] may be written in terms of modified Bessel functions of the first and second kind

$$y = \widetilde{A} I_n(\psi \sqrt{i}) + \widetilde{B} K_n(\psi \sqrt{i}), \tag{4.2}$$

where the modified Bessel function of the first kind of order n $I_n(\psi\sqrt{i})$ and that of the second kind $-K_n(\psi\sqrt{i})$ are written in terms of the

tabulated Thomson (Kelvin) functions [4.6]

$$i^n I_n(\psi\sqrt{i}) = \text{ber}_n\psi + i\,\text{bei}_n\psi,$$
$$i^n K_n(\psi\sqrt{i}) = \text{ker}_n\psi + i\,\text{kel}_n\psi. \tag{4.3}$$

The functions $\text{ber}_n\psi$, $\text{bei}_n\psi$ with subscript n may be defined in terms of the corresponding functions with subscript n - 1 using the following recursion formulas

$$\text{ber}_1\psi = \frac{1}{\sqrt{2}}(\text{ber}'\psi - \text{bei}'\psi),$$
$$\text{bei}_1\psi = \frac{1}{\sqrt{2}}(\text{ber}'\psi + \text{bei}'\psi),$$
$$\text{ber}_{n+1}\psi = -\frac{n\sqrt{2}}{\psi}(\text{ber}_n\psi - \text{bei}_n\psi) - \text{ber}_{n-1}\psi,$$
$$\text{bei}_{n+1}\psi = -\frac{n\sqrt{2}}{\psi}(\text{ber}_n\psi + \text{bei}_n\psi) - \text{bei}_{n-1}\psi; \tag{4.4}$$
$$\text{ber}'_n\psi = -\frac{1}{\sqrt{2}}(\text{ber}_{n-1}\psi + \text{bei}_{n-1}\psi) - \frac{n\,\text{ber}_n\psi}{\psi},$$
$$\text{bei}'_n\psi = \frac{1}{\sqrt{2}}(\text{ber}_{n-1}\psi - \text{bei}_{n-1}\psi) - \frac{n\,\text{bei}_n\psi}{\psi}. \tag{4.5}$$

Similar formulas hold for the Thomson functions of the second kind $\text{ker}_n\psi$, $\text{kel}_n\psi$.

For small values of the argument the asymptotic forms of the Thomson functions are valid

$$\text{ker}\,\psi = -\ln\psi + 0{,}1159 + \frac{\pi\psi^2}{16} + \dots,$$
$$\text{kel}\,\psi = -\left(\frac{\psi^2}{4}\right)\ln\psi - \frac{\pi}{4} + 1{,}1159\frac{\psi^2}{4} + \dots,$$
$$\psi^{-1}\text{ker}'\psi = -\psi^{-2} + \frac{\pi}{8} + \left(\frac{\psi^2}{16}\right)\ln\psi + \dots, \tag{4.6}$$
$$\psi^{-1}\text{kel}'\psi = -\frac{1}{2}\ln\psi - \frac{1}{4} + 0{,}558 + \dots$$

For large values of the argument the following expressions will be the asymptotic representations

$$\begin{matrix}\text{ber}\,\psi \\ \text{bei}\,\psi\end{matrix} = \frac{\exp\alpha(\psi)}{\sqrt{2\pi\psi}}\begin{matrix}\cos \\ \sin\end{matrix}\beta(\psi),$$
$$\begin{matrix}\text{ker}\,\psi \\ \text{kel}\,\psi\end{matrix} = \frac{\exp\alpha(-\psi)}{\sqrt{2\psi/\pi}}\begin{matrix}\cos \\ \sin\end{matrix}\beta(-\psi), \tag{4.7}$$

where

$$\alpha(\psi) \sim \frac{\psi}{\sqrt{2}} + \frac{1}{8\psi\sqrt{2}} - \frac{25}{384\psi^3\sqrt{2}} - \frac{13}{128\psi^4} - \dots,$$
$$\beta(\psi) \sim \frac{\psi}{\sqrt{2}} - \frac{\pi}{8} - \frac{1}{8\psi\sqrt{2}} - \frac{1}{16\psi^2} - \frac{25}{384\psi^3\sqrt{2}} + \dots \tag{4.8}$$

We see from (4.7) that the Thomson functions of the first kind $\text{ber}\,\psi$, $\text{bei}\,\psi$ increase exponentially with increase of the argument, while the functions of the second kind $\text{ker}\,\psi$, $\text{kel}\,\psi$ diminish.

§ 5. Symmetric Deformation of a Spherical Shell
Weakened by a Small Central Opening

Consider a spherical segment with small central opening (Figure 6) subjected to uniform internal pressure p. In this case we take the momentless solution as the particular solution of the problem

$$T_1 = T_2 = p\,\frac{R}{2}. \tag{5.1}$$

We find the general solution of the homogeneous equation (2.3), which for the sphere ($\gamma = 0$, $R_1 = R_2 = R$) takes the form

$$\frac{d\tilde{T}}{d\theta^2} + \mathrm{ctg}\,\theta\,\frac{d\tilde{T}}{d\theta} + i\,\frac{R}{c}\,\tilde{T} = 0. \tag{5.2}$$

With the intention of obtaining a solution which is valid near the small opening, we limit ourselves to the consideration of small angles θ and we set in the equation ctg θ ≈ 1/θ

$$\frac{d\tilde{T}}{d\theta^2} + \frac{1}{\theta}\cdot\frac{d\tilde{T}}{d\theta} + i\,\frac{R}{c}\,\tilde{T} = 0.$$

By the substitution $x = \sqrt{R/c(\theta)}$ this equation is reduced to the Bessel equation (4.1) for n = 0

$$\frac{d\bar{\tilde{T}}}{dx^2} + \frac{1}{x}\cdot\frac{d\bar{\tilde{T}}}{dx} - i\bar{\tilde{T}} = 0, \tag{5.3}$$

where the bar over the complex quantity denotes conjugation.

Its fundamental solution is written in the form of (4.2)

$$\bar{\tilde{T}} = \tilde{C}_1 I_0(x\sqrt{i}) + \tilde{C}_2 K_0(x\sqrt{i}). \tag{5.4}$$

where $I_0(x\sqrt{i})$ is the modified Bessel function of the first kind of zero order; $K_0(x\sqrt{i})$ is the modified Bessel function of the second kind of zero order. We note that for large values of the argument $x = \sqrt{R/c(\theta)}$ (with increasing distance from the edge of the opening) the solution obtained with account for the asymptotic forms of the Bessel functions (4.7) yields the familiar Geckeler approximation.

Considering the behavior of the functions appearing in the solution, and discarding the part of the solution which tends to infinity with increase of the argument, we write the solution in the form
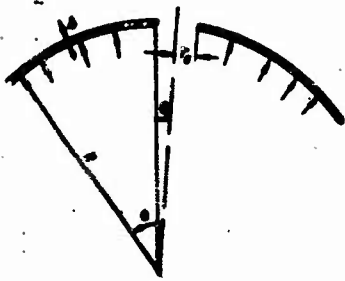
Figure 6.

$$\overline{\overline{T}} = \widetilde{C}_* K_0(x\sqrt{i}) = (A + iB)(\ker x + i \ker x),$$
$$\overline{T} = (A - iB)(\ker x - i \ker x). \tag{5.5}$$

Taking (1.14), (2.4) into account, we obtain the expressions for the meridional and circumferential forces

$$T_1 = T_1' + \sqrt{\frac{c}{R}} \operatorname{ctg}\theta [A \ker' x + B \ker' x],$$
$$T_2 = T_2' + A\left[\ker x - \sqrt{\frac{c}{R}} \operatorname{ctg}\theta \ker' x\right] - \tag{5.6}$$
$$- B\left[\ker x + \sqrt{\frac{c}{R}} \operatorname{ctg}\theta \ker' x\right]$$

and for the meridional and circumferential bending moments

$$M_1 = c\left\{A\left[\ker x + (1-\nu)\sqrt{\frac{c}{R}} \operatorname{ctg}\theta \ker' x\right] + \right.$$
$$+ B\left[\ker x - (1-\nu)\sqrt{\frac{c}{R}} \operatorname{ctg}\theta \ker' x\right]\right\},$$
$$M_2 = c\left\{A\left[\nu \ker x - (1-\nu)\sqrt{\frac{c}{R}} \operatorname{ctg}\theta \ker' x\right] + \right. \tag{5.7}$$
$$+ B\left[\nu \ker x + (1-\nu)\sqrt{\frac{c}{R}} \operatorname{ctg}\theta \ker' x\right]\right\}.$$

The constants of integration are found from the problem boundary conditions. The stresses are determined from the usual formulas (1.8)-(1.10).

We obtain the expressions for the edge compliance (stiffness) coefficients, understanding these to be the angle of rotation and radial displacement of the edge which develop under the influence of unit force and unit moment at the edge. Introducing the notations for the edge values of the Thomson functions

$$\ker x_0 = \varphi_0,$$
$$\ker x_0 = \psi_0 \left(x_0 = \sqrt{\frac{R}{c}}\theta_0\right), \tag{5.8}$$
$$\ker' x_0 = \varphi_0',$$
$$\ker' x_0 = \psi_0'$$

and using (2.5), we write the shearing force Q_0 and bending moment M_0 acting on the edge in the following form

$$Q_0 = Q_1(\theta_0) = Q_0' - \sqrt{\frac{c}{R}} \cdot \frac{1}{\sin\theta_0} [A\psi_0' + B\varphi_0'],$$
$$M_0 = M_1(\theta_0) = c\left\{A\left[\psi_0 + (1+\nu)\sqrt{\frac{c}{R}} \operatorname{ctg}\theta_0\varphi_0'\right] + \right. \tag{5.9}$$
$$+ B\left[\varphi_0 - (1+\nu)\sqrt{\frac{c}{R}} \operatorname{ctg}\theta_0\psi_0'\right]\right\},$$
$$Q_0' = \cos\theta_0 T_1'.$$

Hence the arbitrary constants may be expressed in terms of the shearing force and bending moment given at the edge of the shell

$$A = \sqrt{\frac{R}{c}} \sin \theta_0 \frac{\Phi_0}{\chi_0} (Q_0 - Q_0^*) - \frac{\Psi_0}{\chi_0} \cdot \frac{M_0}{c},$$
$$B = -\sqrt{\frac{R}{c}} \sin \theta_0 \frac{\Psi_0}{\chi_0} (Q_0 - Q_0^*) + \frac{\Phi_0}{\chi_0} \cdot \frac{M_0}{c}, \tag{5.10}$$

where the notations are

$$\Phi_0 = \varphi_0 - (1+\nu) \sqrt{\frac{c}{R}} \operatorname{ctg} \theta_0 \psi_0,$$
$$\Psi_0 = \psi_0 + (1+\nu) \sqrt{\frac{c}{R}} \operatorname{ctg} \theta_0 \varphi_0, \tag{5.11}$$
$$\chi_0 = \Phi_0 \psi_0' - \Psi_0 \varphi_0'.$$

From (2.6), (2.7) we find the edge values of the radial displacement and rotation

$$u_0 = u_\rho(\theta_0) = u_0^* + \frac{R \sin \theta_0}{Eh} [A\Phi_0 - B\Psi_0],$$
$$\vartheta_0 = \vartheta(\theta_0) = -\frac{1}{Eh} \sqrt{\frac{R}{c}} [A\varphi_0' - B\psi_0'] \quad (\vartheta^* = 0). \tag{5.12}$$

Substituting here the values of the arbitrary constants from (5.10), we obtain the final expressions for the edge values of the radial displacement and rotation

$$u_0 = u_0^* + a_{11}(Q_0 - Q_0^*) + a_{12} M_0,$$
$$\vartheta = a_{21}(Q_0 - Q_0^*) + a_{22} M_0, \tag{5.13}$$

where α_{11}, α_{12}, α_{21}, α_{22} denote the edge compliance coefficients

$$a_{11} = \sqrt[4]{12(1-\nu^2)} \left(\frac{R}{h}\right)^{3/2} \sin^2 \theta_0 \frac{\Phi_0^2 + \Psi_0^2}{\chi_0} \cdot \frac{1}{E},$$
$$a_{12} = a_{21} = -\sqrt{12(1-\nu^2)} \frac{R}{h} \sin \theta_0 \frac{\varphi_0 \varphi_0' + \psi_0 \psi_0'}{\chi_0} \cdot \frac{1}{Eh},$$
$$a_{22} = [12(1-\nu^2)]^{3/4} \sqrt{\frac{R}{h}} \cdot \frac{(\varphi_0')^2 + (\psi_0')^2}{\chi_0} \cdot \frac{1}{Eh^3}. \tag{5.14}$$

§ 6. Antisymmetric Deformation of a Spherical Shell with Small Opening in the Center

For the sphere the governing equation of the antisymmetric case (3.6) take the form

$$\frac{d^2 \tilde{T}_{,1}}{d\theta^2} + \frac{\cos \theta}{\sin \theta} \cdot \frac{d\tilde{T}_{,1}}{d\theta} + \left(i \frac{R}{c} - \frac{1}{\sin^2 \theta}\right) \tilde{T}_{,1} = i \frac{R}{c} F(\theta). \tag{6.1}$$

In each particular loading case there is no difficulty in finding the (momentless) problem solution from (3.8), (3.3). Therefore, we

examine the homogeneous equation and, as in the symmetric case, we
make the replacement

$$\cos\theta \approx 1,$$
$$\sin\theta \approx \theta.$$

The equation is then written as

$$\frac{d^2\tilde{T}_{,1}^\theta}{d\theta^2} + \frac{1}{\theta}\cdot\frac{d\tilde{T}_{,1}^\theta}{d\theta} + \left(i\frac{R}{c} - \frac{1}{\theta^2}\right)\tilde{T}_{,1}^\theta = 0.$$

(6.2)

By the substitution

$$x = \sqrt{\frac{R}{c}}\,\theta$$

(6.3)

it is reduced to the Bessel equation of type (4.1) for the value n = 1.
and for the conjugate quantity $\overset{\approx}{T}$, $_1$ it is written as follows

$$\frac{d^2\overline{\tilde{T}}_{,1}}{dx^2} + \frac{1}{x}\cdot\frac{d\overline{\tilde{T}}_{,1}}{dx} - \left(i + \frac{1}{x^2}\right)\overline{\tilde{T}}_{,1} = 0.$$

(6.4)

Using (4.2) its solution will have the form

$$\overline{\tilde{T}}_{,1} = \widetilde{C}_1 I_1(x\sqrt{i}) + \widetilde{C}_2 K_1(x\sqrt{i}),$$

(6.5)

where $I_1(x\sqrt{i})$ is the modified Bessel function of the first kind of
order one; $K_1(x\sqrt{i})$ is the modified Bessel function of the second kind
of order one. Just as in the symmetric case, we set $\tilde{C}_1 \equiv 0$. The
function $K_1(x\sqrt{i})$ is expressed in terms of the Thomson (Kelvin) func-
tions of the second kind as follows (4.3)

$$K_1(x\sqrt{i}) = i(\ker_1 x + i\,\mathrm{kei}_1 x),$$
$$K_1(x\sqrt{i}) = -\,\mathrm{kei}_1 x + i\,\ker_1 x,$$

(6.6)

and between the Thomson functions of first and zero orders we have
the recursion relations (4.4), (4.5)

$$\mathrm{ker}_1\, x = \frac{1}{\sqrt{2}}(\mathrm{ker}'\, x - \mathrm{kei}'\, x),$$

$$\mathrm{kei}_1\, x = \frac{1}{\sqrt{2}}(\mathrm{ker}'\, x + \mathrm{kei}'\, x),$$

$$\mathrm{ker}_1'\, x = -\frac{1}{\sqrt{2}}(\mathrm{ker}\, x + \mathrm{kei}\, x) - \frac{\mathrm{ker}_1\, x}{x},$$

$$\mathrm{kei}_1'\, x = \frac{1}{\sqrt{2}}(\mathrm{ker}\, x - \mathrm{kei}\, x) - \frac{\mathrm{kei}_1\, x}{x}.$$

(6.7)

Short tables of the Thomson functions of the second order with index 1 are presented in [5] for the values of the argument $0 \le x \le 10$.

We finally obtain the following expression for the basic complex function $\widetilde{T}^0{}_{,1}$

$$(\widetilde{C}_2 = A + iB),$$

$$\widetilde{T}_{,1} = -(A - iB)(\mathrm{kei}_1\, x + i\,\mathrm{ker}_1\, x). \tag{6.8}$$

Using (3.7) and (1.14), we find the following expressions for the forces and moments for the antisymmetric case

$$T_{1,1} = T_{1,1}^{\circ} + A\left[\sqrt{\frac{c}{R}}\,\mathrm{ctg}\,\theta\,\mathrm{ker}_1'\, x - \frac{c}{R}\cdot\frac{1}{\sin^2\theta}\,\mathrm{ker}_1\, x\right] - \\ - B\left[\sqrt{\frac{c}{R}}\,\mathrm{ctg}\,\theta\,\mathrm{kei}_1'\, x - \frac{c}{R}\cdot\frac{1}{\sin^2\theta}\,\mathrm{kei}_1\, x\right]. \tag{6.9}$$

$$T_{2,1} = T_{2,1}^{\circ} - A\left[\mathrm{kei}_1\, x + \sqrt{\frac{c}{R}}\,\mathrm{ctg}\,\theta\,\mathrm{ker}_1'\, x - \frac{c}{R}\cdot\frac{1}{\sin^2\theta}\,\mathrm{ker}_1\, x\right] - \\ - B\left[\mathrm{ker}_1\, x - \sqrt{\frac{c}{R}}\,\mathrm{ctg}\,\theta\,\mathrm{kei}_1'\, x + \frac{c}{R}\cdot\frac{1}{\sin^2\theta}\,\mathrm{kei}_1\, x\right];$$

$$M_{1,1} = c\left\{A\left[\mathrm{ker}_1\, x - (1-\nu)\sqrt{\frac{c}{R}}\,\mathrm{ctg}\,\theta\,\mathrm{kei}_1'\, x + \\ + (1-\nu)\frac{c}{R}\cdot\frac{1}{\sin^2\theta}\,\mathrm{kei}_1\, x\right] - B\left[\mathrm{kei}_1\, x + \\ + (1-\nu)\sqrt{\frac{c}{R}}\,\mathrm{ctg}\,\theta\,\mathrm{ker}_1'\, x - (1-\nu)\frac{c}{R}\cdot\frac{1}{\sin^2\theta}\,\mathrm{ker}_1\, x\right]\right\},$$

$$M_{2,1} = -c\left\{A\left[\nu\,\mathrm{ker}_1\, x - (1-\nu)\sqrt{\frac{c}{R}}\,\mathrm{ctg}\,\theta\,\mathrm{kei}_1'\, x + \\ + (1-\nu)\frac{c}{R}\cdot\frac{1}{\sin^2\theta}\,\mathrm{kei}_1\, x\right] - B\left[\nu\,\mathrm{kei}_1\, x + \\ + (1-\nu)\sqrt{\frac{c}{R}}\,\mathrm{ctg}\,\theta\,\mathrm{ker}_1'\, x - (1-\nu)\frac{c}{R}\cdot\frac{1}{\sin^2\theta}\,\mathrm{ker}_1\, x\right]\right\}. \tag{6.10}$$

We write out the values of the edge shearing force and bending moment (3.9)

$$Q_{\rho,1} = Q_{\rho,1}^{\circ} + \sqrt{\frac{c}{R}}\cdot\frac{1}{\sin\theta}\left\{A\left[\mathrm{ker}_1'\, x - \sqrt{\frac{c}{R}}\,\mathrm{ctg}\,\theta\,\mathrm{ker}_1\, x\right] - \\ - B\left[\mathrm{kei}_1'\, x - \sqrt{\frac{c}{R}}\,\mathrm{ctg}\,\theta\,\mathrm{kei}_1\, x\right]\right\},$$

$$M_{1,1} = c\left\{A\left[\mathrm{ker}_1\, x + (1+\nu)\left(\frac{c}{R}\cdot\frac{1}{\sin^2\theta}\,\mathrm{kei}_1\, x - \\ - \sqrt{\frac{c}{R}}\,\mathrm{ctg}\,\theta\,\mathrm{kei}_1'\, x\right)\right] - B\left[\mathrm{kei}_1\, x - (1+\nu)\left(\frac{c}{R}\cdot\frac{1}{\sin^2\theta}\,\mathrm{ker}_1\, x - \\ - \sqrt{\frac{c}{R}}\,\mathrm{ctg}\,\theta\,\mathrm{ker}_1'\, x\right)\right]\right\}. \tag{6.11}$$

If we now, by analogy with the symmetric case, introduce the notations
for the edge values of the Thomson functions of the first order and
their combinations

$$\eta_1 = \ker_1 x_0, \quad \eta_1' = \ker_1' x_0,$$
$$\psi_1 = \kei_1 x_0, \quad \psi_1' = \kei_1' x_0$$
$$\left(x_0 = \sqrt{\frac{R}{c}}\, \theta_0\right); \tag{6.12}$$

$$\Phi_1 = \eta_1 + (1+\nu)\left(\frac{c}{R} \cdot \frac{1}{\sin^2\theta_0}\psi_1 - \sqrt{\frac{c}{R}}\operatorname{ctg}\theta_0\psi_1'\right),$$
$$\Psi_1 = \psi_1 - (1+\nu)\left(\frac{c}{R} \cdot \frac{1}{\sin^2\theta_0}\eta_1 - \sqrt{\frac{c}{R}}\operatorname{ctg}\theta_0\eta_1'\right), \tag{6.13}$$
$$\chi_1 = \Phi_1\left(\psi_1' - \sqrt{\frac{c}{R}}\operatorname{ctg}\theta_0\psi_1\right) - \Psi_1\left(\eta_1' - \sqrt{\frac{c}{R}}\operatorname{ctg}\theta_0\eta_1\right).$$

after solving (6.11) for the arbitrary constants, we obtain for the
latter expressions in terms of the shearing force $Q_0 = Q_{\rho,\,1}(\theta_0)$ and
bending moment $M_0 = M_{1,\,1}(\theta_0)$, given at the edge

$$A = -\sqrt{\frac{R}{c}}\sin\theta_0\frac{\Psi_1}{\chi_1}(Q_0 - Q_0') + \frac{\psi_1' - \sqrt{\frac{c}{R}}\operatorname{ctg}\theta_0\psi_1}{\chi_1} \cdot \frac{M_0}{c};$$
$$B = -\sqrt{\frac{R}{c}}\sin\theta_0\frac{\Phi_1}{\chi_1}(Q_0 - Q_0') + \frac{\eta_1' - \sqrt{\frac{c}{R}}\operatorname{ctg}\theta_0\eta_1}{\chi_1} \cdot \frac{M_0}{c}. \tag{6.14}$$

Using (3.10), we obtain for the elastic rotation and relative elonga-
tion of the edge

$$\eta_1 = \eta^* - \frac{r}{Eh}\left\{A\left[\kei_1 x + (1+\nu)\sqrt{\frac{c}{R}}\operatorname{ctg}\theta\ker_1' x - (1+\nu)\frac{c}{R} \cdot \frac{1}{\sin^2\theta}\ker_1 x\right] + B\left[\ker_1 x - (1+\nu)\sqrt{\frac{c}{R}}\operatorname{ctg}\theta\kei_1' x + (1+\nu)\frac{c}{R} \cdot \frac{1}{\sin^2\theta}\kei_1 x\right]\right\},$$
$$\chi = \frac{1}{Eh}\sqrt{\frac{R}{c}}\left\{A\left[\kei_1' x - \sqrt{\frac{c}{R}}\operatorname{ctg}\theta\kei_1 x\right] + B\left[\ker_1' x - \sqrt{\frac{c}{R}}\operatorname{ctg}\theta\ker_1 x\right]\right\}, \tag{6.15}$$

where

$$\eta^* = \frac{r}{Eh}(T_{2,1}^\circ - \nu T_{1,1}^\circ),$$
$$\chi^* = 0, \quad r = R\sin\theta.$$

Denoting

$$\vartheta_0 = \chi(\theta_0),$$
$$u_0 = (\eta)_0, \tag{6.16}$$
$$u_0^\circ = (\eta^*)_0,$$

using the previously introduced notations (6.12), (6.13) and substitut-
ing into (6.15) the values of the arbitrary constants, we obtain the
following form of the desired expressions

$$u_0 = u_0^\circ + a_{11}^1(Q_0 - Q_0') + u_{12}^1 M_0,$$
$$\vartheta_0 = a_{21}^1(Q_0 - Q_0') + a_{22}^1 M_0. \tag{6.17}$$

Here, as before, α_{11}, α_{12}, α_{21}, α_{22} are the shell edge compliance coefficients, and in the present case they have the form

$$
\begin{aligned}
\alpha_{11}^1 &= \sqrt[4]{12(1-\nu^2)}\left(\frac{R}{h}\right)^{3/2}\sin^2\theta_0\,\frac{\sigma_1^2+\tau_1^2}{\chi_1}\cdot\frac{1}{E}, \\
\alpha_{12}^1 &= \alpha_{21}^1 = -\sqrt{12(1-\nu^2)}\,\frac{R}{h}\sin\theta_0\,\frac{\chi_2}{\chi_1}\cdot\frac{1}{Eh}, \\
\alpha_{22}^2 &= [12(1-\nu^2)]^{3/4}\left(\frac{R}{h}\right)^{1/2}\frac{\chi_2}{\chi_1}\cdot\frac{1}{Eh^2}.
\end{aligned}
\tag{6.18}
$$

In addition to the notations used previously (6.12), (6.13), here we have used the two additional notations

$$
\begin{aligned}
\chi_1 &= \sigma_1\left(\tau_1' - \sqrt{\frac{c}{R}}\,\mathrm{ctg}\,\theta_0\tau_1\right) + \tau_1\left(\sigma_1' - \sqrt{\frac{c}{R}}\,\mathrm{ctg}\,\theta_0\sigma_1\right), \\
\chi_2 &= \left(\tau_1' - \sqrt{\frac{c}{R}}\,\mathrm{ctg}\,\theta_0\tau_1\right)^2 + \left(\sigma_1' - \sqrt{\frac{c}{R}}\,\mathrm{ctg}\,\theta_0\sigma_1\right)^2.
\end{aligned}
\tag{6.19}
$$

The derived relations (5.13) and (6.17) are essentially deformation boundary conditions of a special form. Their use facilitates the solution, particularly of problems of the mating of shells.

§ 7. Calculation of Symmetric Loading of an Ellipsoid of Revolution

The principal radii of curvature for an ellipsoid of revolution are

$$
\begin{aligned}
R_1 &= \frac{a^2}{b(1+\gamma\sin^2\theta)^{3/2}}, \\
R_2 &= \frac{a^2}{b(1+\gamma\sin^2\theta)^{1/2}},
\end{aligned}
\tag{7.1}
$$

where a, b are the ellipse semimajor and semiminor axes, respectively, and

$$
\gamma = \frac{a^2}{b^2} - 1.
\tag{7.2}
$$

Fundamental resolvent (2.3) takes the form

$$
\frac{d^2\widetilde{T}}{d\theta^2} + \frac{1+2\gamma\sin^2\theta}{1+\gamma\sin^2\theta}\cdot\frac{\cos\theta}{\sin\theta}\cdot\frac{d\widetilde{T}}{d\theta} + i\,\frac{a^2}{cb(1+\gamma\sin^2\theta)^{3/2}}\,\widetilde{T} =
$$
$$
= i\,\frac{a^2}{cb(1+\gamma\sin^2\theta)^{3/2}}\,F(\theta).
$$

We take as the particular solution the momentless solution, which for a uniform internal pressure p acting on the ellipsoid has the form

$$
\begin{aligned}
T_1^\circ &= \frac{pa^2}{2b}\cdot\frac{1}{(1+\gamma\sin^2\theta)^{1/2}}, \\
T_2^\circ &= \frac{pa^2}{2b}\cdot\frac{1-\gamma\sin^2\theta}{(1+\gamma\sin^2\theta)^{1/2}}.
\end{aligned}
\tag{7.3}
$$

We find the general solution of the homogeneous equation

$$\frac{d^2\widetilde{T}}{d\theta^2} + \frac{1+2\gamma\sin^2\theta}{1+\gamma\sin^2\theta}\cdot\frac{\cos\theta}{\sin\theta}\cdot\frac{d\widetilde{T}}{d\theta} + i\frac{a^2}{c\theta(1+\gamma\sin^2\theta)^{5/2}}\widetilde{T}=0,$$

or for the conjugate

$$\frac{d^2\overline{\widetilde{T}}}{d\theta^2} + \frac{1+2\gamma\sin^2\theta}{1+\gamma\sin^2\theta}\cdot\frac{\cos\theta}{\sin\theta}\cdot\frac{d\overline{\widetilde{T}}}{d\theta} - i\frac{a^2}{c\theta(1+\gamma\sin^2\theta)^{5/2}}\overline{\widetilde{T}}=0. \qquad (7.4)$$

We seek the solution by the reference equation method, for which we take the Bessel equation (see § 4) of zero order

$$\frac{d^2y}{d\xi^2} + \frac{1}{\xi}\cdot\frac{dy}{d\xi} - iy=0. \qquad (7.5)$$

We write initial equation (7.4) as follows

$$\frac{d^2z}{d\theta^2} + p(\theta)\frac{dz}{d\theta} - \lambda^2 q(\theta)z=0, \qquad (7.6)$$

where we have set

$$\begin{aligned}
z(\theta) &= \overline{\widetilde{T}}(\theta), \\
\lambda^2 &= \frac{a^2}{bc}, \\
p(\theta) &= \frac{1+2\gamma\sin^2\theta}{1+\gamma\sin^2\theta}\cdot\frac{\cos\theta}{\sin\theta} = \frac{d}{d\theta}\{\ln[(1+\gamma\sin^2\theta)^{1/2}\sin\theta]\}, \\
q(\theta) &= \frac{1}{(1+\gamma\sin^2\theta)^{5/2}}.
\end{aligned} \qquad (7.7)$$

We seek the general solution of (7.6) in the form

$$z = \eta(\theta)\, y\,[\xi(\theta)]. \qquad (7.8)$$

Hence

$$\begin{aligned}
\frac{dz}{d\theta} &= (\eta\xi')\,y' + \eta'y, \\
\frac{d^2z}{d\theta^2} &= (\eta\xi'^2)\,y'' + (2\eta'\xi' + \eta\xi'')\,y' + \eta''y.
\end{aligned} \qquad (7.9)$$

Assuming that $y(\xi)$ is the solution of reference equation (7.5), replacing y'' and substituting (7.8), (7.9) into (7.6), we obtain

$$\begin{aligned}
&\left\{-\eta\frac{\xi'^2}{\xi} + \eta\xi'' + 2\eta'\xi' + p(\theta)\,\eta\xi'\right\}y' + \\
&+ \{\eta'' + p(\theta)\eta' + i\eta\xi'^2 - \lambda^2 q(\theta)\eta\}\,y = 0.
\end{aligned} \qquad (7.10)$$

Equating the first bracket to zero

$$\frac{\xi''}{\xi'} + 2\frac{\eta'}{\eta} - \frac{\xi'}{\xi} + p(\theta) = 0 \qquad (7.11)$$

and integrating with account for (7.7), we obtain

$$\eta(\theta) = C\sqrt{\frac{\xi}{\xi'(1+\gamma\sin^2\theta)^{1/2}\sin\theta}}. \qquad (7.12)$$

Now we equate the second bracket to zero

$$\frac{\zeta''}{\eta} + \rho(\theta)\frac{\zeta'}{\eta} + \xi'^2 - \lambda^2 q(\theta) = 0 \tag{7.13}$$

and replace here with account for (7.11)

$$\frac{\eta''}{\eta} + \rho(\theta)\frac{\eta'}{\eta} = -\frac{1}{2}\cdot\frac{\zeta''}{\zeta'} + \frac{3}{4}\left(\frac{\zeta''}{\zeta'}\right)^2 - \frac{1}{4}\left(\frac{\zeta'}{\zeta}\right)^2 - \frac{1}{2}\rho'(\theta) - \frac{1}{4}\rho^2(\theta).$$

Equation (7.13) may be satisfied by setting

$$\xi'^2 = \lambda^2 q(\theta),$$
$$\xi(\theta) = \lambda\int_0^\theta \frac{d\theta}{(1+\gamma\sin^2\theta)^{1/4}}. \tag{7.14}$$

Since we are considering the shell edge near a small opening at the apex, we can limit ourselves to examination of small angles θ, taking (in the first approximation)

$$\sin\theta \approx \theta,$$
$$\xi(\theta) \approx \lambda\theta,$$
$$\rho(\theta) \approx \frac{1}{\theta},$$
$$\rho'(\theta) \approx -\frac{1}{\theta^2}.$$

It is obvious that (7.13) is immediately satisfied.

We take

$$\xi(\theta) = \lambda\theta,$$
$$\eta(\theta) = \sqrt{\frac{\theta}{(1+\gamma\sin^2\theta)^{1/2}\sin\theta}}. \tag{7.15}$$

Now, with account for (4.2) the general solution of the homogeneous equation may be written

$$z = \eta(\theta)\left\{\widetilde{C}_1 I_0(\lambda\theta\sqrt{i}) + \widetilde{C}_2 K_0(\lambda\theta\sqrt{i})\right\}. \tag{7.16}$$

We drop the part of the solution which grows with increase of the argument and convert to the unknown function $\widetilde{T}^0$, writing the solution in terms of Thomson functions (4.3)

$$\widetilde{T}^0 = \eta(\theta)\left\{(A - iB)(\ker\lambda\theta - i\ker\lambda\theta)\right\}. \tag{7.17}$$

The function $\eta(\theta)$ changes slowly and for small angles is close to one (Figure 7). We neglect the variability of this function in comparison with the variability of the Thomson functions and thereby obtain a simplified formula for $d\widetilde{T}^0/d\theta$

$$\frac{d\tilde{T}_0}{ds} = \lambda \eta(\theta) \{(A - \iota B)(\text{ker}'\lambda\theta - \iota \text{ kei}'\lambda\theta)\}.$$

With the aid of (1.14) and (2.4) we obtain, the expression for the forces and moments

$$T_1 = T_1^\circ + \lambda^{-1}\eta(\theta)\,\text{ctg}\,\theta(1 + \gamma\sin^2\theta)^{3/2}\,[A\,\text{ker}'\lambda\theta + B\,\text{kei}'\lambda\theta],$$

$$T_2 = T_2^\circ + \eta(\theta)\{A\,[\text{ker}\,\lambda\theta - \lambda^{-1}\text{ctg}\,\theta(1+\gamma\sin^2\theta)^{3/2}\,\text{kei}'\lambda\theta] - B\,[\text{kei}\,\lambda\theta + \lambda^{-1}\text{ctg}\,\theta(1+\gamma\sin^2\theta)^{3/2}\,\text{ker}'\lambda\theta]\};$$ (7.18)

$$M_1 = c\eta(\theta)\{A\,[\text{kei}\,\lambda\theta + (1-\nu)\lambda^{-1}\text{ctg}\,\theta(1+\gamma\sin^2\theta)^{3/2}\,\text{ker}'\lambda\theta] + B\,[\text{ker}\,\lambda\theta - (1-\nu)\lambda^{-1}\text{ctg}\,\theta(1+\gamma\sin^2\theta)^{3/2}\,\text{kei}'\lambda\theta]\},$$

$$M_2 = c\eta(\theta)\{A\,[\nu\,\text{kei}\,\lambda\theta - (1-\nu)\lambda^{-1}\text{ctg}\,\theta(1+\gamma\sin^2\theta)^{3/2}\,\text{ker}'\lambda\theta] + B\,[\nu\,\text{ker}\,\lambda\theta + (1-\nu)\lambda^{-1}\text{ctg}\,\theta(1+\gamma\sin^2\theta)^{3/2}\,\text{kei}'\lambda\theta]\}.$$ (7.19)

The constants of integration are found from the boundary conditions.

The edge compliance coefficients for the ellipsoid may be obtained just as was done for the sphere. Without repeating the previous arguments, we present the final results. The arbitrary constants are

$$A = \frac{\lambda\sin\theta_0}{\eta(\theta_0)(1+\gamma\sin^2\theta_0)^{3/2}}\cdot\frac{\phi_0}{T_0}(Q_0 - Q_0^\circ) - \frac{M_0}{c_1(\theta_0)}\cdot\frac{\dot{\phi}_0}{T_0},$$

$$B = -\frac{\lambda\sin\theta_0}{\eta(\theta_0)(1+\gamma\sin^2\theta_0)^{3/2}}\cdot\frac{\phi_0}{T_0}(Q_0 - Q_0^\circ) + \frac{M_0}{c_1(\theta_0)}\cdot\frac{\dot{\phi}_0}{T_0}$$ (7.20)

We obtain for the edge horizontal displacement and angle of rotation

$$u_0 = u_0^\circ + a_{11}^\circ(Q_0 - Q_0^\circ) + a_{12}^\circ M_0,$$

$$\theta_0 = a_{21}^\circ(Q_0 - Q_0^\circ) + a_{22}^\circ M_0.$$ (7.21)

where the compliance coefficients have the form

$$a_{11}^\circ = \sqrt[4]{12(1-\nu^2)}\left(\frac{a^2}{bh}\right)^{3/2}\frac{\sin^2\theta_0}{(1+\gamma\sin^2\theta_0)^2}\cdot\frac{\phi_0^2+\phi_0^2}{T_0}\cdot\frac{1}{E},$$

$$a_{12}^\circ = a_{21}^\circ = -\sqrt{12(1-\nu^2)}\left(\frac{a^2}{bh}\right)\frac{\sin\theta_0}{(1+\gamma\sin^2\theta_0)^{1/2}}\cdot\frac{\phi_0\dot{\phi}_0+\phi_0\dot{\phi}_0}{T_0}\cdot\frac{1}{Eh},$$ (7.22)

$$a_{22}^\circ = [12(1-\nu^2)]^{3/4}\left(\frac{a^2}{bh}\right)^{1/2}(1+\gamma\sin^2\theta_0)\frac{\dot{\phi}_0^2+\dot{\phi}_0^2}{T_0}\cdot\frac{1}{Eh^2}.$$

We note that here, as before,

$$\phi_0 = \text{ker}\,\lambda\theta_0, \qquad \dot{\phi}_0 = \text{ker}'\lambda\theta_0,$$

$$\psi_0 = \text{kei}\,\lambda\theta_0, \qquad \dot{\psi}_0 = \text{kei}'\lambda\theta_0,$$

$$\lambda = \sqrt[4]{12(1-\nu^2)}\sqrt{\frac{a^2}{bh}},$$

$$\gamma = \frac{a^2}{b^2} - 1.$$ (7.23)
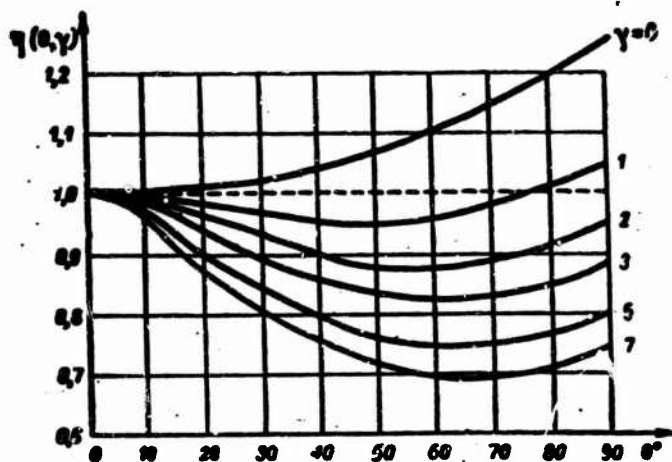
. Figure 7.

Moreover, we have introduced the notations

$$d_0 = \varphi_0 - (1 + \nu)\lambda^{-1}\,\text{ctg}\,\theta_0(1 + \tau\sin^2\theta_0)^{3/2}\psi_0',$$
$$e_0 = \psi_0 + (1 + \nu)\lambda^{-1}\,\text{ctg}\,\theta_0(1 + \tau\sin^2\theta_0)^{3/2}\varphi_0,$$
$$\Gamma_0 = d_0\psi_0' - e_0\varphi_0',$$

(7.24)

and also

$$x_0^* = \frac{r_0}{Eh}(T_2^* - \nu T_1^*),$$
$$Q_0^* = \cos\theta_0 T_1^*.$$

(7.25)

The case of antisymmetric loading is analyzed similarly.

§ 8. Calculation Examples

As examples we shall consider spherical and elliptical end closures with small central opening, subjected to uniform internal pressure.

Example 1. For the spherical segment (see Figure 6) with a small central opening at the apex we take two versions of the boundary conditions at the edge of the opening:

a) the opening edge is rigidly clamped so that the radial displacement and angle of rotation are zero

$$u_r = 0,$$
$$\vartheta = 0 \text{ for } \theta = \theta_0;$$

(8.1)

b) the opening edge is free of forces and moments

$$M_1 = 0,$$
$$T_1 = 0 \text{ for } \theta = \theta. \tag{8.2}$$

Using the relations of § 5, for the first boundary condition version we obtain the following expressions for the stresses on the opening contour

$$\sigma_{T_1} = \frac{pR}{2h}\left[1 - (1-\nu)\sqrt{\frac{c}{R}}\operatorname{ctg}\theta_0 \frac{\varphi_0'^2 + \psi_0'^2}{\chi_0}\right],$$

$$\sigma_{T_2} = \nu\sigma_{T_1},$$

$$\sigma_{M_1} = -\frac{3(1-\nu)}{\sqrt{3(1-\nu^2)}}\cdot\frac{pR}{2h}\left[\frac{\varphi_0\varphi_0' + \psi_0\psi_0'}{\chi_0}\right]. \tag{8.3}$$

On the freely-supported opening contour we have

$$\sigma_{T_2} = \frac{pR}{2h}\left[2 - \sqrt{\frac{R}{c}}\operatorname{tg}\theta_0 \frac{\varphi_0\varphi_0' + \psi_0\psi_0'}{\chi_0}\right]. \tag{8.4}$$

Here the previous notations of (5.8) and (5.11) are used everywhere.

The expressions in the square brackets in (8.3) and (8.4), characterizing the stress increase in the sphere in comparison with the momentless case

$$\sigma_{T_1}^0 = \sigma_{T_2}^0 = \frac{pR}{2h},$$

were calculated for different values of the wall curvature-thickness ratios and different angles of the opening edge in the sphere. Their values are shown in the table, where the notations are

$$l_1 = \left[2 - \sqrt{\frac{R}{c}}\operatorname{tg}\theta_0 \frac{\varphi_0\Phi_0 + \psi_0\Psi_0}{\chi_0}\right],$$

$$l_2 = \left[1 - (1-\nu)\sqrt{\frac{c}{R}}\operatorname{ctg}\theta_0 \frac{\varphi_0'^2 + \psi_0'^2}{\chi_0}\right],$$

$$l_3 = -\frac{3(1-\nu)}{\sqrt{3(1-\nu^2)}}\cdot\frac{\varphi_0\varphi_0' + \psi_0\psi_0'}{\chi_0}. \tag{8.5}$$

Example 2. We consider the symmetric deformation of an elliptical end closure with small central opening which is reinforced by an elastic ring.

We assume that the ring is symmetric about the horizontal plane and that its linear dimensions are small in comparison with the radius r_k (distance from the ring center of gravity to the axis of revolution).

R/a	φ	I_1	I_2	I_3	R/a	φ	I_1	I_2	I_3
20	5	2.35	1.45	−0.337	200	5	4.12	1.28	−0.776
	10	3.10	1.36	−0.602		10	7.22	1.17	−0.990
	15	4.02	1.29	−0.764		15	10.50	1.12	−1.079
	30	7.62	1.17	−1.005		30	21.70	1.06	−1.180
	45	12.20	1.11	−1.120		45	37.00	1.04	−1.2.0
	60	20.56	1.07	−1.200		60	63.60	1.02	−1.250
80	5	2.75	1.39	−0.806	500	5	5.88	1.21	−0.925
	10	4.14	1.28	−0.775		10	10.90	1.12	−1.065
	15	5.72	1.21	−0.917		15	16.10	1.08	−1.150
	30	11.24	1.12	−1.097		30	33.90	1.04	−1.210
	45	18.87	1.07	−1.180		45	58.20	1.02	−1.240
	60	32.14	1.04	−1.230		60	100.20	1.01	−1.260
100	5	3.29	1.34	−0.644					
	10	5.40	1.22	−0.895					
	15	7.88	1.16	−1.008					
	30	15.57	1.08	−1.150					
	45	26.40	1.05	−1.200					
	60	46.20	1.03	−1.240					
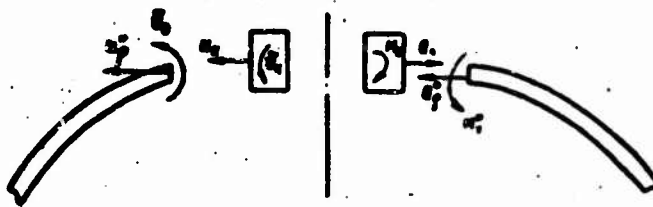
Figure 8.

The displacement in the radial direction and the rotation angle about the ring center of gravity are

$$u_k = \frac{r_k^2}{E_k \Omega_k} Q_k,$$
$$\vartheta_k = \frac{r_k^2}{E_k I_k} M_k,$$

(8.6)

where E_k is the ring elastic modulus, Ω_k is the ring section area, I_k is the ring section moment of inertia about the horizontal axis passing through its center of gravity, Q_k is the spreading force in the ring, and M_k is the torsional moment.

The conditions of the elastic coupling of the ring with the shell have the form (Figure 8)

$$u_k = u_0, \quad M_k = M_0,$$
$$\vartheta_k = \vartheta_0, \quad Q_k = Q_0.$$

(8.7)

With the aid of (7.21) and (8.6) these conditions may be rewritten as

$$\frac{r_s^2}{E_s Q_s} Q_0 = \kappa_0^s + a_{11}^s (Q_0 - Q_0^s) + a_{12}^s M_0,$$

$$\frac{r_s^2}{E_s J_s} M_0 = a_{21}^s (Q_0 - Q_0^s) + a_{22}^s M_0$$

and solved for the unknown edge force and moment

$$Q_0 = \frac{1}{\Delta}\left[(a_{12}^s)^2 Q_0^s - \left(a_{22}^s - \frac{r_s^2}{E_s J_s}\right)(a_{11}^s Q_0^s - \kappa_0^s)\right],$$

$$M_0 = \frac{a_{12}^s}{\Delta}\left(\frac{r_s^2}{E_s Q_s} Q_0^s - \kappa_0^s\right). \tag{8.8}$$

where

$$\Delta = (a_{12}^s)^2 - \left(a_{11}^s - \frac{r_s^2}{E_s Q_s}\right)\left(a_{22}^s - \frac{r_s^2}{E_s J_s}\right). \tag{8.9}$$

On the right in (8.8) are known quantities which depend on the geometry of the shell and ring, and also on the momentless problem solution, which may be considered known. Then (8.8) and (7.20) yield the values of the arbitrary constants for our problem.

§ 9. Refinement of the Theory

By means of the substitution $z = \tilde{T}\sqrt{\sin\theta}$ the resolvent (5.2) for the symmetrically loaded spherical shell

$$\frac{d^2\tilde{T}}{d\theta^2} + \operatorname{ctg}\theta \frac{d\tilde{T}}{d\theta} + i\frac{R}{c}\tilde{T} = 0$$

is reduced to the form

$$\frac{d^2 z}{d\theta^2} + \left[\frac{1}{4}\left(\frac{1}{\sin^2\theta} - \frac{1}{\theta^2}\right) + \frac{1}{4} + \frac{1}{4\theta^2} + i\frac{R}{c}\right]z = 0. \tag{9.1}$$

The underlined small terms (values of the function $f(\theta) = \frac{1}{4}\left(\frac{1}{\sin^2\theta} - \frac{1}{\theta^2}\right) + \frac{1}{4}$ are shown in Figure 9) may be neglected in comparison with the other terms. We obtain the following form of the Bessel equation

$$\frac{d^2 z}{d\theta^2} + \left[\frac{1}{4\theta^2} + i\frac{R}{c}\right]z = 0. \tag{9.2}$$

The solution of this equation is a cylinder function of zero order

$$z = \sqrt{\theta}\, G_0\left(\sqrt{i\frac{R}{c}}\,\theta\right).$$

which may be written in terms of Bessel functions of the first and second kind or in terms of their modifications. Dropping the part of the solution which tends to infinity with increase of the argument and writing the Bessel function which appears in the solution in terms of Thomson functions of the second kind, as was done in § 5,

$$K_0(x\sqrt{-i}) = \ker x - i \operatorname{kei} x,$$
$$x = \sqrt{\frac{R}{c}}\,\theta,$$

we obtain the following expression for the basic complex function

$$\widetilde{T} = \sqrt{\frac{\theta}{\sin\theta}}\,\widetilde{C_1}K_0(x\sqrt{-i}) =$$
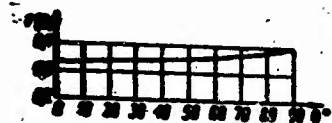$$\sqrt{\frac{\theta}{\sin\theta}}(A_1 + iB_1)(\ker x - i\operatorname{kei} x). \tag{9.3}$$

Fig. 9.

We obtained (9.2) from the original equation by neglecting quantities of order c/R in comparison with one. This permits considering the resulting solution as "exact," i.e., its error is a quantity of order h/R.

Denoting

$$F(\theta) = \frac{d}{d\theta}\left(\sqrt{\frac{\theta}{\sin\theta}}\right). \tag{9.4}$$

we obtain the expressions for the shell forces and moments

$$T_1 = T_1' + \frac{c}{R}\operatorname{ctg}\theta\left\{A_1\left[F(\theta)\operatorname{kei} x + \sqrt{\frac{\theta}{\sin\theta}}\sqrt{\frac{R}{c}}\operatorname{kei}'x\right] - B_1\left[F(\theta)\ker x + \sqrt{\frac{\theta}{\sin\theta}}\sqrt{\frac{R}{c}}\ker'x\right]\right\}, \tag{9.5}$$
$$T_2 = T_2' + A_1\left[\sqrt{\frac{\theta}{\sin\theta}}\ker x - \frac{c}{R}\operatorname{ctg}\theta F(\theta)\operatorname{kei} x - \sqrt{\frac{\theta}{\sin\theta}}\sqrt{\frac{c}{R}}\operatorname{ctg}\theta\operatorname{kei}'x\right] + B_1\left[\sqrt{\frac{\theta}{\sin\theta}}\operatorname{kei} x + \frac{c}{R}\operatorname{ctg}\theta F(\theta)\ker x + \sqrt{\frac{\theta}{\sin\theta}}\sqrt{\frac{c}{R}}\operatorname{ctg}\theta\ker'x\right],$$
$$M_1 = c\left\{A_1\left[\sqrt{\frac{\theta}{\sin\theta}}\operatorname{kei} x + (1-\nu)\left(\frac{c}{R}\operatorname{ctg}\theta F(\theta)\ker x + \sqrt{\frac{\theta}{\sin\theta}}\sqrt{\frac{c}{R}}\operatorname{ctg}\theta\ker'x\right)\right] - B_1\left[\sqrt{\frac{\theta}{\sin\theta}}\ker x - (1-\nu)\left(\frac{c}{R}\operatorname{ctg}\theta F(\theta)\operatorname{kei} x + \sqrt{\frac{\theta}{\sin\theta}}\sqrt{\frac{c}{R}}\operatorname{ctg}\theta\operatorname{kei}'x\right)\right]\right\}, \tag{9.6}$$

$$M_1 = c \left\{ A_1 \left[\nu \sqrt{\frac{\theta}{\sin\theta}} \, \text{kei}\, x - (1-\nu) \left(\frac{c}{R} \text{ctg}\,\theta F(\theta) \, \text{ker}\, x + \right. \right. \right.$$
$$\left. + \sqrt{\frac{\theta}{\sin\theta}} \sqrt{\frac{c}{R}} \text{ctg}\,\theta\, \text{ker}'x \right) \Big] - B_1 \left[\nu \sqrt{\frac{\theta}{\sin\theta}} \, \text{ker}\, x + \right.$$
$$\left. \left. + (1-\nu) \left(\frac{c}{R} \text{ctg}\,\theta F(\theta) \, \text{kei}\, x + \sqrt{\frac{\theta}{\sin\theta}} \sqrt{\frac{c}{R}} \text{ctg}\,\theta\, \text{kei}'x \right) \right] \right\}.$$

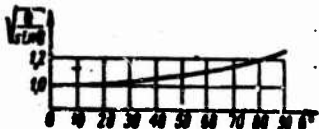The values of the functions $\sqrt{\theta/\sin\theta}$ and $F(\theta)$ are taken from Figures 10 and 11.
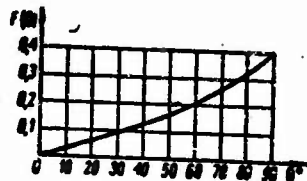
Figure 10.   Figure 11.

We have for the edge shearing force

$$Q_\varphi = A_1 \left[\frac{c}{R} \cdot \frac{1}{\sin\theta} F(\theta) \, \text{kei}\, x + \sqrt{\frac{\theta}{\sin\theta}} \sqrt{\frac{c}{R}} \cdot \frac{1}{\sin\theta} \, \text{kei}'x \right] -$$
$$- B_1 \left[\frac{c}{R} \cdot \frac{1}{\sin\theta} F(\theta) \, \text{ker}\, x + \sqrt{\frac{\theta}{\sin\theta}} \sqrt{\frac{c}{R}} \cdot \frac{1}{\sin\theta} \, \text{ker}'x \right]. \qquad (9.7)$$

Using the same notations for the values of the Thomson functions (5.8) at the edge and using arguments similar to the preceding, we find the relations between the edge values of the radial displacement and rotation angle and the values of the shearing force and bending moment at the edge

$$u_0 = u_0^* + A_{11}(Q_0 - Q_0^*) + A_{12}M_0,$$
$$\theta_0 = A_{21}(Q_0 - Q_0^*) + A_{22}M_0. \qquad (9.8)$$

In this case the edge compliance coefficients are

$$A_{11} = \sqrt{12(1-\nu^2)} \left(\frac{R}{h}\right)^2 \sin^2\theta_0 \, \frac{W_1^2 + W_2^2}{W_0} \cdot \frac{1}{E},$$
$$A_{12} = A_{21} = -\sqrt{12(1-\nu^2)} \, \frac{R}{h} \sqrt{\theta_0 \sin\theta_0} \, \frac{\alpha_0 \alpha_0 + \psi_0 \theta_0}{W_0} \cdot \frac{1}{Eh}, \qquad (9.9)$$
$$A_{22} = \sqrt{12(1-\nu^2)} \, \frac{\alpha_0^2 + \beta_0^2}{W_0} \cdot \frac{1}{Eh^2},$$

where we have the additional notation

$$\alpha_0 = F(\theta_0)\varphi_0 + \sqrt{\frac{R}{c}} \sqrt{\frac{\theta_0}{\sin\theta_0}} \varphi_0',$$
$$\beta_0 = F(\theta_0)\psi_0 + \sqrt{\frac{R}{c}} \sqrt{\frac{\theta_0}{\sin\theta_0}} \psi_0'; \qquad (9.10)$$

$$W_1 = \sqrt{\frac{\theta_0}{\sin\theta_0}} \psi_0 + (1+\nu)\frac{c}{R}\text{ctg}\,\theta_0 \alpha_0,$$
$$W_2 = \sqrt{\frac{\theta_0}{\sin\theta_0}} \varphi_0 - (1+\nu)\frac{c}{R}\text{ctg}\,\theta_0 \beta_0,$$
$$W_0 = \beta_0 W_2 - \alpha_0 W_1. \qquad (9.11)$$

In order to evaluate the accuracy of the solutions, we calculated the compliance coefficients corresponding to three methods: 1) the conventional Geckeler method [2, page 123], 2) the Bessel asymptotic solution treatment (using the relations of § 5, which for brevity we term the Bessel solution), and 3) the modified solution presented in the present section. The latter is more exact and is used as the comparison standard. The angle θ_0, characterizing the size of the central opening in the sphere, was assigned various values from 5 to 90°. In addition, several values of the curvature-thickness ratio were used $h/R = 1/20$, $1/50$, $1/100$, $1/200$, $1/500$.
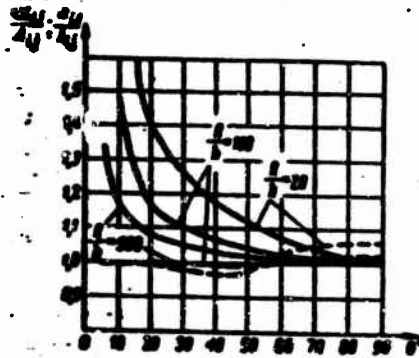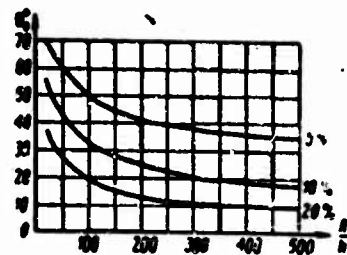
Figure 12.   Figure 13.

The compliance coefficients corresponding to the Bessel solution (Formulas (5.14)) were close to the modified values obtained using (9.9). The difference did not exceed 5% for any values of the parameters.

As an example Figure 12 shows the values of the ratios α_{1j}/A_{1j} (solid curves) and a_{1j}/A_{1j} (dashed) for three values of the curvature-thickness ratio R/h = 20, 100 and 500, where α_{1j} are the compliance coefficients corresponding to the Geckeler solution, a_{1j} are for the Bessel solution, and A_{1j} are the modified solution. The Geckeler asymptotic solution gives good agreement for the compliance coefficients with the modified solution for thin spherical shells and for angles θ_0 greater than 30°. The worst of the ratios α_{1j}/A_{1j} was used to plot the curves of Figure 13, which make it possible to evaluate the applicability of the considerably simpler Geckeler asymptotic solution as a function of the shell parameters. Here the curves correspond to 5, 10 and 20% error of the Geckeler solution in comparison with the modified solution. Selecting a shell curvature-thickness

ratio and the desired accuracy, we can use the figure to obtain the value of the angle θ_0 for which the Bessel solution may be replaced by the Geckeler solution.

This analysis permits us to conclude that:

1) The proposed version of the Bessel solution is valid for all "hemispheres" to within shell theory accuracy. Therefore, its further refinement is not worthwhile.

2) For θ_0 exceeding some limiting value which is characteristic for each curvature-thickness ratio (Figure 13), the simpler Geckeler solution may be used.

§ 10. Literature Survey

The following survey (laying no claim to completeness) includes primarily studies of the stress state in shells of revolution with a small central opening. The closely related studies of the effect of a concentrated force or of a load distributed over the area of a small circle with center at the pole of a shallow shell are not covered in this survey.

The symmetric deformation of a spherical shell weakened by a circular cutout was studied by Shevlyakov [7]. Using the Vlasov shallow shell equilibrium equations [8], he reduced the solution to the single equation

$$LL\sigma - iL\sigma = 0,$$

(10.1)

where

$$L = \frac{d^2}{d\alpha^2} + \frac{1}{\alpha} \cdot \frac{d}{d\alpha},$$

α is a dimensionless parameter

$$r = k\alpha, \quad k = \sqrt[4]{\frac{R^2 h^2}{12(1-\nu^2)}}.$$

The solution was obtained in the form $\sigma = \sigma_1 + \sigma_2$, where σ_1 and σ_2 are solutions of the equations

$$\frac{d^2 \sigma_1}{dz^2} + \frac{1}{z} \cdot \frac{d\sigma_1}{dz} = 0,$$
$$\frac{d^2 \sigma_2}{dz^2} + \frac{1}{z} \cdot \frac{d\sigma_2}{dz} - i\sigma_2 = 0,$$

(10.2)

and σ_2 is the solution in terms of Bessel functions

$$\sigma_2 = (A_1 + iB_1) J_0(\alpha \sqrt{-i}) + (A_2 + iB_2) K_0(\alpha \sqrt{-i}).$$

(10.3)

The cases of free and clamped opening were considered. Unfortunately, an error was made in the argument in the solution of (10.3). In reality the function $K_0(\alpha \sqrt{i})$ will be the second solution in (10.3).

The results of this study were used in [9] to solve the problem of stress concentration in a spherical closure which is coupled through a toroidal segment with a cylindrical tube.

The axisymmetric problem was also examined by Sokolov [10] who used the Lur'ye relations [11] to write the solution for a spherical shell with small circular opening at the pole in terms of the same Thomson functions ker x and kei x. Then, retaining in the general solution the function which decreases with reduction of the angle θ (ber x, bei x), Sokolov obtained also a solution for a closed spherical shell in which the angle corresponding to the shell edge is small. He wrote out the expressions for the edge values of the basic quantities—forces, moments and displacements, for two versions of the boundary conditions at the edge of the opening: 1) given meridional bending moment (M_0) and horizontal force (Q_0), 2) given horizontal displacement (u_0) and rotation (ϑ_0).

The combinations of Thomson functions were calculated for the sphere with an opening

$$C(x) = \frac{\ker'^2 x + \kei'^2 x}{x}, \quad D(x) = \ker' x \kei x - \kei' x \ker x,$$
$$E(x) = \ker'^2 x + \kei'^2 x, \quad F(x) = \ker' x \ker x + \kei' x \kei x,$$
$$f(x) = \frac{F(x)}{xC(x)}, \quad e(x) = \frac{E(x)}{xC(x)}, \quad d(x) = \frac{D(x)}{xC(x)},$$

(10.5)

where the values of the functions f(x), e(x), d(x) are presented in a table $(x \leq 10)$.

Comparing his solution with the conventional asymptotic solution, Sokolov concludes that it may be used for large values of the angle θ.

We know that the Geckeler approximation, valid for not very small angles θ, consists in neglecting the unknown function and its first derivative in comparison with the second derivative in the Meissner equation [12]

$$Q_{1n}'' + ctg\,\theta Q_{1n}' - (ctg^2\theta - \nu)\,Q_{1n} = Eh\vartheta,$$
$$\vartheta'' + ctg\,\theta\vartheta' - (ctg^2\theta + \nu)\vartheta = -\frac{12(1-\nu^2)R^2}{Eh^2}Q_{1n}$$

(10.6)

(ϑ is the meridian rotation angle, Q_{1n} is the shearing force). This leads to exclusion of terms with trigonometric factors from the equation.

Hoff [13] attempted to account approximately for the meridian curvature of a spherical shell by replacing ctg θ by the first two terms of its Taylor series expansion in the fourth-order system (10.6), trans rmed to a single equation, i.e., writing

$$ctg\,\theta = ctg(\theta_0 + x) = ctg\,\theta_0 - \frac{x}{\sin^2\theta_0},$$

where θ_0 corresponds to the shell edge in question, and x is measured from the shell edge. He shows that this approximation is valid for $\theta_0 \geq 30°$ for R/h = 100 and for $\theta_0 \geq 45°$ for R/h = 50. Here the influence coefficients corresponding to the new approximation differ from the Geckeler values only by correction factors which are close to unity in the region where the new solution is applicable.

The numerical values of the influence coefficients for a hemisphere with opening with the basic parameters

$$\frac{R}{h} = 15,\ 25,\ 50,\ 75,\ 100,\ 125,\ 150,\ 200,\ 250;$$
$$\theta_0 = 50,\ 40,\ 30,\ 20,\ 10°$$

were obtained by Galletly [14] by integrating the Meissner equations (10.6) using the Runge-Kutta method with $1°$ step.

In his previous study [15] Galletly made a comparison of the influence coefficients for the hemisphere with circular central opening obtained using three different methods: 1) Geckler method, 2) Esslinger method, [16] which amounts to reducing the governing equation to a Bessel equation by the change ctg θ ≈ 1/θ, and 3) the Love method [17], which reduces the equation to a form whose solutions are Legendre

functions of a complex variable. In calculating the latter, Galletly used either asymptotic representations (method 3a) or their expressions in terms of hypergeometric series (method 3b). Method 3b (very cumbersome, but more precise) was used as the standard for comparison with the other methods. On the basis of comparison of the influence coefficients for one specific hemisphere with the parameters R/h = 90.5 and θ_0 = 10°30', he recommends using method 2 (Bessel asymptotic method) for cases when the opening total central angle $2\theta_0 < \pi/6$. In the case in question, its error was 5% in comparison with method 3b, while the Geckeler method gave a maximal deviation of 15%.

In a discussion of Galletly's article his supporters [18] expand the study, including two additional methods which are convenient for practical application: method 4 of Burrows-Graves and method 5, which is an approximate solution based on the Langer asymptotic treatment. The Langer ideas will be discussed later. The Burrows-Graves technique extends the asymptotic solution of Hildebrand [19].

The latter reduces the system of the type (10.6) for the shell of revolution of arbitrary shape to a form which does not contain the first derivative

$$X'' - F_1 X + 2k^2 \Phi^2 Y = 0,$$
$$Y'' - F_2 Y - 2k^2 \Phi^2 X = - 2k^2 \Phi^2 X_0.$$

Here $k^2 = \sqrt{3(1-\nu^2)} \frac{R_1^2}{R_2 h}$ and the functions F_1, F_2, Φ, which depend on the shell geometry, under the assumption of smoothness of the geometric parameters are quantities of order one. The asymptotic solution is sought in the form

$$X = x e^{k\zeta},$$
$$Y = y e^{k\zeta},$$

where $\zeta = \bullet \int \Phi d\xi$, $\omega^2 = 2i$, and the functions x and y are taken in the form of series in powers of 1/k

$$x = \sum_{n=0}^{\cdot} x_n(\xi) k^{-n}, \quad y = \sum_{n=0}^{\cdot} y_n(\xi) k^{-n}.$$

In the previously mentioned discussion a comparison was made of the influence coefficients for a hemisphere with ratio 2R/h = 30

using all four methods with the results of an exact solution similar
to the Love method (method 3b) and led the authors to conclude: 1)
the Geckeler approximation is valid for a comparatively thin closed
hemisphere; 2) the Bessel approximations are satisfactory near central
openings in relatively thin spherical segments; 3) method 4 is usable
for comparatively thin segments which are nearly hemispherical; and
4) method 5 (Langer) is valid at all points of relatively thick closed
or unclosed spherical segments, including the complete sphere.

We note that the Hetenyi approximation [20], also presented in Timo-
shenko's book [21], which is more exact than the Geckeler approximation
and involves neglecting only the function itself in comparison with the
second derivative in initial equations (10.6), yields poorer results than
the Burrows-Graves method and the Bessel asymptotic solution for the
hemisphere in question.

We note that not all the approximate methods were investigated
for the angles $2\theta_0 > \pi/6$ and for other values of the curvature-
thickness ratio.

Several analyses have been based on the methods developed by
Langer [22-24] for asymptotic integration of differential equations
containing a large parameter. Langer's first study [22] examined
asymptotic integration of the equation

$$u''(x) + [\lambda^2\Phi^2(x) - \chi(x)]\, u(x) = 0,$$

(10.7)

where λ is the large parameter; $\Phi^2(x)$ may vanish at a single point of
the interval of x variation (for example, x = 0) as follows

$$\Phi^2(x) = x^\nu (a_0 + a_1 x + \ldots) \quad (\nu \geqslant 0),$$

and $\chi(x)$ is assumed finite.

Detailed studies are made of the solutions

$$y_\pm = \frac{\left\{\int_0^x \Phi(x)\,dx\right\}^{\frac{1}{2}-\mu}}{[\Phi(x)]^{\frac{1}{2}}} \, \zeta^\mu G_{\pm\mu}(\zeta)$$

(10.8)

$$\left(\mu = \frac{1}{\nu + 2}, \quad \xi = \lambda \int_0^x \Phi(x)\,dx, \right.$$

$$\left. \Omega = \frac{\int_0^x \Phi(x)\,dx}{\Phi(x)}, \right.$$

where $G_\mu(\xi)$, $G_{-\mu}(\xi)$ are cylinder functions of an equation related to the initial equation (10.7);

and

$$y''(x) + \{\lambda^2 \Phi^2(x) - \omega(x)\}\, y(x) = 0 \qquad (10.9)$$

$$\omega(x) = \frac{1}{4\Omega^2}\{(\Omega^2)'' - 3(\Omega')^2 + 4\mu^2\}$$

is finite in the function interval being considered. The solution of (10.7) is given in terms of $y_+(x)$ and $y_-(x)$, where the Hankel functions are used as the cylinder functions. The more general equation is considered in [24]

$$\frac{d^2u}{dx^2} + [\lambda^2 q_0(x) + \lambda q_1(x) + R(x, \lambda)]\, u = 0,$$

where

$$|\lambda| > N, \quad R(x, \lambda) = \sum_{\nu=0}^{\infty} \frac{r_\nu(x)}{\lambda^\nu},$$

and $q_0(x)$ may or may not vanish.

Asympototic solutions of (10.7) for singularities of the coefficient $\Phi^2(x)$ of more complex form were obtained by Dorodnitsyn [3].

Naghdi and de Silva [25, 26] introduce an auxiliary complex function to reduce the system of two equations for a shallow shell of revolution obtained by Reissner [27] to a single second-order differential equation of the type (10.7), valid for shells of constant thickness and for those of a large class of variable thickness

$$W'' + [2\beta^2 \mu^2 \Psi^2(\xi) + \Lambda(\xi)]\, W = \left[\frac{h}{h_0} \cdot \frac{r}{a}\right]^{\frac{1}{2}} f(\xi)\,[F + ikG]. \qquad (10.10)$$

Its asymptotic solution is found by the Langer method

$$W = [\Psi^{-1} \int \Psi\,d\xi]^{\frac{1}{2}} \left\{ A J_{-\frac{1}{2}}(\eta_i) + B J_{\frac{1}{2}}(\eta) \right\},$$

$$\eta_i = (2\beta^2)^{\frac{1}{2}} \mu \int \Psi\,d\xi. \qquad (10.11)$$

This method is used in [28] to obtain a solution valid at the apex for a thin ellipsoidal shell of constant thickness subject to an

axisymmetric load. The solution is written in terms of Thomson functions (See § 7). It is shown that in the limit this solution becomes the familiar solution for a shallow spherical shell [29].

The Dingle method [30] for finding the asymptotic solutions of ordinary differential equations leads to the same results as the Langer method. By the usual substitution any second order differential equation is reduced to the standard form

$$\frac{d^2 u(x)}{dx^2} = \tau(x) u(x).$$

(10.12)

The Dingle method involves comparing the original equation with

$$\frac{d^2 U(\sigma)}{d\sigma^2} = \Gamma(\sigma) U(\sigma),$$

(10.13)

for which analytic solutions in terms of tabulated special functions are known. Dingle's study presents a table of the comparison function $\Gamma(\sigma)$ and the corresponding solutions for various typical shells of revolution. Here the unknown solution is written in terms of the solution of (10.13) in the form

$$u(x) = \left(\frac{d\sigma}{dx}\right)^{-\frac{1}{2}} U(\sigma),$$

or in the first approximation

$$u(x) \sim \left(\frac{\Gamma(\sigma)}{\tau(x)}\right)^{\frac{1}{4}} U(\sigma),$$

(10.14)

with a simple technique being given for estimating the omitted correction terms.

The study [31] of Galletly and Radok indicates that the Dingle method includes the Langer method as a particular case and permits a simpler and less formal analytic interpretation of the asymptotic solution of the equations. Moreover, in the Langer method the argument of the Thomson functions includes an integral of the type

$$\Phi = \int_0^t \frac{t}{(1-t^2)^{\frac{1}{2}}} dt$$
$$\left(t = \sin \frac{\theta_0}{2}\right),$$

which is not tabulated anywhere. In order to compare the Langer approximate solution with the more exact solution, the authors give

a comparison for two particular forms of shells of revolution – ellipsoid with opening and torus of negative Gaussian curvature – in terms of the compliance coefficients between the two asymptotic solutions (Langer and Dingle) and the solution obtained by numerical integration of the equilibrium equations. They conclude that the agreement between these methods is satisfactory.

The effect of symmetric and antisymmetric loadings on a spherical shell with small opening is studied in [32]. The bending moment is transmitted to the shell through a thin-wall cylindrical tube. The purpose of the paper is to study the effect of cylinder thickness on the magnitude of the stresses and deformations in the sphere. The Reissner solution for a shallow shell [29] is used for the sphere. A numerical example shows that the cylinder thickness has a large influence on the stresses and displacements in the sphere and in the limit. With increase of the cylinder thickness, the solution becomes the familiar solution of the problem of the effect of a concentrated force and moment acting on a spherical shell through a cylindrical adapter [33].

REFERENCES

1. Novozhilov, V. V., Teoriya tonkikh obolochek (Thin Shell Theory), Leningrad, Sudpromgiz, 1962.

2. Chernykh, K. F., Lineynaya teoriya obolochek (Linear Shell Theory), Part 1, LGU, Press 1962.

3. Dorodnitsyn, A. A., "Asymptotic eigenvalue distribution laws for some particular forms of second-order differential equations," UMN, Vol. 7, NO. 6, 1952.

4. Watson, G. N., Theory of Bessel Functions, Moscow, IL, 1949.

5.

6.

7. Shevlyakov, Yu., A., "Stresses in a spherical cap weakened by a circular cutout", Inzh. Sbornik, Vol. 24, 1956.

8. Vlasov, V. Z., Obshchaya teoriya obolochek i yeye prilozheniya v tekhnike, (General Shell Theory and its Application in Engineering), Moscow, Gostekhizdat, 1949.

9. Rozenberg, L. B., and L. A. Bespal'ko, "Stress concentration in a spherical cap around a circular opening," DAN SSSR, Vol. 2, 1959.

10. Sokolov, F. A., "Spherical shell subjected to axisymmetric loading," IAN SSSR, OTN, No. 2, 1962.

11. Lur'ye, A. I., Statika tonkostennykh uprugikh obolochek (Statics of Thin Elastic Shells), OGIZ,(Ob'yedineniye gosudarstvennykh izdatel'stv) 1947.

12. Geckeler, J. W., Statics of Elastic Bodies, Moscow-Leningrad, GTTI (Gostekhizdat), 1934.

13. Hoff, N. F., "Effect of meridional curvature on the influence coefficients of thin spherical shells," In: Problems of Continuum Mechanics, Volume in honor of the 70th anniversary of Academician N. I. Muskhelishvili, Moscow, 1961.

14. Galletly, G. D., Influence coefficients for open-grown hemispheres. Transactions ASME, A-82, dNo. 1, 1960, pp 73-81 .

15. Galletly, G. D., Influence coefficients for hemispherical shells with small openings at the vertex. JAM, Vol. 22, No. 1 p. 20, No. 3, p 443, 1955.

16. Esslinger, M., Statische Berechnung von Kesselboden Inlius Springer. (Static Calculation of Vessel Bottoms). Berlin, 1952.

17. Love, A., Mathematical Theory of Elasticity, ONTI, 1935.

18. Burrows, W. R., R. L. Graves, P. G. Stevens Discussion on the paper:Influence coefficients for hemispherical shells with small openings at the vertex". JAM, Vol. 25, No. 3, 1955, p. 443.

19. Hildebrand, F. B., On asymptotic integration in shell theory. Proceedings symposia in appl. math., Vol. 3. N.Y., 1950.

20. Hetenyi, M., Spherical shells subject to axial symmetrical beeding. Pub. Intern. Assoc. Bridge Struct. Eng., Vol. 5, 1938.

21. Timoshenko, S. P., Plastinki i Obolochki (Plates and shells), Moscow-Leningrad, Gostekhizdat, 1948.

22. Langer, R. E., On the asymptotic solution of ordinary differential equations. Trans. Amer. math. soc., Vol. 33, 1931. pp. 23-64.

23. Langer, R. E., On the asymptotic solution of ordinary differential equations with reference to the Stokes' phenomenon about a singular point. Trans. amer. math. soc., vol. 37., No. 3, 1935.

24. Langer, R. E., The asymptotic solutions of ordinary linear differential equations of the second order with special reference to a turning point. Trans. Amer. math. soc., Vol. 67, No. 2, 1949.

25. Naghdi, P. M., C. Nevin de Silva. On the deformation of elastic shells of revolution. Quart. appl. math., Vol. 12, No. 4, 1955, p. 369.

26. Naghdi, P. M., C. Nevin de Silva. Asymptotic solutions of a class of elastic shells of revolution with variable thickness. Quart. appl. math., Vol. 15, No. 2, 1957.

27. Reissner, E., On the theory of thin elastic shells. H. Reissner's anniversary volume. Contributions to appl. mech., J. W. Edwards, Ann Arbor, Michigan, 1949, p. 231.

28. Naghdi, P. M., C. Nevin de Silva. Deformation of elastic ellipsoidal shells of revolution. Proceedings of the 2d U. S. National Congress of applied mechanics., 1954.

29. Reissner, E. Stresses and small displacement of shallow spherical shells. I and II. J. Math. a. phys., Vol. 25, 1946, pp. 80-85, 279-300, Vol. 27, 1948, p 240.

30. Dingle, R. B., The method of comparison equations in the solution of linear second-order differential equations. Applied Scientific Research, ser. B. Vol. 5, No. 5, 1956, pp. 345-367.

31. Galletly, G. D., J. R. M. Radok. On the accuracy of some shell solutions. Paper Amer. soc. mech. eng., NAPM-30, 1959.

32. Bailey, R., R. Hicks. Localized loads applied to a spherical pressure vessel through a cilindrical insert. J. mech. Eng. Sci., Vol. 2, No. 4, 1960.

33. Bijlaard, P. P. Computation of the stresses from local loads in spherical pressure vessels or pressure vessel heads. Welding research council bulletin series, No. 34, 1957.

34. Nosova, L. N. Tablitsy funktsiy Tomsona i ikh pervykh proizvod-nykh (Tables of the Thompson Functions and Their First Derivatives), Moscow, Izdatel'stvo AN SSSR, 1960.

35. Jahnke, E., and F. Emde, Tables of Functions with Formulas and Curves, Moscow, Fizmatgiz, 1959.

STUDY OF STRESS CONCENTRATION IN TURBINE BLADE T-SHAPED HEADS
IN ELASTIC AND CREEP CONDITIONS

I. I. Bugakov, V. P. Smirnova and S. P. Shikhobalov

This article presents the results of a study using photoelastic
and photocreep methods of stress concentration in the T-shaped
heads of turbine blades with relative dimensions $D/d = 1.58$ and $h/d =$
$= 0.625$ (Figure 1). The study was made by the Optical Laboratory of
the Scientific Research Institute of Mathematics and Mechanics
of Leningrad State University for the "22-nd Session of the CPSU"
Leningrad Metals Plant.
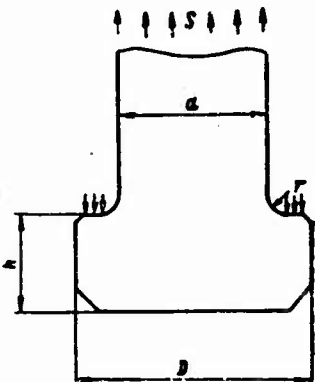
Figure 1

The study was made using two-
dimensional models subjected to a
constant external load simulating
the blade centrifugal force. The
models were fabricated using metal
templates with relative dimensions
$r/d = 0.010; 0.0417; 0.0625;$ and
0.1250 (Figure 1).

The elastic problem was studied
on models made from a solution of
PN-1 in 30% styrene, solidified
with gradual temperature increase to 80° after adding 10% styrene to
increase the material optical activity and 1-2% hydroperoxide. The

models were studied by "freezing" the deformations. In the "freezing" process the model was mounted on a ring simulating the turbine disc rim. The studies were made using three mounting techniques: a) the model was supported on the ring through metal bars located at the edges of the collars; b) the bars were located at the radii r; c) the model rested directly on the ring. The loaded model was transformed into the highly elastic state by gradual heating to 90°, after which it was slowly cooled.

The optical path difference δ was measured at those points where, under elastic conditions, the highest stresses arise, namely at the midpoints of the arcs of radii r. Exceptions were the models with ratios r/d = 0.010, in which the highest stresses were observed and measured not on the r contour itself, but 0.2 - 0.4 mm above this contour, at points of the rectilinear part of the contour (Figure 1). The δ measurements were made in white light on a KSP-6 synchronized coordinate polarimeter using a SKK-2 mica compensator [1].

The stress concentration factor k was determined from the formula

$$k = \sigma_{max} \, S,$$

(1)

where σ_{max} is the measured stress; S is the nominal stress in the neck part of the head (see Figure 1). The values of k are presented in the table.

The creep problem was studied using models made from transparent technical celluloid. The techniques for modeling creep of T-heads were discussed in [2].

As the creep law, we used the aging theory equation

$$\varepsilon_{ij} = \frac{1+v}{E}\left(s_{ij} + \frac{1-2v}{1+v}\sigma\Delta_{ij}\right) + \varphi(t)\exp(bT)s_{ij},$$
$$i, j = 1, 2, 3,$$

(2)

where ε_{ij} are the deformation tensor components; s_{ij} are the stress deviator components; $\sigma = \frac{1}{3}\sigma_{ii}$ is the average pressure; $T = \sqrt{0.5 s_{ij} s_{ij}}$ is the tangential stress intensity; t is time; E is the elasticity

modulus; ν is Poisson's ratio; b is a function of temperature; and Δ_{ij} are unit tensor components.

The mechanical and piezo-optical properties of the celluloid were determined from data of specimen tests under constant stresses of 50, 100, 150 and 200 kgf/cm^2 and a temperature of 35° in simple tension; the tests lasted five hours. The creep curves were reduced using the equation

$$\epsilon_i = \frac{\sigma_i}{E} + \frac{2}{3}\,\varphi(t)\exp\left(\frac{b\sigma_i}{\sqrt{3}}\right)\sigma_i.$$

(3)

which follows from (2), in the case of simple tension.

The specimen deformation as a function of time was measured using Martens tensiometers [3]. The modulus E = 18,000 kgf/cm^2 was determined from the results of the first measurement as the ratio of the stress to the measured value of the deformation. Then the experimental results were plotted on a plane in the coordinates $\ln\left(\frac{\epsilon_i}{\sigma_i} - \frac{1}{E}\right), \sigma_i$. Isochrones were then drawn through points relating to the same moments of time (Figure 2).

It follows from (3) that

$$\ln\left(\frac{\epsilon_i}{\sigma_i} - \frac{1}{E}\right) = \ln\left[\frac{2}{3}\varphi(t)\right] + \frac{b\sigma_i}{\sqrt{3}}.$$

Thus, the slope of the lines in Figure 2 defines the quantity $\frac{b}{\sqrt{3}}$. From Figure 2, we find b = 0.026 cm^{2}kgf.
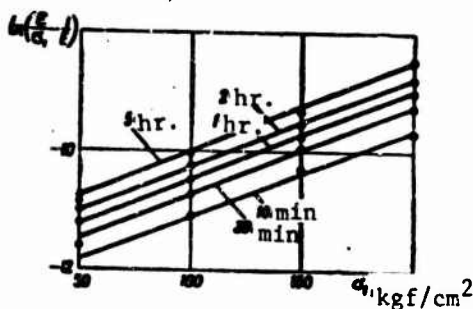
Figure 2
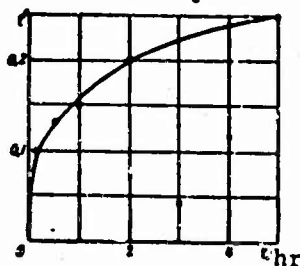
Figure 3

Since time enters into (2) as a parameter, the function ϕ is not determined specifically. The quantity $t^\circ = E\phi(t)$, which defines the connection between analogous moments of times on the model and full-scale [2], was calculated in accordance with (3) using the formula

$$t^\circ = \tfrac{3}{2}\left(\tfrac{E_{\epsilon_1}}{\sigma_1} - 1\right)\exp\left(-\tfrac{b\sigma_1}{\sqrt{3}}\right).$$

The curve of t° has the shape of creep curves (Figure 3).

Studies have shown that the values of t° increase with increase of the material temperature. In order to cover a wide range of values of t°, the specimen and model tests were conducted at elevated temperatures.

The optical path difference δ in these tests of the celluloid specimens was measured by the Senarmon method in polarized light which was nearly monochromatic with wavelength 546 mμ. From the measured values of δ, we plotted isochrones in the coordinates $\delta\sigma_1$ (Figure 4).

The celluloid models were tested at 35° under various constant values of the nominal stresses S. The values of S are shown in the table. Also shown are the values of the dimensionless parameter $S^\circ = bS$, which are necessary for conversion from the model to full scale. The models were mounted directly on a celluloid ring (it was shown in [2] that the contact conditions of the head with the disk under creep conditions does not have a significant effect on the value of the stress concentration factor). Each test lasted five hours. The δ measurements were made as a function of time at the same points as used on the PN-1 models, using the measurement technique described in [2]. The conversion from δ to the stress σ_{max} was accomplished with the aid of the isochronic curves (see Figure 4). The particular isochrone used depended on the moment at which δ was measured.
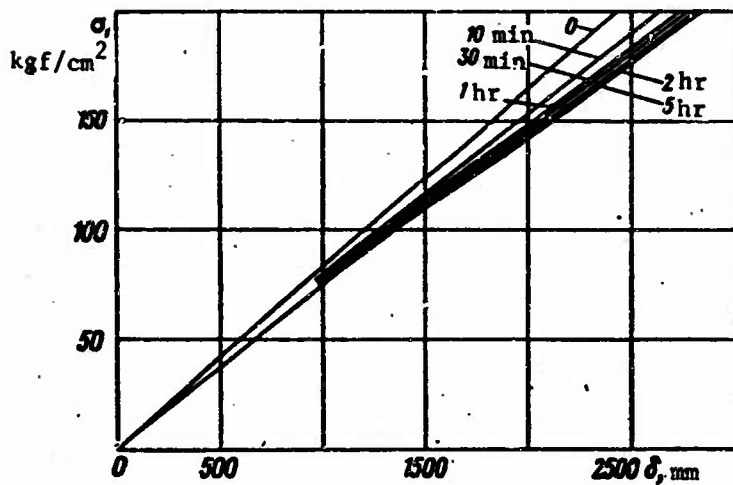
Figure 4.

The stress concentration factor k was found from (1).

The variation of k with time for the celluloid models with
r/d = 0.0417 is shown in Figure 5.

The dimensionless time t_*^0 of steady state creep onset was
determined from the conditions [2]

$$\ell_* = 0.5 \exp\left(-\frac{S^0}{\sqrt{3}}\right). \tag{4}$$

Then Figure 3 was used to determine the physical time t_* of steady
state creep onset (dashed curve in Figure 5). The values of $\ell_*, \; t_*$
and the stress concentration factors k for steady state creep
for $t \geqslant t_*$) are shown in the table. Since the values of k for $\frac{r}{d} = 0.0417$,
$S^0 = 0.345$ and S^0 = 0.695 vary little with time (Figure 5), we consider
that steady state creep corresponds to the values of k for t =
5 hours.

Figure 6 shows the variation of k in steady state creep as a
function of the ratio r/d (solid curves). The curve S^0 = 0 corres-
ponds to the solution of the elastic problem or the solution of the
problem for a material for which the creep deformation depends linearly

FTD-HC-23-361-69

r/d	Model No.	Support technique	δ	k_{av}	Model No.	S, kgf/cm²	ν	q	t*, hr	δ
0,0100	1	a	9,2	9,2	13	46,5	1,21	0,26	5	3,95
	2	c	8,3							
	3	c	10,1							
0,0417	4	a	7,7	7,5	14	13,3	0,345	0,41	5	6,1
	5	a	7,6		15	26,7	0,695	0,33	5	5,35
	6	a	7,6		16	46,5	1,21	0,26	5	3,55
	7	b	7,0		17	73,0	1,90	0,17	1	2,8
					18	93,0	2,42	0,12	0,5	2,35
0,0625	8	a	6,8	6,8	19	46,5	1,21	0,25	5	3,7
	9	a	7,0		20	46,5	1,21	0,25	5	3,65
	10	b	6,5							
0,1250	11	a	5,2	5,1	21	45,5	1,21	0,25	5	3,4
	12	b	4,3		22	55,5	1,47	0,21	3	3,3
					23	73,0	1,90	0,17	1	2,55

on the stress. This curve is plotted from the results of PN-1 model testing. The other curves are plotted from the results of celluloid model testing. The crosses correspond to the data of Hetenyi [4], obtained under creep conditions.

In [2], a study was made of the stress concentration in a T-head with relative dimensions $\frac{D}{d} = 1.78$, $\frac{h}{d} = 0.645$ (see Figure 1) for $S^0 = 0$ (elastic problem) and $S^0 = 1.47$ for values of r/d in the range 0.0715-0.1785. Values of k for the same values of S^0 were later obtained for r/d = 0.009. The results of the study of these blade heads are shown by the dashed curves in Figure 6. We see that the values of k in theses heads and in those studied above are practically the same for the same values of S^0 and r/d.

The data of Figure 6 are used to plot in Figure 7 the variation of k with S^0 under steady state creep conditions. The parameter for each curve is the ratio r/d. The ordinate $S^0 = 0$ defines the solution of the elastic problem.
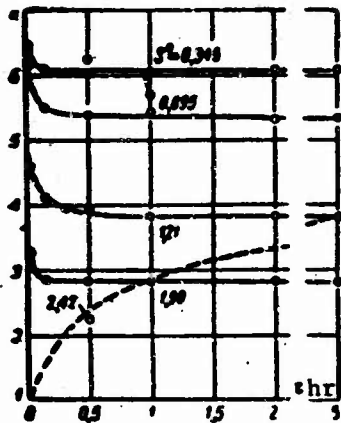
Figure 5
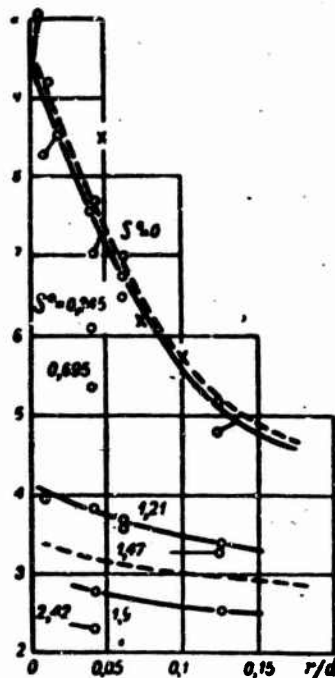
Figure 6

We see from Figure 6 that with an increase of the parameter S^0 (level of the nominal stress in the head or degree of nonlinearity of the connection between creep deformation and stress for the head material) the value of k decreases, and the dependence of k on the ratio r/d also diminishes. It follows similarly from Figure 7 that the values of k and the dependence of k on S^0 diminish with increase of the ratio r/d.

These results make it possible to determine the stress concentration factor in metal T-heads in steady state creep conditions, if they have the relative profile dimensions indicated. It is assumed that the head is loaded only by the constant blade centrifugal force S — which does not cause bending — the stress state in the head is plane, the head is uniformly heated and its temperature is constant.

From the results of testing the head material in simple tension under creep conditions, we can determine the values of b and t^0,
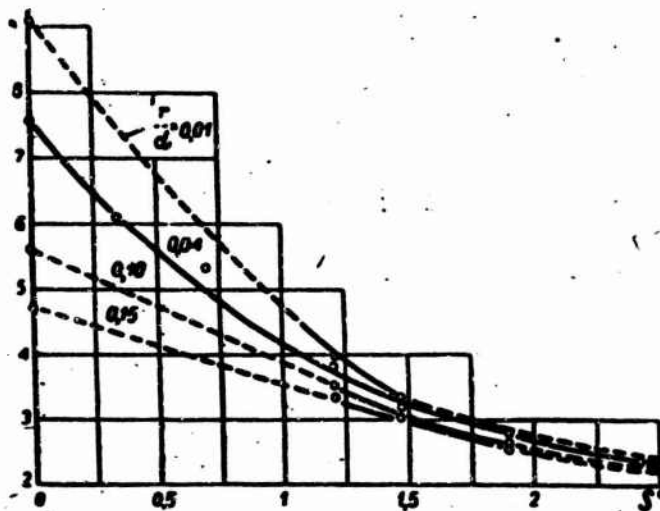
Figure 7

similarly to the way this was done above for celluloid. We note
that the use of the exponential dependence of the creep deformation
on the stress in accordance with (2) usually leads to good results.
The tests should be conducted at the working temperature and with
stresses in a range no less than the expected stress range in the
head. Then, the parameter $S^0 = bS$ is calculated, and (4) is used
to obtain the dimensionless time t_*^0 of steady state creep onset,
and then the physical time t_* for onset of this state. The value
of k for steady state creep $(t \geq t_*)$, is found from the values of
S^0 and r/d using the curves of Figures 6 and 7. From the curves of
Figure 5, we can find the variation of k with time in the unsteady
state creep condition for the head with ratio r/d = 0.0417. The
analogous moments of time for the model and full scale are defined
by the same values of t^0 [2]. Therefore, we can use Figure 3 to
convert the curves of Figure 5 to the coordinates k, t^0, and we can
use the curve of t^0, t to convert for the full-scale material back
into the k, t coordinates, where now t is the time after loading of
the full scale head.

REFERENCES

1. Edel'shteyn, Ye. I., "Instruments of the Scientific Research Institute of Mathematics and Mechanics of Leningrad State University for Studying Stresses by the Optical Polarization Technique." In the collection: Polyarizatsionno-opticheskiy metod issledovaniya napryazheniy (Optical Polarization Techniques for Stress Analysis) LGU Press (Leningrad State University Press) 1960, p. 174.

2. Bugakov, I. I., V. P. Smirnova and S. P. Shikhobalov, "Modeling creep of T-head turbine blades," Issledovaniya po uprugosti i plastichnosti (Studies in Elasticity and Plasticity), Collection 3, LGU Press, 1964, p. 192

3. Bugakov, I. I., "Equipment for Plastic Creep Studies" In the collection: Issledovaniya po uprugosti i plastichnosti (Studies in Elasticity and Plasticity), Collection 1, LGU Press, 1961, p. 213.

4. Hetényi, M., Stress-concentration factors for T-heads. J. Appl. Mech., Vol. 26, No. 1/2, p. 130, 1959.

Received 7 April 1964.

ESTIMATING THE FUNDAMENTAL VIBRATION FREQUENCY OF

A BAR OF VARIABLE CROSS SECTION

L. I. Kuznetsov

The problem of finding the natural frequencies of the longitudinal vibrations of a bar, one end of which is clamped while the other carries an absolutely rigid weight, leads to finding those values of ω_k for which the equation

$$[S(x)f'(x)]' + \frac{\gamma \omega^2}{E} S(x)f(x) = 0 \tag{1}$$

has a nonzero solution [1], under the boundary conditions

$$\begin{aligned} f(0) &= 0, \\ M\omega^2 f(l) - ES(l)f'(l) &= 0 \end{aligned} \tag{2}$$

Here γ is the bar material density; $\underline{l}$ is the bar length; $S(x)$ is the cross section area; E is the modulus of elasticity; M is the mass of the bar.

For estimating the upper limit of the first (fundamental) vibration frequency, we have the simple but in many cases adequately precise Rayleigh formula [2, 3], which for the mode corresponding to a static load is

$$\omega_1^2 < \omega_\infty^2 = \frac{E}{M\sigma(l) + \frac{1}{\sigma(l)}\int_0^l \sigma^2(x)S(x)dx}, \tag{3}$$

where ω_1 is the fundamental vibration frequency, and

$$\sigma(x) = \int_0^x \frac{dx}{S(x)}. \tag{4}$$

It is desirable to have an equally simple formula for estimating the lower limit of the fundamental frequency, as this would be useful for practical calculations. Such an estimate is obtained immediately with the aid of the principle of contracting mappings [5]. However, this method is not found in handbooks and texts on vibration theory, and this is the reason for the present article.

Let us consider the problem of forced vibrations of a bar with a weight under the influence of a "distributed" loading of the form $F(x, t) = \varphi(x)\sin \omega t$, where $\phi(x)$ is a function which is continuous in [0,1] . Then we obtain

$$[S(x)f'(x)]' + \frac{M\omega^2}{E}S(x)f(x) = \varphi(x) \tag{5}$$

with the same boundary conditions.

Let $\omega < \omega_1$. Then there exists a Green's function of the operator $[S(x)f'(x)]'$ with the conditions (2)[4]

$$G(x, y) = \begin{cases} \frac{\sigma(x)}{E - M\omega^2\sigma(l)}\{E - M\omega^2[\sigma(l) - \sigma(y)]\}, & x \leqslant y, \\ \frac{\sigma(y)}{E - M\omega^2\sigma(l)}\{E - M\omega^2[\sigma(l) - \sigma(x)]\}, & x > y, \end{cases} \tag{6}$$

and we can write the integral equation

$$f(x) = \frac{M\omega^2}{E}\int_0^l G(x, y)S(y)f(y)dy + \Phi(x), \tag{7}$$

where

$$\Phi(x) = -\int_0^l G(x, y)\varphi(y)dy.$$

We note the following. Since $\omega < \omega_1$, we find from (3) and (4) that

$$E - M\omega^2\sigma(l) > 0$$

$$(8)$$

and

$$0 < E - M\omega^2[\sigma(l) - \sigma(x)] < E.$$

$$(9)$$

We require that

$$\frac{T\omega^2}{E} \max_{x \in [0, l]} \int_0^l G(x, y)S(y)\,dy < 1.$$

$$(10)$$

We achieve this if we consider that $\omega < \omega_*$, where

$$\omega_*^2 = \frac{E}{M\sigma(l) + T\int_0^l \sigma(x)S(x)\,dx},$$

$$(11)$$

In fact, it follows from (4), (6) and (9) that for all $x \in [0, l]$ we have

$$\int_0^l G(x, y)S(y)\,dy < \frac{E}{E - M\sigma(l)\omega^2}\int_x^l \sigma(y)S(y)\,dy +$$

$$+ \frac{E\sigma(x)}{E - M\omega^2\sigma(l)}\int_x^l S(y)\,dy < \frac{E}{E - M\omega^2\sigma(l)}\int_0^l \sigma(x)S(x)\,dx$$

and

$$\frac{T\omega^2}{E} \max_{x \in [0, l]} \int_0^l G(x, y)S(y)\,dy <$$

$$< \frac{T\omega^2}{E} \cdot \frac{E}{E - M\omega^2\sigma(l)}\int_0^l \sigma(x)S(x)\,dx = 1.$$

Then it follows from the principle of contraction mappings [5] that a solution of (7) exists for any $\omega < \omega_*$. And this means that ω_* is no greater than ω_1.

For illustration, consider the simple example: S = const. If we take $v = \frac{\omega l}{c}$, $\mu = \frac{m}{M}$ (m is the bar mass), then we obtain from (3) and (11)

$$v_* = \sqrt{\frac{2\mu}{2 + \mu}}, \quad v_{**} = \sqrt{\frac{3\mu}{3 + \mu}}.$$

The exact value of the fundamental frequency is determined by the smallest positive root of the equation [3].

$$v \, tg \, v = \mu.$$

The following table is constructed from the calculations.

μ	0,1	0,3	0,5	1	10	100	∞
v_0	0,309	0,511	0,633	0,817	1,292	1,400	1,414
v_1	0,311	0,520	0,653	0,861	1,429	1,566	1,571
v_{∞}	0,311	0,523	0,655	0,866	1,520	1,706	1,732

We see from the table that for small μ the error of (11) is not large (however,(3) is more accurate). However, for large μ the error of both formulas is of the same order.

It is interesting to note that the error of the average value $v_{av} = \frac{1}{2}(v_0 + v_{\infty})$ does not exceed 2.5% for all the values of μ presented in the table.

It is clear that (3) and (11) are also suitable for estimating the fundamental frequency of torsional vibrations of a bar. In place of E, S(x), M we need only write G (shear modulus), I (x) (polar moment of the section), and I (moment of inertia of the weight).

Formulas (3) and (11) will also hold for transverse vibrations of a clamped bar with a point weight at the end (without account for rotational inertia and shear). However, in this case

$$\sigma(x) = \int_0^x \int_0^{\xi} \frac{(l - \eta) \, d\eta}{I(\eta)} d\xi,$$

where EI(x) is the bending stiffness.

REFERENCES

1. Babakov, I. M., Teoriya kolebaniy (Vibration Theory), Moscow, GITTL, 1958.

2. Den Hartog, J. P., Mekhanicheskiye kolebaniya (Mechanical Vibrations), Moscow, Fizmatgiz, 1960.

3. Timoshenko, S. P., Kolebaniya v inzhenernom dele (Vibration Problems in Engineering), Moscow, Fizmatgiz, 1959.

4. Smirnov, V. I., Kurs vysshey matematiki (Course of Higher Mathematics), Vol. 4, Moscow, GITTL, 1951.

5. Kantorovich, L. V., and Akilov, G. P., Funktsional'nyy analiz v normirovannykh prostranstvakh (Functional Analysis in Normed Spaces), Moscow, Fizmatgiz, 1959.

FORCED AXISYMMETRIC VIBRATIONS OF A
CIRCULAR THICK PLATE

G. N. Bukharinov

In this article we solve the problem of forced axisymmetric
vibrations of a circular thick plate under the influence of uniformly
distributed normal forces which are harmonic time functions applied
to one of the faces of the plate. The boundary conditions on the
faces are satisfied exactly. Satisfaction of the boundary conditions
at the side surfaces reduces to calculating the coefficients in
the expansion of the displacements into series of functions of the
z coordinate, where oᶻ is the axis of symmetry.

In the axisymmetric deformation case, the radial displacement u
and the axial displacement w, as is known, satisfy the following
differential equations of motion

$$
\frac{1-\mu}{1-2\mu}\cdot\frac{\partial^2 u}{\partial r^2}+\frac{1-\mu}{1-2\mu}\cdot\frac{1}{r}\cdot\frac{\partial u}{\partial r}-\frac{1-\mu}{1-2\mu}\cdot\frac{u}{r^2}+\frac{1}{2}\cdot\frac{\partial^2 u}{\partial z^2}+
$$
$$
+\frac{1}{2(1-2\mu)}\cdot\frac{\partial^2 w}{\partial z\partial r}=\frac{\rho(1+\mu)}{E}\cdot\frac{\partial^2 u}{\partial t^2}.
$$
$$
\frac{1}{2(1-2\mu)}\cdot\frac{1}{r}\cdot\frac{\partial u}{\partial z}+\frac{1}{2(1-2\mu)}\cdot\frac{\partial^2 u}{\partial r\partial z}+\frac{1-\mu}{1-2\mu}\cdot\frac{\partial^2 w}{\partial z^2}+
$$
$$
+\frac{1}{2r}\cdot\frac{\partial w}{\partial r}+\frac{1}{2}\cdot\frac{\partial^2 w}{\partial r^2}=\frac{\rho(1+\mu)}{E}\cdot\frac{\partial^2 w}{\partial t^2}.
$$

$$(1)$$

184

where t is time; r and z are cylindrical coordinates; μ is Poisson's ratio; E is the normal elasticity modulus: ρ is the density. We take the plane z = 0 as the middle plane. We denote the plate thickness by 2h and the face radius by r_0.

The normal σ_z and tangential τ_{rz} stresses are known to have the form, respectively,

$$\sigma_z = \frac{2G}{1-2\mu}\left\{(1-\mu)\frac{\partial w}{\partial r} + \mu\left(\frac{\partial u}{\partial r} + \frac{u}{r}\right)\right\}.$$
$$\tau_{rz} = G\left(\frac{\partial u}{\partial z} + \frac{\partial w}{\partial r}\right). \tag{2}$$

where G is the shear modulus.

We specify the following boundary conditions at the faces of the plate

$$\sigma_z = \begin{cases} -q_0\sin\omega t & \text{for } z = +h, \\ 0 & \text{for } z = -h \end{cases}$$

$$\text{for } z = \pm h. \tag{3}$$

and

$$\tau_{rz} = 0$$

Substituting (2) into (3), we have

$$\left\{(1-\mu)\frac{\partial w}{\partial z} + \mu\left(\frac{\partial u}{\partial r} + \frac{u}{r}\right)\right\}\Big|_{z=+h} = -\frac{1-2\mu}{2G}q_0\sin\omega t, \tag{4}$$
$$\left\{(1-\mu)\frac{\partial w}{\partial z} + \mu\left(\frac{\partial u}{\partial r} + \frac{u}{r}\right)\right\}\Big|_{z=-h} = 0$$

and

$$\left(\frac{\partial u}{\partial z} + \frac{\partial w}{\partial r}\right)\Big|_{z=\pm h} = 0. \tag{5}$$

We seek the solution corresponding to forced vibrations in the form

$$u = u^*(r,\ z)\sin\omega t,$$
$$w = \left[\frac{(1-2\mu)\,q_0}{2G(1-\mu)k\sin 2kh}\cos k(z+h) + w^*(r,\ z)\right]\sin\omega t, \tag{6}$$

where

$$k^2 = \frac{\omega^2\rho(1+\mu)(1-2\mu)}{E(1-\mu)}.$$

and it is assumed that the frequency ω of the specified loading satisfies the condition $\sin 2\,kh \neq 0$. Substituting (6) into (1), we find that $u^*(r, z)$ and $\omega^* (r, z)$ must satisfy the following system of differential equations

$$\frac{2(1-\mu)}{1-2\mu} \cdot \frac{\partial^2 u^*}{\partial r^2} + \frac{2(1-\mu)}{1-2\mu} \cdot \frac{1}{r} \cdot \frac{\partial u^*}{\partial r} - \frac{2(1-\mu)}{1-2\mu} \cdot \frac{u^*}{r^2} +$$
$$+ \frac{\partial^2 u^*}{\partial z^2} + \frac{1}{1-2\mu} \cdot \frac{\partial^2 w^*}{\partial r \partial z} + a^2 u^* = 0,$$
$$\frac{1}{1-2\mu} \cdot \frac{1}{r} \cdot \frac{\partial w^*}{\partial z} + \frac{1}{1-2\mu} \cdot \frac{\partial^2 u^*}{\partial r \partial z} + \frac{2(1-\mu)}{1-2\mu} \cdot \frac{\partial^2 w^*}{\partial z^2} + \tag{7}$$
$$+ \frac{1}{r} \cdot \frac{\partial w^*}{\partial r} + \frac{\partial^2 w^*}{\partial r^2} + a^2 w^* = 0,$$

where

$$a^2 = \frac{2\omega^2 \rho\left(\frac{1}{2} + \mu\right)}{E}.$$

The boundary conditions at the faces $z = \pm\ h$ after substituting (6) into (4) and (5) are rewritten in the form

$$\left\{ (1-\mu) \frac{\partial w^*}{\partial z} + \mu \left(\frac{\partial u^*}{\partial r} + \frac{u^*}{r} \right) \right\} \Big|_{z=\pm h} = 0 \tag{8}$$

and

$$\left(\frac{\partial u^*}{\partial z} + \frac{\partial w^*}{\partial r} \right) \Big|_{z=\pm h} = 0. \tag{9}$$

We seek the solution of (7) in the form

$$u^* = - iJ_1(iar)\,\varphi(z),$$
$$w^* = J_0(iar)\,\psi(z), \tag{10}$$

where J_0 and J_1 are Bessel functions.

Substituting (10) into (7), we find the equations for the functions $\phi(z)$ and $\psi(z)$

$$\varphi''(z) + \frac{2(1-\mu)}{1-2\mu} \left[z^2 + \frac{1-2\mu}{2(1-\mu)} a^2 \right] \varphi(z) + \frac{a}{1-2\mu} \psi'(z) = 0, \tag{11}$$
$$\psi''(z) + \frac{1-2\mu}{2(1-\mu)} (a^2 + a^2) \psi(z) + \frac{a}{2(1-\mu)} \varphi'(z) = 0.$$

Integrating (11) we find

$$\varphi(z) = A_1 \cos \lambda_1 z + B_1 \sin \lambda_1 z + \frac{a}{\lambda_2}(-D_2 \cos \lambda_2 z + C_2 \sin \lambda_2 z),$$

$$\psi(z) = \frac{a}{\lambda_1}(B_1 \cos \lambda_1 z - A_1 \sin \lambda_1 z) + C_2 \cos \lambda_2 z + D_2 \sin \lambda_2 z, \tag{12}$$

where A_1, B_1, C_2, L_2 are arbitrary constants and

$$\lambda_1^2 = a^2 + a^2,$$
$$\lambda_2^2 = \frac{1-2\mu}{2(1-\mu)} a^2 + a^2. \tag{13}$$

After introducing (10) into the boundary conditions (8) and (9), they are written in the form

$$(1-\mu)\psi'(h) + \mu 2\varphi(h) = 0,$$
$$(1-\mu)\psi'(-h) + \mu 2\varphi(-h) = 0 \tag{14}$$

and

$$\varphi'(h) + a\psi(h) = 0,$$
$$\varphi'(-h) + a\psi(-h) = 0. \tag{15}$$

Introducing (12) into (14) and (15), we find that (11) and the boundary conditions (14) and (15) will be satisfied by the functions

$$\varphi(z) = A_1 \left[\cos \lambda_1 z - \frac{2a^2}{a^2 + 2a^2} \cdot \frac{\cos \lambda_1 h}{\cos \lambda_2 h} \cdot \cos \lambda_2 z \right],$$

$$\psi(z) = -\frac{a}{\lambda_1} A_1 \left[\sin \lambda_1 z - \frac{a^2 + 2a^2}{2a^2} \cdot \frac{\sin \lambda_1 h}{\sin \lambda_2 h} \cdot \sin \lambda_2 z \right], \tag{16}$$

where λ_1 and λ_2 are expressed in terms of α using (13), and we have the equation

$$\operatorname{tg} \lambda_1 h \operatorname{ctg} \lambda_2 h = \frac{4a^2 \lambda_1 \lambda_2}{(a^2 + 2a^2)^2}. \tag{17}$$

Similarly, the system (11) and the boundary conditions (14) and (15) will be satisfied by the functions

$$\varphi(z) = B_1 \left[\sin \lambda_1 z - \frac{2a^2}{a^2 + 2a^2} \cdot \frac{\sin \lambda_2 h}{\sin \lambda_2 h} \sin \lambda_2 z \right],$$

$$\psi(z) = \frac{a}{\lambda_1} B_1 \left[\cos \lambda_1 z - \frac{a^2 + 2a^2}{2a^2} \cdot \frac{\cos \lambda_1 h}{\cos \lambda_2 h} \cos \lambda_2 z \right], \tag{18}$$

where λ_1 and λ_2 are expressed in terms of α using (13), and the equation holds

$$\operatorname{tg} \lambda_1 h \operatorname{ctg} \lambda_2 h = \frac{(a^2 + 2\sigma^2)^2}{4\sigma^2\lambda_1\lambda_2}.$$

(19)

We denote by α_k $(k=1, 2, 3, \ldots)$ the root of (17). On the basis of (13) this root corresponds to

$$\lambda_{1k}^2 = a^2 + \alpha_k^2,$$
$$\lambda_{2k}^2 = \frac{1-2\mu}{2(1-\mu)} a^2 + \alpha_k^2$$

(20)

and from (16) we have the functions

$$\varphi_k(z) = M_k \left[\cos \lambda_{1k} z - \frac{2\alpha_k^2}{a^2 + 2\alpha_k^2} \cdot \frac{\cos \lambda_{1k} h}{\cos \lambda_{2k} h} \cos \lambda_{2k} z \right],$$

$$\psi_k(z) = -\frac{\alpha_k}{\lambda_{1k}} M_k \left[\sin \lambda_{1k} z - \frac{a^2 + 2\alpha_k^2}{2\alpha_k^2} \cdot \frac{\sin \lambda_{1k} h}{\sin \lambda_{2k} h} \sin \lambda_{2k} z \right],$$

(21)

where $M_k (k=1, 2, 3, \ldots)$ are arbitrary constants.

We denote by $\beta_k, k=1, 2, 3, \ldots,$ the root of (19), i.e.,

$$\operatorname{tg} S_{1k} h \operatorname{ctg} S_{2k} h = \frac{(a^2 + 2\beta_k^2)^2}{4\beta_k^2 S_{1k} S_{2k}},$$

(22)

where

$$S_{1k} = a^2 + \beta_k^2,$$
$$S_{2k} = \frac{1-2\mu}{2(1-\mu)} a^2 + \beta_k^2.$$

(23)

On the basis of (18) the root β_k corresponds to the functions

$$\varphi_k^*(z) = N_k \left[\sin S_{1k} z - \frac{2\beta_k^2}{a^2 + 2\beta_k^2} \cdot \frac{\sin S_{1k} h}{\sin S_{2k} h} \sin S_{2k} z \right],$$

$$\psi_k^*(z) = \frac{\beta_k}{S_{1k}} N_k \left[\cos S_{1k} z - \frac{a^2 + 2\beta_k^2}{2\beta_k^2} \cdot \frac{\cos S_{1k} h}{\cos S_{2k} h} \cos S_{2k} z \right].$$

(24)

where N_k $(k=1, 2, 3, \ldots)$ are arbitrary constants. It follows from (10) that (7) and the boundary conditions (8) and (9) will be satisfied by the following coordinate functions

188

$$u^\bullet = -\sum_{k=1}^{\infty}\left\{ iM_k J_1(i\alpha_k r)\left[\cos\lambda_{1k}z - \frac{2\alpha_k^2}{e^2+2\alpha_k^2}\cdot\frac{\cos\lambda_{1k}h}{\cos\lambda_{2k}h}\cos\lambda_{2k}z\right] +\right.$$
$$\left. + iN_k J_1(i\beta_k r)\left[\sin S_{1k}z - \frac{2\beta_k^2}{e^2+2\beta_k^2}\cdot\frac{\sin S_{1k}h}{\sin S_{2k}h}\sin S_{2k}z\right]\right\},$$

$$w^\bullet = \sum_{k=1}^{\infty}\left\{ -\frac{\alpha_k}{\lambda_{1k}}M_k J_0(i\alpha_k r)\left[\sin\lambda_{1k}z - \frac{e^2+2\alpha_k^2}{2\alpha_k^2}\cdot\frac{\sin\lambda_{1k}h}{\sin\lambda_{2k}h}\sin\lambda_{2k}z\right] +\right. \tag{25}$$
$$\left. + \frac{\beta_k}{S_{1k}}N_k J_0(i\beta_k r)\left[\cos S_{1k}z - \frac{e^2+2\beta_k^2}{2\beta_k^2}\cdot\frac{\cos S_{1k}h}{\cos S_{2k}h}\cos S_{2k}z\right]\right\}.$$

The arbitrary constants M_k and N_k $(k=1, 2, 3, ...)$ must be found from the boundary conditions at the plate side surface.

It is obvious that there is no difficulty in indicating the values of the constants M_k and N_k if we satisfy the boundary conditions at the side surface $(r = r_0)$ in the Saint Venant sense, or if we require satisfaction of these conditions only at a finite number of points from the interval $h < z < +h$.

Received 7 March 1964

EFFECT OF PRELIMINARY PLASTIC DEFORMATION ON THE YIELD
AND ULTIMATE LIMITS OF
COPPER

G. B. Talypov

.

In preceding papers [1, 2] a study of the effect of preliminary
plastic deformation on the yield limit of low and medium carbon
steel established that the shape of the yield limit is independent
of the loading path, and is a circle on the Il'yushin plane [3],
expanding and displacing in the direction of the preliminary plastic
deformation. In the present paper, we present the results of a study
of the effect of preliminary plastic deformation on the yield
limit of annealed technical copper.

§ 1. Specimens and Test Equipment

Tubular specimens (D = 25 mm, d = 23 mm) were fabricated from
35-mm-diameter annealed rods of technical copper. The basic geo-
metric dimensions of the specimens were selected so that the stress
state induced during testing was as near uniform as possible. The
axial load was transmitted to the specimen by means of a UM-5
press and special blank flanges. The axial force measurement ac-
curacy was ± 1%. Internal pressure was transmitted to the specimen
by means of a hydraulic press and was monitored by a reference
manometer. The internal pressure readout accuracy was ± 0.25 atm.

Wire resistance pickups and bridge amplifiers were used to measure
the deformations. The deformation measurement accuracy was $\pm 5 \cdot 10^{-6} \pm 1\%$.
The technique for reducing the test results was described in [1, 2, 4].

§ 2. Yield and Ultimate Limits in the Original Condition

a) <u>Yield Limit</u>   In order to find the initial yield limit
each of the selected specimens was tested to failure along a definite
ray of the first quadrant of the $(\sigma_\theta, \sigma_z)$ plane. For a given ray the
connection between the axial force and the internal pressure was
determined by the relation

$$P = p \frac{\pi d}{4} [nD + (n-1)d].$$

(1)

where n is the slope of the ray to the σ_θ axis. The basic geometric
dimensions of the specimens, the values of the loading path parameter
α, and also the test results are presented in Table 1.

Table 1.

Sample No.	R, мм	d, мм	α°	σ_{1r} kg/cm²	$\sigma_{\theta r}$ kg/cm²	σ_{zr} kg/cm²	$-\frac{\sigma_z}{\sigma_\theta}$	$\gamma = \frac{\sigma_{zr}}{\sigma_{r\theta}}$
1	24,98	22,93	0	1230	1230	0	1,15	0
2	25,00	22,93	15	1130	1160	310	1,08	0,290
3	24,95	22,94	30	·960	1090	630	1,02	0,588
4	25,00	22,93	45	1050	1060	1060	0,99	0,990
5	25,01	22,95	60	920	656	1185	0,613	1,16
6	24,96	22,87	75	1000	299	1115	0,280	1,04
7	24,95	22,93	90	1090	0	1070	0	1,00

The test results are: $E = 1.1 \cdot 10^6$ kg/cm², $\mu = 0.32$, $\sigma_{s0} = 1070$ kg/cm²,
$\sigma_{b0} = 2190$ kg/cm². The experimental initial yield limit points
from the data of Table 1 are plotted in Figure 1. The α = 0 point
should be neglected; a shortage of specimens from this lot of copper
made it impossible to carry out repeat tests for this point. Figure
1 also shows the initial yield limit on the Il'yushin plane, [4],
where
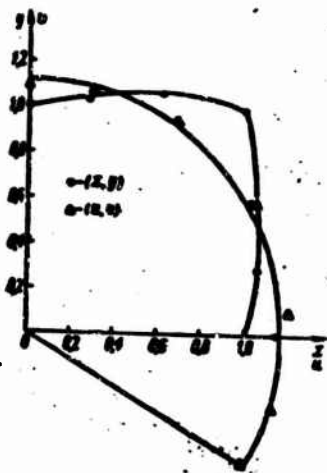
Figure 1
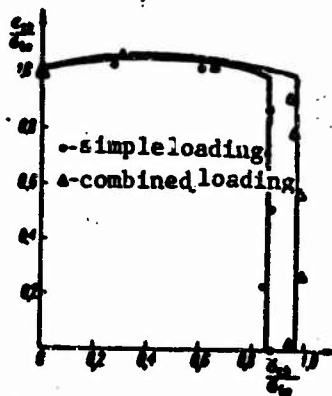
Figure 2

$$u = \frac{x}{\sqrt{2}},$$
$$v = \sqrt{\frac{2}{3}}\,y - \frac{x}{\sqrt{6}}. \tag{2}$$

Figure 1 shows that this copper is isotropic with respect to the initial yield limit.

b) Ultimate Limit.   During the tests the maximal magnitudes of the axial force and internal pressure were recorded. From these quantities we determined the equivalent ultimate stresses $\sigma_{\theta b}$ and σ_{zb} . The test results are presented in Table 2, from which the data are used to plot in Figure 2 the effective ultimate limit . In this case, just as in the case of steel [1], in the region $\sigma_z > \sigma_\theta$ the Huber-Mises strength condition is satisfied

$$\sigma_\theta^2 - \sigma_\theta \sigma_z + \sigma_z^2 = \sigma_{b0}^2, \tag{3}$$

while in the region $\sigma_\theta > \sigma_z$ the condition of maximal tangential stress is satisfied

$$\tau_{max} = \tau_b. \tag{4}$$

Sample No.	$\alpha°$	$p_b,$ kg/cm²	$p_b,$ kg	$q_b,$ kg/cm²	$\sigma_{zb},$ kg/cm²	$\frac{q_b}{q_{90}}$	$\frac{\sigma_{zb}}{\sigma_{90}}$
1	0	170	−700	1900	0	0,868	0
2	15	165	−300	1830	490	0,834	0,224
3	30	167	140	1890	1100	0,864	0,503
4	45	170	780	1880	1900	0,859	0,866
5	60	118	1250	1315	2240	0,600	1,02
6	75	53	1590	586	2320	0,268	1,06
7	75	54	1530	610	2300	0,278	1,05
8	90	0	1660	0	2190	0	1,00
9	90	0	1670	0	2200	0	1,00

Table 2.

§ 3. Yield and Ultimate Limits
After Preliminary Plastic Deformation

The data of Table 2 show that the ultimate strength in the transverse direction is about 87% of the ultimate strength in the longitudinal direction. Therefore, in order to ensure consistent results the preliminary loading of all the specimens was performed up to $\sigma_z = 1,6\,\sigma_{z9}$ along the ray $\alpha = 90°$. After the preliminary loading and unloading new measurements were made of each of these specimens and loading tables were prepared. The second loading up to failure was accomplished on the day following unloading.

a) <u>Yield Limit</u> From the measured deformation values, we calculated the deformation intensity e_i, and from the corresponding values of the stresses σ_θ and σ_z we calculated the stress intensity σ_i. From the (σ_i, e_i) diagram, we determined the value σ_{is} of σ_i at the effective yield limit. In determining the stresses σ_θ and σ_z we used the new specimen dimensions, so that σ_{is} will in essence represent the true stress [4].

The test results are presented in Table 3. The data of Table 3 were used to plot in Figure 3 the yield limit of the copper after preliminary plastic deformation. In this figure the triangles

Specimen No.	D_1, mm	d_1, mm	$a°$	σ_{1s} kg/cm²	$\sigma_{\theta s}$ kg/cm²	σ_{zs} kg/cm²	$x=\frac{\sigma_z}{\sigma_{s0}}$	$y=\frac{\sigma_{z\theta}}{\sigma_{s0}}$
1	24.14	22.20	0	1740	1740	0	1.62	0
2	24.59	22.73	15	1870	2080	560	1.94	-0.517
3	23.89	21.96	30	1895	2090	1210	1.95	1.13
4	24.04	22.10	45	1830	1830	1830	1.71	1.71
5	24.20	22.26	60	1770	1175	2040	1.10	1.91
6	24.50	22.52	75	1730	516	1875	0.482	1.75
7	24.13	22.18	90	1720	0	1720	0	1.61

Table 3

indicate this same boundary on the Il'yushin plane. The results
show that the loading complexity does not affect the shape of the
yield limit for copper.. This limit remains a circle on the
Il'yushin plane, expanding and displacing in the present case in
a direction which does not coincide with the direction of the pre-
liminary plastic deformation.

b) Ultimate Limit. As indicated above, the second loading
of each specimen after the preliminary plastic deformation was
carried out to failure. The maximal values of the axial force and
the internal pressure recorded during the tests were used to
determine the effective ultimate stresses. The test results are
presented in Table 4 and plotted in
Figure 2. We see from the figure
that preliminary plastic deformation
by axial stretching has no effect
on the ultimate limit in the
region $\sigma_z > \sigma_\theta$, but leads to
some expansion of this limit in
the region $\sigma_\theta > \sigma_z$. .
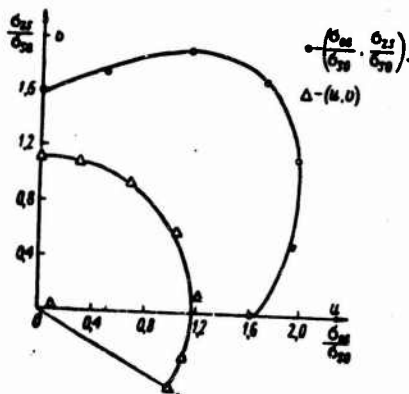
Figure 3

Specimen No.		P_δ, kg/cm²	P_y, kg	kg/cm²	kg/cm²	%/%	%/%
1	0	185	−730	2090	40	0,944	0,018
2	15	192	−356	2170	565	0,991	0,268
3	30	190	147	2130	1200	0,972	0,55
4	30°45′	187	550	2105	1720	0,968	0,784
5	45	187	780	2060	2000	0,937	0,914
6	60	121	1230	1370	2250	0,626	1,03
7	75	57	1550	643	2345	0,293	1,07
8	90	0	1670	0	2150	0	0,983

Table 4

REFERENCES

1. Talypov, G. B., "Yield and Ultimate Limit for Low Carbon Steel in Simple and Complex loading. Effect of aging," IAN SSSR, Mekhanika i mashinostroyeniye, No. 6, 1961.

2. Talypov., G. B., and A. I. Chistyakov, "Effect of large Preliminary Plastic Deformations on the Yield Limit of Low Carbon Steel." Issledovaniya po uprugosti i plastichnosti (Studies in Elasticity and Plasticity), Vol. 3, Leningrad State University Press, 1963.

3. Il'yushin, A. A., Connection Between Stresses and Plastic Deformations in Continuum Mechanics: PMM, No. 6, 1954

4. Talypov, G. B., and V. N. Kamentsev, "Study of the Yield Limits and Certain Other Effects for Complex Loading." Uchenyye Zapiski LGU, No. 280, 1960.

EFFECT OF LARGE PRELIMINARY PLASTIC DEFORMATIONS AND NATURAL AGING ON THE YIELD LIMIT OF LOW CARBON STEEL

G. B. Talypov

It was shown in [1, 2] that natural aging after preliminary plastic deformation has no effect on the shape of the yield and ultimate limits. Therefore,the effect of natural aging on the yield and ultimate limits may be studied by means of experiments in simple tension. The influence of natural aging after preliminary plastic deformation manifests itself in the fact that,along with the increase of the duration of natural aging,the yield limit initially expands continuously and then contracts, i.e., there is a recovery effect. Natural aging has practically no effect on the ultimate limit.

Results were presented in [3] of a study of the effect of small (up to 5%) preliminary plastic tensile deformations and natural aging on the yield and ultimate limits of St. 3 steel. The results of these tests showed that the effect of natural aging on the yield limit of low carbon steel is described quite satisfactorily by the formula

$$\chi = \chi_0 + A e^{-h(t-t_1)^r}, \tag{1}$$
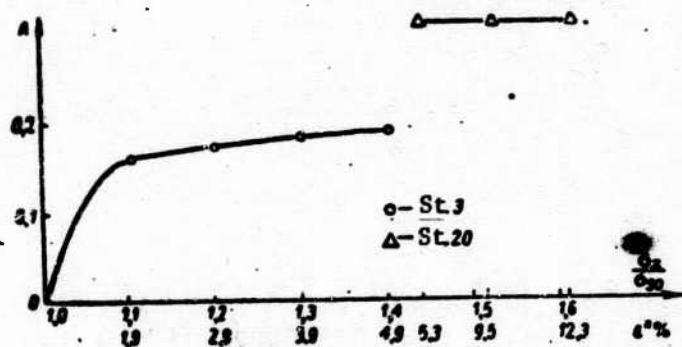
Figure 1

where χ_0 is the ratio of the yield limit σ_s to σ_{s0} in the unaged condition; t_1 is the aging time interval for which maximal expansion of the yield·limit occurs. In the general case the parameters A, k and t_1 depend on the magnitude of the preliminary plastic deformation. Small preliminary plastic deformations were examined in [3] and therefore, account was not taken of the effect of the specimen cross section area change as a result of preliminary deformation on the value of the yield point for the repeat loading. Figure 1 shows' the variation of the parameter A for St. 3 steel as a function of the degree of preliminary plastic deformation, plotted from the results of [3] with account for the specimen cross section area change as a result of preliminary plastic deformation.

In the present paper, we present the results of a study of the effect of large preliminary plastic deformations and natural aging on the yield limit. For the experiments we used four groups of so-called "gagarin" specimens of annealed St. 20 steel. The (three) specimens of the first group were tested in tension to determine the basic mechanical properties of this steel (σ_{s0} = 2280 kg/cm^2, σ_{b0} = = 3860 kg/cm^2). All 27 specimens of the second group were stretched to σ_z = 0.85σ_{b0}. After unloading and recording the new dimensions, 3 samples of the first subgroup were again stretched up to failure on the same day. Each of the three specimens of succeeding subgroups were
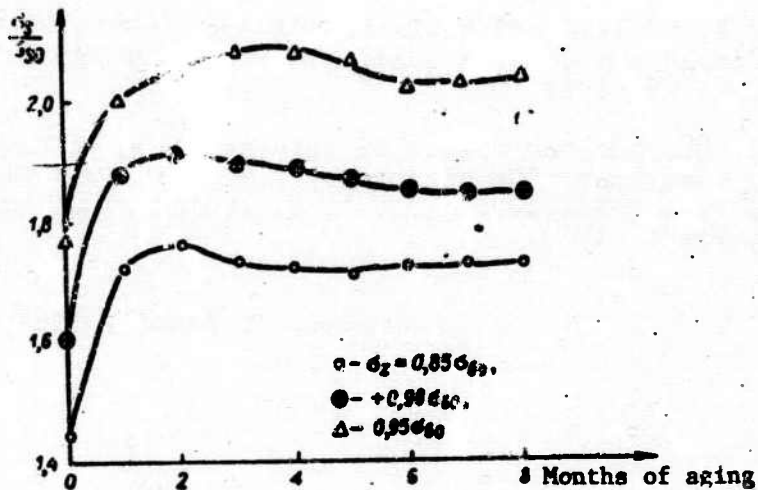
Figure 2

stretched up to failure, after aging for a period of one to two months
and so on. All 27 specimens of the third group were subjected to
preliminary stretching to $\sigma_z = 0.90 \, \sigma_{b0}$ and all the specimens of
the fourth group were stretched to $\sigma_z = 0.95 \sigma_{b0}$. After unloading the
corresponding subgroups of these groups of specimens were subjected
to the same operations as were the corresponding subgroups of the
second group. The test results are shown in Figure 2 and are described
satisfactorily by (1). In this case the parameter A remains constant,
equal to 0.31, and its values are shown by the triangles in Figure 1.
Thus, we find that the extent of the maximal expansion of the yield
limit for natural aging depends not only on the magnitude of the
preliminary plastic deformation, but also on the steel grade. While
in the case of St. 3 steel this expansion reached 20%, for St. 20
steel it reached 30%. ·

REFERENCES

1. Talypov, G. B. and V. N. Kamentsev, "Effect of Preliminary
    Plastic Deformation and Natural aging on Yield and Ultimate
    Limits". Issledovaniya po uprugosti i plastichnosti
    (Studies in Elasticity and Plasticity), Vol. 1, Leningrad State
    University Press, 1961.

2. Talypov, G. B., "Yield and Ultimate Limits of Low Carbon Steel in Simple and Complex Loading. Effect of Aging,", IAN SSSR, OTN, No. 6, 1961.

3. Talypov, G. B., "On the effect of Natural Aging on the Yield Limit." Issledovaniya po uprugosti i plastichnosti (Studies in Elasticity and Plasticity,) Vol. 3, Leningrad State University Press, 1963.

FAILURE TIME OF TUBES SUBJECTED TO
INTERNAL PRESSURE AND AXIAL FORCE

Ye. M. Levitas

In [1] Hoff showed the practical value of the concept in which failure time is determined from an analysis of the unbounded quasi-viscous flow of a body. Discussion and literature references on the problem of "viscous" failure are presented in [2].

One of the most important practical problems of this kind is that of tube failure. In [3] Kats found the time for viscous failure of a tube under the influence of the internal pressure p. In the following, we consider a more general problem in which the load is made up of the internal pressure p and the axial force P.

Let a and b be the instantaneous internal and external radii of the tube. In accordance with the Hoff scheme, failure occurs when a→b $\left(\frac{b}{a} = \beta \rightarrow 1\right)$.

Let us derive the differential equation for β. We start from the obvious relation

$$\frac{d\beta}{dt} = \frac{1}{a}\left(\frac{db}{dt} - \frac{b}{a} \cdot \frac{da}{dt}\right). \tag{1}$$

The following formula for the creep deformation rate in the
tangential direction was obtained in [4], devoted to an analysis
of the stress state of a tube under the influence of internal pressure
p and axial force P

$$\xi_\tau = \frac{c'}{r^2} - \frac{k}{2},$$
(2)

where

$$c' = \frac{3p^2}{2\lambda_p} k;$$
$$\lambda_p = \frac{P - p\pi a^2}{p\pi a^2};$$

2   (creep rate in the axial direction).

Introducing the value (2) into the expressions

$$\frac{db}{dt} = v_r|_{r=b} = (r\xi_\tau)|_{r=b}, \quad \frac{da}{dt} = (r\xi_\tau)|_{r=a},$$
(3)

substituting the result into (1) and noting the connection
between k and c', we obtain

$$\frac{2}{3} \cdot \frac{\lambda_p}{k} \cdot \frac{d\beta}{\beta(\beta^2 - 1)} = -dt.$$
(4)

In the new notations

$$\bar{k} = \frac{k}{Bp^m}, \quad \bar{t} = Bp^m t$$

(B is a coefficient and m is the creep index) we rewrite (4) as

$$\frac{2}{3} \cdot \frac{\lambda_p}{\bar{k}} \cdot \frac{d\beta}{\beta(\beta^2 - 1)} = -d\bar{t}.$$
(4')

We write the formula for the radial stress σ_r obtained in [4]
in the form

$$\bar{\sigma}_r \equiv \frac{\sigma_r}{p} = 2 \cdot 3^{\frac{1+m}{m}} \beta^2 \frac{\bar{k}^{\frac{1}{m}}}{\lambda_p} \mathbf{F}(\beta, \lambda_p, \beta, m) - 1,$$
(5)

where

$$\Psi(\rho, \lambda_p, \beta, m) = \int_1^\rho \left(1 + \frac{3}{\lambda_p^2} \cdot \frac{\beta^4}{\rho^4}\right)^{\frac{1-m}{2m}} \frac{d\rho}{\rho^3} \quad \left(\rho = \frac{r}{a}\right).$$

Considering $\lambda_p = \text{const}$, we find $\bar{k}$ from the boundary condition $\bar{\sigma}_r |_{r=a} = 0$ and substitute it into (4')

$$2^{m+1} 3^{\frac{m-1}{2}} \frac{\Psi^m(\beta, \lambda_p, m)}{\lambda_p^{m-1}} \cdot \frac{\beta^{2m-1} d\beta}{\beta^2 - 1} = -d\bar{t}. \tag{6}$$

where

$$\Psi(\rho, \lambda_p, m) = \Psi(\rho, \lambda_p, \beta, m) |_{\rho = \beta}.$$

We introduce the function

$$Q(\beta, \lambda_p, m) = \frac{1}{\lambda_p^{m-1}} \int_1^\beta \Psi^m(\beta, \lambda_p, m) \frac{\beta^{2m-1}}{\beta^2 - 1} d\beta.$$

Then, integrating (6) with the condition $\beta |_{\bar{t}=0} = \beta_0$, we obtain

$$2^{m+1} 3^{\frac{m-1}{2}} [Q(\beta_0, \lambda_p, m) - Q(\beta, \lambda_p, m)] = \bar{t}. \tag{7}$$

Considering that $Q(1, \lambda_p, m) = 0$, we find the failure time

$$\tag{8}$$

$$\bar{t}_q = 2^{m+1} 3^{\frac{m-1}{2}} Q(\beta_0, \lambda_p, m).$$

REMARKS.

1. If $P = p\pi a^2$, then $\lambda_p = 0$. Considering the relation $\frac{k}{c^2} = \frac{2\lambda_p}{36\pi}$, after transformation, we obtain

$$Q(\beta, 0, m) = \frac{m^m}{2^m 3^{\frac{m-1}{2}}} \int_1^\beta \left(1 - \beta^{-\frac{2}{m}}\right)^m \frac{\beta d\beta}{\beta^2 - 1}.$$

Table 1

Values of the Function $\Psi(\lambda, \lambda_p, m)\cdot 10$

λ	λ_p=1					λ_p=3					λ_p=5				
	m=1	m=3	m=5	m=7	m=9	m=1	m=3	m=5	m=7	m=9	m=1	m=3	m=5	m=7	m=9
1.00	0.000	0.000	0.000	0.000	0.000	0.000	0.000	0.000	0.000	0.000	0.000	0.000	0.000	0.000	0.000
1.05	0.286	0.359	0.246	0.143	0.280	0.355	0.359	0.355	0.419	0.410	0.406	0.405
1.10	0.620	0.469	0.449	0.440	0.609	0.669	0.657	0.660	0.774	0.787	0.750	0.746
1.15	0.712	0.640	0.611	0.598	0.986	0.922	0.994	0.994	1.228	1.061	1.040	1.034
1.20	0.870	0.890	0.742	0.723	1.191	1.133	1.199	1.098	1.395	1.200	1.288	1.277
1.25	1.000	0.980	0.846	0.823	1.379	1.208	1.270	1.263	1.436	1.612	1.493	1.483
1.30	1.107	1.052	0.930	0.904	1.587	1.433	1.419	1.400	1.741	1.691	1.691	1.656
1.35	1.193	1.109	0.997	0.967	1.669	1.573	1.533	1.511	1.905	1.843	1.815	1.801
1.40	1.264	1.154	1.049	1.017	1.760	1.671	1.626	1.602	2.041	1.989	1.938	1.923
1.45	1.321	1.189	1.089	1.065	1.871	1.750	1.701	1.675	2.157	2.103	2.041	2.052
1.50	1.367	1.215	1.130	1.084	1.946	1.814	1.761	1.731	2.254	2.236	2.125	2.104
1.55	1.403	1.234	1.143	1.104	2.007	1.865	1.808	1.776	2.335	2.343	2.196	2.172
1.60	1.431	1.247	1.169	1.119	2.057	1.906	1.843	1.809	2.405	2.380	2.250	2.223
1.65	1.452	1.255	1.166	1.128	2.096	1.934	1.869	1.834	2.461	2.409	2.294	2.268
1.70	1.468	1.259	1.175	1.135	2.127	1.966	1.938	1.851	2.527	2.430	2.328	2.300
1.75	1.178	1.260	1.175	1.130	2.160	1.971	1.906	1.861	2.544	2.444	2.371	2.324
1.80	1.485	1.258	1.173	1.128	2.167	1.989	1.908	1.886	2.573	2.452	2.382	2.339
1.85	1.488	1.263	1.166	1.119	2.178	1.993	1.802	1.860	2.595	2.455	2.387	2.349
1.90	1.488	1.248	1.155	1.110	2.184	1.993	1.895	1.852	2.611	2.464	2.388	2.351
1.95	1.484	1.238	1.147	1.100	2.187	1.978	1.895	1.841	2.621	2.353	2.352
2.00	1.90	1.238			2.185	1.971	1.986		2.627		2.384	2.346

We have obtained the formulas found by Kats [3] for viscous failure of a tube under the influence of the internal pressure p.

2. It is not difficult to show that for p = 0 β = const.

In fact, introducing the expression for the creep rate in the tangential direction

$$\xi_\varphi = \frac{1}{2} BT^{m-1}(s_\varphi - \sigma) = -\frac{1}{2 \cdot 3^{\frac{m+1}{2}}} B\sigma_\delta^m \quad \left(\sigma = \frac{s_r + s_\varphi + s_z}{3}\right)$$

into (3) and substituting the result into (1) we obtain

$$\beta = const = \beta_o.$$ (5)

Consequently the method of solution based on analysis of the variations of β is not suitable. Therefore, the Hoff solution [1] for a bar in tension does not follow from (8).

We present a table of the values of:

1). the functions $\Psi(\beta, \lambda_p, m) = \int \left(1 + \frac{3}{\lambda_p^2} \cdot \frac{\beta^4}{t^4}\right)^{\frac{1-m}{2m}} \frac{d\rho}{\rho^3}$, calculated for $\lambda_p = 1, 2, 3; \ m = 3, 5, 7, 9$ with β varying from 1.00 to 2.00 (0.05 steps);

Table 2

Values of the Function $t_o(\beta, \lambda_p, m) \cdot 10$

β	$\lambda_p=1$				$\lambda_p=2$				$\lambda_p=3$			
	$m-3$	$m-5$	$m-7$	$m-9$	$m-3$	$m-5$	$m-7$	$m-9$	$m-3$	$m-5$	$m-7$	$m-9$
1.50	2,480	3,498	9,193	27,283	1,586	1,220	1,749	2,900	1,005	0,441	0,265	0,337
2.00	8,500	10,770	18,745	39,813	6,310	5,591	6,154	7,630	4,530	2,868	2,203	1,845

2). the function $\bar{t}_o(\beta, \lambda_p, m)$ for a) $\beta_0 = 1.50$, b) $\beta_0 = 2.00$ for the same λ_p and m.

Curves of the functions $\Psi(\beta, \lambda_p, m) \cdot 10$ and $\bar{t}_o(\beta, \lambda_p, m) \cdot 10$ are shown in Figures 1 and 2.
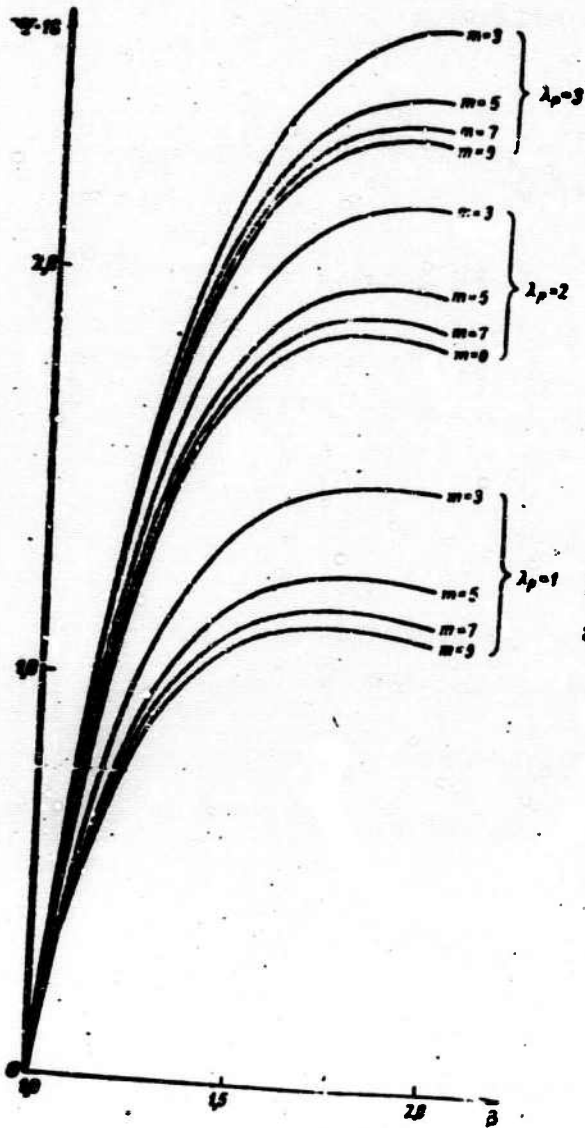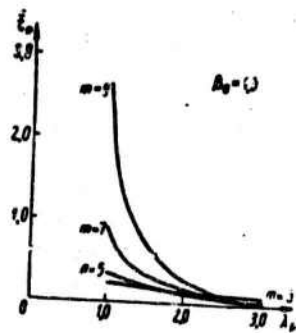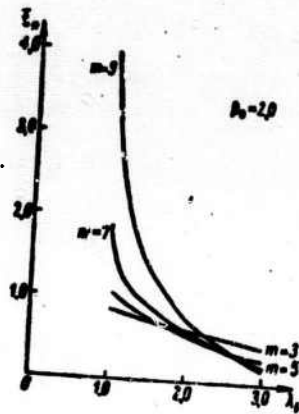
Figure 1

Figure 2

REFERENCES

1. Hoff, N., The necking and the rupture of rods subjected to constant tensile loads. J. appl. mech., 1953, Vol. 20, No.1.

2. Kachanov, L. M., "Some questions of Failure Under Creep Conditions," In: Polzuchest'i dlitel'naya prochnost' (Creep and Long-Term Strength), Novosibirsk, Press of the Siberian Division of the Academy of Sciences of the USSR, 1963.

3. Kats, Sh. N., "Creep and Failure of Tubes Subjected to Internal Pressure," IAN SSSR, OTN, NO. 10, 1957.

4. Finnie, I., Steady-state Creep of a Thick-Walled Cylinder under Combined Axial Load and Internal Pressure. Transactions of the ASME, 1960, ser. D-82, No. 3.

Received 1 April 1964

EFFECT OF PRELIMINARY PLASTIC DEFORMATION
ON THE YIELD LIMIT OF ST. 45 STEEL

A. I. Chistyakov

Tubular specimens were prepared from 55-mm-diameter annealed rods. A plane stress state at points of the specimen cross section was created by simultaneous application of an axial force and internal pressure. The axial force was measured to within $\pm$ 1%, the internal pressure to within 1 kg/cm^2.

The longitudinal and transverse deformations of the specimen were measured by wire resistance pickups with base length 24 mm and bridge amplifiers. In order to account for the possible slight eccentricity in the specimen installation, the longitudinal gages were mounted along two opposite generators.

§ 1. Yield Limit for Simple Stress

To construct the yield limit, we tested nine specimens using the following stress paths α = 0, 15, 30, 45, 60, 75, 90°, and in order to determine more precisely the yield point σ_{so} for the St. 45 steel three specimens were tested with α = 90°.

As is known, under simultaneous application of the axial force P and the internal pressure p, the effective stresses are determined from the formulas

$$\sigma_\theta = p \frac{d}{2\delta},$$
$$\sigma_z = \frac{P}{F} + p \frac{\pi d^2}{4F}. \qquad (1)$$

Since small elasto-plastic deformations are considered, the effective stresses will be close to the true stresses.

The loading path in the $(\sigma_z,\ \sigma_\theta)$ plane is defined by the expression

$$\frac{\sigma_z}{\sigma_\theta} = \operatorname{tg}\alpha = n. \qquad (2)$$

Substituting into this equality the expressions (1) for σ_θ and σ_z, we obtain the dependence of P on p

$$P = p \frac{\pi d}{4}\left[nD + (n-1)d\right]. \qquad (3)$$

To determine the yield point we plotted the curves $\sigma_i = f(e_i)$, where

$$e_i = \sqrt{\sigma_\theta^2 - \sigma_\theta \sigma_z + \sigma_z^2},$$
$$e_i = \frac{\sqrt{2}}{3}\sqrt{(e_\theta - e_z)^2 + (e_z - e_r)^2 + (e_r - e_\theta)^2}. \qquad (4)$$

The deformation e_r in the elastic region was found from the formula

$$e_r = -\frac{\mu}{1-\mu}(e_\theta^y + e_z^y). \qquad (5)$$

and in the plastic region from

$$e_r = -\frac{\mu}{1-\mu}(e_\theta^y + e_z^y) - (e_\theta^n + e_z^n). \qquad (6)$$

The relative permanent elongation 0.2% at the effective yield limit for $\mu = 0.27$ corresponds to the intensity $e_{is} = 0.17\%$. From the value of e_{is}, we find the values of the stress intensity σ_{is} and in Figure 1 we plot the Mises ellipse in the relative coordinates $\frac{\sigma_{zz}}{\sigma_{s0}}; \frac{\sigma_{\theta\theta}}{\sigma_{s0}}$, where $\sigma_{s0} = 3100$ kg/cm^2 is defined as the average value for the three specimens with deviation from the mean of $\pm 1.5\%$.
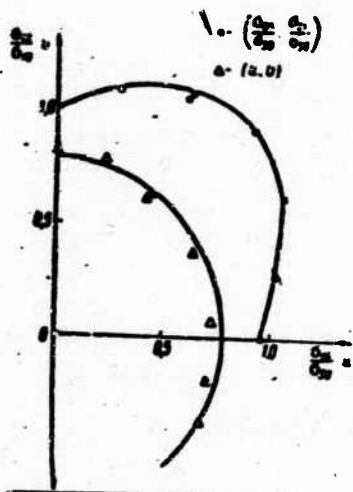
Figure 1

We can also plot the yield limit on the Il'yushin plane if we use the transformation to the new variables σ_1 and σ_2 on the basis of the formulas

$$\sigma_1 = \sqrt{3}\,z_1,$$
$$\sigma_2 = \sqrt{\tfrac{3}{2}}\,\sigma_1 + \frac{z_2}{\sqrt{2}}. \qquad (7)$$

In so doing the Mises ellipse will be transformed into a circle with the same center.

If we denote

$$x = \frac{\sigma_{11}}{z_{20}}; \; y = \frac{\sigma_{22}}{\sigma_{20}},$$
$$u = \frac{\sigma_{11}}{\sigma_{20}}; \; v = \frac{\sigma_{22}}{\sigma_{20}}, \qquad (8)$$

then we have from (7)

$$u = \frac{x}{\sqrt{2}}; \; v = \sqrt{\tfrac{2}{3}}\,y - \frac{x}{\sqrt{6}}.$$
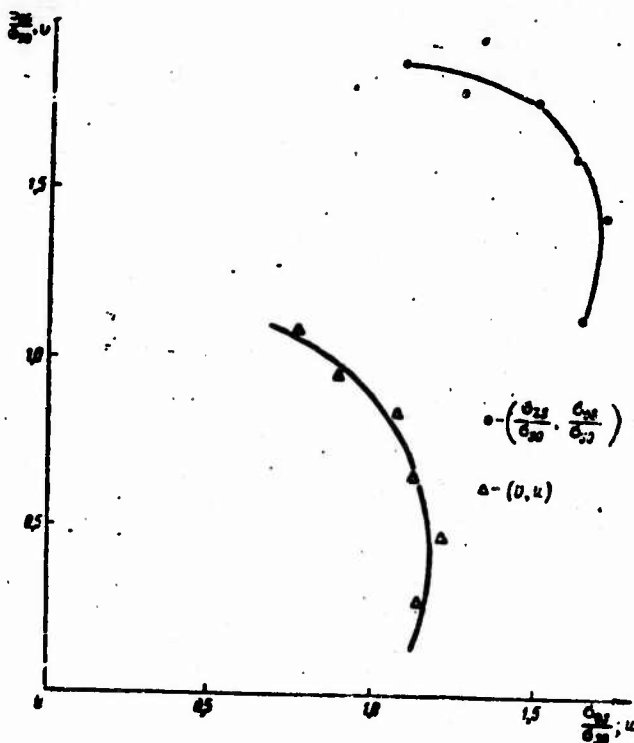
Figure 2

The yield limit on the Il'yushin plane is plotted in this same figure.

For an isotropic material the yield curve must be a circle on the Il'yushin plane.

In our case the curve in Figure 1 differs somewhat from a circle in the direction of the σ_θ axis. This can apparently be explained by the fact that the specimen material has a lower yield limit in the transverse direction than in the longitudinal direction.

§ 2. Yield Limit for Compound Loading

Six specimens of a given lot were loaded to $\sigma_1 = 1.7\sigma_{s0}$ in the direction $\alpha = 45°$ and then were unloaded along the same path. After unloading the specimen dimensions were measured and each specimen was again loaded along a given direction.

The following directions were used for the second loading in the experiment: $\alpha = 35, 40, 45, 50, 55, 60°$. From the test data, we found the yield points and plotted the yield curve in the relative coordinates (Figure 2)

$$\frac{\sigma_{22}}{\sigma_{s0}} ; \frac{\sigma_{12}}{\sigma_{s0}} .$$

Figure 2 also shows the yield curve on the Il'yushin plane, which indicates that the yield limit is shifted in the direction coinciding with the direction of the preliminary plastic deformation and does not have angular points.

The shape of the yield limit for the plane stress state is independent of the loading direction and is a circle in the Il'yushin plane.

In conclusion, the auther wishes to thank Docent G. B. Talypov for guidance in setting up the experiments.

REFERENCES

1. Talypov, G. B., and V. N. Kamentsev, "Study of the Yield Limit and Certain other Effects under Compound Loading", Scientific Notes of Leningrad State University, Mathematical Sciences Series, No. 35, 1964.

PHOTOELASTIC STUDY OF THE EFFECT OF BOTTOM SHAPE ON THE STRESS STATE OF THICK-WALL VESSELS

T.D. Maksutova

The present article is an extension of the description of the results of an optical polarization study of thick-wall cylindrical vessels. The purpose of the study is to obtain the most complete possible description of the stress state as a function of the values of the parameters characterizing the vessel geometry.

Table 1.

Models	R_1/R_0	t	h	ρ_0	ρ_1
Model 1	2	1	1	0.167	0
Model 2	2	1	1	0.167	1.167
Model 3	2	1	1	1	2

In a preceding study[1], we examined the effect of the cylinder outer/inner radii ratio R_1/R_0 on the stress state of a thick-wall vessel with flat bottom and constant wall thickness. In the present article, we use the example of a cylindrical vessel with ratio R_1/R_0 equal to two to examine the effect of the geometry of the region where the vessel wall joins the bottom, and the shape of the bottom on the stress state. To clarify the posed question, we consider three vessel geometries (Figure 1, Table 1). The quantities which characterize the vessel geometry are given in dimensionless form, and we take as the characteristic dimension, just as in the preceding article, the magnitude

(Footnote 1. See page 225.)

R_0 of the cylinder inner radius. Consequently, the stress state of
the vessels is described in the dimensionless variables $\rho = r/R_0$,
$\zeta = z/R_0$, and the vessel geometry is characterized by the dimension-
less quantities: bottom height (h), wall thickness (t), inner (ρ_0)
and outer (ρ_1) bond radii.
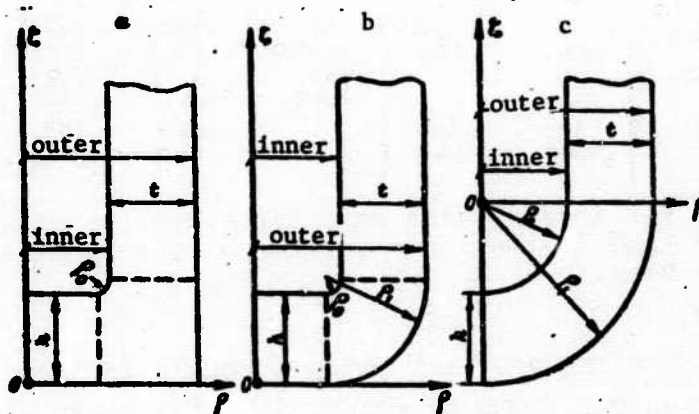
Figure 1. Geometry of vessels with different bottom shape.

As the basic version (Figure 1a), we considered the model with
flat bottom, small inner bond radius ($\rho_0 \simeq 0.167$) and outer square
corner ($\rho_1 = 0$). As the second characteristic case (Figure 1c), we
studied the stress state of a vessel with hemispherical bottom
($\rho_0 = 1$; $\rho_1 = 2$). The vessel with a flat bottom, small inner bond
radius $\rho_0 \simeq 0.167$) and outer corner cut at the radius ($\rho_1 = \rho_0 + t$)
is an intermediate version (Figure 1b).

In models 1 and 2, the distribution of the stress state components
in the bottom and a portion of the adjacent transition region is deter-
mined along the lines ρ = const, parallel to the vessel axis of
symmetry. To calculate σ_z in this region, we use the second equili-
brium equation in cylindrical coordinates, which leads to the familiar
formula[2]

$$\bar{\sigma}_s = \bar{\sigma}_s^0 - \int_0^z \left(\frac{\partial \bar{\tau}_{zr}}{\partial r} + \frac{\bar{\tau}_{zr}}{r} \right) dz. \tag{1}$$

As usual, $\partial \bar{\tau}_{zr}/\partial r$ is calculated from the corresponding values in two
auxiliary sections, $\bar{\tau}_{zr}$ are the values of the tangential stress at
the points of the basic section being considered, and r, the distance

(Footnote 2. See page 225.

from the axis of symmetry, is a constant along the entire path of integration. The normal stress σ_z at points of the axis of symmetry cannot be calculated directly from (1), since along this line $r = 0$ and $\tau_{zr} = 0$. Therefore, we must first eliminate the indeterminancy, which leads in final form to the following expression

$$\bar{\sigma}_z = \bar{\sigma}_z^0 - 2 \int_0^z \frac{\partial \bar{\tau}_{zr}}{\partial r} dz. \tag{2}$$

Thus, to determine σ_z in the bottom and in the adjacent portion of the transition region we need only have available data obtained on the basis of measurements of the optical quantities in the radial section $\rho\zeta$ whose middle plane coincides with the vessel plane of symmetry.

To calculate σ_r in the vessel wall and in the portion of the transition region directly adjacent to it, it is natural to use the first equilibrium equation in cylindrical coordinates. In this case, we have

$$\bar{\sigma}_r = \bar{\sigma}_r^0 - \int_{R_1}^r \left(\frac{\partial \bar{\tau}_{rz}}{\partial z} + \frac{\bar{\sigma}_r - \bar{\sigma}_\theta}{r} \right) dr. \tag{3}$$

The calculation of σ_r using (3) requires that we have data along two mutually perpendicular planes — along the lines $\zeta = $ const in the radial plane and along the radius in the corresponding plane $\zeta = $ const.

In calculating both σ_z and σ_r, the origin for the integration path was selected at points on the free surface of the model, so that as a result of the calculations we determined the value of the corresponding component of the stress state normal to the inner loaded surface, and at the end of the integration path nominally equal to the magnitude of the internal pressure. Naturally, for different sections ($\rho = $ const or $\zeta = $ const) we obtain different, but only slightly differing, values of the stress state component σ_ν normal to the surface.

The resultant of the tangential stresses $\bar{\tau}_{zr}$, acting on a cylindrical surface of radius ρ isolated from the bottom is equilibrated by the resultant of the internal pressure p. On the basis of the corresponding area, $2\pi\rho\bar{T}_{zr}$ equals $\pi\rho^2\bar{p}$, where $\bar{T}_{zr}$ is the area of the

corresponding tangential stress diagram. Since the quantities $\bar{T}_{zr}$ are determined from experimental data, this equilibrium condition is not satisfied exactly. Consequently, the quantities $\bar{p}_1$ calculated for different cylindrical elements of radii ρ_1 differ somewhat from one another: $\bar{p}_1 = 2\bar{T}_{zr}^1/\rho_1$.

In reducing the experimental data, it was found to be advisable to determine the magnitude of the internal pressure as the average of all the values $\bar{\sigma}_z$ and $\bar{\sigma}_r$ determined by integration at the points of the inner surface of the model and the $\bar{p}_1$, calculated from the resultant of the tangential stresses in the bottom

$$\bar{p}_{av} = \frac{\sum\limits_1^k \bar{\sigma}_z^i + \sum\limits_1^l \bar{\sigma}_r^i + \sum\limits_1^m \bar{p}_i}{k+l+m}$$

In this case, the optical activity coefficient C is calculated from the formula $C = \bar{p}_{av}/dp$, where p is the internal pressure acting on the vessel model, measured by a manometer.

The deviations of $\Delta\bar{\sigma}_r$ and $\Delta\bar{\sigma}_z$ of $\bar{\sigma}_r$ and $\bar{\sigma}_z$ at the points of the inner surface of the model from the value $\bar{p}_{av}$ and the deviations ($\Delta\bar{T}_{zr}$) of the resultant tangential stresses $\bar{T}_{zr}$ in the bottom from the corresponding values $\bar{p}_{av}\rho/2$ define the accuracy with which the experimental study is carried out (Table 2).

Analysis of the results obtained from all three models showed that the average error in the determination of the stresses normal to the inner surface, calculated by integration, is 2.8% with a maximal deviation from the average value of 9.3%. The error in the determination of the principal vector of the tangential stresses in the bottom is 2.9% with a maximal deviation of 9%.

It is natural to describe the stress state of the hemispherical bottom of model 3 in the polar coordinates ρ, ψ, θ, and that of the wall in cylindrical coordinates ρ, ζ, θ. Within the limits of the bottom, the stress state components were determined along the axis of symmetry ($\psi = 180°$) and along the line where the bottom joins the cylindrical wall of the vessel ($\psi = 90°$, the boundary of the transition

Table 2.

Deviation, %

Models	$\dfrac{\Delta\bar\sigma_r}{\bar p_{av}}$	av	$\dfrac{\Delta\bar\sigma_z}{\bar p_{av}}$	av	$\dfrac{\Delta\bar\sigma_{zr}}{\bar p_{av}\frac{\rho}{2}}$	av	$\dfrac{\Delta\bar\sigma_r}{\bar p_{av}}$	$\dfrac{\Delta\bar\sigma_z}{\bar p_{av}}$	$\dfrac{\Delta\bar T_{zr}}{\bar p_{av}\frac{\rho}{2}}$
							Average	Maximal	
Model 1	$\begin{matrix}1.6\\k=7\end{matrix}$		$\begin{matrix}3.2\\l=6\end{matrix}$		$\begin{matrix}2.7\\m=6\end{matrix}$		$\begin{matrix}+3.5\\-1.4\end{matrix}$	$\begin{matrix}+1.8\\-7.0\end{matrix}$	$\begin{matrix}+5.0\\-4.8\end{matrix}$
Model 2	$\begin{matrix}2.5\\k=12\end{matrix}$		$\begin{matrix}4\\l=5\end{matrix}$		$\begin{matrix}3.1\\m=5\end{matrix}$		$\begin{matrix}+4.7\\-3.7\end{matrix}$	$\begin{matrix}+0.2\\-9.3\end{matrix}$	$\begin{matrix}+9.0\\-1.9\end{matrix}$
Model 3	$\begin{matrix}1.9\\k=8\end{matrix}$		$\begin{matrix}4.9*\\l=4\end{matrix}$		—		$\begin{matrix}+1.8\\-4.1\end{matrix}$	$\begin{matrix}+5.0\\-6.7\end{matrix}$	—

* For model 3 data were taken for the stress normal to the inner surface of the spherical bottom.

region), and also along rays for which ψ equals 150° and 120°. The distribution of σ_r was found by integrating the first equilibrium equation in the rectangular coordinate system $x_1, x_2, x_3 (\sigma_r = \sigma_{x_1}; \sigma_\psi = \sigma_{x_2}; \sigma_\psi = \sigma_{x_3})$, since there is no obvious advantage in calculating σ_r by graphical integration of the corresponding equilibrium equation in polar coordinates. In order to obtain all the required data, it was necessary to perform measurements in two mutually perpendicular planes – the radial plane and that corresponding to the section ψ = const. The pieces and sections cut from the model were marked off using a large tooling microscope, which made it possible to ensure the required precision in performing this operation. Just as in the case of models 1 and 2, the optical activity coefficient C was determined from the formula $C = \bar p_{av}/dp$, and the experimentally determined value of the internal pressure $\bar p_{av}$ was calculated as the average value of all the quantities $\bar\sigma_r$ determined by integration at the points of the inner surface of the bottom and wall: $\bar p_{av} = \sum_{1}^{n}\bar\sigma_r^1/n$.

The patterns of the principal stress trajectories and the distribution of their differences in the $\rho\zeta$ plane (Figures 2 and 3) yield a good intuitive feel for the effect of the bottom shape and the shape of the region where the bottom joins the wall on the stress state in the vessel.
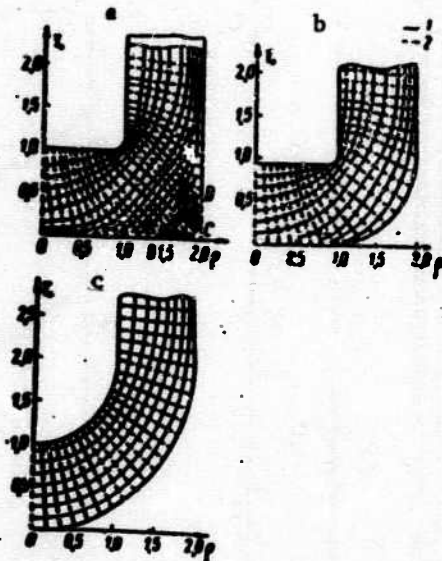
Figure 2. Principal stress trajectories in the $\rho\zeta$ plane: 1) trajectories S_1 of the principal stress σ'_1; 2) trajectories S_2 of the principal stress σ'_2; a-model 1; b-model 2; c-model 3.

The trajectories of the principal stresses in the $\rho\zeta$ plane (Figure 2) were plotted from the corresponding isocline patterns for each model. Comparison of the isostatic curves of the three models shows that the nature of the stress state for models 1 and 2 is the same in the bottom, the wall and the portion of the transition region adjacent to the inner loaded surface of the models. The stresses in the vessel with hemispherical bottom were distributed more uniformly than in the vessels with flat bottom and small inner bend radius, for which a marked crowding of the trajectories σ'_1, is observed near the inner surface of the region where the bottom and wall join, which indicates a significant local concentration of this stress. However, the σ'_1 trajectories in model 3 within the limits of the hemispherical bottom are nearly concentric circles, while the σ'_2 trajectories lie nearly in the radial directions.

On the basis of the experimental data obtained on models 1 and 2, in Figure 3 we have plotted the lines δ_{rz}/p = const in the bottom and the portion of the region where the bottom joins the wall directly adjacent to the inner surface of the models, and we have shown the distribution of $\delta_{rz}/\bar{p}$ along the axis of symmetry, along the generator $\rho \simeq 1 - \rho_0$ and along the outer and inner surfaces of the bottom closure. The lines $\delta_{rz}/\bar{p}$ = const within the limits of the bottom are
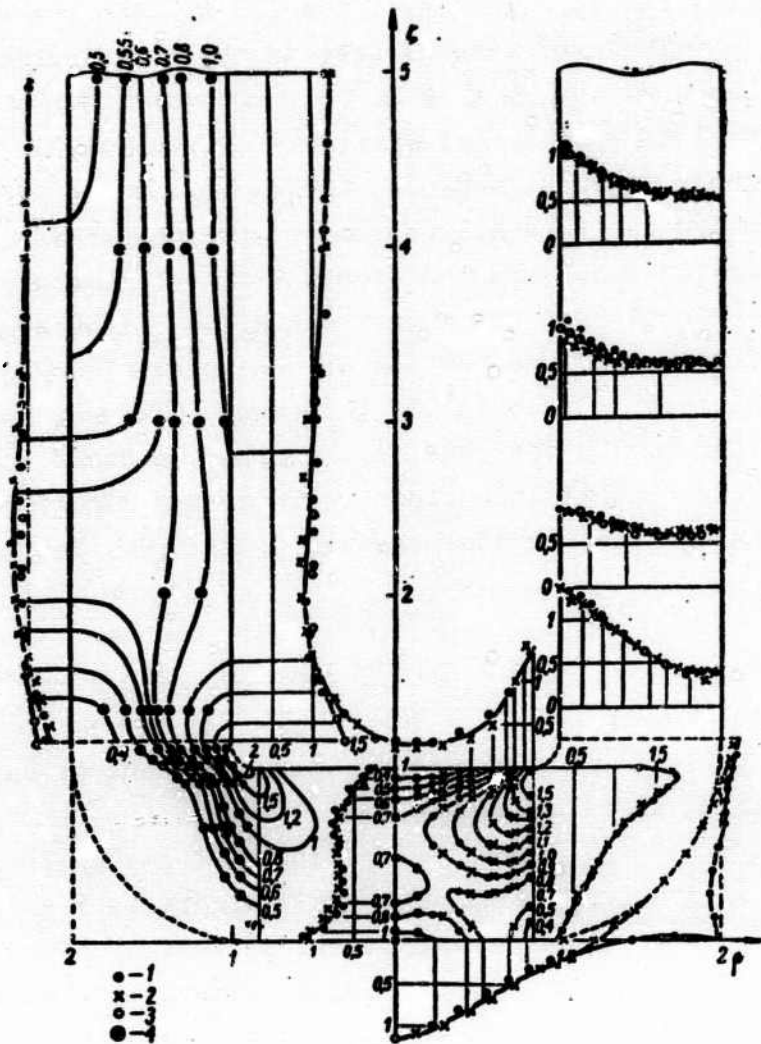
Figure 3. Distribution of $\sigma'_1 - \sigma'_2/p$, characterized by the lines $\sigma'_1 - \sigma'_2/p$ = const in the $\rho\zeta$ plane, by values at points of the inner and outer surfaces and by values at several sections ρ = const and ζ = const.

  • — model 1

  x — model 2

  o — model 3

  ☒ — common data for two (bottom) or three (wall) models

drawn through points plotted in the $\rho\zeta$ plane and taken from the curves $\delta_{rz}/\bar{p}$ constructed for models 1 and 2 in the various sections ρ = const. In those sections ρ = const (or ζ = const) in which experimental data were obtained on both models, the curves $\delta_{rz} = \delta_{rz}(\rho)$ or $\delta_{rz} = \delta_{rz}(\zeta)$ were plotted on the basis of these combined data and then we determined

from these curves the coordinates of the points with the corresponding values of $\delta_{rz}/\bar{p}$. The experimental data on the distribution of the stress state components σ_r, σ_z, σ_θ, τ_{rz} in the bottom and the transition region of models 1 and 2 were processed similarly (Figures 4-7). The results presented in these figures, and also the curves of the stress distribution constructed for several sections of the transition region and along its inner surface, show that for the vessel models with a flat bottom the distribution of all the stress state components within the limits of the bottom and the portion of the transition region adjacent to the inner surface is practically the same. However, the portions of the transition region adjacent to the outer unloaded surfaces have stress state component distributions which differ significantly from one another, though the stresses themselves are very low in magnitude in these regions.

Figures 8a and 8c, respectively, show the general patterns of the distribution of σ_r/p and σ_θ/p in the model with hemispherical bottom, while Figure 8b shows the general pattern of the σ_τ/p distribution, where σ_τ within the limits of the hemispherical bottom coincides with σ_ψ (polar coordinate system) while within the limits of the wall it coincides with σ_z (cylindrical coordinate system). Obviously, the distribution of the stress state components in the hemispherical bottom of model 3 differs considerably from that of the corresponding components in the bottom and the transition region of both models 1 and 2. Thus, the stress state in the hemispherical bottom is characterized by the fact that the normal stresses σ_ψ and σ_θ are tensile and do not change sign through the thickness, while in the models with a flat bottom there are regions of significant compressive normal stresses σ_r and σ_θ near the inner surface, which transition into tensile stresses only at the boundary where the bottom joins the wall. Also, σ_r and σ_θ are positive in a quite broad region of the bottom near the free surface. Finally, there are no marked normal stress concentrations at points of the inner surface of the model with hemispherical bottom. Conversely, at the points of the transition region on the inner surface of the model with a flat bottom there is a high concentration of all the stress state components.

Figure 4. Distribution of σ_r/p, characterized by the lines σ_r/p = const in the $\rho\zeta$ plane, by values at points of the inner and outer surfaces and values in several sections ρ = const and ζ = const.
Notations same as in Figure 3.

There are two possibilities for comparing the stress states in the walls of the three models under consideration: either align the boundaries of the transition regions of models 1 and 2 with the section ζ = 2 of model 3 (Figure 9a), or align the points ζ = 0 of the three models and consider the beginning of the wall to be the section ζ = 2, corresponding to the plane along which the hemispherical bottom joins the cylindrical wall of model 3 (Figure 9b). In the latter case, within the limits of the bottom for the first two models

Figure 5. Distribution of σ_z/p, characterized by the lines $\sigma_z/p = $ Const in the $\rho\zeta$ plane, by values at points of the inner and outer surfaces and values at several sections $\rho = $ const and $\zeta = $ const.

Notations same as in Figure 3.

there is included not only the bottom itself and the transition region, but also a portion of the cylindrical wall.

In constructing the general patterns of the stress state component distribution in the vessel wall we selected the first version for comparison of the data obtained for the three versions of vessel bottom geometry. Namely, we aligned the sections $\zeta = 1.167$ of the first two models with the section $\zeta = 2$ of model 3, and this plane
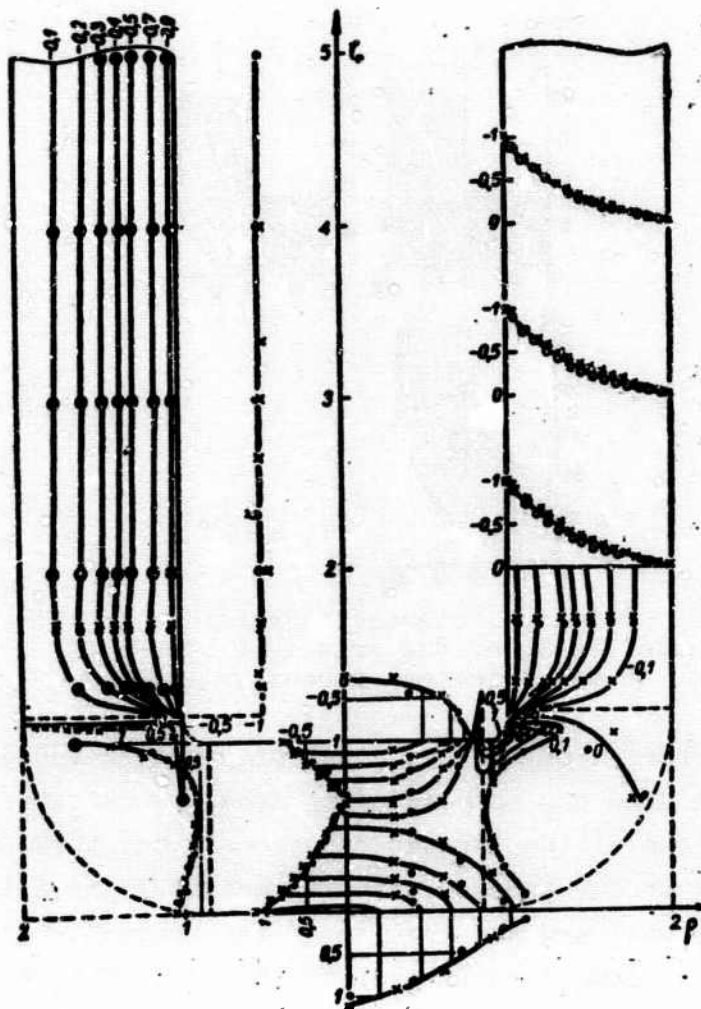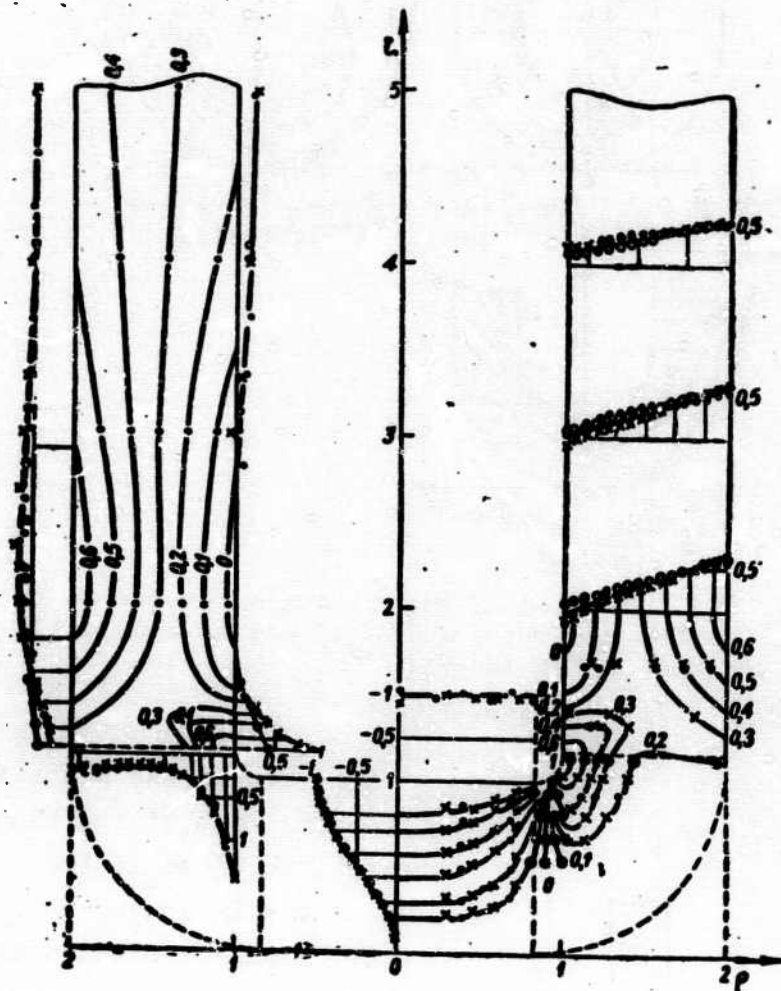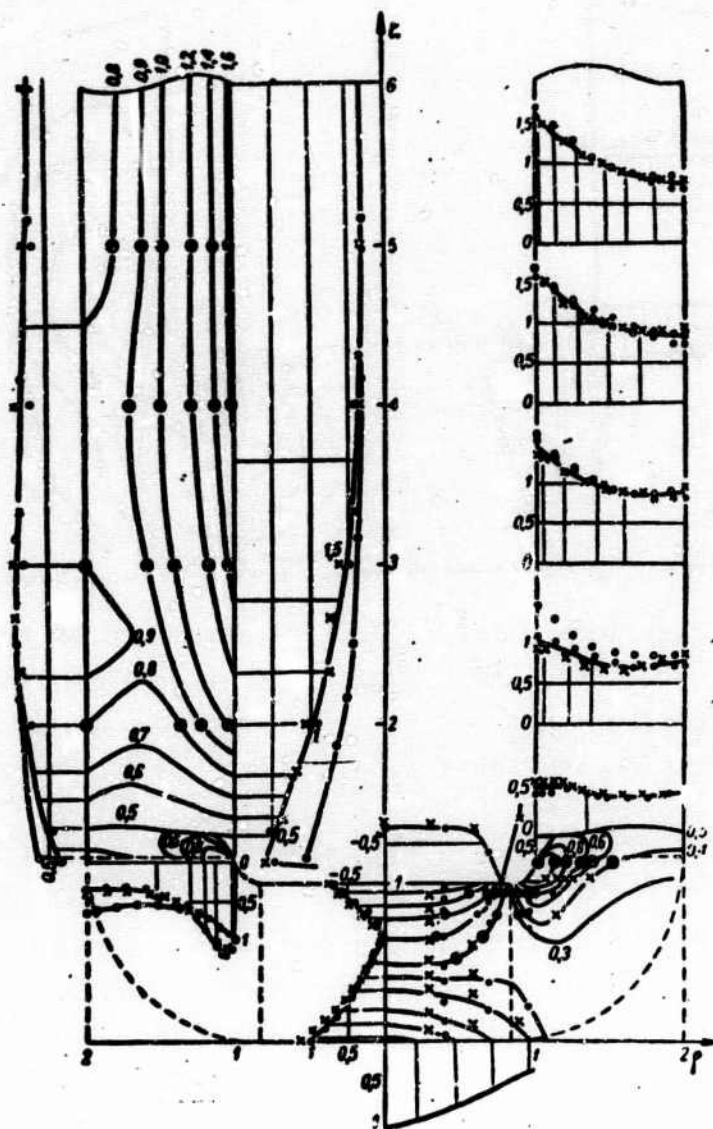
Figure 6. Distribution of σ_θ/p, characterized by the lines σ_θ/p = const in the $\rho\zeta$ plane, by values at points of the inner and outer surfaces and values at several sections ρ = const and ζ = const.

Notations same as in Figure 3.

was taken as the origin for measuring the axial coordinates ζ^* in the vessel wall. From the values of the stress state components calculated in section ζ^*=const (common for the three models) we plotted curves of the variation of the corresponding stresses along the radius.

The experimental data shown in Figures 4-7 show clearly that the distributions of all the stress state components for models 1 and 2
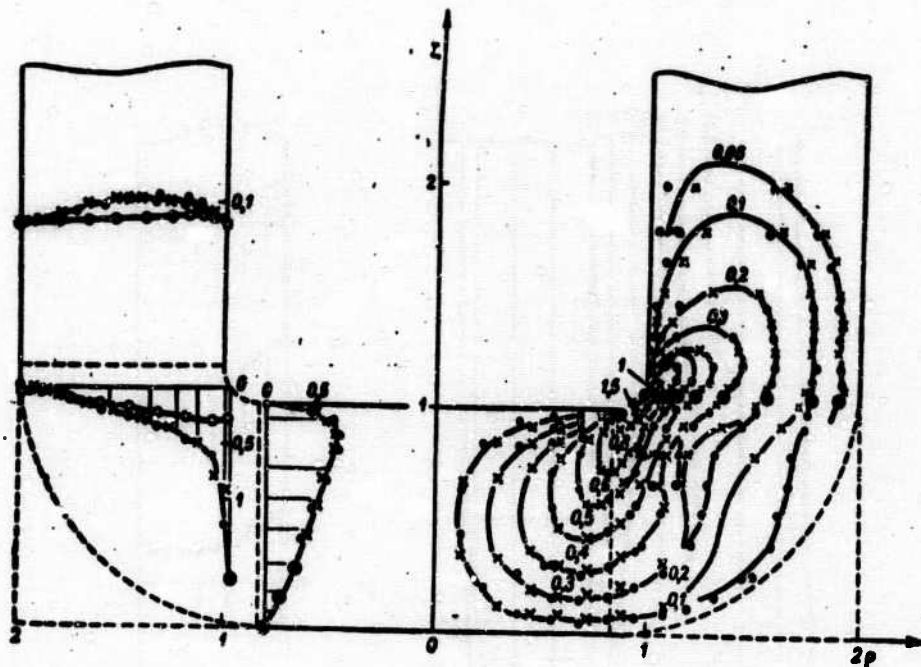
Figure 7. Distribution of τ_{rz}/p, characterized by the lines τ_{rz}/p in the $\rho\zeta$ plane and by values at several sections ρ = const and ζ = const.
Notations same as in Figure 3.

in the wall are also practically identical.

For $\zeta \geq 0.8$; the experimental values of σ_r obtained for model 3 fall on the curve which is common for models 1 and 2, which in turn differs little from the distribution curve for σ_r given by the Lamé solution.

The values of σ_θ obtained experimentally in the sections of model 3 lie on curves which are common for models 1 and 2 for $\zeta^* \geq 1.8$. Agreement of the experimental values with those calculated following Lamé is observed only for $\zeta^* > 2.8$. Here the experimental data systematically exceed the theoretical data near the free surface[3]. These deviations at individual points do not exceed 0.2p or 21% of the theoretical values at the same points, with the average deviation of $\sigma_{\theta\ exp}$ from $\sigma_{\theta\ Lamé}$ being of the order of 4%.

(Footnote 3. See page 225.)
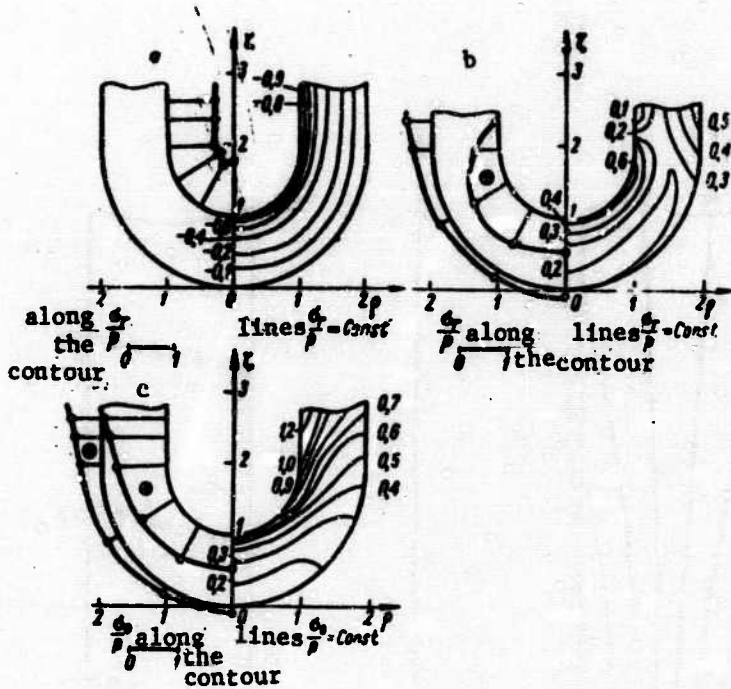
Figure 8. Distribution of stress state components in hemispherical bottom and the portion of the wall directly adjacent to the bottom for model 3.

a) σ_r/p; b) σ_τ/p, c) σ_θ/p
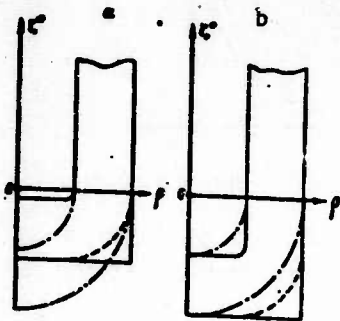
Figure 9. Two model comparison versions.

Analysis of the distributions of σ_z, the smallest of the three normal stresses, obtained in the vessel wall leads to the following conclusions: first, the experimental data obtained on model 3 lie on the curves which are common for models 1 and 2 for $\zeta^* \geq 0.8$; second, the distribution of σ_z through the thickness of the wall is nearly linear; and third, equilization of σ_z across the section $\zeta^* = $ const takes place extremely slowly and for $\zeta^* = 2.8$ the distribution of σ_z still differs significantly from the uniform distribution required by the theoretical Lamé solution (for $\rho = 1, \sigma_z = 0.16p$; for $\rho = 2, \sigma_z = 0.48p$).

FOOTNOTES

1. T.D. Maksutova, "Photoelastic study of thick-wall vessels with flat bottom," Studies in Elasticity and Plasticity, vol 3, Press of Leningrad State University, 1964. (see page 212)

2. Here and hereafter we use the previously introduced notations

$$\tau_r = \frac{\bar{\sigma}_r}{Cd}, \quad \tau_\theta = \frac{\bar{\sigma}_\theta}{Cd}, \quad \tau_z = \frac{\bar{\sigma}_z}{Cd}, \quad \tau_{zr} = \frac{\bar{\tau}_{zr}}{Cd},$$

where C is the material optical activity coefficient; d is the reduced section thickness. The tangential stresses in the $\rho\zeta$ plane were calculated from the formulas

$$\bar{\tau}_{zr} = \frac{\bar{\sigma}_z}{2} \sin 2\varphi_{zr}, \quad \bar{\tau}_{rz} = \frac{\bar{\sigma}_z}{2} \sin 2\varphi_{rz},$$

where ϕ_{rz} is the angle formed by the (algebraically greater in the section plane) principal stress σ'_1 with the positive direction of the radius, and ϕ_{zr} is the angle between σ'_1 and the positive direction of the z(ζ) axis. (see page 213)

3. This is easily explained by the neglected initial path difference $\delta^0_{r\theta} = 0$, which develops during polymerization of the cylindrical blanks, distributed nonuniformly across the section and not completely eliminated by annealing ($\delta^0_{r\theta} = 0$ at points of the axis of symmetry and distributed parabolically along the radius). (see page 223)

CALCULATING THE LOAD-CARRYING CAPACITY OF
IDEALLY PLASTIC AXISYMMETRIC SHELLS

V.I. Rozenblyum

The yield condition expressed in terms of forces and moments
("finite relation") is of fundamental importance in the theory of
limit equilibrium of ideally plastic shells. At the present time
these finite relations have been formulated for the cases of the Mises
medium [1-4] and for the Tresca-Saint Venant medium [5,6], and also
for certain other types of plastic media [7].[1] These finite relations
(within the framework of the usual hypotheses of thin shell theory
they may be considered as exact relations) have a very complex struc-
ture. In this connection considerable attention has also been devoted
to the question of the approximation of these exact yield conditions
by means of relatively simple surfaces which are more convenient for
application. The greatest simplicity is achieved if we take the
yield surfaces in the form of polygons[2], for example,

$$\max\{|t_1|,\ |t_2|,\ |t_1-t_2|,\ |m_1|,\ |m_2|,\ |m_1-m_2|\}=1,$$

where

$$(0.1)$$

$$t_1=\frac{T_1}{h\sigma_s},\quad m_1=\frac{M_1}{h^2\sigma_s\, t}$$

and so on, are dimensionless forces and moments; h is the shell thick-
ness, σ_s is the tensile yield limit.

The piecewise linear yield condition in the form (0.1) has been
widely used in many particular problems [8, 9, and others]. However,
the results obtained and the comparisons made with certain more exact

(Footnotes 1 and 2. See page 239.)

solutions[10] suggest that, generally speaking, the approximation of the actual yield surface by the piecewise linear relation (0.1) is too crude and in many cases may lead to unacceptable errors. The reason for this is, in part, that in the yield condition (0.1) we have ignored to a considerable degree the interaction of the force and moment factors, which has a significant effect on the plastic behavior (as follows, for example, from the elementary theory of plastic arches).

Under these conditions the question arises of the choice of a "compromise" version of the theory, possibly more complex in comparison with the simplest formulation based on (0.1), but at the same time leading to a more realistic description of the actual structural behavior.

In this connection we consider in the following the "quadratic" yield condition [11, 12]

$$(t_1^2 - t_1 t_2 + t_2^2) + (m_1^2 - m_1 m_2 + m_2^2) = 1$$

(0.2)

and its "semilinear" modification

$$\tau^2 + \mu^2 = 1,$$

(0.3)

where

$$\tau = \max \{|t_1|, |t_2|, |t_1 - t_2|\},$$
$$\mu = \max \{|m_1|, |m_2|, |m_1 - m_2|\}.$$

(0.4)

The results presented later for the axisymmetrically loaded shell of revolution show that the nonlinearity present in (0.2) and (0.3) appears to make it possible to approach more closely the exact solution than when using the piecewise linear condition (0.1); although the solutions are somewhat more complex in this instance, in many cases quite effective solutions may be obtained.

1. We first consider the quadratic yield condition (0.2), which on the basis of the associated flow law corresponds to the middle surface deformation rates

$$\dot{\epsilon}_1 = \lambda \left(t_1 - \frac{1}{2} t_2 \right), \quad \dot{x}_1 = \frac{4}{h} \lambda \left(m_1 - \frac{1}{2} m_2 \right),$$
$$\dot{\epsilon}_2 = \lambda \left(t_2 - \frac{1}{2} t_1 \right), \quad \dot{x}_2 = \frac{4}{h} \lambda \left(m_2 - \frac{1}{2} m_1 \right).$$

(1.1)

where λ is a nonnegative coefficient of proportionality. The yield condition (0.2) may be satisfied by taking

$$l_1 = \frac{2}{\sqrt{3}} \sin\omega\cos\left(\psi - \frac{\pi}{6}\right), \quad m_1 = \frac{2}{\sqrt{3}} \cos\omega\cos\left(\theta - \frac{\pi}{6}\right),$$
$$l_2 = \frac{2}{\sqrt{3}} \sin\omega\cos\left(\psi + \frac{\pi}{6}\right), \quad m_2 = \frac{2}{\sqrt{3}} \cos\omega\cos\left(\theta + \frac{\pi}{6}\right). \tag{1.2}$$

Substitution of these expressions into (1.1) yields

$$\dot\epsilon_1 = \lambda \sin\omega\cos\left(\psi - \frac{\pi}{6}\right), \quad \dot\varkappa_1 = \frac{4\lambda}{h}\cos\omega\cos\left(\theta - \frac{\pi}{3}\right),$$
$$\dot\epsilon_2 = \lambda \sin\omega\cos\left(\psi + \frac{\pi}{3}\right), \quad \dot\varkappa_2 = \frac{4\lambda}{h}\cos\omega\cos\left(\theta + \frac{\pi}{3}\right). \tag{1.3}$$

If we substitute (1.2) into the usual system of (three) equilibrium equations of the axisymmetric shell

$$\frac{dA_2T_1}{d\alpha_1} - \frac{dA_2}{d\alpha_1}T_2 + \frac{N_1}{R_1}A_1A_2 + q_1A_1A_2 = 0,$$
$$\frac{dA_2N_1}{d\alpha_1} - \left(\frac{T_1}{R_1} + \frac{T_2}{R_2}\right)A_1A_2 + q_nA_1A_2 = 0, \tag{1.4}$$
$$\frac{dA_2M_1}{d\alpha_1} - \frac{dA_2}{d\alpha_1}M_2 - N_1A_1A_2 = 0$$

(R_1, R_2 are the principal radii of curvature, A_1, A_2 are the Lamé parameters, α_1 is the coordinate corresponding to the meridional direction) and if we substitute (1.3) into the two equations for deformation compatibility, then as a result we obtain a system of five differential equations in terms of the unknown functions λ, ω, ψ, θ and the shearing force N_1. Generally speaking, the solution may be obtained by numerical methods· However, the energy approach, which leads to two-sided estimates of the limit load [11], is far more effective. In order to obtain the lower estimate we must construct a statically possible force and moment field which satisfies the static equations (1.4), the static boundary conditions, and does not contradict the yield condition (0.2). The upper estimate is found by equating the internal energy dissipation and the eternal force intensity A at kinematically possible rates

$$\frac{2}{\sqrt{3}} T_s \iint \Gamma A_1 A_2 d\alpha_1 d\alpha_2 = A, \tag{1.5}$$

where

$$\Gamma = \sqrt{(\dot\epsilon_1^2 + \dot\epsilon_1\dot\epsilon_2 + \dot\epsilon_2^2) + \frac{h^2}{16}(\dot\varkappa_1^2 + \dot\varkappa_1\dot\varkappa_2 + \dot\varkappa_2^2)}. \tag{1.6}$$

We note that by virtue of the known inequalities

$$\frac{\sqrt{3}}{2}\tau < (t_1^2 - t_1 t_2 + t_2^2)^{1/2} < \tau,$$
$$\frac{\sqrt{3}}{2}\mu < (m_1^2 - m_1 m_2 + m_2^2)^{1/2} < \mu$$

(1.7)

every statically permissible (or exact) solution satisfying the semi-linear yield condition (0.3) is also statically permissible with relation to the quadratic condition (0.2). This makes it possible to use for the construction of the lower estimates the simpler condition (0.3) (or its linearized version (2.6), introduced later).

2. In using the semilinear relation (0.3) we must differentiate the regular and singular regimes. In the first case the usual associated flow law yields

$$\dot{\varepsilon}_1 = \lambda \tau \frac{\partial \tau}{\partial t_1}, \quad \dot{\varkappa}_1 = \frac{a}{h} \mu \frac{\partial \mu}{\partial m_1},$$
$$\dot{\varepsilon}_2 = \lambda \tau \frac{\partial \tau}{\partial t_2}, \quad \dot{\varkappa}_2 = \frac{a}{h} \mu \frac{\partial \mu}{\partial m_2}.$$

(2.1)

In the singular regime case (when one of the conditions: $t_1 = t_2$, $t_1 = 0$, $t_2 = 0$, $m_1 = m_2$, $m_1 = 0$, $m_2 = 0$ is met) the flow law is constructed in the form of a suitable linear combination of the regular laws in a fashion which is completely analogous to the corresponding construction in general plasticity theory. For example, let

$$\tau = t_1 = t_2, \quad \mu = m_1.$$

Then

$$\dot{\varepsilon}_1 = \alpha \dot{\varepsilon}_1^{(1)} + (1-\alpha) \dot{\varepsilon}_1^{(2)}, \qquad (0 < \alpha < 1),$$
$$\dot{\varepsilon}_2 = \alpha \dot{\varepsilon}_2^{(1)} + (1-\alpha) \dot{\varepsilon}_2^{(2)}$$

(2.2)

where the superscripts (1) and (2) denote the deformation rates calculated using (2.1) for the regular regimes $\tau = t_1$, $\tau = t_2$, respectively:

$$\dot{\varepsilon}_1^{(1)} = \lambda t_1, \quad \dot{\varepsilon}_1^{(2)} = 0,$$
$$\dot{\varepsilon}_2^{(1)} = 0, \quad \dot{\varepsilon}_2^{(2)} = \lambda t_2.$$

(2.3)

Combining (2.2) and (2.3) we obtain

$$\dot{\varepsilon}_1 + \dot{\varepsilon}_2 = \lambda t_1.$$

(2.4)

Moreover, for $\mu = m_2$ we have from (2.1)

$$\dot{\varkappa}_2 = \frac{a}{h} m_2, \quad \dot{\varkappa}_1 = 0.$$

(2.5)

We obtain the complete system of (four) equations of the flow law by adding to the three relations (2.4) and (2.5) the adopted condition

$$t_1 = t_2.$$

We note that in the case of singular regimes the problem of determining the stress state of the axisymmetric shell in the corresponding plastic regions becomes (internally) statically determinate.

To obtain a statically determinate problem in the general case (which is important for obtaining the lower bounds with the aid of statically permissible solutions), we can use the following approximate technique [11]. We replace one yield condition (0.3) by the following two conditions

$$\max\{|t_1|, |t_2|, |t_1 - t_2|\} = \delta_t,$$
$$\max\{|m_1|, |m_2|, |m_1 - m_2|\} = \delta_m.$$

$$(2.6)$$

where δ_t, δ_m are constants subject to the conditions

$$0 < \delta_t < 1, \quad 0 < \delta_m < 1,$$
$$\delta_t^2 + \delta_m^2 = 1.$$

$$(2.7)$$

These constants are determined in the final stage of the solution so as to obtain the maximal value for the limit load. The yield conditions (2.6) are analogous in form to the classical Tresca-Saint Venant yield condition and are formed by hexagons in the t_1, t_2 and m_1, m_2 planes (Figure 1). We note that an analogous technique is also possible in the case of the quadratic yield condition (0.2), for which we take

$$t_1^2 - t_1 t_2 + t_2^2 = \delta_t^2,$$
$$m_1^2 - m_1 m_2 + m_2^2 = \delta_m^2.$$

$$(2.8)$$
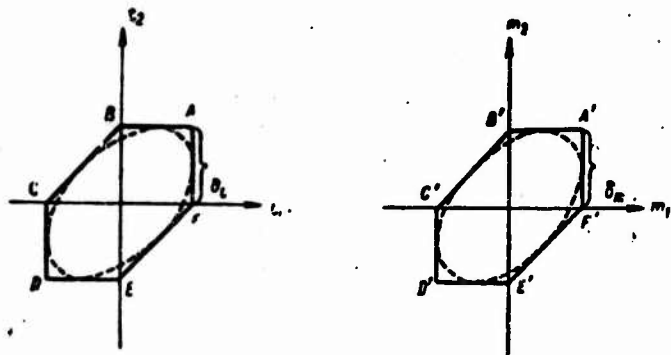
Figure 1

In Figure 1 ellipses inscribed in the hexagons (2.6) correspond to these conditions.

Let us consider some examples which clarify the use of these
techniques.
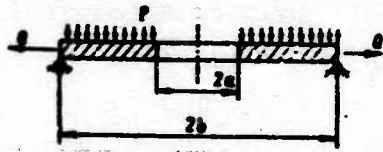
Figure 2.

3. It is convenient to make the com-
parison with other solutions on the basis
of combined bending and tension of an an-
nular plate (Figure 2), which has been
studied in detail by Hodge [9, 10]. We shall use the semilinear yield
condition (0.3) and assume the plastic regime

$$\tau = t_2, \quad p = m_2. \tag{3.1}$$

Then from (0.3)

$$t_2^2 + m_2^2 = 1. \tag{3.2}$$

Then the flow law (2.1) yields

$$\dot{\epsilon}_1 = 0, \quad \dot{x}_1 = 0,$$
$$\dot{\epsilon}_2 = \lambda t_2, \quad \dot{x}_2 = \frac{4}{h} \lambda m_2, \tag{3.3}$$

where

$$\dot{\epsilon}_1 = \frac{du}{dr}, \quad \dot{x}_1 = -\frac{d^2w}{dr^2},$$
$$\dot{\epsilon}_2 = \frac{u}{r}, \quad \dot{x}_2 = -\frac{1}{r} \cdot \frac{dw}{dr} \tag{3.4}$$

(u and w are the radial displacement and bending deflection rates).

We obtain the complete system of equations by combining with (3.2),
(3.3), (3.4) the equilibrium equations

$$\frac{d}{dr}(r t_1) - t_2 = 0,$$
$$\frac{d}{dr}(r m_1) - m_2 = -p \frac{r^2 - a^2}{2} \tag{3.5}$$

($\bar{p}$ = P/M$_s$; P is the uniform pressure on the plate) and the boundary
conditions

for $r = a$ $t_1 = 0, \quad m_1 = 0,$

for $r = b$ $t_1 = q = \frac{Q}{T_s}, \quad m_1 = 0, \quad w = 0.$ (3.6)

In spite of the static indeterminancy of the problem and the nonlinear-
ity of the yield condition (3.2), the exact solution in this case is
quite elementary. From (3.4) with account for the conditions ϵ_1 = 0,
κ_1 = 0 we obtain

$$\dot{\iota}_1 = \frac{C_1}{r}, \quad \dot{\iota}_2 = \frac{C_2}{r},$$ (3.7)

where C_1, C_2 are arbitrary constants. Since from (3.3) $\bar{m}_2/t_2 = h\kappa_2/4\varepsilon_2$, as a result of (3.7) we obtain

$$\frac{m_2}{t_2} = const = C.$$ (3.8)

Solving this equation together with (3.2) we immediately obtain

$$t_2 = \frac{1}{\sqrt{1+C^2}}, \quad m_2 = \frac{C}{\sqrt{1+C^2}}.$$ (3.9)

Substitution of these values into (3.5) and integration with account for the boundary conditions at r = a yield

$$t_1 = \frac{r-a}{r} \cdot \frac{1}{\sqrt{1+C^2}},$$
$$m_1 = \frac{r-a}{r} \cdot \frac{C}{\sqrt{1+C^2}} - \frac{p}{6} \cdot \frac{r-a}{r}(r^2 + ar - 2a^2).$$ (3.10)

Then the two remaining boundary conditions at r = b serve for determining the constant C and the limiting relation between the values of the loads p and q. The latter may be written in the form

$$\left(\frac{p}{p_0}\right)^2 + \left(\frac{q}{q_0}\right)^2 = 1,$$ (3.11)

where p_0 and q_0 denote the limiting values of the pressure and radial force, acting separately

$$p_0 = 6(b^2 + ab - 2a^2), \quad q_0 = \frac{b-a}{b}.$$ (3.12)

(These expressions are the exact solutions of the bending and tension problems for a flat plate under the Tresca-Saint Venant condition.)

Figure 3 shows the circle (3.11) and also the polygon AOB corresponding to the analogous solution [9] based on the piecewise linear yield condition (0.1). The difference between the solutions in this case is quite large, and the circular arc AB is closer to the exact solution, which Hodge showed [9] must lie within the hatched strip in Figure 3.

4. Now let us consider a shallow shell of revolution supported along the contour and loaded axisymmetrically by the normal pressure P(r).
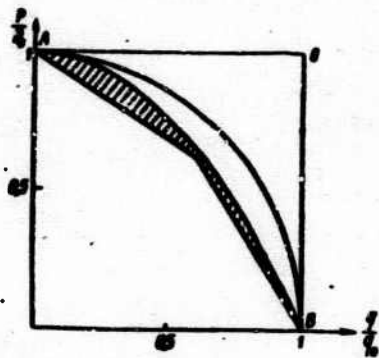
Figure 3

Figure 4.

The shell middle surface is given by the equation $z = z(r)$, where r is the distance to the axis of symmetry (Figure 4).
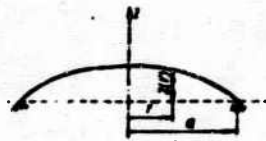
Under the usual assumptions of shallow shell theory, the equilibrium equations and the expressions for the deformations of the middle surface may be written in the form

$$\frac{d}{dr}(rt_1) - t_2 = 0, \quad \left(p = \frac{Pa^2}{c_s h^2}\right): \tag{4.1}$$

$$\frac{d}{dr}(rm_1) - m_2 + \frac{4rz'}{h}t_1 = -\frac{4}{a^2}\int_0^r p(r)\,r\,dr,$$

$$\dot{\epsilon}_1 = \frac{du}{dr} - z'w, \quad \dot{x}_1 = \frac{d\theta}{dr}, \quad \left(\theta = -\frac{dw}{dr}\right) \tag{4.2}$$

$$\dot{\epsilon}_2 = \frac{u - z'w}{r}, \quad \dot{x}_2 = \frac{\theta}{r}.$$

where the prime denotes differentiation with respect to r.

We shall use the yield condition (0.3) and consider the singular (statically determinate) plastic regime $\tau = t_1 = t_2$, $\mu = m_2$ to which corresponds the finite relation

$$t_1^2 + m_2^2 = 1 \tag{4.3}$$

and the flow law (derived in § 2)

$$\dot{x}_1 = 0, \quad \frac{\dot{\epsilon}_1 + \dot{\epsilon}_2}{\dot{x}_2} = \frac{h}{4} \cdot \frac{t_1}{m_2}. \tag{4.4}$$

Using the condition $t_1 = t_2$ we obtain from the first equilibrium equation

$$t_1 = t_2 = c. \tag{4.5}$$

From (4.3) and (4.1) we obtain the bending moments

$$m_2 = \sqrt{1 - c^2}, \tag{4.6}$$

$$m_1 = \sqrt{1 - c^2} - \frac{4c}{h}\int_0^r z'r\,dr - \frac{4}{a^2 r}\int_0^r dr \int_0^r p(r)\,r\,dr. \tag{4.7}$$

After transforming the second term we integrate by parts and noting the boundary condition $m_1 = 0$ on the contour $r = a$, we obtain (for $p = $ const)

$$\frac{2}{3}p = \sqrt{1-c^2} + \frac{4c}{ha}\int_0^a z\,dr. \tag{4.8}$$

If an external meridional force $t_1 = q$ is applied on the contour, the problem will be completely statically determinate; for constant c we find in this case, in accordance with (4.5), the value $c = q$ and (4.8) defines the limit loads·

$$\frac{p}{p_0} = \sqrt{1-q} + 4q\frac{z^*}{h}. \tag{4.9}$$

Here $p_0 = 3/2$ is the limiting pressure for the flat plate case; z^* denotes the average shell height

$$z^* = \frac{1}{a}\int_0^a z\,dr. \tag{4.10}$$

Now let the kinematic condition

$$w = u = 0 \quad (\text{for } r = a). \tag{4.11}$$

be given on the contour. In this case, in order to complete the solution we must examine the velocity field. Introducing the values for t_1, m_2 into (4.4), we obtain

$$\frac{d^2w}{dr^2} = 0,$$
$$\frac{d}{dr}(ru) - w\frac{d(rz')}{dr} = -\frac{h}{4}\cdot\frac{c}{\sqrt{1-c^2}}\cdot\frac{dw}{dr}. \tag{4.12}$$

Integrating these equations with account for (4.11) we obtain for velocities u, w and constant c,

$$w = w_0\left(1 - \frac{r}{a}\right), \tag{4.13}$$

$$u = z'w + w_0\frac{z}{a} \quad \frac{w_0}{ra}\int_0^r z\,dr + \frac{h}{4}\cdot\frac{c}{\sqrt{1-c^2}}:$$
$$\tag{4.14}$$

$$c = 4\frac{z^*}{h}\left[1 + \left(4\frac{z^*}{h}\right)^2\right]^{-\frac{1}{2}},$$

where w_0, the velocity scale, remains arbitrary. Introducing (4.14) into (4.8), we obtain the expression for the limiting pressure

$$p = p_0\sqrt{1 + \left(4\frac{z^*}{h}\right)^2}. \tag{4.15}$$

We see from this formula that the limiting pressure on the shallow shell depends not on the details of its shape, but only on the average height z^*. For the solution to be correct, it is necessary that the bending moment m_1 satisfy the condition $0 \leq m_1 \leq m_2$. This condition

is easily verified for specific classes of shells. It is obviously satisfied, for example, for the spherical shell, for shells of the form $z = z_0 \left[1 - \left(\frac{r}{a} \right)^n \right]$ (for $1 \leq n/2 \leq (h/4z^*)^2$) and in many other cases.

5. We shall examine the construction of bilateral estimates of the limiting load on the example of a spherical shell which is clamped along the contour and subjected to pressure loading (Figure 5). To obtain the lower estimate, we use the yield condition in the form (2.6). We assume the plastic regime.

$$0 \leqslant t_2 < t_1, \quad 0 < m_1 < m_2. \tag{5.1}$$

Then (2.6) provide two yield conditions

$$t_1 = \delta_t, \quad m_2 = \delta_m. \tag{5.2}$$

Combining with these relations the equilibrium equations

$$\frac{d}{d\varphi}(t_1 \sin \varphi) - t_2 \cos \varphi + \frac{\sin^2 \varphi}{\cos \varphi} t_1 = \frac{ph}{2R} \cdot \frac{\sin^2 \varphi}{\cos \varphi},$$

$$\frac{d}{d\varphi}(m_1 \sin \varphi) - m_2 \cos \varphi - 4 \frac{R}{h} \cdot \frac{\sin^2 \varphi}{\cos \varphi} t_1 = -2p \frac{\sin^2 \varphi}{\cos \varphi}$$

$$\left(p = \frac{P}{\sigma_s} \cdot \frac{R^2}{h^2} \right), \tag{5.3}$$

we obtain a statically possible regime which satisfies the necessary conditions at the apex of the shell (for $\phi = 0$) in the form

$$t_2 = \frac{\delta_t}{\cos^2 \varphi} - \frac{ph}{2R} \cdot \frac{\sin^2 \varphi}{\cos^2 \varphi},$$

$$m_1 = \delta_m + 2 \left(2\delta_t \frac{R}{h} - p \right) S(\varphi), \tag{5.4}$$

where the notations are

$$S(\varphi) = \frac{1}{\sin \varphi} \ln \operatorname{tg} \left(\frac{\varphi}{2} + \frac{\pi}{4} \right) - 1. \tag{5.5}$$

The edge condition $m_1 = 0$ for $\varphi = \alpha$ yields

$$p = 2\delta_t \frac{R}{h} + \frac{\delta_m}{2S(\alpha)}. \tag{5.6}$$

After determining here δ_t, δ_m from the condition of a maximum of p with the additional condition (2.7) and returning to dimensional variables, we obtain finally

$$\frac{P}{P_0} = \left[1 + \left(\frac{h}{4RS(\alpha)} \right)^2 \right]^{1/2}, \tag{5.7}$$

where $P_0 = 2\sigma_s (h/R)$ denotes the momentless solution.

To obtain the upper estimate we specify the rate field

$$u = 0, \quad w = w_0 \frac{\sin \alpha - \sin \varphi}{\sin \alpha},$$

(5.8)

to which correspond the following deformation rates

$$\dot{\varepsilon}_1 = \frac{du}{R d\varphi} + \frac{w}{R} = \frac{w_0}{R} \cdot \frac{\sin \alpha - \sin \varphi}{\sin \alpha},$$

$$\dot{\varepsilon}_2 = \frac{u}{R} \operatorname{ctg} \varphi + \frac{w}{R} = \frac{w_0}{R} \cdot \frac{\sin \alpha - \sin \varphi}{\sin \alpha},$$

$$\dot{\vartheta} = \frac{u}{R} - \frac{dw}{R d\varphi} = \frac{w_0}{R} \cdot \frac{\cos \varphi}{\sin \alpha},$$

$$\dot{\varkappa}_1 = \frac{d\vartheta}{R d\varphi} = -\frac{w_0}{R^2} \cdot \frac{\sin \varphi}{\sin \alpha}, \quad \dot{\varkappa}_2 = \frac{w_0}{R^2} \cdot \frac{\cos^2 \varphi}{\sin \alpha \sin \varphi}.$$

Substituting these values into (1.5) we obtain

$$\frac{P}{T_0} \leqslant \frac{\int_0^\alpha \left[(\sin \alpha - \sin \varphi)^2 + \frac{h^2}{4R^2} \cdot \frac{1 - \frac{3}{4} \sin^2 2\varphi}{\sin^2 \varphi} \right]^{1/2} \sin \varphi \, d\varphi}{\int_0^\alpha (\sin \alpha - \sin \varphi) \sin \varphi \, d\varphi}$$

(5.9)

The results of calculations using this formula for certain values of h/R are shown (for $10° \leq \alpha \leq 90°$) in Figure 6. Also shown there are the corresponding curves constructed using (5.7) (lower estimate). For small values of α (5.7) is in good agreement with the exact solution (4.15) for the shallow shell. In this case the upper estimate (5.9) differs from the solution (5.7) by at most 15%.
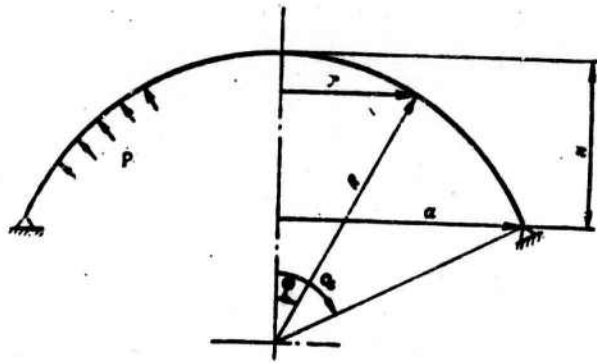
Figure 5.
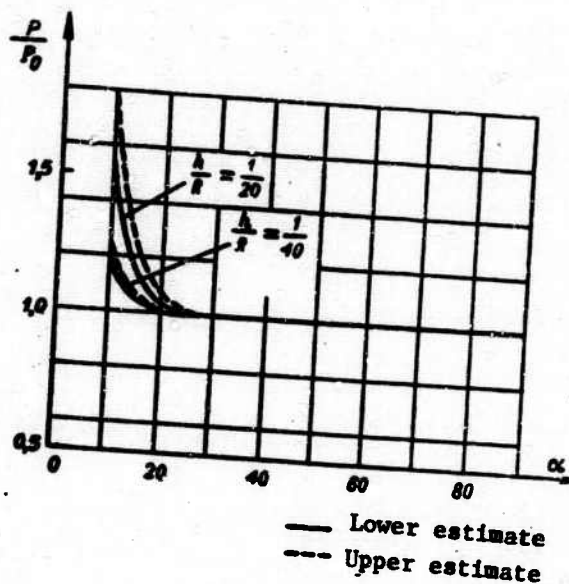
Figure 6.

REFERENCES

1. Il'yushin, A. A., Plastichnost' (Plasticity), Moscow, Gostek-hizdat, 1948.

2. Sawezuk, A., J. Rychlewski. On yield surfaces for plastic shells. Arch. mech. stosowanei, 1960, 12, No. 1.

3. Hodge, P. The Mises yield condition for rotationally symmetric shells. Quart. appl. math. 1960. No. 4.

4. Shapiro, G. S., "On yield surfaces for perfectly plastic shells". In: Problemy mekhaniki sploshnoy sredy (Problems of Continuum Mechanics), 1961.

5. Hodge, P. Rigid plastic analysis of symmetrically loaded cylindrical shells. J. appl. mech., 1954, No. 4.

6. Onat, E., and W. Prager. "Limiting equilibrium of shells of revolution," Mekhanika, No. 5, 1955.

7. Ivlev, D. D., "On the theory of limiting equilibrium of shells of revolution for peicewise linear plasticity conditions," IAN SSSR, OTN, Mekhanika i mashinostroyeniye, No. 6, 1962.

8. Eason, Shield. The influence of free ends on the load carrying capacities of cylindrical shells. J. mech. phys. Solids, 1955. 4, No. 1.

9. Hodge, P. G., "Boundary Value problems of plasticity theory": In: Plastichnost' i termoplastichnost' (Plasticity and Thermoplasticity), IL, 1962.

10. Hodge, P. G., "Comparison of the yield conditions in plastic shell theory," In: Problemy mekhaniki sploshnoy sredy. (Problems of Continuum mechanics), 1961.

11. Rozenblyum, V. I., "Approximate theory of plastic shell equilibrium," PMM, No. 3, 1954.

12. Rozenblyum, V. I., "On the plasticity condition for thin-wall shells," PMM, No. 2, 1960.

FOOTNOTES

1. In the last two cases, the finite relationships were derived only for axisymmetrically loaded shells of revolution. (see page 226)

2. In this case, there are specific difficulties connected with selecting the suitable plastic regimes. (see page 226)

DOCUMENT CONTROL DATA - R & D

(Security classification of title, body of abstract and indexing annotation must be entered when the overall report is classified)

1. ORIGINATING ACTIVITY (Corporate author)	2a. REPORT SECURITY CLASSIFICATION
Foreign Technology Division Air Force Systems Command U. S. Air Force	UNCLASSIFIED
	2b. GROUP

3. REPORT TITLE

EQUATIONS OF ANISOTROPIC PLATE THEORY

4. DESCRIPTIVE NOTES *(Type of report and inclusive dates)*

Translation

5. AUTHOR(S) *(First name, middle initial, last name)*

Ponyatovskiy, V. V.

6. REPORT DATE	7a. TOTAL NO. OF PAGES	7b. NO. OF REFS
1965	32	13

8a. CONTRACT OR GRANT NO.	9a. ORIGINATOR'S REPORT NUMBER(S)
F33657-70-D-0607	
b. PROJECT NO. 72301-78	
	FTD-HC-23-361-69
c.	9b. OTHER REPORT NO(S) *(Any other numbers that may be assigned this report)*
d.	Acc. Nr. L8379-66

10. DISTRIBUTION STATEMENT

Distribution of this document is unlimited. It may be released to the Clearinghouse, Department of Commerce, for sale to the general public.

11. SUPPLEMENTARY NOTES	12. SPONSORING MILITARY ACTIVITY
	Foreign Technology Division Wright-Patterson AFB, Ohio

13. ABSTRACT

In this paper the method of [1] is used to construct a theory of anisotropic plates. It is assumed that the plate is elastically uniform through its thickness and has at every point a plane of elastic symmetry parallel to the median plane. As is known, in this case the problem of the stresses in the plate breaks down into two independent problems which are symmetric and antisymmetric with respect to the median plane, respectively. The equations of the bending problem for transversely isotropic plates are examined in detail. In this case, the stress state is represented as the sum of two qualitatively different stress states: "rotational" and "potential" [2]. To solve the bending problem we use asymptotic integration of differential equations with a small parameter in the derivatives [3,4].

DD FORM 1473
NOV 65

14. KEY WORDS	LINK A		LINK B		LINK C	
	ROLE	WT	ROLE	WT	ROLE	WT
Anisotropic Plate Differential Equation Asymptotic Solution Linear Differential Equation Constant Coefficient Integral Equation Elasticity Theory						

DOCUMENT CONTROL DATA - R & D

(Security classification of title, body of abstract and indexing annotation must be entered when the overall report is classified)

1. ORIGINATING ACTIVITY (Corporate author)	2a. REPORT SECURITY CLASSIFICATION
Foreign Technology Division	UNCLASSIFIED
Air Force Systems Command	2b. GROUP
U. S. Air Force	

3. REPORT TITLE

SOME QUESTIONS OF UNCOUPLING AND DISCRETIZATION OF SHELL THEORY EQUATIONS

4. DESCRIPTIVE NOTES (Type of report and inclusive dates)

Translation

5. AUTHOR(S) (First name, middle initial, last name)

Rozin, L. A.

6. REPORT DATE	7a. TOTAL NO. OF PAGES	7b. NO. OF REFS
1965	27	7
8a. CONTRACT OR GRANT NO.	9a. ORIGINATOR'S REPORT NUMBER(S)	
F33657-70-D-0607		
b. PROJECT NO. 72301-78		
	FTD-HC-23-361-69	
c.	9b. OTHER REPORT NO(S) (Any other numbers that may be assigned this report)	
d.	Acc. Nr. L8379-66	

10. DISTRIBUTION STATEMENT

Distribution of this document is unlimited. It may be released to the Clearinghouse, Department of Commerce, for sale to the general public.

11. SUPPLEMENTARY NOTES	12. SPONSORING MILITARY ACTIVITY
	Foreign Technology Division
	Wright-Patterson AFB, Ohio

13. ABSTRACT

In plate and shell theory, it is of interest to construct problem solution methods which can be ascribed definite physical relevance. This is because physical considerations are often useful in constructing computational algorithms. Moreover, this approach makes possible a more profound and simpler analysis of the various assumptions and simplifications. Some techniques were indicated for decoupling the operators of the differential equations of shell theory and these techniques were used to construct solution schemes having definite physical relevance. In particular, it was possible to reduce the problem to the caluclation of a crossed bar system. It was found that this sort of system is not a crossed bar system in the usual sense. Its individual bars do not bend relative to the normal to the shell middle surface. Their twist takes place with a rigidity proportional to the moment of inertial, additional forces and moments acting on the bars appear, the calculation result does not depend on the relative width of the bars etc. The resulting bar system differs in this aspect from the conventional crossed bar system. The latter sometimes appears in those studies where an attempt is made to construct computational schemes not on the basis of the fundamental mathematical formulation of the problem, but by means of unconvincing and at times erroneous arguments based on "engineering" intuition.

DD FORM 1473
NOV 65

16. KEY WORDS	LINK A		LINK B		LINK C	
	ROLE	WT	ROLE	WT	ROLE	WT
Shell Theory Differential Equation Elasticity Theory Algorithm Integral Equation						

DOCUMENT CONTROL DATA - R & D

(Security classification of title, body of abstract and indexing annotation must be entered when the overall report is classified)

1. ORIGINATING ACTIVITY (Corporate author)	2a. REPORT SECURITY CLASSIFICATION
Foreign Technology Division	UNCLASSIFIED
Air Force Systems Command	2b. GROUP
U. S. Air Force	

3. REPORT TITLE

ON THE DETERMINATION OF THE MOMENTLESS STRESS STATE IN COVERINGS WITH POLYGONAL PLANFORM

4. DESCRIPTIVE NOTES (Type of report and inclusive dates)

Translation

5. AUTHOR(S) (First name, middle initial, last name)

Pavilaynen, V. Ya.

6. REPORT DATE	7a. TOTAL NO. OF PAGES	7b. NO. OF REFS
1965	16	3

8a. CONTRACT OR GRANT NO.	9a. ORIGINATOR'S REPORT NUMBER(S)
F33657-70-D-0607	
b. PROJECT NO. 72301-78	FTD-HC-23-361-69
c.	9b. OTHER REPORT NO(S) (Any other numbers that may be assigned this report)
d.	Acc. Nr. L8379-66

10. DISTRIBUTION STATEMENT

Distribution of this document is unlimited. It may be released to the Clearinghouse, Department of Commerce, for sale to the general public.

11. SUPPLEMENTARY NOTES	12. SPONSORING MILITARY ACTIVITY
	Foreign Technology Division
	Wright-Patterson AFB, Ohio

13. ABSTRACT

Shells which cover a space with nonrectangular planform find application in the construction of pavilions, trade centers, and other structures. Here the most efficient shells are those in which the midsurface has positive Gaussian curvature, since these shells provide a stress state which is nearly moment-free under the primary design loads (dead weight, snow). In this case a considerable portion of the shell, with the exception of small regions near the edge, operates in uniform compression and this permits effective use of the material in reinforced concrete designs. In the present paper we suggest a method for calculating coverings with nonrectangular planform which differs from that of [3]. The Pucher system of equations is generalized to the case of an oblique Cartesian coordinate system. We examine several cases of the application of the resulting equations to the analysis of coverings which have an arbitrary parallelogram planform, and also the questions of direct determination of the tangential forces at the shell corners.

DD FORM 1473
(1 NOV 65)

14. KEY WORDS	LINK A		LINK B		LINK C	
	ROLE	WT	ROLE	WT	ROLE	WT
Stress Analysis Shell Theory Cartesian Coordinate Polygonal Curved Plate Poisson Equation						

DOCUMENT CONTROL DATA - R & D

(Security classification of title, body of abstract and indexing annotation must be entered when the overall report is classified)

1. ORIGINATING ACTIVITY (Corporate author)	2a. REPORT SECURITY CLASSIFICATION
Foreign Technology Division Air Force Systems Command U. S. Air Force	UNCLASSIFIED 2b. GROUP

3. REPORT TITLE

SOME CASES OF TORSION OF BARS WITH VARYING ELASTIC MODULI

4. DESCRIPTIVE NOTES (Type of report and inclusive dates)

Translation

5. AUTHOR(S) (First name, middle initial, last name)

Lekhnitskiy, S. G.

6. REPORT DATE	7a. TOTAL NO. OF PAGES	7b. NO. OF REFS
1965	17	3

8a. CONTRACT OR GRANT NO. F33657-70-D-0607 b. PROJECT NO. 72301-78 c. d.	9a. ORIGINATOR'S REPORT NUMBER(S) FTD-HC-23-361-69 9b. OTHER REPORT NO(S) (Any other numbers that may be assigned this report) Acc. Nr. L8379-66

10. DISTRIBUTION STATEMENT

Distribution of this document is unlimited. It may be released to the Clearinghouse, Department of Commerce, for sale to the general public.

11. SUPPLEMENTARY NOTES	12. SPONSORING MILITARY ACTIVITY Foreign Technology Division Wright-Patterson AFB, Ohio

13. ABSTRACT

The problem of torsion of an elastic bar of constant cross section in the classical formulation, i.e., under the assumption that the deformations are small and the material obeys the generalized Hooke's law, is known to reduce to the determination of a stress function which satisfies in the region of the cross section a second-order linear equation and takes a constant value on the contour. For a homogeneous bar this equation has constant coefficients which depend on the modulus of elasticity. However, if the elastic moduli are continuous functions of the coordinates we obtain for the stress function a second-order differential equation with variable coefficients, and the question of finding an effective solution for the torsion problem becomes much more complex. It appears that this problem has been solved only for a bar in the form of a solid or hollow circular cylinder having cylindrical anisotropy, with elastic moduli which are constant along the length. In the present article we consider several cases of bars with variable moduli for which an effective solution of the torsion problem may be obtained elementarily, using the same methods used in solving the corresponding problems for the homogeneous isotropic bar.

DD FORM 1473
I NOV 65

14. KEY WORDS	LINK A		LINK B		LINK C	
	ROLE	WT	ROLE	WT	ROLE	WT
Elasticity Theory Constant Coefficient Linear Equation Differential Equation Torsion Stress						

DOCUMENT CONTROL DATA - R & D

(Security classification of title, body of abstract and indexing annotation must be entered when the overall report is classified)

1. ORIGINATING ACTIVITY (Corporate author)	2a. REPORT SECURITY CLASSIFICATION
Foreign Technology Division	UNCLASSIFIED
Air Force Systems Command	2b. GROUP
U. S. Air Force	

3. REPORT TITLE

CYLINDRICAL SHELL AND PLATE SUBJECTED TO A MOVING HEAT SOURCE

4. DESCRIPTIVE NOTES (Type of report and inclusive dates)

Translation

5. AUTHOR(S) (First name, middle initial, last name)

Kozhakhmetov, K. Kh. and Finkel'shteyn, R. M.

6. REPORT DATE	7a. TOTAL NO. OF PAGES	7b. NO. OF REFS
1965	20	

8a. CONTRACT OR GRANT NO.	9a. ORIGINATOR'S REPORT NUMBER(S)
F33657-70-D-0607	
b. PROJECT NO. 72301-78	FTD-HC-23-361-69
c.	9b. OTHER REPORT NO(S) (Any other numbers that may be assigned this report)
d.	Acc. Nr. L8379-66

10. DISTRIBUTION STATEMENT

Distribution of this document is unlimited. It may be released to the Clearinghouse, Department of Commerce, for sale to the general public.

11. SUPPLEMENTARY NOTES	12. SPONSORING MILITARY ACTIVITY
	Foreign Technology Division
	Wright-Patterson AFB, Ohio

13. ABSTRACT

We consider thin circular cylindrical shells of radius R and a semi-infinite flat plate under the influence of a moving heat source. The temperature is distributed linearly through the thickness of the shells and plate.

DD FORM 1473
I NOV 65

14. KEY WORDS	LINK A		LINK B		LINK C	
	ROLE	WT	ROLE	WT	ROLE	WT
Thin Shell Structure						
Thin Plate Structure						
Cylindric Shell Structure						
Heat Transfer Coefficient						
Thermoelasticity						
Integral Equation						

DOCUMENT CONTROL DATA - R & D

(Security classification of title, body of abstract and indexing annotation must be entered when the overall report is classified)

1. ORIGINATING ACTIVITY *(Corporate author)*	2a. REPORT SECURITY CLASSIFICATION
Foreign Technology Division	UNCLASSIFIED
Air Force Systems Command	2b. GROUP
U. S. Air Force	

3. REPORT TITLE

INTEGRALS OF THE EQUATIONS OF AXISYMMETRIC VIBRATIONS OF SHELLS OF REVOLUTION

4. DESCRIPTIVE NOTES *(Type of report and inclusive dates)*

Translation

5. AUTHOR(S) *(First name, middle initial, last name)*

Tovstik, P. Ye.

6. REPORT DATE	7a. TOTAL NO. OF PAGES	7b. NO. OF REFS
1965	13	4

8a. CONTRACT OR GRANT NO.	9a. ORIGINATOR'S REPORT NUMBER(S)
F33657-70-D-0607	
b. PROJECT NO. 72301-78	FTD-HC-23-361-69
c.	9b. OTHER REPORT NO(S) *(Any other numbers that may be assigned this report)*
d.	Acc. Nr. L8379-66

10. DISTRIBUTION STATEMENT

Distribution of this document is unlimited. It may be released to the Clearinghouse, Department of Commerce, for sale to the general public.

11. SUPPLEMENTARY NOTES	12. SPONSORING MILITARY ACTIVITY
	Foreign Technology Division
	Wright-Patterson AFB, Ohio

13. ABSTRACT

The asymptotic method for integrating equations with small parameters in the higher derivatives is employed to integrate the system of equations of small axisymmetric vibrations of a thin elastic shell of revolution. In some frequency range the resolvent equation has a reversal point. In this article we consider the case in which the coefficient of the second derivative in the resolvent has a simple root (simple reversal point), and we find the Stokes multipliers relating the integrals of the resolvent to the right and left of the reversal point. Moreover, the integrals in the immediate vicinity of the reversal point are calculated. As an example, we examine the problem of the natural vibration frequencies of a shell with clamped edges. The present article is an extension of the study initiated by Alumyae for a conical shell.

14. KEY WORDS	LINK A		LINK B		LINK C	
	ROLE	WT	ROLE	WT	ROLE	WT
Integral Equation						
Asymptotic Solution						
Shell Vibration						
Shell of Revolution						

DOCUMENT CONTROL DATA - R & D

(Security classification of title, body of abstract and indexing annotation must be entered when the overall report is classified)

1. ORIGINATING ACTIVITY (Corporate author)	2a. REPORT SECURITY CLASSIFICATION
Foreign Technology Division	UNCLASSIFIED
Air Force Systems Command	2b. GROUP
U. S. Air Force	

3. REPORT TITLE

REGULAR INTEGRALS OF THE EQUATIONS FOR AXISYMMETRIC VIBRATIONS OF A DOME

4. DESCRIPTIVE NOTES (Type of report and inclusive dates)

Translation

5. AUTHOR(S) (First name, middle initial, last name)

Tovstik, P. Ye.

6. REPORT DATE	7a. TOTAL NO. OF PAGES	7b. NO. OF REFS
1965	7	6

8a. CONTRACT OR GRANT NO.	9a. ORIGINATOR'S REPORT NUMBER(S)
F33657-70-D-0607	
b. PROJECT NO. 72301-78	
	FTD-HC-23-361-69
c.	9b. OTHER REPORT NO(S) (Any other numbers that may be assigned this report)
d.	Acc. Nr. L8379-66

10. DISTRIBUTION STATEMENT

Distribution of this document is unlimited. It may be released to the Clearinghouse, Department of Commerce, for sale to the general public.

11. SUPPLEMENTARY NOTES	12. SPONSORING MILITARY ACTIVITY
	Foreign Technology Division
	Wright-Patterson AFB, Ohio

13. ABSTRACT

is known that the general solution of the system of equations of free axisymmetric vibrations of a thin elastic shell of revolution is made up of two integrals of the momentless equations and four integrals with a large variability index. The asymptotic expressions for these four integrals may be found easily in intervals which do not contain either so-called reversal points or singular points of the shell vibration equations. The behavior of the integrals in the vicinity of a simple reversal point is examined. The equations for the vibrations of a shell in the form of a dome have a regular singular point at the shell apex. In the present study, we construct the regular integrals with large variability index at the dome apex, and find their asymptotic expressions far from the apex of the dome. We need to know these integrals in order to determine the natural vibration frequency of the dome.

DD FORM NOV 1473

14. KEY WORDS	LINK A		LINK B		LINK C	
	ROLE	WT	ROLE	WT	ROLE	WT
Integral Equation Shell of Revolution Shell Vibration Vibration Frequency						

DOCUMENT CONTROL DATA - R & D

(Security classification of title, body of abstract and indexing annotation must be entered when the overall report is classified)

1. ORIGINATING ACTIVITY *(Corporate author)*	2a. REPORT SECURITY CLASSIFICATION
Foreign Technology Division Air Force Systems Command U. S. Air Force	UNCLASSIFIED
	2b. GROUP

3. REPORT TITLE

SHELLS OF REVOLUTION WITH A SMALL CENTRAL OPENING SUBJECTED TO SYMMETRIC AND ANTISYMMETRIC LOADING

4. DESCRIPTIVE NOTES *(Type of report and inclusive dates)*

Translation

5. AUTHOR(S) *(First name, middle initial, last name)*

Kruglyakova, V. I.

6. REPORT DATE	7a. TOTAL NO. OF PAGES	7b. NO. OF REFS
1965	37	35

8a. CONTRACT OR GRANT NO. F33657-70-D-0607	9a. ORIGINATOR'S REPORT NUMBER(S)
b. PROJECT NO. 72301-78	FTD-HC-23-361-69
c.	9b. OTHER REPORT NO(S) *(Any other numbers that may be assigned this report)*
d.	Acc. Nr. L8379-66

10. DISTRIBUTION STATEMENT

Distribution of this document is unlimited. It may be released to the Clearinghouse, Department of Commerce, for sale to the general public.

11. SUPPLEMENTARY NOTES	12. SPONSORING MILITARY ACTIVITY
	Foreign Technology Division Wright-Patterson AFB, Ohio

13. ABSTRACT

This article presents a unified method for determining the stresses near a small central opening in shells of revolution subjected to symmetric and antisymmetric loads. Primary emphasis is placed on reducing the solution to a form convenient for practical application. In particular, the edge stiffness coefficients are obtained. In most studies on this question symmetric deformation of a shallow shell is examined. In contrast to these studies, the proposed method contains a simplification involving replacement of sin θ by θ only in the equation coefficients. The trigonometric multipliers are retained in the expressions for the stresses and displacements. Comparison of the resulting solution with a specially constructed more exact solution has shown its acceptability for a wide range of values of a given angle; corresponding to the edge of the opening in the shell. The region of values of the basic parameters in which the suggested Bessel solution may be replaced by the much simpler familiar Geckeler solution, is determined. A brief review of the studies known to the author is presented.

DD FORM 1473
I NOV 65

14. KEY WORDS	LINK A		LINK B		LINK C	
	ROLE	WT	ROLE	WT	ROLE	WT
Shell of Revolution						
Symmetric Load						
Antisymmetric Load						
Gauss Differential Equation						
Bessel Function						
Bessel Differential Equation						

DOCUMENT CONTROL DATA - R & D

(Security classification of title, body of abstract and indexing annotation must be entered when the overall report is classified)

1. ORIGINATING ACTIVITY (Corporate author)	2a. REPORT SECURITY CLASSIFICATION
Foreign Technology Division	UNCLASSIFIED
Air Force Systems Command	2b. GROUP
U. S. Air Force	

3. REPORT TITLE

STUDY OF STRESS CONCENTRATION IN TURBINE BLADE T-SHAPED HEADS IN ELASTIC AND CREEP CONDITIONS

4. DESCRIPTIVE NOTES (Type of report and inclusive dates)

Translation

5. AUTHOR(S) (First name, middle initial, last name)

Bugakov, I. I., Smirnova, V. P. and Shikhobalov, S. P.

6. REPORT DATE	7a. TOTAL NO. OF PAGES	7b. NO. OF REFS
1965	9	4

8a. CONTRACT OR GRANT NO. F33657-70-D-0607	9a. ORIGINATOR'S REPORT NUMBER(S)
b. PROJECT NO. 72301-78	FTD-HC-23-361-69
c.	9b. OTHER REPORT NO(S) (Any other numbers that may be assigned this report)
d.	Acc. Nr. L8379-66

10. DISTRIBUTION STATEMENT

Distribution of this document is unlimited. It may be released to the Clearinghouse, Department of Commerce, for sale to the general public.

11. SUPPLEMENTARY NOTES	12. SPONSORING MILITARY ACTIVITY
	Foreign Technology Division Wright-Patterson AFB, Ohio

13. ABSTRACT

This article presents the results of a study using photoelastic and photocreep methods of stress concentration in the T-shaped heads of turbine blades with relative dimensions given. The study was made by the Optical Laboratory of the Scientific Research Institute of Mathematics and Mechanics of Leningrad State University for the "22-nd Session of the CPSU" Leningrad Metals Plant. The study was made using two-dimensional models subjected to a constant external load simulating the blade centrifugal force. The models were fabricated using metal templates with relative dimensions.

DD FORM 1473 (1 NOV 65)

14. KEY WORDS	LINK A		LINK B		LINK C	
	ROLE	WT	ROLE	WT	ROLE	WT
Stress Concentration						
Turbine Blade						
Photoelasticity						
Photocreep						

DOCUMENT CONTROL DATA - R & D

(Security classification of title, body of abstract and indexing annotation must be entered when the overall report is classified)

1. ORIGINATING ACTIVITY (Corporate author)	2a. REPORT SECURITY CLASSIFICATION
Foreign Technology Division	UNCLASSIFIED
Air Force Systems Command	2b. GROUP
U. S. Air Force	

3. REPORT TITLE

ESTIMATING THE FUNDAMENTAL VIBRATION FREQUENCY OF A BAR OF VARIABLE CROSS SECTION

4. DESCRIPTIVE NOTES (Type of report and inclusive dates)

Translation

5. AUTHOR(S) (First name, middle initial, last name)

Kuznetsov, L. I.

6. REPORT DATE	7a. TOTAL NO. OF PAGES	7b. NO. OF REFS
1965	5	5

8a. CONTRACT OR GRANT NO.	9a. ORIGINATOR'S REPORT NUMBER(S)
F33657-70-D-0607	
b. PROJECT NO. 72301-78	FTD-HC-23-361-69
c.	9b. OTHER REPORT NO(S) (Any other numbers that may be assigned this report)
d.	Acc. Nr. L8379-66

10. DISTRIBUTION STATEMENT

Distribution of this document is unlimited. It may be released to the Clearinghouse, Department of Commerce, for sale to the general public.

11. SUPPLEMENTARY NOTES	12. SPONSORING MILITARY ACTIVITY
	Foreign Technology Division
	Wright-Patterson AFB, Ohio

13. ABSTRACT

The problem of finding the natural frequencies of the longitudinal vibrations of a bar, one end of which is clamped while the other carries an absolutely rigid weight, leads to finding a given value for which a given equation has a nonzero solution, under given boundary conditions. Here gamma is the bar material density; 1 is the bar length; $S(x)$ is the cross section area; E is the modulus of elasticity; M is the mass of the bar. For estimating the upper limit of the first (fundamental) vibration frequency, we have the simple but in many cases adequately precise Rayleigh formula, which for the mode corresponding to a static load is a given equation. It is desirable to have an equally simple formula for estimating the lower limit of the fundamental frequency, as this would be useful for practical calculations. Such an estimate is obtained immediately with the aid of the principle of contracting mappings. However, this method is not found in handbooks and texts on vibration theory, and this is the reason for the present article.

DD FORM 1473 (1 NOV 65)

14. KEY WORDS	LINK A		LINK B		LINK C	
	ROLE	WT	ROLE	WT	ROLE	WT
Vibration Frequency						
Static Load						
Rayleigh Formula						
Green's Function						
Cross Section Bar						

DOCUMENT CONTROL DATA - R & D

(Security classification of title, body of abstract and indexing annotation must be entered when the overall report is classified)

1. ORIGINATING ACTIVITY (Corporate author)	2a. REPORT SECURITY CLASSIFICATION
Foreign Technology Division	UNCLASSIFIED
Air Force Systems Command	2b. GROUP
U. S. Air Force	

3. REPORT TITLE

FORCED AXISYMMETRIC VIBRATIONS OF A CIRCULAR THICK PLATE

4. DESCRIPTIVE NOTES (Type of report and inclusive dates)

Translation

5. AUTHOR(S) (First name, middle initial, last name)

Bukharinov, G. N.

6. REPORT DATE	7a. TOTAL NO. OF PAGES	7b. NO. OF REFS
1965	6	

8a. CONTRACT OR GRANT NO.	9a. ORIGINATOR'S REPORT NUMBER(S)
F33657-70-D-0607	
b. PROJECT NO. 72301-78	FTD-HC-23-361-69
c.	9b. OTHER REPORT NO(S) (Any other numbers that may be assigned this report)
d.	Acc. Nr. L8379-66

10. DISTRIBUTION STATEMENT

Distribution of this document is unlimited. It may be released to the Clearinghouse, Department of Commerce, for sale to the general public.

11. SUPPLEMENTARY NOTES	12. SPONSORING MILITARY ACTIVITY
	Foreign Technology Division
	Wright-Patterson AFB, Ohio

13. ABSTRACT

In this article we solve the problem of forced axisymmetric vibrations of a circular thick plate under the influence of uniformly distributed normal forces which are harmonic time functions applied to one of the faces of the plate. The boundary conditions on the faces are satisfied exactly. Satisfaction of the boundary conditions at the side surfaces reduces to calculating the coefficients in the expansion of the displacements into series of functions of the z coordinate, where oz is the axis of symmetry.

DD FORM 1473
NOV 1473

14. KEY WORDS	LINK A		LINK B		LINK C	
	ROLE	WT	ROLE	WT	ROLE	WT
Forced Vibration						
Differential Equation						
Circular Plate						

DOCUMENT CONTROL DATA - R & D

(Security classification of title, body of abstract and indexing annotation must be entered when the overall report is classified)

1. ORIGINATING ACTIVITY (Corporate author)	2a. REPORT SECURITY CLASSIFICATION
Foreign Technology Division	UNCLASSIFIED
Air Force Systems Command	2b. GROUP
U. S. Air Force	

3. REPORT TITLE

EFFECT OF PRELIMINARY PLASTIC DEFORMATION ON THE YIELD AND
ULTIMATE LIMITS OF COPPER

4. DESCRIPTIVE NOTES (Type of report and inclusive dates)

Translation

5. AUTHOR(S) (First name, middle initial, last name)

Talypov, G. B.

6. REPORT DATE	7a. TOTAL NO. OF PAGES	7b. NO. OF REFS
1965	6	4

8a. CONTRACT OR GRANT NO.	9a. ORIGINATOR'S REPORT NUMBER(S)
F33657-70-D-0607	
b. PROJECT NO. 72301-78	
	FTD-HC-23-361-69
c.	9b. OTHER REPORT NO(S) (Any other numbers that may be assigned this report)
d.	Acc. Nr. L8379-66

10. DISTRIBUTION STATEMENT

Distribution of this document is unlimited. It may be released to
the Clearinghouse, Department of Commerce, for sale to the general
public.

11. SUPPLEMENTARY NOTES	12. SPONSORING MILITARY ACTIVITY
	Foreign Technology Division
	Wright-Patterson AFB, Ohio

13. ABSTRACT

In preceding papers a study of the effect of preliminary
plastic deformation on the yield limit of low and medium
carbon steel established that the shape of the yield
limit is independent of the loading path, and is a circle
on the Il'yushin plane expanding and displacing in the
direction of the preliminary plastic deformation. In the
present paper, we present the results of a study of the
effect of preliminary plastic deformation on the yield
limit of annealed technical copper.

DD FORM 1473
1 NOV 65

14. KEY WORDS	LINK A		LINK B		LINK C	
	ROLE	WT	ROLE	WT	ROLE	WT
Plastic Deformation Copper Annealing						

DOCUMENT CONTROL DATA - R & D

(Security classification of title, body of abstract and indexing annotation must be entered when the overall report is classified)

1. ORIGINATING ACTIVITY (Corporate author)	2a. REPORT SECURITY CLASSIFICATION
Foreign Technology Division Air Force Systems Command U. S. Air Force	UNCLASSIFIED 2b. GROUP

3. REPORT TITLE

EFFECT OF LARGE PRELIMINARY PLASTIC DEFORMATIONS AND NATURAL
AGING ON THE YIELD LIMIT OF LOW CARBON STEEL

4. DESCRIPTIVE NOTES *(Type of report and inclusive dates)*

Translation

5. AUTHOR(S) *(First name, middle initial, last name)*

Talypov, G. B.

6. REPORT DATE	7a. TOTAL NO. OF PAGES	7b. NO. OF REFS
1965	4	3

8a. CONTRACT OR GRANT NO. F33657-70-D-0607 b. PROJECT NO. 72301-78 c. d.	9a. ORIGINATOR'S REPORT NUMBER(S) FTD-HC-23-361-69 9b. OTHER REPORT NO(S) (Any other numbers that may be assigned this report) Acc. Nr. L8379-66

10. DISTRIBUTION STATEMENT

Distribution of this document is unlimited. It may be released to
the Clearinghouse, Department of Commerce, for sale to the general
public.

11. SUPPLEMENTARY NOTES	12. SPONSORING MILITARY ACTIVITY Foreign Technology Division Wright-Patterson AFB, Ohio

13. ABSTRACT

In the present paper, we present the results of a study of the
effect of large preliminary plastic deformations and natural aging
on the yield limit. For the experiments we used four groups of so-
called "gagarin" specimens of annealed St. 20 steel. The (three)
specimens of the first group were tested in tension to determine
the basic mechanical properties of this steel. All 27 specimens of
the second group were stretched to a given equation. After unload-
ing and recording the new dimensions, 3 samples of the first sub-
group were again stretched up to failure on the same day. Each of
the three specimens of succeeding subgroups were stretched up to
failure, after aging for a period of one to two months etc. All 27
specimens of the third group were subjected to preliminary stretch-
ing to a given equation and all the specimens of the fourth group
were stretched to a given equation. After unloading the correspond-
ing subgroups of these groups of specimens were subjected to the
same operations as were the corresponding subgroups of the second
group. The test results are shown in a figure and are described
satisfactorily. In this case the parameter A remains constant,
equal to 0.31, and its values are shown by the triangles in a
figure. Thus, we find that the extent of the maximal expansion of
the yield limit for natural aging depends not only on the magnitude
of the preliminary plastic deformation, but also on the steel grade.

DD FORM 1473

14. KEY WORDS	LINK A		LINK B		LINK C	
	ROLE	WT	ROLE	WT	ROLE	WT
Plastic Deformation						
Carbon Steel						

DOCUMENT CONTROL DATA - R & D

(Security classification of title, body of abstract and indexing annotation must be entered when the overall report is classified)

1. ORIGINATING ACTIVITY *(Corporate author)*	2a. REPORT SECURITY CLASSIFICATION
Foreign Technology Division	UNCLASSIFIED
Air Force Systems Command	2b. GROUP
U. S. Air Force	

3. REPORT TITLE

FAILURE TIME OF TUBES SUBJECTED TO INTERNAL PRESSURE AND AXIAL FORCE

4. DESCRIPTIVE NOTES *(Type of report and inclusive dates)*

Translation

5. AUTHOR(S) *(First name, middle initial, last name)*

Levitas, Ye. M.

6. REPORT DATE	7a. TOTAL NO. OF PAGES	7b. NO. OF REFS
1965	7	4

8a. CONTRACT OR GRANT NO.	9a. ORIGINATOR'S REPORT NUMBER(S)
F33657-70-D-0607	
b. PROJECT NO. 72301-78	FTD-HC-23-361-69
c.	9b. OTHER REPORT NO(S) *(Any other numbers that may be assigned this report)*
d.	Acc. Nr. L8379-66

10. DISTRIBUTION STATEMENT

Distribution of this document is unlimited. It may be released to the Clearinghouse, Department of Commerce, for sale to the general public.

11. SUPPLEMENTARY NOTES	12. SPONSORING MILITARY ACTIVITY
	Foreign Technology Division
	Wright-Patterson AFB, Ohio

13. ABSTRACT

Hoff showed the practical value of the concept in which failure time is determined from an analysis of the unbounded quasi-viscous flow of a body. Discussion and literature references on the problem of "viscous" failure are presented. One of the most important practical problems of this kind is that of tube failure. Kats found the time for viscous failure of a tube under the influence of the internal pressure p. A more general problem in which the load is made up of the internal pressure p and the axial force P is considered.

14. KEY WORDS	LINK A		LINK B		LINK C	
	ROLE	WT	ROLE	WT	ROLE	WT
Tube Failure						
Differential Equation						
Internal Pressure						
Axial Force						

DOCUMENT CONTROL DATA - R & D

(Security classification of title, body of abstract and indexing annotation must be entered when the overall report is classified)

1. ORIGINATING ACTIVITY (Corporate author)	2a. REPORT SECURITY CLASSIFICATION
Foreign Technology Divi ..on Air Force Systems Comm: U. S. Air Force	UNCLASSIFIED 2b. GROUP

3. REPORT TITLE

EFFECT C PRELIMINARY PLASTIC DEFORMATION ON THE YIELD LIMIT
OF ST. 45 STEEL

4. DESCRIPTIVE NOTES (Type of report and inclusive dates)
Translation

5. AUTHOR(S) (First name, middle initial, last name)

Chistyakov, A. I.

6. REPORT DATE	7a. TOTAL NO. OF PAGES	7b. NO. OF REFS
1965	15	1

8a. CONTRACT OR GRANT NO. F33657-70-D-0607 b. PROJECT NO. 72301-78 c. d.	9a. ORIGINATOR'S REPORT NUMBER(S) FTD-HC-23-361-69 9b. OTHER REPORT NO(S) (Any other numbers that may be assigned this report) Acc. Nr. L8379-66

10. DISTRIBUTION STATEMENT

Distribution of this document is unlimited. It may be released to
the Clearinghouse, Department of Commerce, for sale to the general
public.

11. SUPPLEMENTARY NOTES	12. SPONSORING MILITARY ACTIVITY Foreign Technology Division Wright-Patterson AFB, Ohio

13. ABSTRACT

Tubular specimens were prepared from 55-mm-diameter annealed
rods. A plane stress state at points of the specimen cross
section was created by simultaneous application of an axial
force and internal pressure. The axial force was measured
to within plus or minus 1 percent, the internal pressure to
within 1 kg/cm(superscript 2). The longitudinal and trans-
verse deformations of the specimen were measured by wire re-
sistance pickups with base lengths 24 mm and bridge ampli-
fiers. In order to account for the possible slight eccentri-
city in the specimen installation, the longitudinal gages
were mounted along two opposite generators.

DD FORM 1473
1 NOV 65

14. KEY WORDS	LINK A		LINK B		LINK C	
	ROLE	WT	ROLE	WT	ROLE	WT
Plastic Deformation						
Stress Analysis						
Carbon Steel						
Annealed Rod						
Yield Limit						

DOCUMENT CONTROL DATA - R & D

(Security classification of title, body of abstract and indexing annotation must be entered when the overall report is classified)

1. ORIGINATING ACTIVITY (Corporate author)	2a. REPORT SECURITY CLASSIFICATION
Foreign Technology Division	UNCLASSIFIED
Air Force Systems Command	2b. GROUP
U. S. Air Force	

3. REPORT TITLE

PHOTOELASTIC STUDY OF THE EFFECT OF BOTTOM SHAPE ON THE STRESS
STATE OF THICK-WALL VESSELS

4. DESCRIPTIVE NOTES (Type of report and inclusive dates)

Translation

5. AUTHOR(S) (First name, middle initial, last name)

Maksutova, T. D.

6. REPORT DATE	7a. TOTAL NO. OF PAGES	7b. NO. OF REFS
1965	14	

8a. CONTRACT OR GRANT NO.	9a. ORIGINATOR'S REPORT NUMBER(S)
F33657-70-D-0607	
b. PROJECT NO. 72301-78	FTD-HC-23-361-69
c.	9b. OTHER REPORT NO(S) (Any other numbers that may be assigned this report)
d.	Acc. Nr. L8379-66

10. DISTRIBUTION STATEMENT

Distribution of this document is unlimited. It may be released to
the Clearinghouse, Department of Commerce, for sale to the general
public.

11. SUPPLEMENTARY NOTES	12. SPONSORING MILITARY ACTIVITY
	Foreign Technology Division
	Wright-Patterson AFB, Ohio

13. ABSTRACT

The present article is an extension of the description of the
results of an optical polarization study of thick-wall cylin-
drical vessels. The purpose of the study is to obtain the
most complete possible description of the stress state as a
function of the values of the parameters characterizing the
vessel geometry.

DD FORM NOV 65 **1473**

14. KEY WORDS	LINK A		LINK B		LINK C	
	ROLE	WT	ROLE	WT	ROLE	WT
Photoelasticity						
Stress Analysis						
Cylindrical Vessel						
Vessel Geometry						

DOCUMENT CONTROL DATA - R & D

(Security classification of title, body of abstract and indexing annotation must be entered when the overall report is classified)

1. ORIGINATING ACTIVITY (Corporate author)	2a. REPORT SECURITY CLASSIFICATION
Foreign Technology Division Air Force Systems Command U. S. Air Force	UNCLASSIFIED
	2b. GROUP

3. REPORT TITLE

CALCULATING THE LOAD-CARRYING CAPACITY OF IDEALLY PLASTIC
AXISYMMETRIC SHELLS

4. DESCRIPTIVE NOTES (Type of report and inclusive dates)

Translation

5. AUTHOR(S) (First name, middle initial, last name)

Rozenblyum, V. I.

6. REPORT DATE	7a. TOTAL NO. OF PAGES	7b. NO. OF REFS
1965	14	12

8a. CONTRACT OR GRANT NO. F33657-70-D-0607 b. PROJECT NO. 72301-78	9a. ORIGINATOR'S REPORT NUMBER(S) FTD-HC-23-361-69
c. d.	9b. OTHER REPORT NO(S) (Any other numbers that may be assigned this report) ACC. Nr. L8379-66

10. DISTRIBUTION STATEMENT

Distribution of this document is unlimited. It may be released to
the Clearinghouse, Department of Commerce, for sale to the general
public.

11. SUPPLEMENTARY NOTES	12. SPONSORING MILITARY ACTIVITY
	Foreign Technology Division Wright-Patterson AFB, Ohio

13. ABSTRACT

The yield condition expressed in terms of forces and moments
("finite relation") is of fundamental importance in the theory
of limit equilibrium of ideally plastic shells. At the present
time these finite relations have been formulated for the cases
of the Mises medium and for the Tresca-Saint medium, and also
for certain other types of plastic media. These finite rela-
tions (within the framework of the usual hypothesis of thin
shell theory they may be considered as exact relations) have a
very complex structure. In this connection considerable atten-
tion has also been devoted to the question of the approximation
of these exact yield conditions by means of relatively simple
surfaces which are more convenient for application.

DD FORM 1 NOV 65 1473

14. KEY WORDS	LINK A		LINK B		LINK C	
	ROLE	WT	ROLE	WT	ROLE	WT
Thin Shell Structure Plastic Shells Shell of Revolution Equilibrium Constant						